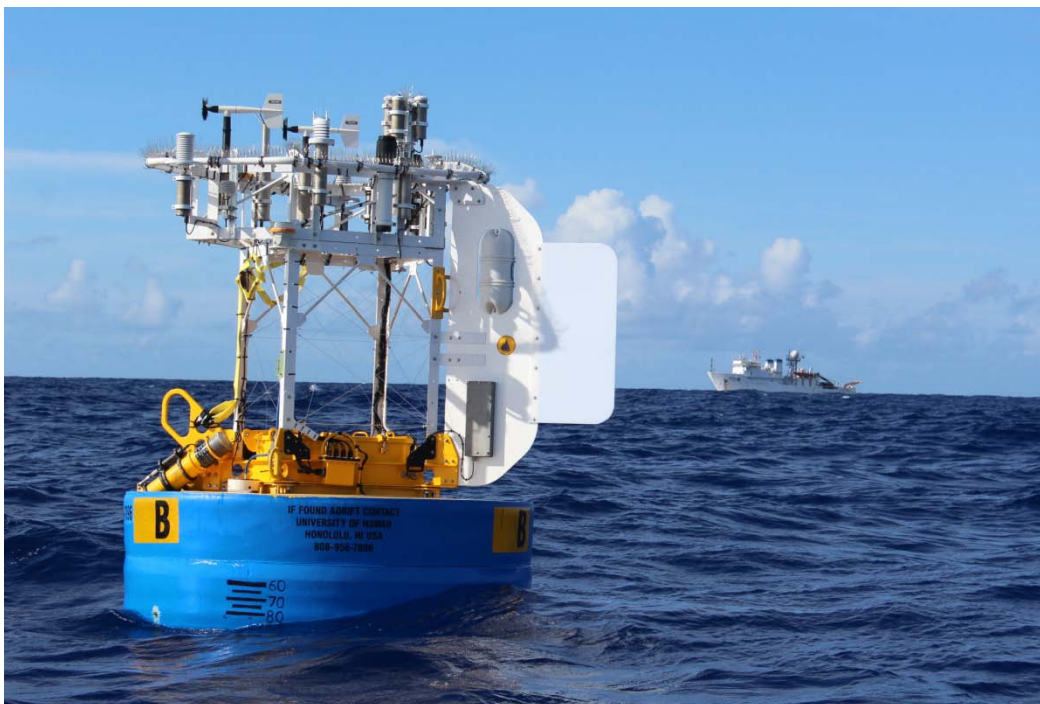


Hydrographic Observations
at the
Woods Hole Oceanographic Institution
Hawaii Ocean Time-series Site:
2013 – 2014
Data Report #10

Fernando Santiago-Mandujano, Daniel McCoy, R. Walter Deppe, Albert
Plueddemann, Robert Weller, Roger Lukas, Jeffrey Snyder, Sean Whelan and
Nan Galbraith

September, 2016



SCHOOL OF OCEAN AND EARTH
SCIENCE AND TECHNOLOGY
UNIVERSITY OF HAWAII AT HONOLULU

SOEST Publication no. 9821

Acknowledgments

Many people participated in the WHOTS mooring deployment/recovery cruises. They are listed in Tables 2.1 and 2.4. We gratefully acknowledge their contributions and support. Thanks are due to all the personnel of the Upper Ocean Processes Group (UOP) at WHOI who prepared the WHOTS buoy's instrumentation and mooring; to Cameron Fumar, Ethan Roth, Jennifer George, Branden Nakahara, Thanh-Van Tran, Kelly Lance, and Ryan Tabata, for their technical assistance with the moored and shipboard instrumentation; to Kellie Terada for her excellent project support, and to Joseph Gum for his shore-based support. We gratefully acknowledge the support from the colleagues at Sea-Bird for helping us maintain the quality of the CTD data. We would also like to thank the captains and crew of the NOAA Ship *Hi'ialakai* for their efforts. The WHOTS Ocean Reference Station mooring is funded by the National Oceanic and Atmospheric Administration (NOAA) through the Cooperative Institute for Climate and Ocean Research (CICOR) under Grant No. NA09OAR4320129 to the Woods Hole Oceanographic Institution. Support for preparation and processing of subsurface instrumentation at WHOI is via a subcontract from the UH NSF project (OCE - 1260164).

Table of Contents

1.	Introduction.....	1
2.	Description of the WHOTS-10 Mooring Cruises	3
A.	WHOTS-10 Cruise: WHOTS-10 Mooring Deployment	3
B.	WHOTS-11 Cruise: WHOTS-10 Mooring Recovery.....	5
3.	Description of WHOTS-10 Mooring.....	7
4.	WHOTS-10 and -11 cruise shipboard observations	10
A.	Conductivity, Temperature and Depth (CTD) profiling.....	10
1.	Data acquisition and processing.....	11
2.	CTD sensor calibration and corrections.....	11
Pressure	11	
Temperature/Conductivity	12	
Dissolved Oxygen.....	12	
B.	Water sampling and analysis	12
1.	Salinity	12
C.	Thermosalinograph data acquisition and processing	13
1.	WHOTS-10 Cruise.....	13
Temperature Calibration	14	
Nominal Conductivity Calibration.....	14	
Data Processing.....	14	
Bottle Salinity and CTD Salinity Comparisons	15	
CTD Temperature Comparisons	15	
2.	WHOTS-11 Cruise.....	16
Temperature Calibration	16	
Nominal Conductivity Calibration.....	16	
Data Processing.....	16	
Bottle Salinity and CTD Salinity Comparisons	17	
CTD Temperature Comparisons	17	
D.	Shipboard ADCP	18
1.	WHOTS-10 Deployment Cruise.....	18
2.	WHOTS-11 Deployment Cruise.....	18
5.	Moored Instrument Observations	19
A.	MicroCAT/SeaCAT data processing procedures.....	19
1.	Internal Clock Check and Missing Samples	20
2.	Pressure Drift Correction and Pressure Variability	20
3.	Temperature Sensor Stability.....	21
Comparisons with VMCM and ADCP temperature sensors	24	
4.	Conductivity Calibration.....	29
B.	Acoustic Doppler Current Profiler.....	39
1.	Compass Calibrations	39
2.	ADCP Configurations.....	42
3.	ADCP data processing procedures.....	43
C.	Vector Measuring Current Meter (VMCM)	53
D.	Global Positioning System Receiver and ARGOS Positions	58
E.	MAVS Acoustic Velocity Sensor	61
6.	Results.....	64

A.	CTD Profiling Data.....	66
B.	Thermosalinograph data.....	77
C.	MicroCAT/SeaCAT data	82
D.	Moored ADCP data.....	98
E.	Moored and Shipboard ADCP comparisons.....	109
F.	Next Generation Vector Measuring Current Meter data (VMCM)	129
G.	GPS data.....	130
H.	Mooring Motion.....	131
7.	References.....	133
8.	Appendices.....	135
A.	Appendix 1: WHOTS-10 300 kHz ADCP Configuration	135
B.	Appendix 2: WHOTS-10 600 kHz ADCP Configuration	136
C.	Appendix 3: WHOTS-10 VMCM report.....	137

1. Introduction

In 2003, Robert Weller (Woods Hole Oceanographic Institution [WHOI]), Albert Plueddemann (WHOI) and Roger Lukas (University of Hawaii [UH]) proposed to establish a long-term surface mooring at the Hawaii Ocean Time-series (HOT) Station ALOHA (22°45'N, 158°W) to provide sustained, high-quality air-sea fluxes and the associated upper ocean response as a coordinated part of the HOT program, and as an element of the global array of ocean reference stations supported by the National Oceanic and Atmospheric Administration's (NOAA) Office of Climate Observation.

With support from NOAA and the National Science Foundation (NSF), the WHOI HOT Site (WHOTS) surface mooring has been maintained at Station ALOHA since August 2004. The objective of this project is to provide long-term, high-quality air-sea fluxes as a coordinated part of the HOT program and contribute to the goals of observing heat, fresh water and chemical fluxes at a site representative of the oligotrophic North Pacific Ocean. The approach is to maintain a surface mooring outfitted for meteorological and oceanographic measurements at a site near Station ALOHA by successive mooring turnarounds. These observations are being used to investigate air-sea interaction processes related to climate variability and change.

The original mooring system is described in the mooring deployment/recovery cruise reports (Plueddemann et al., 2006; Whelan et al., 2007). Briefly, a Surlyn foam surface buoy is equipped with meteorological instrumentation including two complete Air-Sea Interaction Meteorological (ASIMET) systems (Hosom et al. (1995), Colbo and Weller (2009)), measuring air and sea surface temperatures, relative humidity, barometric pressure, wind speed and direction, incoming shortwave and longwave radiation, and precipitation. Complete surface meteorological measurements are recorded every minute, as required to compute air-sea fluxes of heat, freshwater and momentum. Each ASIMET system also transmits hourly averages of the surface meteorological variables via the Argos satellite system and via iridium. The mooring line is instrumented in order to collect time series of upper ocean temperatures, salinities and velocities with the surface forcing record. This includes vector measuring current meters, conductivity, salinity and temperature recorders, and two Acoustic Doppler current profilers (ADCPs). See the WHOTS-10 mooring diagram in Figure 1-1.

The subsurface instrumentation is located vertically to resolve the temporal variations of shear and stratification in the upper pycnocline to support study of mixed layer entrainment. Experience with moored profiler measurements near Hawaii suggests that Richardson number estimates over 10 m scales are adequate. Salinity is clearly important to the stratification, as salt-stratified barrier layers are observed at HOT and in the region (Kara et al., 2000), so we use Sea-Bird MicroCATs with vertical separation ranging from 5-20 m to measure temperature and salinity. We use an RDI ADCP to obtain current profiles across the entrainment zone and another in the mixed layer. Both ADCPs are in an upward-looking configuration, one is at 126 m, using 4 m bins, and the other is a 47.5 m using 2 m bins. To provide near-surface velocity (where the ADCP estimates are less reliable) we deploy two Vector Measuring Current Meters (VMCMs). The nominal mooring design is a balance between resolving extremes versus typical annual cycling of the mixed layer (see WHOTS Data Report 1-2, Santiago-Mandujano et al., 2007). A

pair of SeaCATs have been included near the bottom of the mooring since the WHOTS-9 deployment (June 2012) to measure the abyssal temperature and salinity.

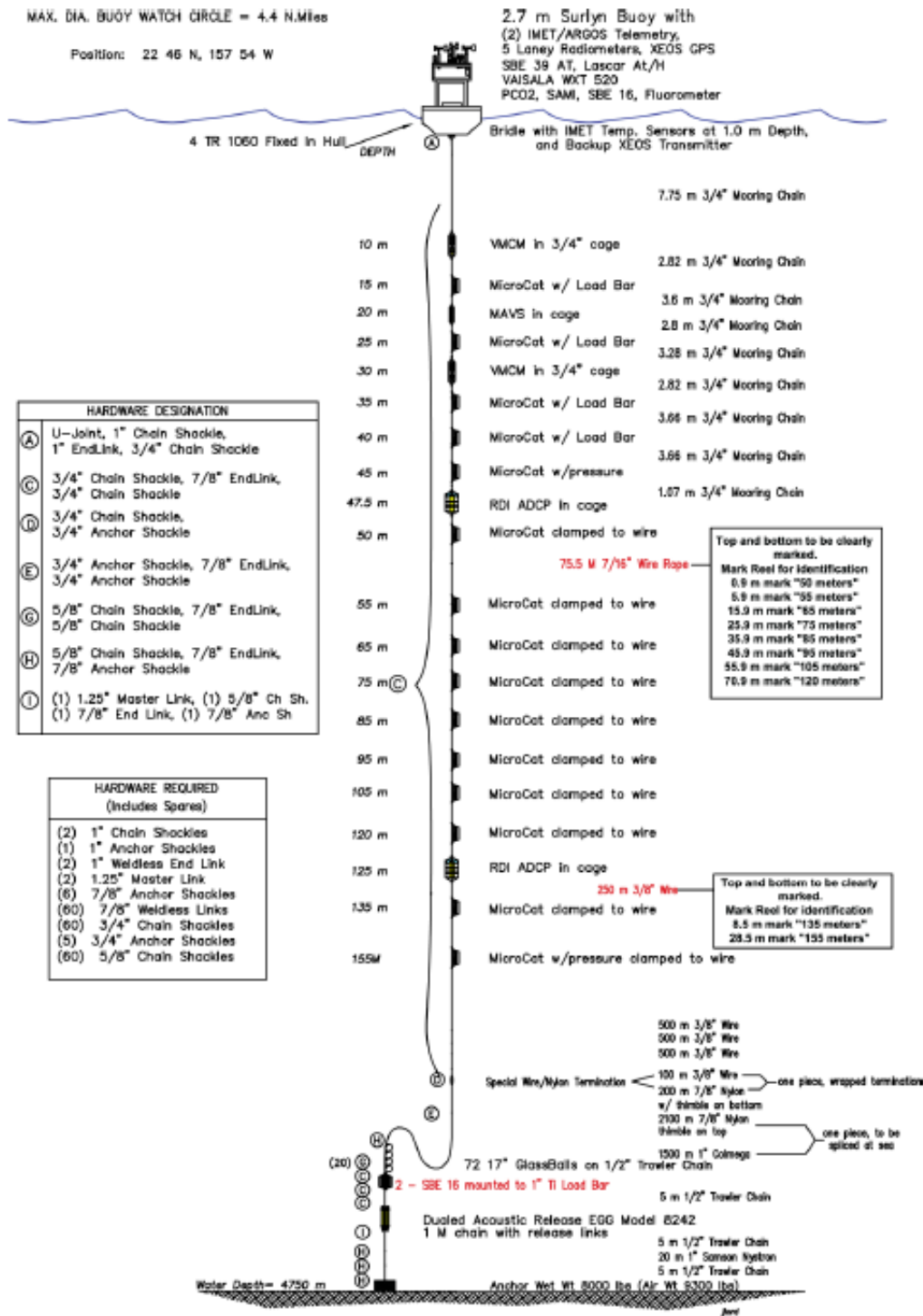


Figure 1-1. WHOTS-10 mooring design.

The tenth WHOTS mooring (WHOTS-10 mooring) was deployed in July 2013 during an 8-day cruise (WHOTS-10 cruise), and it was recovered in July 2014 during a 9-day cruise (WHOTS-11 cruise); both cruises aboard the NOAA Ship *Hi'ialakai*. An eleventh mooring (WHOTS-11 mooring) was deployed during the WHOTS-11 cruise; to be recovered in July 2015.

This report documents and describes the oceanographic observations made on the tenth WHOTS mooring during a period of nearly one year, and from shipboard during the two cruises when the mooring was deployed and recovered. Sections 2 and 3, respectively, include a detailed description of the cruises and the mooring. Sampling and processing procedures of the hydrographic casts, thermosalinograph, and shipboard ADCP data collected during cruises are in Section 4. Section 5 includes the processing procedures for the data collected by the moored instruments: SeaCATs, MicroCATs, VMCMs, and moored ADCP. Plots of the resulting data and a preliminary analysis are included in Section 6.

2. Description of the WHOTS-10 Mooring Cruises

A. WHOTS-10 Cruise: WHOTS-10 Mooring Deployment

The Woods Hole Oceanographic Institution Upper Ocean Processes Group (WHOI/UOP), with the assistance of the UH group conducted the tenth deployment of the WHOTS mooring on board the NOAA Ship *Hi'ialakai* during the WHOTS-10 cruise between 9 and 16 July 2013. The WHOTS-10 mooring was deployed at HOT Station 52 on 11 July 2013 at 04:26 UTC at 22° 40.12'N, 157° 57.01'W. The scientific personnel that participated during the cruise are listed in Table 2-1.

Table 2-1. Scientific personnel on Ship *Hi'ialakai* during the WHOTS-10 deployment cruise.

Cruise	Name	Title or function	Affiliation
WHOTS-10	Plueddeman, Albert	Chief Scientist	WHOI
	Lukas, Roger	Professor/PI	UH
	Whelan, Sean	Senior Engineering Assistant	WHOI
	Pietro, Ben	Engineering Assistant	WHOI
	Snyder, Jeffrey	Marine Electronic's Technician	UH
	Fumar, Cameron	Research Associate	UH
	McCoy, Daniel	Research Associate	UH
	Roth, Ethan	Marine Research Engineer	UH
	George, Jennifer	Marine Research Technician	UH
	Nakahara, Branden	Marine Research Technician	UH
	Wolfe, Dan	Scientist	NOAA/CIRES

The shipboard oceanographic observations during the cruise were conducted by the UH group.

A Sea-Bird CTD (conductivity, temperature and depth) system was used to measure T, S, and O₂ profiles during ten CTD casts. The time, location, and maximum CTD pressure for each of the profiles are listed in Table 2-2. One cast was conducted to 1020 dbar at a test site near Oahu. Five CTD casts were made at Station 52 near the WHOTS-10 mooring for comparison with subsurface instruments after the WHOTS-10 mooring deployment; each cast was to 500 dbar. Five CTD casts were conducted at HOT Station 50 near the WHOTS-9 mooring for comparison with subsurface instruments before its recovery; each cast was to 500 dbar. These casts were sited approximately 200 to 500 m from the buoys and consisted of 4 yo-yo cycles between 10 dbar and 200 dbar and then to 500 dbar (5th yo-yo cycle of each cast). Four salinity samples were taken from each 500 dbar cast to calibrate the conductivity sensors used for the CTD profiling.

Table 2-2. CTD stations occupied during the WHOTS-10 cruise

Station/cast	Date	Time (GMT)	Location (using NMEA data)	Maximum pressure (dbar)
TEST	7/10/13	01:03	21° 28.49' N, 158° 20.97' W	1026
52 / 1	7/11/13	16:11	22° 40.88' N, 157° 58.70' W	518
52 / 2	7/11/13	19:56	22° 41.04' N, 157° 58.67' W	502
52 / 3	7/11/13	23:55	22° 41.12' N, 157° 58.75' W	506
52 / 4	7/12/13	04:05	22° 41.24' N, 157° 58.55' W	506
52 / 5	7/12/13	07:59	22° 41.03' N, 157° 58.35' W	506
50 / 1	7/13/13	15:58	22° 47.43' N, 157° 54.09' W	502
50 / 2	7/13/13	20:02	22° 47.63' N, 157° 54.38' W	504
50 / 3	7/13/13	23:58	22° 47.79' N, 157° 53.69' W	504
50 / 4	7/14/13	04:02	22° 47.79' N, 157° 53.50' W	504
50 / 5	7/14/13	07:51	22° 47.84' N, 157° 53.60' W	504

In addition, continuous acoustic Doppler current profiler (ADCP) and near surface thermosalinograph data were obtained while underway.

The Ship *Hi'ialakai* was equipped with an RD Instruments Ocean Surveyor 75 kHz ADCP, set to function in broadband and narrowband configurations. Configurations for each system are shown in Table 2-3. The ADCP used input from a S.G. Brown gyrometer and a Furuno GP 90 GPS receiver to establish the heading and attitude of the ship while an Applanix POSMV4 system archived attitude data for use in post-processing.

A complete description of these operations is available in the WHOTS-10 cruise report (Plueddemann *et al.*, 2014).

Table 2-3. Configuration of the Ocean Surveyor 75kHz ADCP on board the Ship *Hi'ialakai* during the WHOTS-10 cruise.

	OS75BB	OS75NB
Sample interval (s)	900	900
Number of bins	80	60
Bin Length (m)	8	16
Pulse Length (m)	8	16
Transducer depth (m)	5	5
Blanking length (m)	16	24

Near-surface temperature and salinity data during the WHOTS-10 cruise were acquired through the use of a thermosalinograph (TSG) system aboard Ship *Hi'ialakai*. The system was comprised of a Sea-Bird model SBE-21 thermosalinograph with internal temperature and conductivity sensors sampling water from the ship's flow through system, and an SBE-38 external temperature sensor located near the intake. These instruments were set to record data every 60 seconds. Ship *Hi'ialakai* has a thermosalinograph intake depth of 2 m. The data were acquired continuously during the WHOTS-10 deployment cruise, with salt calibration samples taken roughly three times per day from an outlet in the flow through system located less than 0.5 m from the TSG.

B. WHOTS-11 Cruise: WHOTS-10 Mooring Recovery

The WHOI/UOP Group conducted the mooring turnaround operations during the WHOTS-11 cruise between 15 and 23 July 2014. The WHOTS-10 mooring was recovered, and the WHOTS-11 mooring was deployed at Station 50 on 17 July 2014 at 22 45.98 'N, 157 53.96 'W.

The scientific personnel that participated during the cruise are listed in Table 2-4.

Table 2-4. Scientific personnel on Ship *Hi'ialakai* during the WHOTS-11 cruise (WHOTS-10 mooring recovery).

Cruise	Name	Title or function	Affiliation
WHOTS-11	Plueddeman, Albert	Chief Scientist	WHOI
	Whelan, Sean	Senior Engineering Assistant	WHOI
	Pietro, Ben	Engineering Assistant	WHOI
	Snyder, Jeffrey	Marine Electronic's Technician	UH
	Santiago-Mandujano, Fernando	Research Associate	UH
	McCoy, Daniel	Research Associate	UH
	Tabata, Ryan	Marine Research Technician	UH
	Nakahara, Branden	Marine Research Technician	UH
	Tran, Thanh-Van	Undergraduate Student	UH

Cruise	Name	Title or function	Affiliation
	Lance, Kelly	Undergraduate Student	UH
	Blomquist, Byron	Researcher	NOAA

The shipboard oceanographic observations during the cruise were conducted by the UH group. A complete description of these operations is available in the WHOTS-11 cruise report (Plueddemann *et al.*, 2015).

A Sea-Bird CTD system was used to measure T, S, and O₂ profiles during ten CTD casts. The time, location, and maximum CTD pressure for each of the profiles are listed in Table 2-5. One cast was conducted at a test site near Oahu to 1020 dbar. Five CTD casts were made at station 50 near the WHOTS-11 mooring for comparison with subsurface instruments after the WHOTS-11 mooring deployment; each cast was to 200 dbar. Five CTD casts were conducted at station 52 near the WHOTS-10 mooring for comparison with subsurface instruments before its recovery; each cast was to 200 dbar. Following these casts, one more CTD cast to 200 dbar was made at station 50 near the WHOTS-11 mooring. These casts were sited approximately 200 to 500 m from the buoys and consisted of 5 yo-yo cycles between 10 dbar and 200 dbar. Four salinity samples were taken from each 200 dbar cast to calibrate the conductivity sensors used for the CTD profiling. One final CTD cast to 1000 dbar was conducted at Station ALOHA and six salinity samples were taken.

Table 2-5. CTD stations occupied during the WHOTS-11 cruise (WHOTS-10 mooring recovery).

Station/cast	Date	Time (UTC)	Location (using NMEA data)	Maximum pressure (dbar)
1 / 1	7/16/14	00:41	21° 28.04' N, 158° 21.07' W	1024
50 / 1	7/17/14	16:10	22° 46.38' N, 157° 57.37' W	945
50 / 2	7/17/14	19:54	22° 45.79' N, 157° 56.15' W	206
50 / 3	7/18/14	00:05	22° 46.77' N, 157° 55.64' W	206
50 / 4	7/18/14	04:28	22° 46.40' N, 157° 55.86' W	201
50 / 5	7/18/14	08:11	22° 46.50' N, 157° 55.87' W	203
52 / 1	7/18/14	16:09	22° 40.42' N, 157° 58.79' W	205
52 / 2	7/18/14	19:57	22° 40.72' N, 157° 58.78' W	206
52 / 3	7/18/14	23:49	22° 40.89' N, 157° 58.56' W	204
52 / 4	7/19/14	03:53	22° 41.04' N, 157° 58.74' W	205
52 / 5	7/19/14	07:45	22° 40.99' N, 157° 58.74' W	208
50 / 6	7/22/14	16:02	22° 47.07' N, 157° 55.65' W	204
2 / 1	7/23/14	01:59	22° 44.93' N, 157° 59.55' W	1001

In addition, continuous acoustic Doppler current profiler (ADCP) and near surface thermosalinograph data were obtained while underway.

The Ship *Hi'ialakai* was equipped with an RD Instruments Ocean Surveyor 75 kHz ADCP, set to function in broadband and narrowband configurations. Broadband data was unavailable for this cruise. The configuration information is shown in Table 2-6. The ADCP used input from a S.G. Brown gyrometer and a Furuno GP 90 GPS receiver to establish the heading and attitude of the ship while an Applanix POSMV4 system archived attitude data for use in post-processing.

Table 2-6. Configuration of the Ocean Surveyor 75kHz ADCP on board the Ship *Hi'ialakai* during the WHOTS-11 cruise.

	OS75NB
Sample interval (s)	300
Number of bins	60
Bin Length (m)	16
Pulse Length (m)	16
Transducer depth (m)	5
Blanking length (m)	8

Near-surface temperature and salinity data during the WHOTS-11 cruise were acquired through the use of a thermosalinograph (TSG) system aboard Ship *Hi'ialakai*. The system was comprised of a Sea-Bird model SBE-21 thermosalinograph with internal temperature and conductivity sensors sampling water from the ship's flow through system, and an SBE-38 external temperature sensor located near the intake. These instruments were set to record data every 60 seconds. Ship *Hi'ialakai* has a thermosalinograph intake depth of 2 m. The data were acquired continuously during the WHOTS-11 deployment cruise, with salt calibration samples taken roughly three times per day from an outlet in the flow through system located less than 0.5 m from the TSG.

3. Description of WHOTS-10 Mooring

The WHOTS-10 mooring, deployed on 10 July 2013 from NOAA's Ship *Hi'ialakai*, was outfitted with two complete sets (L08 and L15) of ASIMET sensors on the buoy and underneath, and subsurface instruments from 10 to 155 m depth (Figure 1-1). The WHOTS-10 recovery on 20-21 July 2014 resulted in about 375 days on station.

The buoy tower also contains a radar reflector, two marine lanterns, and two independent Argos satellite transmission systems that provide continuous monitoring of buoy position. A Xeos Melo Global Positioning System (GPS) receiver, a SBE-39 temperature sensor adapted to measure air temperature and a Vaisala WXT-520 multi-variable (temperature, humidity, pressure, wind and precipitation) were also mounted on the tower. A fourth positioning system (SiS Argos transmitter) was mounted beneath the hull. Several other instruments were mounted on the buoy. A pCO₂ system, a pumped SBE-16 CTD and a SAMI-2 pH sensor were mounted to

the underside of the buoy. The SHB-16 hosted turbidity and dissolved oxygen sensors. Five radiometers and a chlorophyll fluorometer were also mounted in one of the buoy access tubes.

Four internally-logging RBR TR-1060 temperature sensors (SN 14813, 14879, 14875, and 19714) and two SBE-37 MicroCATs (SN 1834 and 1841) were bolted to the underside of the buoy hull measuring sea surface temperature (SST) and salinity. The RBRs measured once every 60 sec between 82-96 cm below the surface, and the MicroCATs measuring every 300 sec were at 1.51 m.

Instrumentation provided by UH for the WHOTS-10 mooring included 15 SBE-37 Microcats, an RDI 300 kHz Workhorse ADCP, an RDI 600 kHz Workhorse ADCP (this instrument, SN 1825 is owned by WHOI, but maintained by UH), and a Nobska MAVS acoustic velocity sensor. The Microcats all measured temperature and conductivity, with 5 also measuring pressure. WHOI provided two Vector Measuring Current Meters (VMCMs), and two Seacats (SBE-16) installed near the bottom of the mooring.

Table 3-1 provides a listing of the WHOTS-10 subsurface instrumentation at their nominal depths on the mooring, along with serial numbers, sampling rates and other pertinent information. A cold water spike was induced to the UH Microcats before deployment and after recovery by placing an ice pack in contact with their temperature sensor to check for any drift in their internal clock.

The RDI 300 kHz Workhorse Sentinel ADCP, SN 4891, with an additional external battery pack, was deployed at 125 m with transducers facing upwards. The instrument was set to ping at 4-second intervals for 160 seconds every 10 minutes. This burst sampling was designed to minimize aliasing by occasional large ocean swell orbital motions. Bin size was set for 4 m. This instrument also measured temperature.

The RDI 600 kHz Workhorse Sentinel ADCP, SN 1825, with an additional external battery pack, was deployed at 47.5 m with transducers facing upwards. The instrument was set to ping at 2-second intervals for 160 seconds every 10 minutes. This burst sampling was designed to minimize aliasing by occasional large ocean swell orbital motions. Bin size was set for 2 m. This instrument also measured temperature. A spike was induced to both ADCPs before deployment and after recovery by gently rubbing each of the transducers to check for any drift in their internal clocks.

The two VMCMs, SN 016 and 019 were deployed at 10 m and 30 m depth respectively. The instruments were prepared for deployment by the WHOI/UOP group and set to sample at 1-minute intervals. These instruments also measured temperature.

A Nobska MAVS SN 10260 acoustic velocity sensor was deployed a 20 m in a downward orientation. The instrument was set to ping at 2-second intervals for 160 seconds every 30 minutes. This burst sampling was designed to minimize aliasing by occasional large ocean swell orbital motions. Data return from all transducers on the MAVS was good until January 2014, when transducer 'A' began to show questionable data. Transducers 'C' and 'D' failed after April 2014.

Table 3-1. WHOTS-10 mooring subsurface instrument deployment information. All times are in UTC.

SN:	Instrument	Depth	Pressure SN	Sample Interval (sec)	Start Logging Data(UTC)		Spike begin (UTC)		Spike end (UTC)		Time in Water (UTC)	
16	VMCM	10	N/A	60	7/3/2013	18:52:30	N/A	N/A	N/A	N/A	07/10/13	18:33
6893	Microcat	15	N/A	60	07/06/13	0:00:00	07/08/13	19:30:30	07/08/13	20:00:30	07/10/13	18:33
10260	MAVS	20	N/A	1800	07/06/13	0:00:00	07/08/13	21:30:30	07/08/13	22:35:00	07/10/13	18:27
6894	Microcat	25	N/A	60	07/06/13	0:00:00	07/08/13	19:30:30	07/08/13	20:00:30	07/10/13	18:14
19	VMCM	30	N/A	60	7/3/2013	18:54:30	N/A	N/A	N/A	N/A	07/10/13	18:08
6895	Microcat	35	N/A	60	07/06/13	0:00:00	07/08/13	19:30:30	07/08/13	20:00:30	07/10/13	18:07
6896	Microcat	40	N/A	60	07/06/13	0:00:00	07/08/13	19:30:30	07/08/13	20:00:30	07/10/13	18:03
6887	Microcat	45	2651319	75	07/06/13	0:00:00	07/08/13	19:30:30	07/08/13	20:00:30	07/10/13	17:58
1825	600 kHz ADCP	47.5	N/A	600	07/06/13	0:00:00	07/06/13	22:10:10	07/06/13	22:10:40	07/10/13	19:22
6897	Microcat	50	N/A	60	07/06/13	0:00:00	07/08/13	19:30:30	07/08/13	20:00:30	07/10/13	19:22
6898	Microcat	55	N/A	60	07/06/13	0:00:00	07/08/13	19:30:30	07/08/13	20:00:30	07/10/13	19:23
6899	Microcat	65	N/A	60	07/06/13	0:00:00	07/08/13	19:30:30	07/08/13	20:00:30	07/10/13	19:24
3618	Microcat	75	N/A	180	07/06/13	0:00:00	07/08/13	19:30:30	07/08/13	20:00:30	07/10/13	19:25
6888	Microcat	85	3418742	75	07/06/13	0:00:00	07/08/13	19:30:30	07/08/13	20:00:30	07/10/13	19:27
3617	Microcat	95	N/A	180	07/06/13	0:00:00	07/08/13	19:30:30	07/08/13	20:00:30	07/10/13	19:27
6889	Microcat	105	2651321	75	07/06/13	0:00:00	07/08/13	19:30:30	07/08/13	20:00:30	07/10/13	19:28
6890	Microcat	120	2651322	75	07/06/13	0:00:00	07/08/13	19:30:30	07/08/13	20:00:30	07/10/13	19:29
4891	300 kHz ADCP	125	N/A	600	07/06/13	0:00:00	07/08/13	22:00:10	07/08/13	22:00:40	07/10/13	19:34
3634	Microcat	135	N/A	180	07/06/13	0:00:00	07/08/13	19:30:30	07/08/13	20:00:30	07/10/13	19:35
6891	Microcat	155	2651323	75	07/06/13	0:00:00	07/08/13	19:30:30	07/08/13	20:00:30	07/10/13	19:36
1882	SBE 16	36m off bottom	N/A	1800	7/3/2013	18:30:00	NA		7/21/4014	22:40:00	07/11/13	3:24
2325	SBE 16	36m off bottom	N/A	1800	7/3/2013	18:30:00	NA		7/21/2014	22:40:00	07/11/13	3:24

All WHOTS-10 instruments were successfully recovered; recovery information for the C-T instruments is shown in Table 3-2. All MicroCATs were in good condition after recovery. The data were downloaded on board ship, and all instruments returned full data records, except for SN 3634 which had a 20 minute gap on October 20, 2013, 21:21Z. The data from this instrument were downloaded again in the shore lab after the cruise and the missing data were recovered. Both deep SeaCATs were missing their anti-foulant plugs on recovery. Table 3-2 has an initial evaluation of the data quality; more details are in Section 5A.

Table 3-2. WHOTS-10 MicroCAT Recovery Information. All times stated are in UTC.

Depth (m)	Sea-Bird Serial #	Time out of water	Time of Spike	Time Logging Stopped	Samples Logged	Data Quality
15	37SM31486-6893	07/21/2014 05:14	07/21/2014 07:41:00	07/22/2014 05:51:30	548,992	good
25	37SM31486-6894	07/21/2014 05:21	07/21/2014 07:41:00	07/21/2014 08:48:30	547,729	good
35	37SM31486-6895	07/21/2014 05:25	07/21/2014 07:41:00	07/21/2014 08:33:00	547,714	good
40	37SM31486-6896	07/21/2014 05:28	07/21/2014 07:41:00	07/21/2014 08:44:30	547,725	good
45	37SM31486-6887	07/21/2014 05:28	07/21/2014 07:41:00	07/21/2014 08:41:00	438,177	good
50	37SM31486-6897	07/21/2014 03:22	07/21/2014 07:41:00	07/21/2014 08:07:00	547,687	good
55	37SM31486-6898	07/21/2014 03:21	07/21/2014 07:41:00	07/21/2014 08:11:30	547,693	good
65	37SM31486-6899	07/21/2014 03:20	07/21/2014 07:41:00	07/21/2014 08:15:00	547,696	good

75	37SM31486-3618	07/21/2014 03:19	07/21/2014 07:41:00	07/22/2014 05:29:30	182,990	good
85	37SM31486-6888	07/21/2014 03:18	07/21/2014 07:41:00	07/21/2014 08:19:00	438,160	good
95	37SM31486-3617	07/21/2014 03:17	07/21/2014 07:41:00	07/22/2014 05:36:00	182,992	good
105	37SM31486-6889	07/21/2014 03:16	07/21/2014 07:41:00	07/22/2014 05:43:00	439,187	good
120	37SM31486-6890	07/21/2014 03:15	07/21/2014 07:41:00	07/22/2014 05:47:00	439,190	good
135	37SM31486-3634	07/21/2014 03:11	07/21/2014 07:41:00	07/22/2014 05:33:00	182,991	20 min gap (recovered after a second data download)
155	37SM31486-6891	07/21/2014 03:08	07/21/2014 07:41:00	07/22/2014 05:26:00	439,173	good
36 mab	SBE-16-04-1882	07/20/2014 20:53	07/21/2014 22:40:00	07/22/2014 02:04:00	18,401	Antifoulant plug missing. Conductivity offset lasting one month
36 mab	SBE-16-04-2325	07/20/2014 20:53	07/21/2014 22:40:00	07/22/2014 02:04:00	18,401	Antifoulant plug missing. Conductivity drift

The data from the upward-looking 300 kHz ADCP at 125 m was good; the instrument was pinging upon recovery. The total number of ensemble records was 54, 892. The first ensemble was at 7/06/2013 00:00:00Z, and the last was at 7/22/2014 04:19:59Z. The after recovery spike was from 19:02:00 to 19:03:30 on 7/21/2014. There were no obviously questionable data from this ADCP apart from near-surface artifacts; more details are in Section 5B.

The data from the upward-looking 600 kHz ADCP at 47.5 m was also good; the instrument was pinging upon recovery. The total number of ensemble records was 54,893. The first ensemble was at 7/06/2013 00:00:00Z, and the last was at 7/22/2014 04:30:00Z. The after recovery spike was from 20:17:30 to 20:18:30 on 7/21/2014. There were no initial questionable data from this ADCP apart from near-surface artifacts; more details are in Section 5B.

4. WHOTS-10 and -11 cruise shipboard observations

The hydrographic profile observations made during the WHOTS cruises were obtained with a Sea-Bird CTD package with dual temperature, salinity and oxygen sensors. This CTD was installed on a rosette-sampler with 5 L Niskin bottles for calibration water samples. In addition, the *Hi'ialakai* came equipped with a thermosalinograph system which provided a continuous depiction of temperature and salinity of the near-surface layer. Horizontal currents over the depth range of 30-1000 m were measured from the shipboard 75 kHz Ocean Surveyor (OS75) ADCP (narrowband) with a vertical resolution of 16m for the WHOTS-10 and WHOTS-11 cruises. Broadband mode for the OS75 was available in addition for WHOTS-10 cruise, providing additional current data over the range of 20-650 m with a vertical resolution of 8m. Broadband mode was unavailable for the WHOTS-11 cruise due to problem with one of the ADCP cables.

A. Conductivity, Temperature and Depth (CTD) profiling

Continuous measurements of temperature, conductivity, dissolved oxygen and pressure were made with the UH Sea-Bird SBE-9/11Plus CTD underwater unit #09P43777-0850 (referred to as

#0850) during the WHOTS-10 and WHOTS-11 cruises. The CTD was equipped with an internal Digiquartz pressure sensor and pairs of external temperature, conductivity, and oxygen sensors.

Each of the temperature-conductivity sensor pairs used a Sea-Bird TC duct which circulated seawater through independent pump and plumbing installations. The CTD configuration also included two oxygen sensors, installed in the plumbing for each sensor set. In both cruises, the CTD was mounted in a vertical position in the lower part of a rosette sampler, with the sensors' water intakes located at the bottom of the 12-place rosette.

The package was deployed on a conducting cable, which allowed for real-time data acquisition and display. The deployment procedure consisted in lowering the package to 10-15 dbar and waiting until the CTD pumps started operating. The CTD was then raised until the sensors were close to the surface to begin the CTD cast. The time and position of each cast was obtained via a GPS connection to the CTD deck box. Six Niskin bottles were used on the rosette. Four salinity samples were taken on each cast for calibration of the conductivity sensors.

1. Data acquisition and processing.

CTD data were acquired at the instrument's highest sampling rate of 24 samples per second. Digital data were stored on a laptop computer and, for redundancy, the analog signal was recorded on VHS video tapes. Backups of CTD data were made onto USB storage cards.

The raw CTD data were quality controlled and screened for spikes as described in the WHOTS Data Report 1 (Santiago-Mandujano et al., 2007). Data alignment, averaging, correction and reporting were done as described in Tupas *et al.* (1993). Spikes in the data occur when the CTD samples the disturbed water of its wake. Therefore, samples from the downcast were rejected when the CTD was moving upward or when its acceleration exceeded 0.5 m s^{-2} in magnitude. The data were subsequently averaged into 2-dbar pressure bins after calibrating the CTD conductivity with the bottle salinities.

The data were additionally screened by comparing the T-C sensor pairs. These differences permitted identification of problems with the sensors. The data from only one T-C pair, whichever was deemed most reliable, is reported here. Only data from the downcast are reported, as upcast data are contaminated by rosette wake effects.

Temperature is reported in the ITS-90 scale. Salinity and all derived units were calculated using the UNESCO (1981) routines; salinity is reported in the practical salinity scale (PSS-78). Oxygen is reported in $\mu\text{mol kg}^{-1}$.

2. CTD sensor calibration and corrections

Pressure

The pressure calibration strategy for CTD pressure transducer SN 101430 used during WHOTS-10 and WHOTS-11 cruises employed a high-quality quartz pressure transducer as a

transfer standard. Periodic recalibrations of this lab standard were performed with a primary pressure standard. The only corrections applied to the CTD pressures were a constant offset determined at the time that the CTD first enters the water on each cast. In addition, a span correction determined from bench tests on the sensor against the transfer standard was applied. These procedures and corrections are thoroughly documented in the HOT-2013 and 2014 data reports (Fujieki, et al. 2016a, 2016b).

Temperature/Conductivity

Sea-Bird SBE-3-Plus temperature and SBE 4C conductivity transducers were used during WHOTS-10 and -11 cruises. The history and performance of these sensors have been monitored during HOT cruises, and calibrations and drift corrections applied during WHOTS cruises are thoroughly documented in the HOT-2013 and 2014 data reports (Fujieki, et al. 2016a, 2016b).

Dissolved Oxygen

Sea-Bird SBE-43 oxygen sensors were used during the WHOTS-10 and -11 cruises. Oxygen data from the WHOTS-10 cruise were calibrated using empirical calibration coefficients obtained during the HOT-253 cruise conducted on 24-28 June 2013, before the WHOTS-10 cruise, which used the same oxygen sensors. Similarly, the WHOTS-11 oxygen data were calibrated using calibration coefficients obtained during the HOT-264 cruise conducted on 29 June to 3 July 2014, before the WHOTS-11 cruise, which used the same oxygen sensors. Fujieki, et al. (2016a, 2016b) have details on these calibrations. The CTD empirical calibration was conducted using oxygen water samples and the procedure from Owens and Millard (1985). See Tupas et al. (1997) for details on these calibrations procedures.

B. Water sampling and analysis

1. Salinity

Salinity samples were collected by rosette sampler during CTD casts at selected depths during WHOTS-9 and -10, and sub-sampled in 250 ml glass bottles. The top of each bottle and thimble were thoroughly dried before being tightly capped to prevent water from being trapped between the cap or thimble and the bottle's mouth. It has been observed that residual water trapped in this way increases its salinity due to evaporation, and it can leak into the sample when the bottle is opened for measuring. Samples from each cruise were measured after the cruise in the laboratory at the UH using a Guildline Autosol 8400B (SN 70168). IAPSO¹ standard seawater samples were measured to standardize the Autosol, and samples from a large batch of "secondary standard" (substandard) seawater were measured after every 24-48 samples to detect drift in the Autosol. Standard deviations of the secondary standard measurements were less than ± 0.001 for WHOTS-10 and -11 cruises (Table 4-1).

¹ International Association for Physical Sciences of the Ocean

The substandard water was collected by rosette sampler from 1020 m at station ALOHA during HOT cruises and drained into a 50-liter Nalgene plastic carboy. In the laboratory, the water was then thoroughly mixed in a glass carboy for 20 minutes by manually shaking, rolling and tilting the carboy vigorously, after which a 2-inch protective layer of white oil was added on top to deter evaporation. The substandard water was allowed to stand for approximately three days before it was used, and was stored in the same temperature controlled room as the Autosal, protecting it from the light with black plastic bags to inhibit biological growth. Substandard seawater batches #55 and #57 were prepared on 19 July 2013, and 12 Mar 2014, respectively and used for WHOTS-10 and -11 samples respectively.

Salinity samples from the WHOTS-10 cruise were measured during the same session as the HOT-253 samples. Samples from WHOTS-11 cruise were measured during the same session as the HOT-264 samples. The substandard statistics in Table 4-1 include the substandard samples measured for the WHOTS-10 and WHOTS-11 samples .

Table 4-1. Precision of salinity measurements of secondary lab standards.

Cruise	Mean Salinity +/- SD	# Samples	Substandard Batch #	IAPSO Batch #
WHOTS-10 / HOT-253	34.4976 +/- 0.0001	19	55	P154
WHOTS-11 / HOT-264	34.4728 +/- 0.0001	25	57	P154

C. Thermosalinograph data acquisition and processing

1. WHOTS-10 Cruise

Near-surface temperature and salinity data for the WHOTS-10 cruise were acquired through the use of the thermosalinograph system aboard the Ship *Hi'ialakai* described above. The system included an SBE-21 (SN 3155) thermosalinograph sensor measuring conductivity and internal temperature; and an SBE-38 (SN 0215) external temperature sensor installed near the seawater intake.

Temperature data were acquired every 60 seconds for the duration of the cruise, but the conductivity sensor stopped recording data just prior to 16 July 2013. Salinity samples were taken periodically throughout the cruise for calibration from an outlet in the flowthrough system located less than 0.5 m from the SBE-21.

Although a SBE-38 external temperature sensor was installed, no data were available from this sensor as the data were not properly recorded during the cruise.

Temperature Calibration

Since the external temperature data from the SBE-38 sensor was not available, data from the SBE-21 internal temperature sensor (last calibrated at Sea-Bird on 18 November 2011) were used as a measure of the seawater temperature. However after applying an offset correction obtained by comparing to the data collected during CTD casts, these temperatures were found unreliable as the water was subject to heating and cooling as it passed through the ship. These data were flagged as uncalibrated.

Nominal Conductivity Calibration

Data from the SBE-21 conductivity and temperature sensors were used to calculate the intake seawater salinity. These sensors were last calibrated at Sea-Bird on 18 November 2011. All conductivity data from the thermosalinograph were nominally calibrated with coefficients from this calibration. However, all the final salinity data reported here were calibrated against bottle data as explained below.

Data Processing

Daily files containing navigation data recorded every 60 seconds were concatenated with the thermosalinograph data. The thermosalinograph data were then screened for gross errors, with upper and lower bounds of 18 °C and 35 °C for temperature and 3 Siemens m⁻¹ and 6 Siemens m⁻¹ for conductivity. There were three points outside the valid temperature range and no points outside the valid conductivity range.

A 5-point running median filter was used to detect one- or two-point temperature and conductivity glitches in the thermosalinograph data. Glitches in temperature and conductivity detected by the 5-point median filter were immediately replaced by the median. Threshold values of 0.3 °C for temperature and 0.1 Siemens m⁻¹ for conductivity were used for the median filter. After running the filter, there were 140 conductivity points replaced by the median. A 3-point triangular running mean filter was used to smooth the temperature and conductivity data after passing the glitch detection.

The thermosalinograph aboard the Ship *Hi'ialakai* was set to record data every 60 seconds, but occasionally, due to an error in the acquisition software rounding routine, a record is written at a longer interval. However, there were no timing errors observed.

Data were visually scanned to flag glitches probably caused by contamination due to the introduction of bubbles to the flowthrough system during transit or during rough conditions. Of a total of 9791 data points, 1391 conductivity data points were flagged as bad. These bad points mostly occurred between 10 July 2013 and 13 July 2013. Data quality improved after. Underway conductivity stopped recording data just prior to 16 July 2013. Therefore, the final 1076 data points for conductivity are not available and set as Not a Number (NaN).

Bottle Salinity and CTD Salinity Comparisons

The thermosalinograph salinity was calibrated by comparing it to bottle salinity samples drawn from a water intake next to the thermosalinograph every 8 hours throughout the cruise. Of the 21 bottles sampled, 5 were considered outliers, while the final 4 bottles were sampled after the system stopped collecting conductivity data. The remaining twelve salinity samples were analyzed as described in Section 0. The comparison was made in conductivity in order to eliminate the effects of temperature. The conductivity of the bottle sample was computed using the salinity of the bottle, thermosalinograph temperature and a pressure of 3.44 dbar, which includes the pressure of the flowthrough system's pump.

Salinity samples were drawn from the flowthrough system, located less than 0.5 m from the SBE-21 and consequently there should be virtually no delay between when the water passes through the thermosalinograph and it being sampled. A 90 second average centered on the sample draw time was chosen for processing purposes.

The CTD salinity data at 2 dbar from the 11 casts conducted during the cruise was used to compare with the thermosalinograph conductivity. Using the thermosalinograph temperature data and a pressure of 3.44 dbar the CTD conductivity was calculated for the 11 casts conducted while the thermosalinograph was running. One CTD cast (station 1 cast 1) was excluded from the processing as it was an obvious outlier. The SBE-21 conductivity sensor had a mean offset of 0.0071 Sm^{-1} with respect to the CTD data.

A cubic spline was fit to the time series of the differences between the bottle and thermosalinograph conductivity and a correction was obtained for the thermosalinograph conductivities. Salinity was calculated using these corrected conductivities, the thermosalinograph temperatures, and 6-dbar pressure. After correction, the mean difference between the bottle and thermosalinograph salinities was -0.0001 with a standard deviation of 0.0102 . The mean CTD - thermosalinograph difference was 0.0024 with a standard deviation of 0.0095 .

CTD Temperature Comparisons

There were 11 CTD casts conducted during the WHOTS-10 cruise. The 2 dbar CTD temperature data were used to compare with the thermosalinograph internal temperature. One CTD cast (station 1 cast 1) was excluded from the processing as it was an obvious outlier. No external temperature data were available post-cruise, despite a SBE-38 sensor being installed (see Sect. 4.C.2), therefore the internal temperature from the SBE-21 thermosalinograph is reported here as external temperature after adding an offset to match it to the CTD temperature data. The mean difference between the internal sensor and the CTD was $-0.1995 \text{ }^\circ\text{C}$, with a standard deviation of $\pm 0.0168 \text{ }^\circ\text{C}$. All the reported temperatures were flagged as uncalibrated.

2. WHOTS-11 Cruise

Near-surface temperature and salinity data for the WHOTS-11 cruise were acquired through the use of the thermosalinograph system aboard the Ship *Hi'ialakai* described above. The system included an SBE-21 (SN 3233) thermosalinograph sensor measuring conductivity and internal temperature; and an SBE-38 (SN 0277) external temperature sensor installed near the seawater intake. Temperature data were acquired every 10 seconds for the duration of the cruise. Salinity samples were taken periodically throughout the cruise for calibration from an outlet in the flowthrough system located less than 0.5 m from the SBE-21.

Temperature Calibration

External temperature data from the SBE-38 sensor (last calibrated at Sea-Bird on 04 December 2012) were used as a measure of the seawater temperature. These data were compared to the data collected during CTD casts, since internal temperatures were found unreliable as the water was subject to heating and cooling as it passed through the ship.

Nominal Conductivity Calibration

Data from the SBE-21 conductivity and temperature sensors were used to calculate the intake seawater salinity. These sensors were last calibrated at Sea-Bird on 27 November 2012. All conductivity data from the thermosalinograph were nominally calibrated with coefficients from this calibration. However, all the final salinity data reported here were calibrated against bottle data as explained below.

Data Processing

Daily files containing navigation data recorded every 10 seconds were concatenated with the thermosalinograph data. The thermosalinograph data were then screened for gross errors, with upper and lower bounds of 18 °C and 35 °C for temperature and 3 Siemens m⁻¹ and 6 Siemens m⁻¹ for conductivity. There were no points outside the valid temperature and conductivity ranges.

A 5-point running median filter was used to detect one- or two-point temperature and conductivity glitches in the thermosalinograph data. Glitches in temperature and conductivity detected by the 5-point median filter were immediately replaced by the median. Threshold values of 0.3 °C for temperature and 0.1 Siemens m⁻¹ for conductivity were used for the median filter. After running the filter, there were 346 conductivity points replaced by the median. A 3-point triangular running mean filter was used to smooth the temperature and conductivity data after passing the glitch detection.

The thermosalinograph aboard the Ship *Hi'ialakai* was set to record data every 10 seconds, but occasionally, due to an error in the acquisition software rounding routine, a record is written at a longer interval. However, there were no timing errors observed.

Data were visually scanned to flag glitches probably caused by contamination due to the introduction of bubbles to the flowthrough system during transit or during rough conditions. Of a total of 67,158 data points, 6081 conductivity data points were flagged as bad for spikes on conductivity.

Bottle Salinity and CTD Salinity Comparisons

The thermosalinograph salinity was calibrated by comparing it to bottle salinity samples drawn from a water intake next to the thermosalinograph every 8 hours throughout the cruise. Of the 24 bottles sampled, 2 were considered outliers, while the final 3 bottles were sampled after the system stopped collecting conductivity data. The remaining 21 salinity samples were analyzed as described in Section 0. The comparison was made in conductivity in order to eliminate the effects of temperature. The conductivity of the bottle sample was computed using the salinity of the bottle, thermosalinograph temperature and a pressure of 3.44 dbar, which includes the pressure of the flowthrough system's pump.

Salinity samples were drawn from the flowthrough system, located less than 0.5 m from the SBE-21 and consequently there should be virtually no delay between when the water passes through the thermosalinograph and it being sampled. A 90 second average centered on the sample draw time was chosen for processing purposes.

The CTD salinity data at 2 dbar from the 12 casts conducted during the cruise were used to compare with the thermosalinograph conductivity. Using the thermosalinograph temperature data and a pressure of 3.44 dbar the CTD conductivity was calculated for the 12 casts conducted while the thermosalinograph was running. Two CTD casts (station 1 cast 1 and station 50 cast 6) were excluded from the processing as outliers. The SBE-21 conductivity sensor had a mean offset of 0.0043 Sm^{-1} with respect to the CTD data.

A cubic spline was fit to the time series of the differences between the bottle and thermosalinograph conductivity and a correction was obtained for the thermosalinograph conductivities. Salinity was calculated using these corrected conductivities, the thermosalinograph temperatures, and 6-dbar pressure. After correction, the mean difference between the bottle and thermosalinograph salinities was 0.000001 with a standard deviation of 0.0142. The mean CTD - thermosalinograph difference was -0.00221 with a standard deviation of 0.0105.

CTD Temperature Comparisons

There were 12 CTD casts conducted during the WHOTS-11 cruise. The 2 dbar CTD temperature data were used to compare with the thermosalinograph external temperature. Two

CTD casts (station 1 cast 1 and station 50 cast 6) were excluded from the processing as outliers. The mean difference between the external sensor and the CTD was -0.17127 ± 0.03063 °C, while the mean difference between the internal sensor and the CTD was -0.22439 ± 0.02666 °C.

D. Shipboard ADCP

1. WHOTS-10 Deployment Cruise

Currents measured by the *Hi'ialakai's* Ocean Surveyor 75 kHz narrowband and broadband ADCP were processed using the CODAS ADCP processing suite. Horizontal velocity data, latitude and longitude were processed with 15 minute ensemble averages and 10 m depth resolution. The times of the datasets from the OS75 are shown in Table 4-2.

Table 4-2. ADCP record times (UTC) for the Narrow Band Ocean Surveyor 75 kHz ADCP during the WHOTS-10 cruise.

WHOTS-10	OS75
File beginning time	09-Jul-2013 20:02:58
File ending time	16-Jul-2013 23:38:00

2. WHOTS-11 Deployment Cruise

Currents measured by the Ship *Hi'ialakai's* Ocean Surveyor 75 kHz narrowband ADCP were processed using the CODAS ADCP processing suite. Horizontal velocity data, latitude and longitude were processed with 15 minute ensemble averages and 10 m depth resolution. The times of the datasets from the OS75 are shown in Table 4-3. Broadband mode for the ADCP was not available during the WHOTS-11 cruise due to a cable problem.

Table 4-3. ADCP record times (UTC) for the Narrow Band 75 kHz ADCP during the WHOTS-11 cruise.

WHOTS-11	OS75
File beginning time	11-Jul-2014 21:22:02
File ending time	23-Jul-2014 18:03:49

5. Moored Instrument Observations

A. MicroCAT/SeaCAT data processing procedures

Each moored MicroCAT and SeaCAT temperature, conductivity and pressure (when installed) was calibrated at Sea-Bird prior to their deployment and after their recovery on the dates shown in Table 5-1. The internally-recorded data from each instrument were downloaded on board the ship after the mooring recovery, and the nominally-calibrated data were plotted for a visual assessment of the data quality. The data processing included checking the internal clock data against external event times, pressure sensor drift correction, temperature sensor stability, and conductivity calibration against CTD data from casts conducted near the mooring during HOT and WHOTS cruises. The detailed processing procedures are described in this section.

Table 5-1. WHOTS-10 MicroCAT/SeaCAT temperature sensor calibration dates, and sensor drift during deployments.

Nominal deployment depth (m)	Sea-Bird Serial number	Pre-deployment calibration	Post-recovery calibration	Temperature sensors annual drift during WHOTS-10 (mili°C)
15	SBE37SM-6893	8-Aug-2012	18-Sep-2014	0.10
25	SBE37SM-6894	16- Aug-2012	18-Sep-2014	0.54
35	SBE37SM-6895	21- Aug-2012	18-Sep-2014	-0.20
40	SBE37SM-6896	8- Aug-2012	18-Sep-2014	0.02
45	SBE37SM-6887	7- Aug-2012	18-Sep-2014	-0.01
50	SBE37SM-6897	7- Aug-2012	19-Sep-2014	0.36
55	SBE37SM-6898	11- Aug-2012	19-Sep-2014	-0.20
65	SBE37SM-6899	7- Aug-2012	19-Sep-2014	0.05
75	SBE37SM-3618	8- Aug-2012	18-Sep-2014	-0.25
85	SBE37SM-6888	1- Sep-2012	19-Sep-2014	-0.18
95	SBE37SM-3617	21- Sep-2012	18-Sep-2014	-0.01
105	SBE37SM-6889	16- Aug-2012	18-Sep-2014	0.02
120	SBE37SM-6890	8- Aug-2012	19-Sep-2014	0.14
135	SBE37SM-3634	8- Aug-2012	19-Sep-2014	-0.01
155	SBE37SM-6891	8- Aug-2012	18-Sep-2014	0.00
4720	SBE16-1882	29-Mar-2011	19-Sep-2014	0.02
4720	SBE16-2325	14-Apr-2004	19-Sep-2014	-0.01

1. Internal Clock Check and Missing Samples

Before the WHOTS-10 mooring deployment and after its recovery (before the data logging was stopped), the MicroCATs temperature sensors were placed in contact with an ice pack to create a spike in the data, to check for any problems with their internal clocks, and for possible missing samples (Table 3-2). The cold spike was detected by a sudden decrease in temperature. For all the instruments, the clock time of this event matched correctly the time of the spike (within the sampling interval of each instrument). No missing samples were detected for any of the instruments.

2. Pressure Drift Correction and Pressure Variability

Some of the MicroCATs used in the moorings were outfitted with pressure sensors (Table 3-1). Biases were detected in the pressure sensors by comparing the on-deck pressure readings (which should be zero for standard atmospheric pressure at sea level of 1029 mbar) before deployment and after recovery. Table 5-2 shows the magnitude of the bias for each of the sensors before and after deployment. To correct for this offset, a linear fit between the initial and final on-deck pressure offset as a function of time was obtained, and subtracted from each sensor. Figure 5-1 shows the linearly corrected pressures measured by the MicroCATs during the WHOTS-10 deployment. For all the sensors, the mean difference from the nominal instrument pressure (based on the deployed depth) was less than 1 dbar. The standard deviation of the pressure for the duration of the record was also less than 1 dbar for all sensors, with the deeper sensors showing a slightly larger standard deviation. The range of variability for all sensors was about ± 3 dbar.

The causes of pressure variability can be several, including density variations in the water column above the instrument; horizontal dynamic pressure (not only due to the currents, but also due to the motion of the mooring); mooring position, etc. (see WHOTS Data Report 1, Santiago-Mandujano et al., 2007).

Table 5-2. Pressure bias of MicroCATs with pressure sensor.

Deployment	Depth (m)	Sea-Bird Serial #	Bias before deployment (dbar)	Bias after recovery (dbar)
WHOTS-10	45	37SM31486-6887	0.07	-0.01
WHOTS-10	85	37SM31486-6888	0.80	0.80
WHOTS-10	105	37SM31486-6889	0.10	0.08
WHOTS-10	120	37SM31486-6890	0.05	-0.02
WHOTS-10	155	37SM31486-6891	0.08	0.06

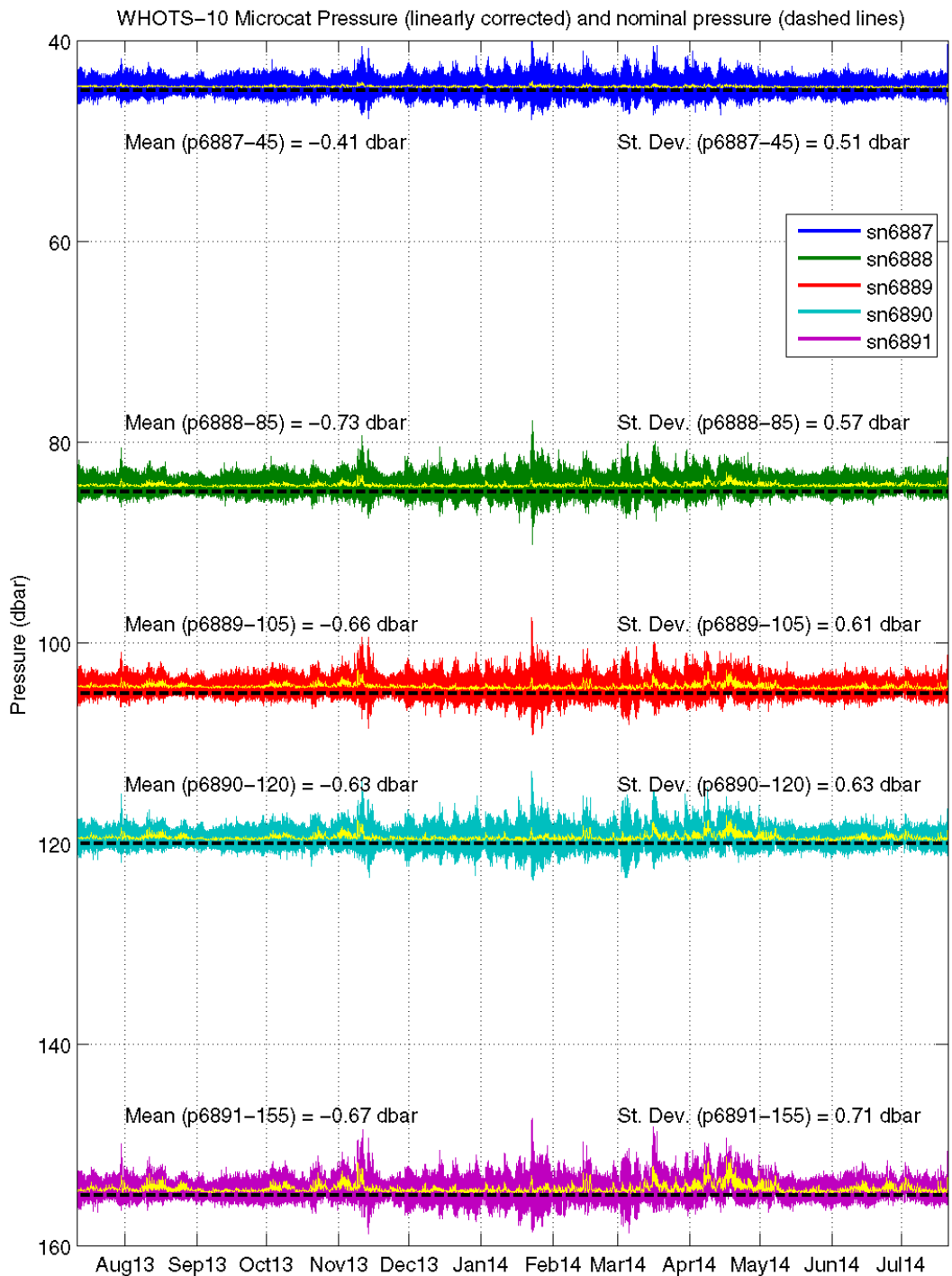


Figure 5-1. Linearly corrected pressures from MicroCATs during WHOTS-10 deployment. The yellow line is a 5-hour running mean. The horizontal dashed line is the sensor's nominal pressure, based on deployed depth.

3. Temperature Sensor Stability

The MicroCAT and SeaCAT temperature sensors were calibrated at Sea-Bird before and after each deployment, and their annual drift evaluations are shown in Table 5-1. These values turned out to be insignificant (not higher than 1 milli °C) for all sensors. Comparisons between the MicroCAT and CTD data from casts conducted near the mooring during HOT cruises confirmed that the temperature drift of the rest of the moored instruments was insignificant. The two SeaCATs (SN 1882 and SN 2325) deployed near the bottom were drift corrected. Figure 5-7 (upper panel) shows the temperature differences between both instruments before and after the correction. After the correction the temperature differences were in the -1.0 to 2.0 m°C range.

Temperature comparisons between one of the WHOTS-10 near-surface MicroCATs (SN 1834) and three of the four RBR surface temperature sensors in the buoy hull (Section 3) are shown in Figure 5-2. Two of the RBR instruments (#14879 and #14875) returned full records; instrument #19714 started showing spikes after Julian day 3750, and it failed a few days after. Instrument #14813 did not return any data. None of the instruments show any obvious bias when compared to the Microcat measurements.

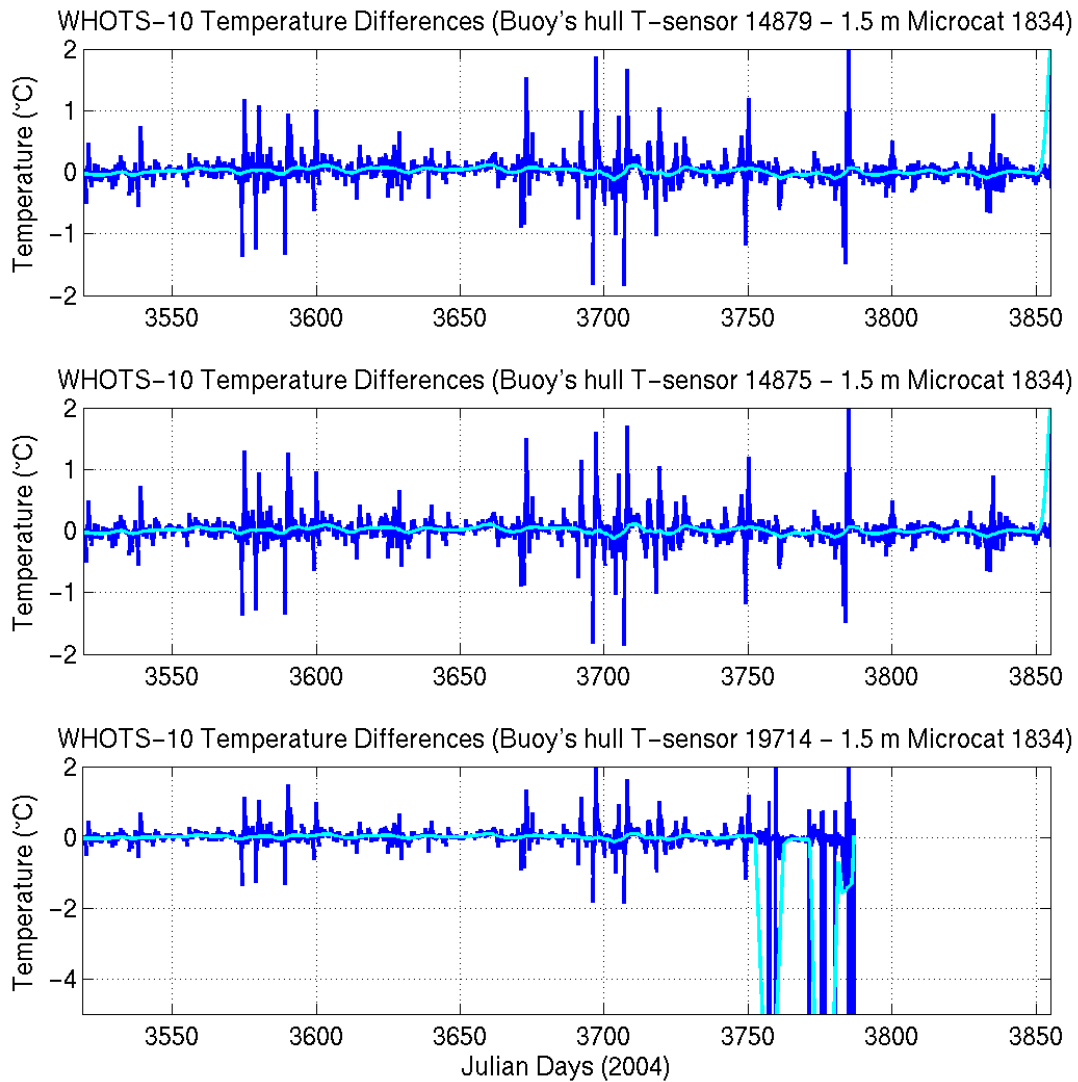


Figure 5-2. Temperature difference between MicroCAT SN 1834 at 1.5 m, and near-surface temperature sensors SN 14879 (upper panel), 14875 (second panel), and 19714 (bottom panel), during WHOTS-10 deployment. The light blue line is a 24-hour running mean of the differences.

In addition to the temperature sensors in the Sea-Bird and the RBR instruments, there were temperature sensors in the VMCMs (at 10 and 30 m), and in the ADCPs (at 47.5 m and 125 m). In order to evaluate the quality of the temperatures from these sensors, comparisons with the temperatures from adjacent MicroCATs were conducted.

Comparisons with VMCM and ADCP temperature sensors

The upper panel of Figure 5-3 shows the difference between the 10-m VMCM and the 15-m MicroCAT temperatures during WHOTS-10, after subtracting a 0.041 °C offset correction to the VMCM. The offset was the mean difference between the uncorrected VMCM and the 15-m MicroCAT data. Also shown for comparison in the lower panel of the figure are the differences between MicroCAT temperatures at 15 and 25 m. The temperature fluctuations in the differences between the 15 and 25-m MicroCATs seem to be around zero.

Temperature differences between the 30-m VMCM and the temperatures from adjacent MicroCATs at 25 and 35-m during WHOTS-10 are shown in Figure 5-4. For comparison, the differences between the MicroCATs temperatures are also shown. These plots indicate that there was no offset in the 30-m VMCM with respect to the adjacent MicroCATs (top and middle plots).

Temperature differences between the 47.5-m ADCP and the temperatures from adjacent MicroCATs at 45 and 50-m during WHOTS-10 are shown in Figure 5-5. For comparison, the differences between the MicroCATs temperatures are also shown. These plots indicate that there was no offset in the 47.5-m ADCP with respect to the adjacent MicroCATs (top and middle plots).

Temperature differences between the 125-m ADCP and the temperatures from adjacent MicroCATs at 120 and 135-m during WHOTS-10 are shown in Figure 5-6. For comparison, the differences between the MicroCATs temperatures are also shown. It is difficult to assess the quality of the ADCP temperature from these comparisons, as these sensors were located at the top of the thermocline, where we expect to find large temperature differences between adjacent sensors. However, an indication of the quality of the ADCP temperatures is given in the upper panel plot, which shows temperatures fluctuating closely around zero.

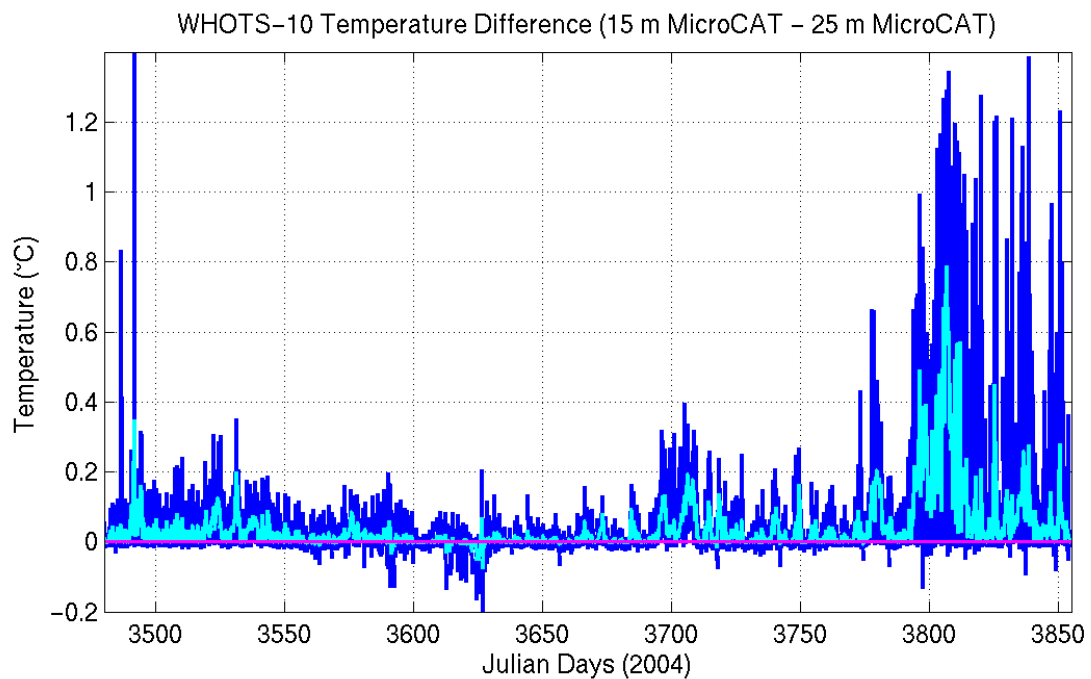
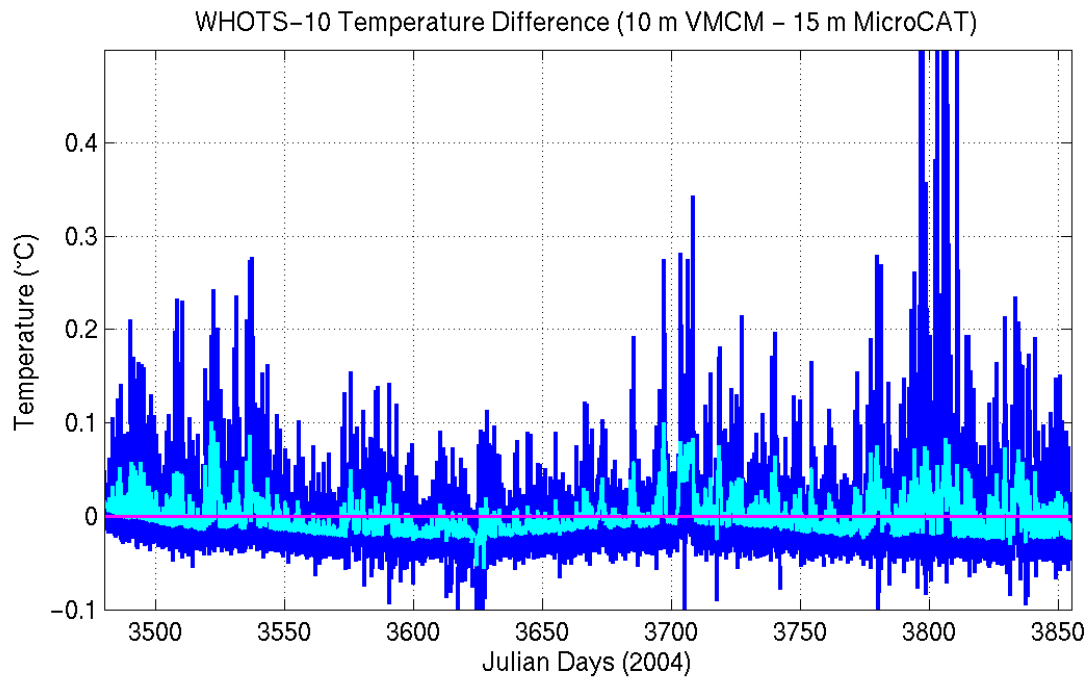


Figure 5-3. Temperature difference between the 10-m VMCM and the 15-m MicroCAT during the WHOTS-10 deployment (upper panel). Temperature difference between the 15-m MicroCAT and the 25-m MicroCAT during the WHOTS-10 deployment (lower panel). The light blue line is a 24-hour running mean of the differences.

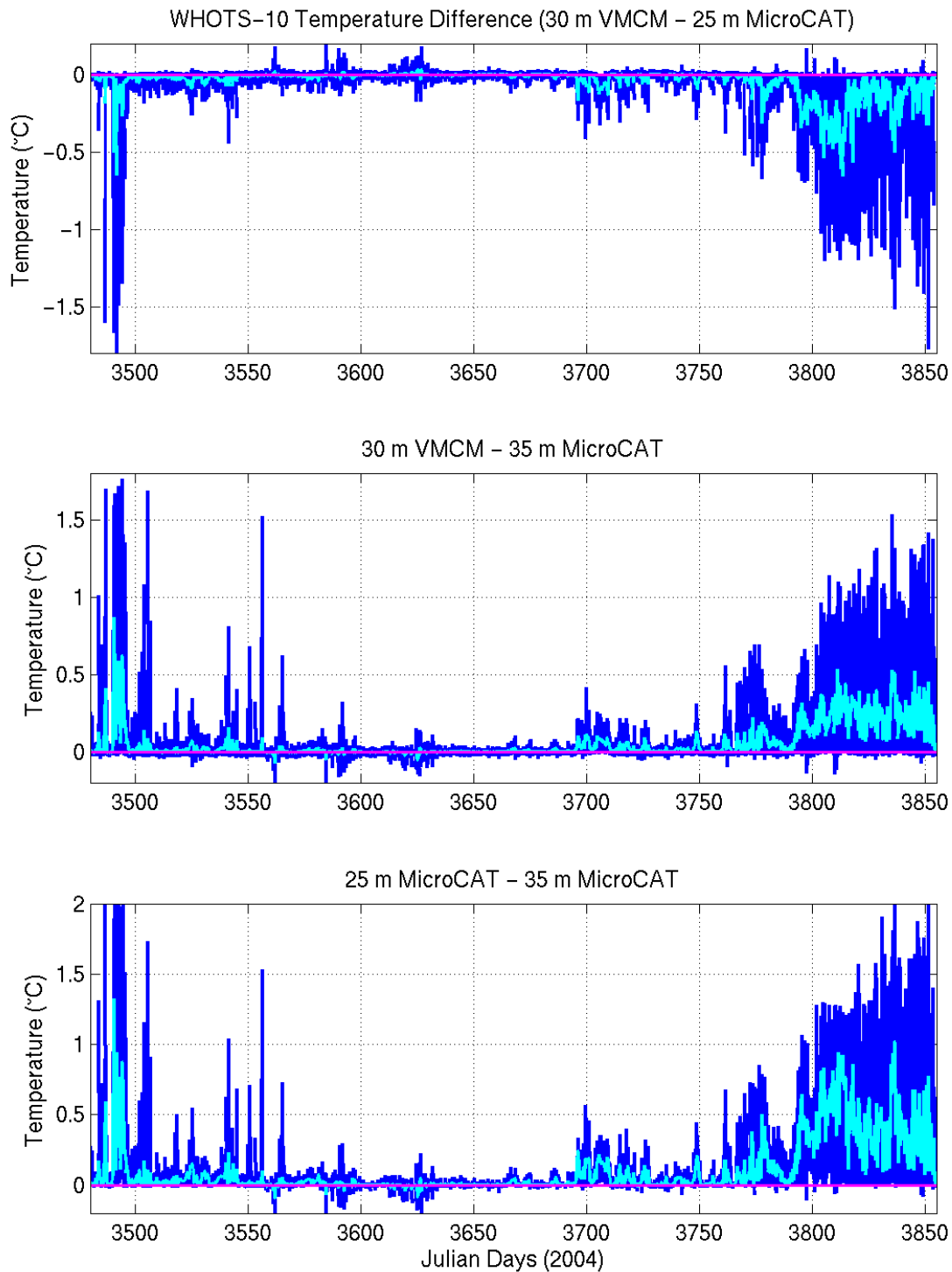


Figure 5-4. Temperature difference between the 30-m VMCM and the 25-m MicroCAT during the WHOTS-10 deployment (upper panel); between the 30-m VMCM and the 35-m MicroCAT (middle panel); and between the 25-m and the 35-m MicroCATs (lower panel). The light blue line is a 24-hour running mean of the differences.

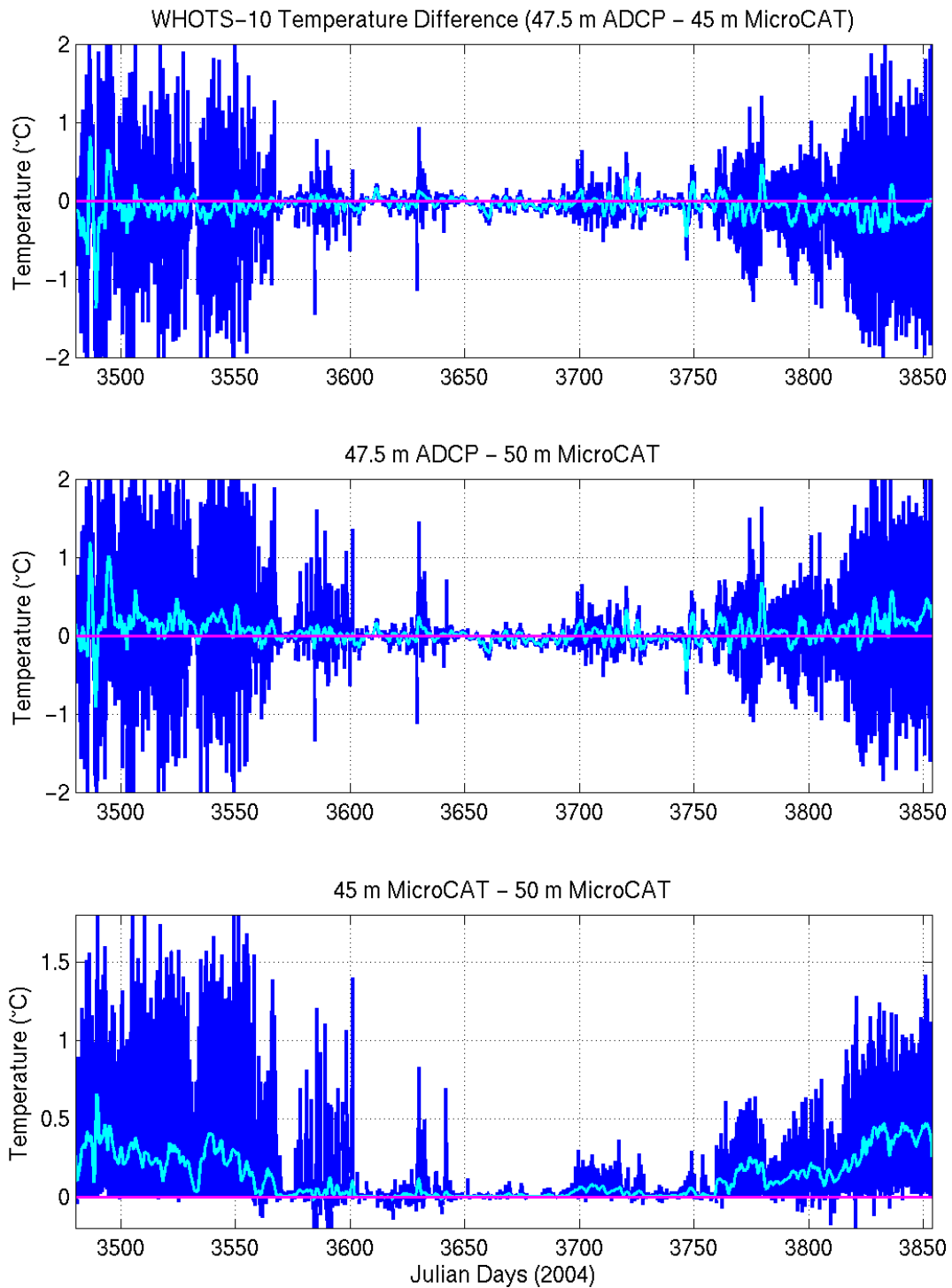


Figure 5-5. Temperature difference between the 47.5-m ADCP and the 45-m MicroCAT during the WHOTS-10 deployment (upper panel); between the 47.5-m ADCP and the 50-m MicroCAT (middle panel); and between the 45-m and the 50-m MicroCATs (lower panel). The light blue line is a 24-hour running mean of the differences.

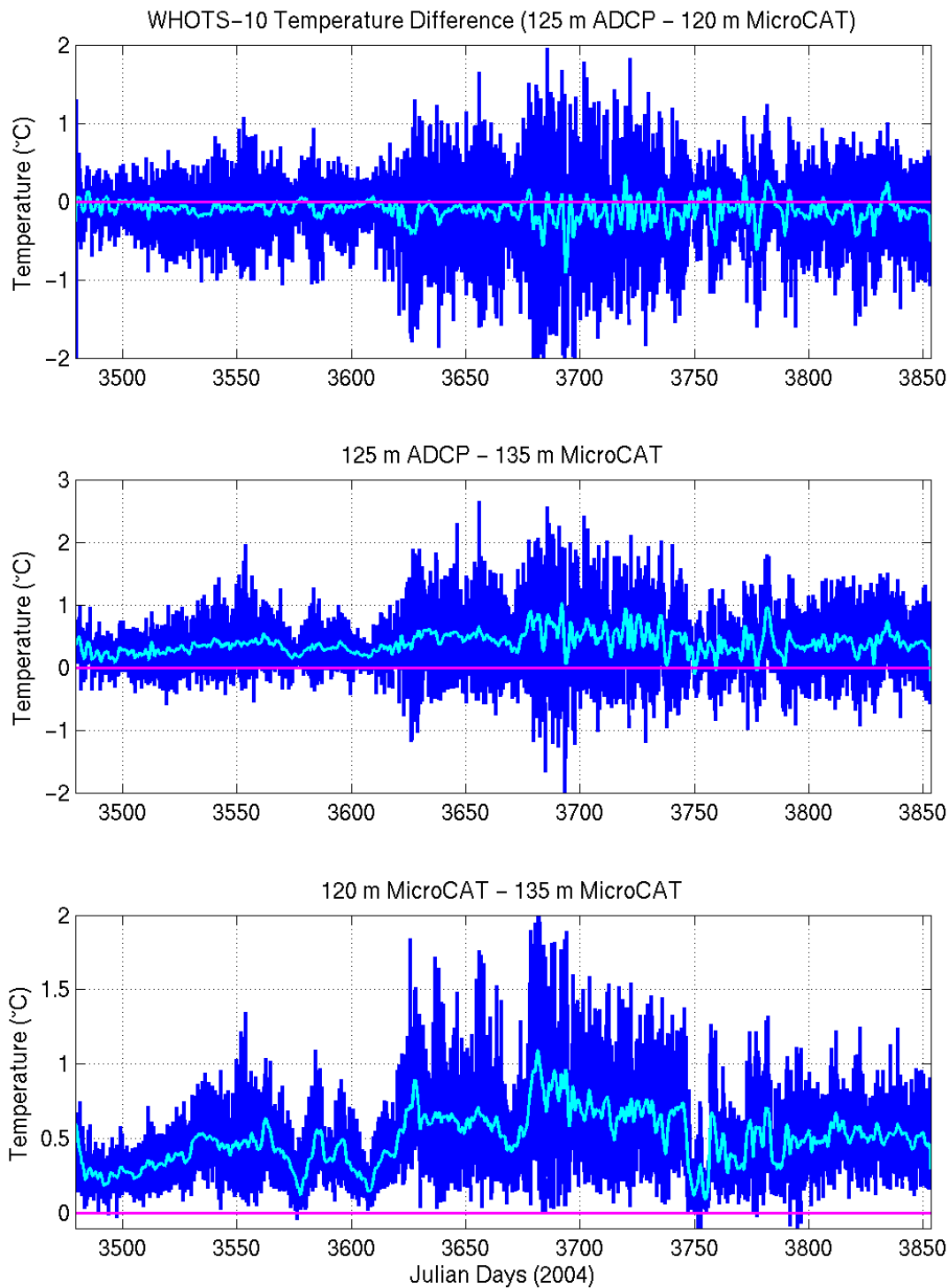


Figure 5-6. Temperature difference between the 125-m ADCP and the 120-m MicroCAT during the WHOTS-10 deployment (upper panel); between the 125-m ADCP and the 135-m MicroCAT (middle panel); and between the 120-m and the 135-m MicroCATs (lower panel). The light blue line is a 24-hour running mean of the differences.

4. Conductivity Calibration

The results of the Sea-Bird post-recovery conductivity calibrations indicated that some of the MicroCAT and SeaCAT conductivity sensors experienced relatively large offsets from their pre-deployment calibration. These were qualitatively confirmed by comparing the mooring data against CTD data from casts conducted between 200 m and 5 km from the mooring during HOT cruises. The causes of the conductivity offsets are not clear, and there may have been multiple causes (see Freitag et. al, (1999) for a similar experience with conductivity cells during COARE). For some instruments the offset was negative, caused perhaps by biofouling of the conductivity cell while for others the offset was positive, caused possibly by scouring of the inside of the conductivity cell (possible by the continuous up and down motion of the instrument in an abundant field of diatoms). A visual inspection of the instruments after recovery did not show any obvious signs of biofouling, and there were no cell scourings reported in the post-recovery inspections at Sea-Bird. However three of the instruments (25, 45 and 50 m) were recovered without their cell guards, and without their anti-fouling device. These instruments experienced large offsets during the deployment as reported below.

Corrections of the MicroCATs conductivity data were conducted by comparing them against CTD data from profiles and yo-yo casts conducted near the mooring during HOT cruises, and during deployment/recovery cruises. Casts conducted between 200 and 1000 m from the mooring were given extra weight in the correction, as compared to those conducted between 1 and 5 km away. Casts more than 5 km away from the mooring were not used. Given that the CTD casts are conducted at least 200 m from the mooring, the alignment between CTD and MicroCAT data was done in density rather than in depth. For cases in which the alignment in density was not possible due to large conductivity offsets (causing unrealistic mooring density values), alignment in temperature space was done. A cubic least-squares fit (LSF) to the CTD-MicroCAT/SeaCAT differences against time was applied as a first approximation, and the corresponding correction was applied.

Some of the sensors had large offsets and/or obvious variability that could not be explained by a cubic LSF (see below). For these sensors, a stepwise correction was applied matching the data to the available CTD cast data, and then using the differences between consecutive sensors to determine when the sensor started to drift. For instance, during periods of weak stratification the conductivity difference between neighboring sensors A, B, and C could reach near-zero values, in particular for instruments near the surface, which are the ones most prone to suffer conductivity offsets. A sudden conductivity offset observed during this period between sensors A and B, but not between sensors A and C could indicate the beginning of an offset for sensor B.

Given that the deepest instruments on the mooring are less likely to be affected by biofouling and consequent sudden conductivity drift, the deep instruments served as a good reference to find any possible malfunction in the shallower ones. Therefore the deepest instruments' conductivity was corrected first, and the correction was continued sequentially upwards toward the shallower ones.

As a quality control to the conductivity corrections, the buoyancy frequency between neighboring instruments was calculated using finite differences. Over- or under-corrected conductivities yielded instabilities in the water column (negative buoyancy frequency) that were easy to detect and were obviously not real when lasting for several days. Based on this, the conductivity correction of the corresponding sensors was revised.

Corrections of the deep SeaCATs conductivity data were conducted following similar procedures as for the shallow instruments by comparing them against CTD data from near-bottom profiles conducted during HOT cruises.

Another characteristic of the offsets in the conductivity sensors is that their development is not always linear in time, and their behavior can be highly variable (see WHOTS Data Report 1, Santiago-Mandujano et al., 2007).

A correction was also applied to the deep SeaCATs conductivities. Both instruments were deployed at the same depth (4720 m). Comparisons with near-bottom CTD data showed that instrument #1882 had a large drift (see Figure 5-7) which was corrected as mentioned earlier. Instrument #2325 had a large offset from the beginning of the record until before 16 August 2013, this section of the data could not be corrected and the data were flagged as bad. After correction, the salinity differences between both instruments were in the ± 0.002 g/kg range.

The corrections applied to each of the conductivity sensors during WHOTS-10 can be seen in Figure 5-8. Most of the instruments had a drift of less than 0.01 Siemens/m for the duration of the deployment, which was corrected with a linear or cubic least-squares fit. Most of the instruments deployed above 55 m showed a sharp negative drift starting about two months before the end of the deployment, apparently due to the expiration of the anti-foulant.

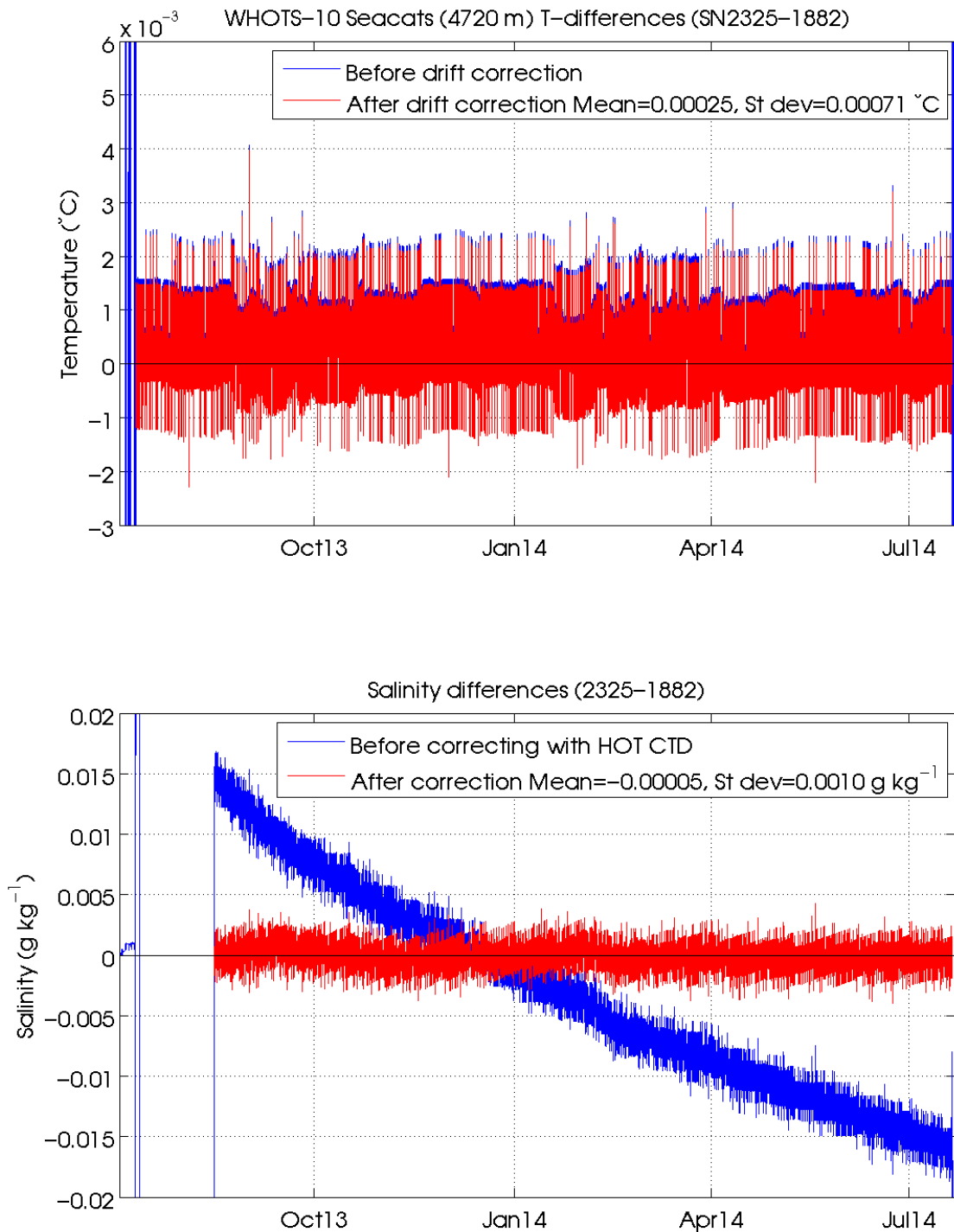


Figure 5-7. Temperature differences (top panel), and salinity differences (bottom panel) between SeaCATs #1882 and #2325 during WHOTS-10. The blue (red) lines are the differences before (after) correcting the data following procedures indicated in the text.

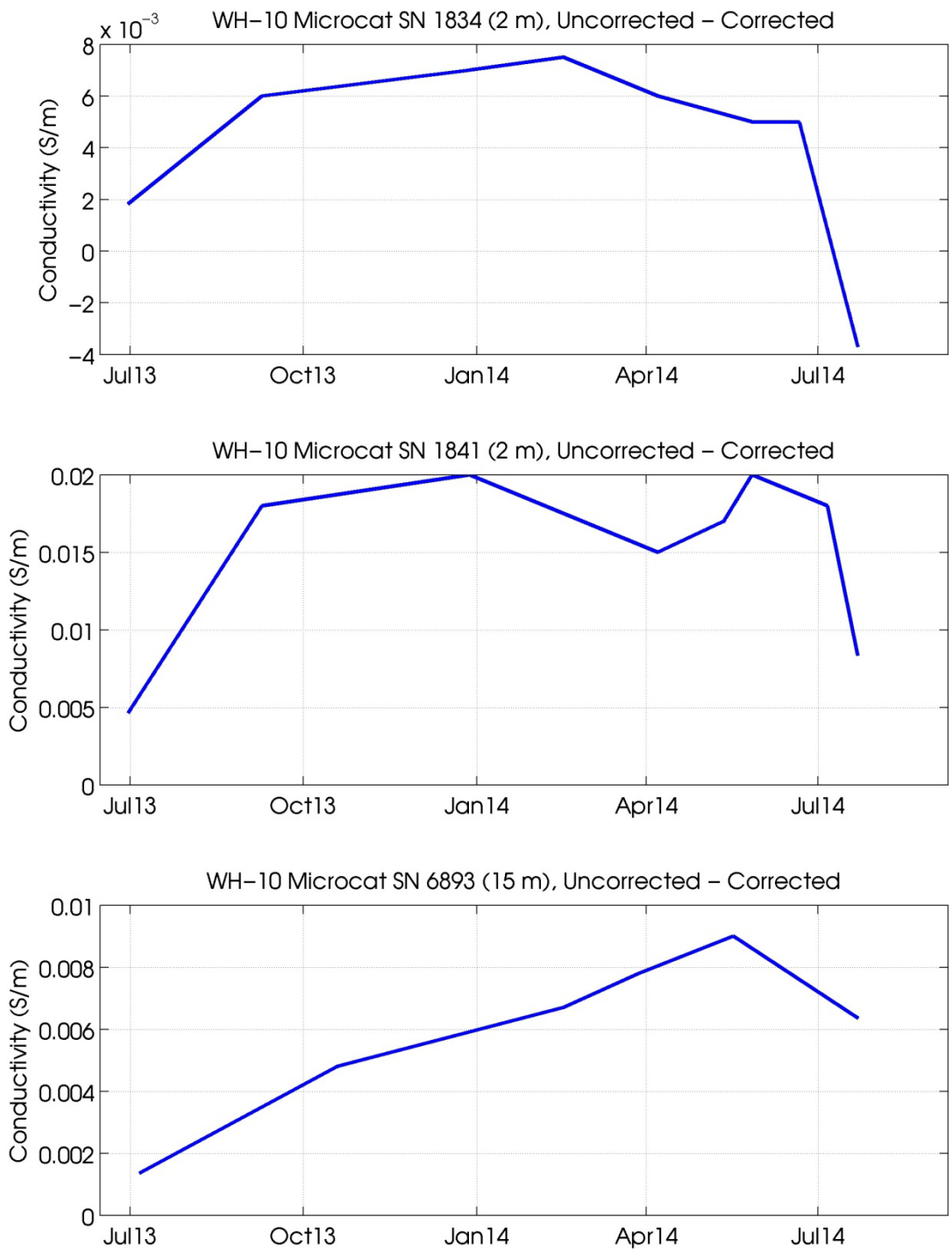


Figure 5-8 Conductivity sensor corrections for MicroCATs and SeaCATs during WHOTS-10

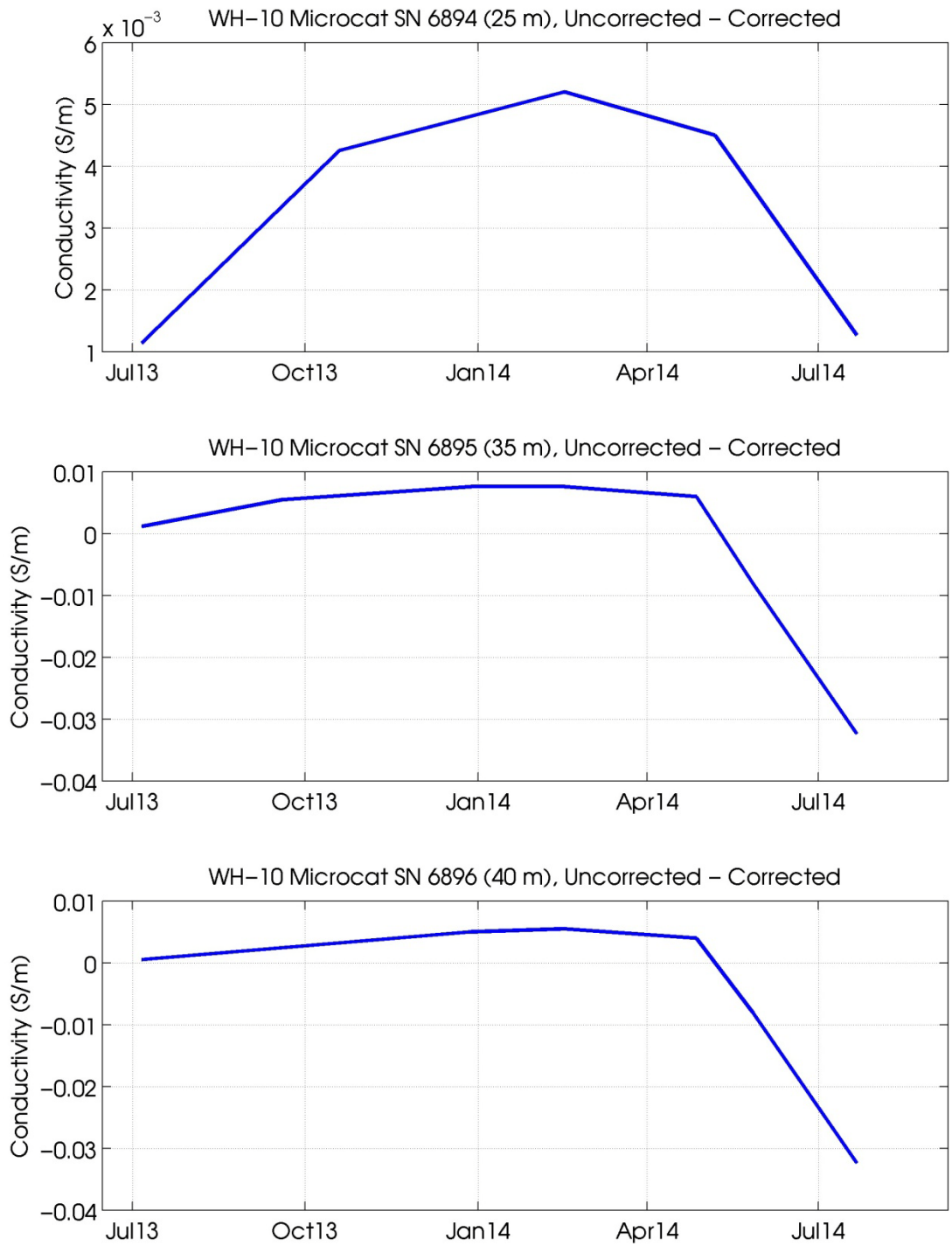


Figure 5-8. (Contd.)

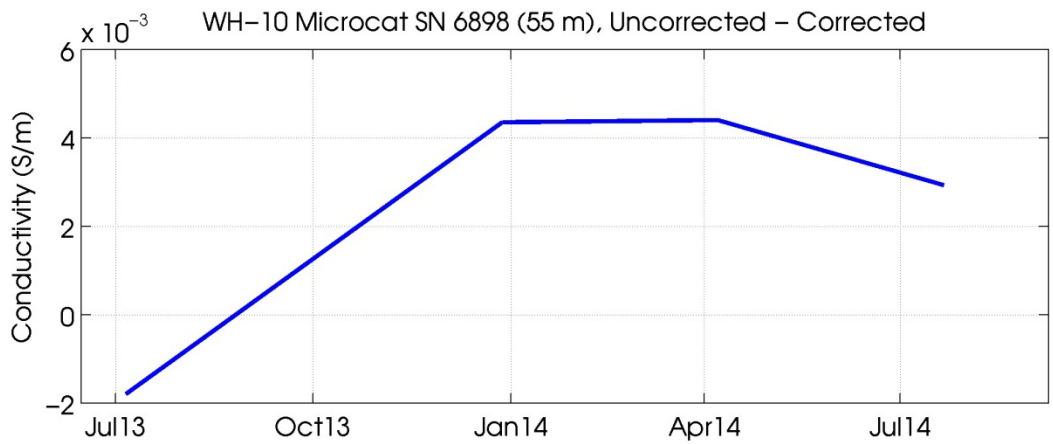
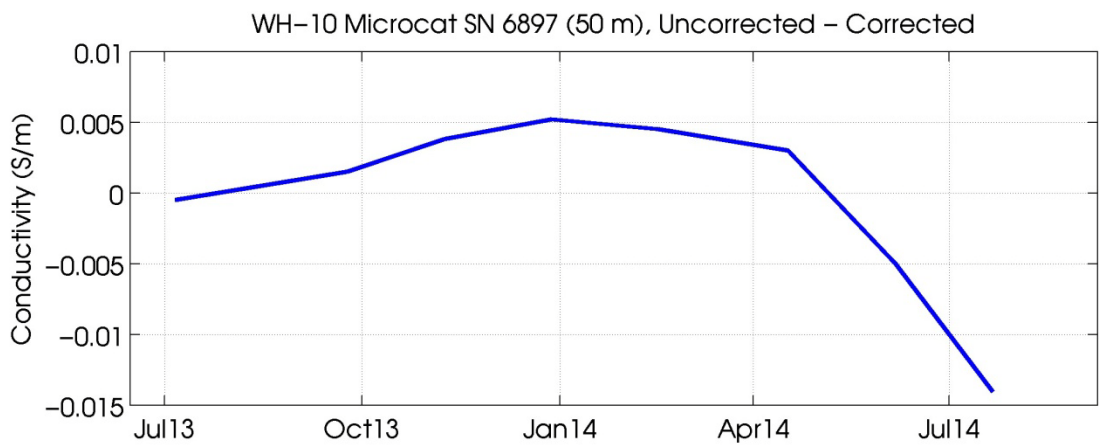
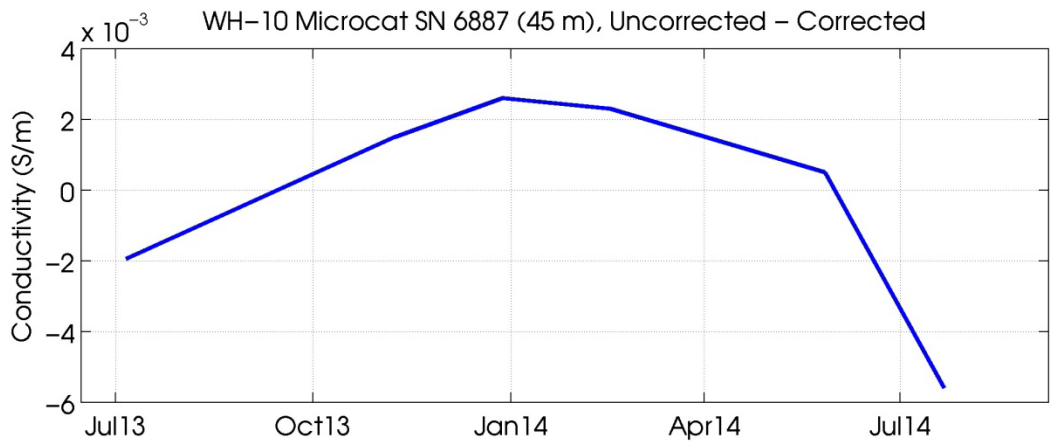


Figure 5-8. (Contd.)

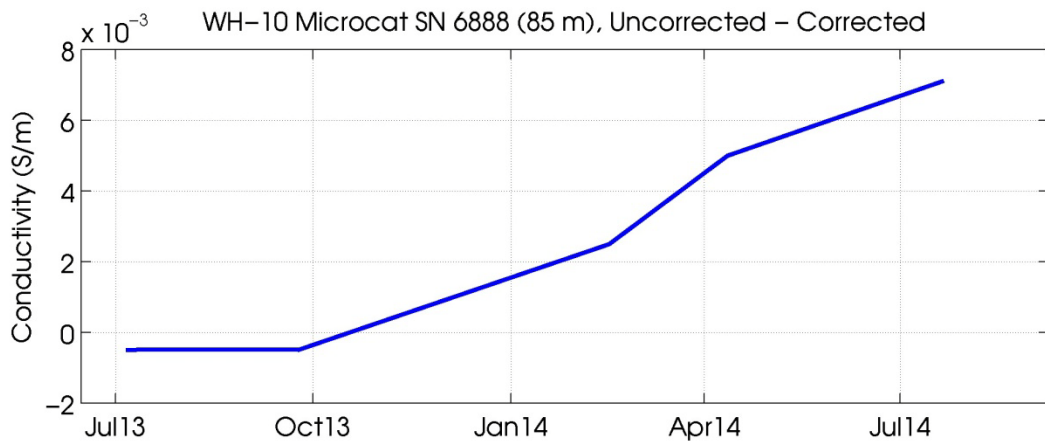
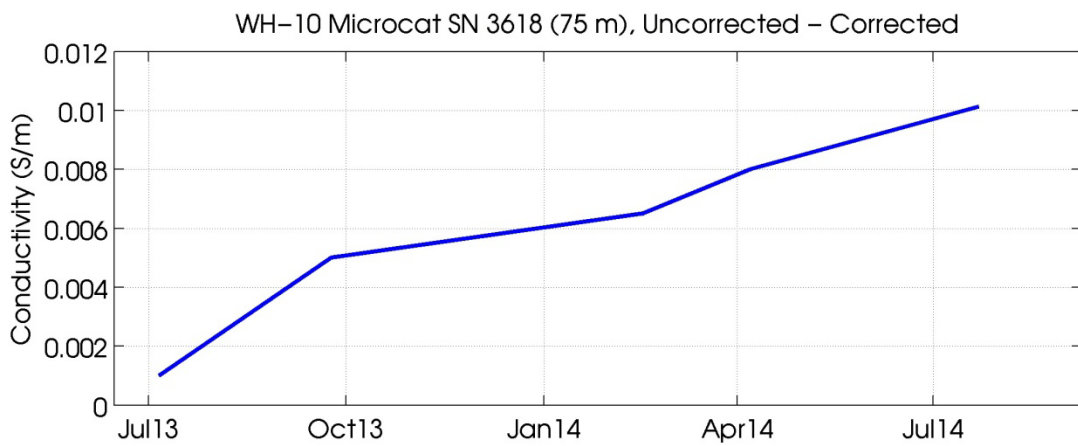
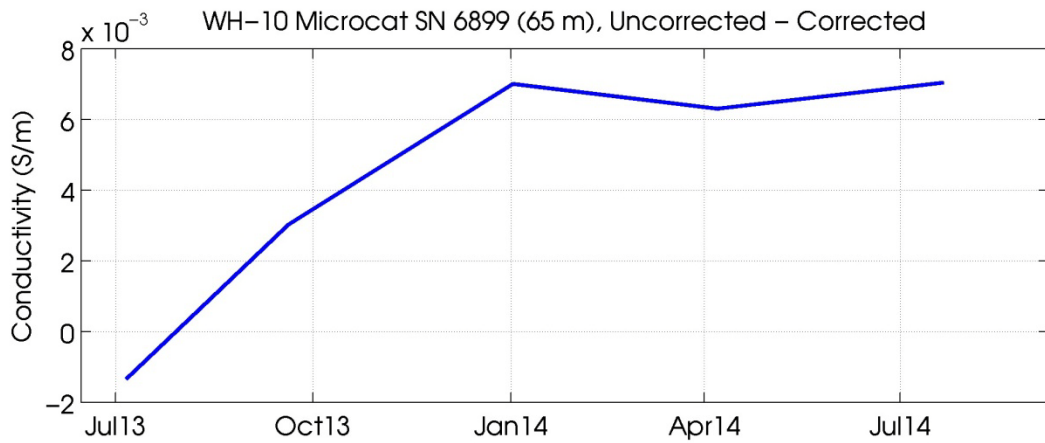


Figure 5-8. (Contd.)

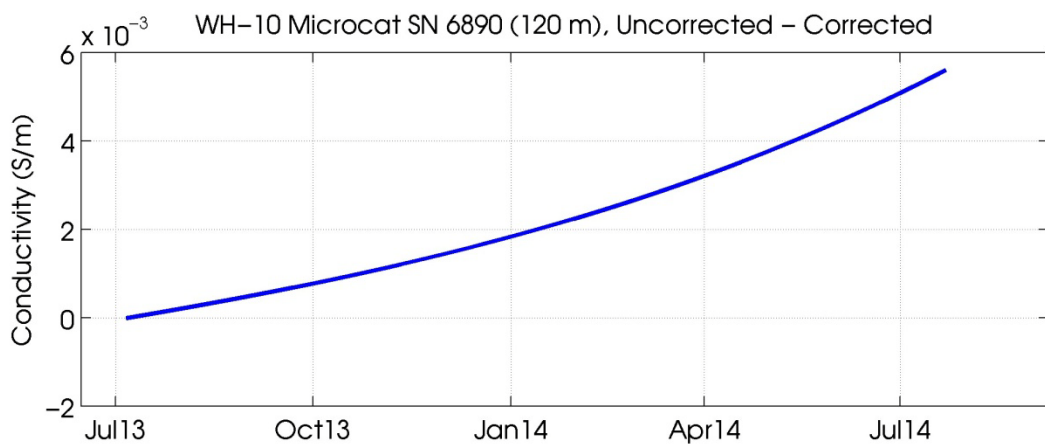
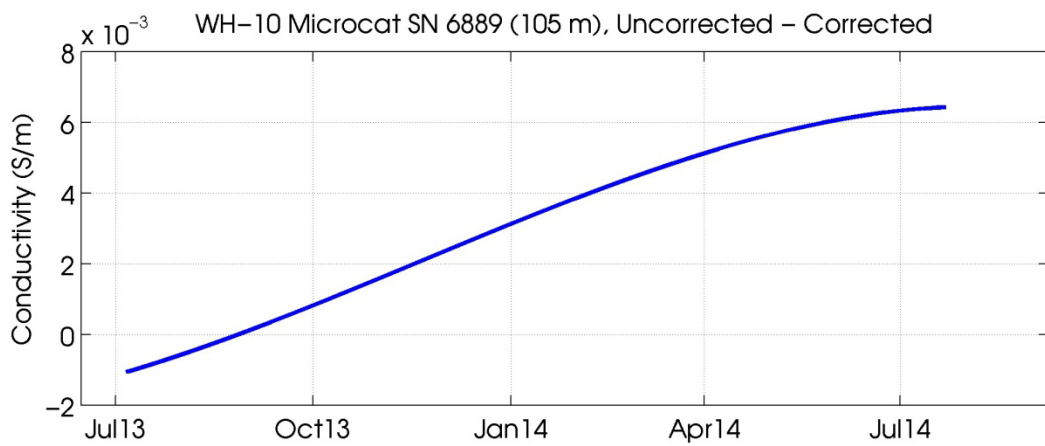
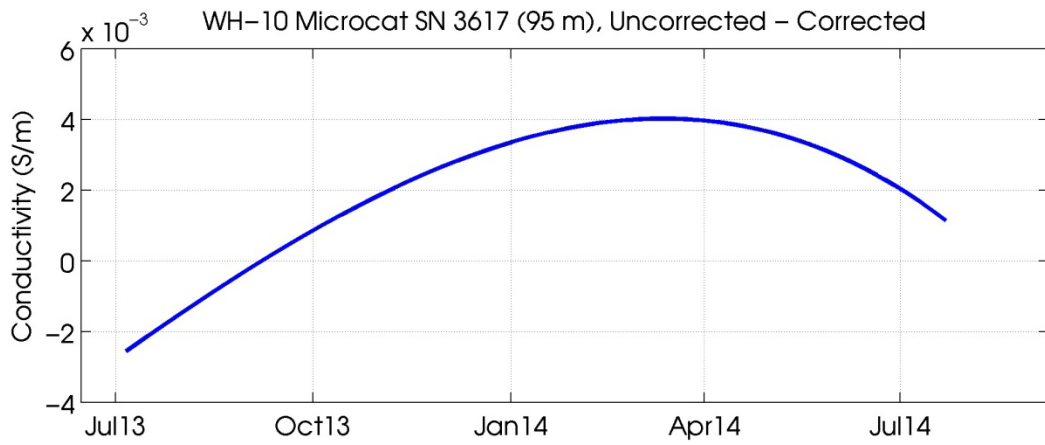


Figure 5-8. (Contd.)

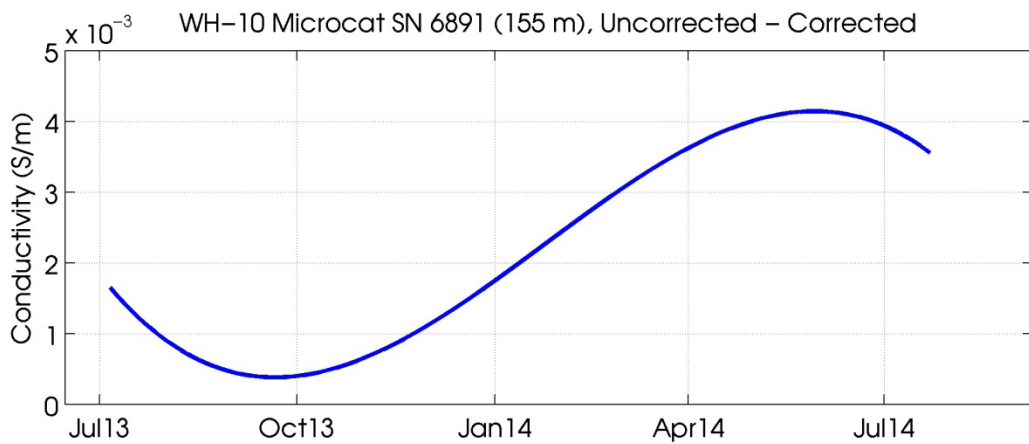
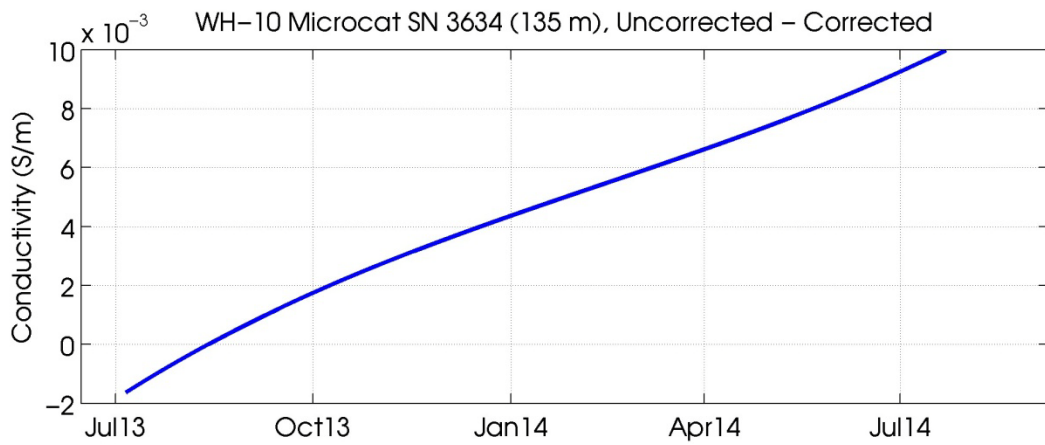


Figure 5-8. (Contd.)

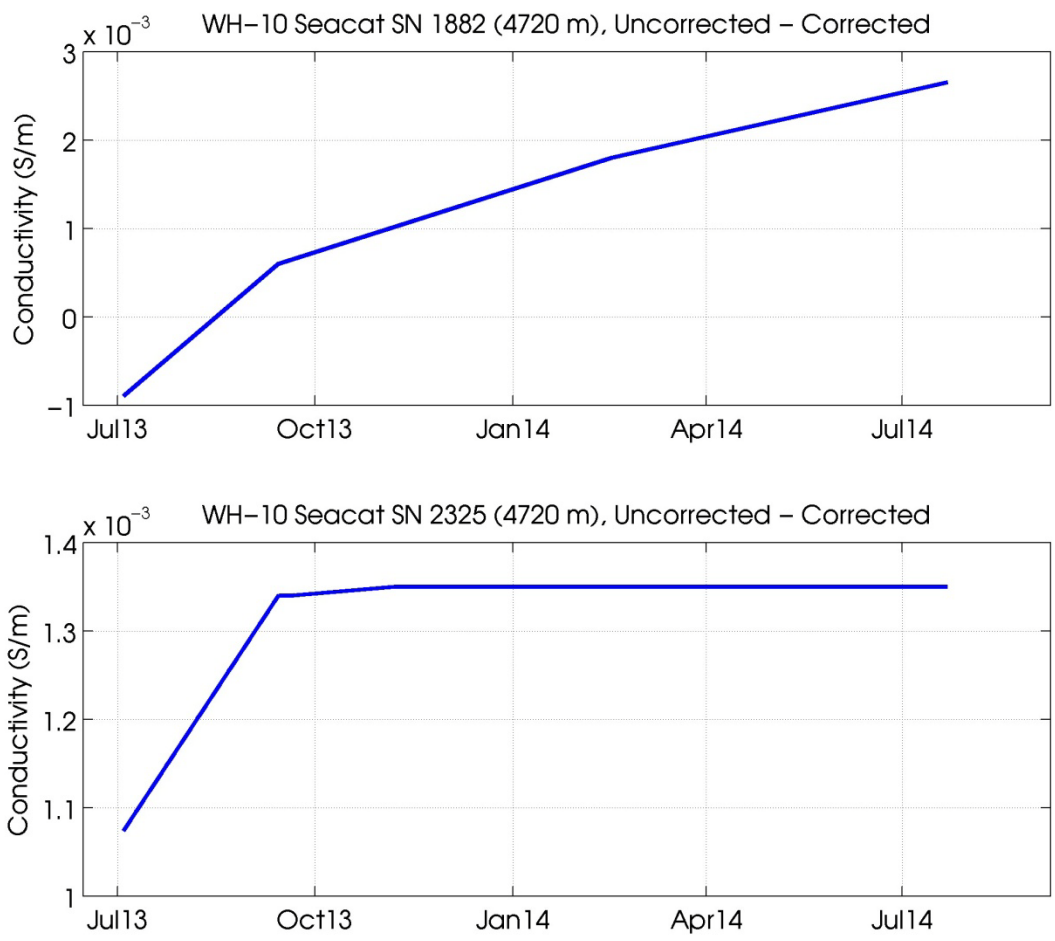


Figure 5-8. (Contd.)

B. Acoustic Doppler Current Profiler

Two Teledyne/RD Instruments broadband Workhorse Sentinel ADCP's were deployed on the WHOTS-10 mooring. A 600 kHz ADCP was deployed at 47.5 m depth in the upward-looking configuration, and a 300 kHz ADCP was deployed at 125 m, also in the upward-looking configuration. The instruments were installed in aluminum frames along with an external battery module to provide sufficient power for the intended period of deployment. The four ADCP beams were angled at 20° from the vertical line of the instrument. The ADCP was set to profile across 30 range cells of 4 m with the first bin centered 6.2 m from the transducer. The maximum range of the instrument was just short of 125 m. The specifications of the instrument are shown in Table 5-3.

Table 5-3. Specifications of the ADCP's used for the WHOTS-10 mooring.

Instrument	Description
ADCP	<i>RDI Workhorse Sentinel, 300KHz</i> Model: WHS300-I-UG186; Serial Number: 4891
	<i>RDI Workhorse Sentinel, 600KHz</i> Model: WHS600-I; Serial Number: 1825
Battery module	<i>300 kHz</i> Model: WH-EXT-BATTERY; Serial Number: 3169
	<i>600 kHz</i> Model: WH-EXT-BCL; Serial Number: 182

1. Compass Calibrations

Pre-Deployment

Prior to the WHOTS-10 deployment a field calibration of the internal ADCP compass was performed at the soccer field of the University of Hawai'i at Manoa on 30 May 2013 for both the 300 kHz and the 600 kHz instruments. Each instrument was mounted in the deployment cage along with the external battery module and was located away from potential sources of magnetic field disturbances. The ADCP was mounted to a turntable, which was aligned with magnetic north using a surveyor's compass. Each ADCP, before performing the calibration on the instrument, was spun on the turntable and its readings were checked every 45° against magnetic north. The results from this pre-calibration spin are shown by the red lines in Figure 5-9 and Figure 5-10. Following this, a built-in RDI compass performance evaluation was conducted to assess pre-calibration errors while rotating the instrument 360 degrees at less than 5°/sec. Following this evaluation, using the built-in RDI calibration procedure, the instrument was tilted in one direction between 10 and 20 degrees and then rotated through 360 degrees at less than 5°/sec. The ADCP was then tilted in a different direction and a second rotation made. Based on the results from the first two rotations, calibration parameters are temporarily loaded into the instrument and the new, post-calibration data are displayed. Next, the ADCP is returned to the upright position and was once again spun on the turntable and its readings were checked every

45° against magnetic north. The results from this post-calibration spin are shown by the blue lines in Figure 5-9 and Figure 5-10. Results from each pre-deployment field calibration are shown in Table 5-4.

Table 5-4. Results from the WHOTS-10 pre-deployment ADCP compass field calibration procedure.

300 kHz (SN 4891)	Single Cycle Error (°)	Double Cycle Error (°)	Largest Double + Single Cycle Error (°)	RMS of 3 rd Order and Higher + Random Error (°)	Overall Error (°)	Pitch Mean and Standard Deviation (°)	Roll Mean and Standard Deviation (°)
Before Calibration	2.82	0.70	3.52	0.12	3.08	1.10 ± 0.89	-1.22 ± 0.85
After Calibration	0.22	0.20	0.41	0.12	0.35	-17.09 ± 0.90	-1.23 ± 0.90

600 kHz (SN 1825)	Single Cycle Error (°)	Double Cycle Error (°)	Largest Double + Single Cycle Error (°)	RMS of 3 rd Order and Higher + Random Error (°)	Overall Error (°)	Pitch Mean and Standard Deviation (°)	Roll Mean and Standard Deviation (°)
Before Calibration	2.81	0.05	2.87	0.13	2.81	-0.13 ± 0.82	-1.44 ± 1.05
After Calibration	0.03	0.15	0.19	0.15	0.18	0.35 ± 1.05	14.20 ± 0.96

Post-Deployment

After the WHOTS-10 mooring was recovered, the performance of the ADCP compass was tested at the soccer field of the University of Hawai'i at Manoa on 30 July 2014 and was set up in the same way as during the pre-deployment calibration. Each ADCP was spun on the turntable and its readings were checked every 45° against magnetic north. The results from this post-deployment assessment spin are shown by the green lines in Figure 5-9 and Figure 5-10. Following this, a built-in RDI compass performance evaluation was conducted to assess the post-deployment compass errors while rotating the instrument 360 degrees at less than 5 °/sec.

Results from the WHOTS-10 post-deployment ADCP compass assessment are listed in Table 5-5.

Table 5-5. Results from the WHOTS-10 post-deployment ADCP compass field calibration procedure

300 kHz	Single Cycle Error (°)	Double Cycle Error (°)	Largest Double + Single Cycle Error (°)	RMS of 3 rd Order and Higher + Random Error (°)	Overall Error (°)	Pitch Mean and Standard Deviation (°)	Roll Mean and Standard Deviation (°)
After Calibration	1.97	0.32	2.29	0.21	2.06	-0.01 ± 0.20	0.82 ± 0.73

600 kHz	Single Cycle Error (°)	Double Cycle Error (°)	Largest Double + Single Cycle Error (°)	RMS of 3 rd Order and Higher + Random Error (°)	Over all Error (°)	Pitch Mean and Standard Deviation (°)	Roll Mean and Standard Deviation (°)
After Calibration	0.73	0.11	0.84	0.27	0.76	-2.48 ± 0.89	-0.43 ± 0.75

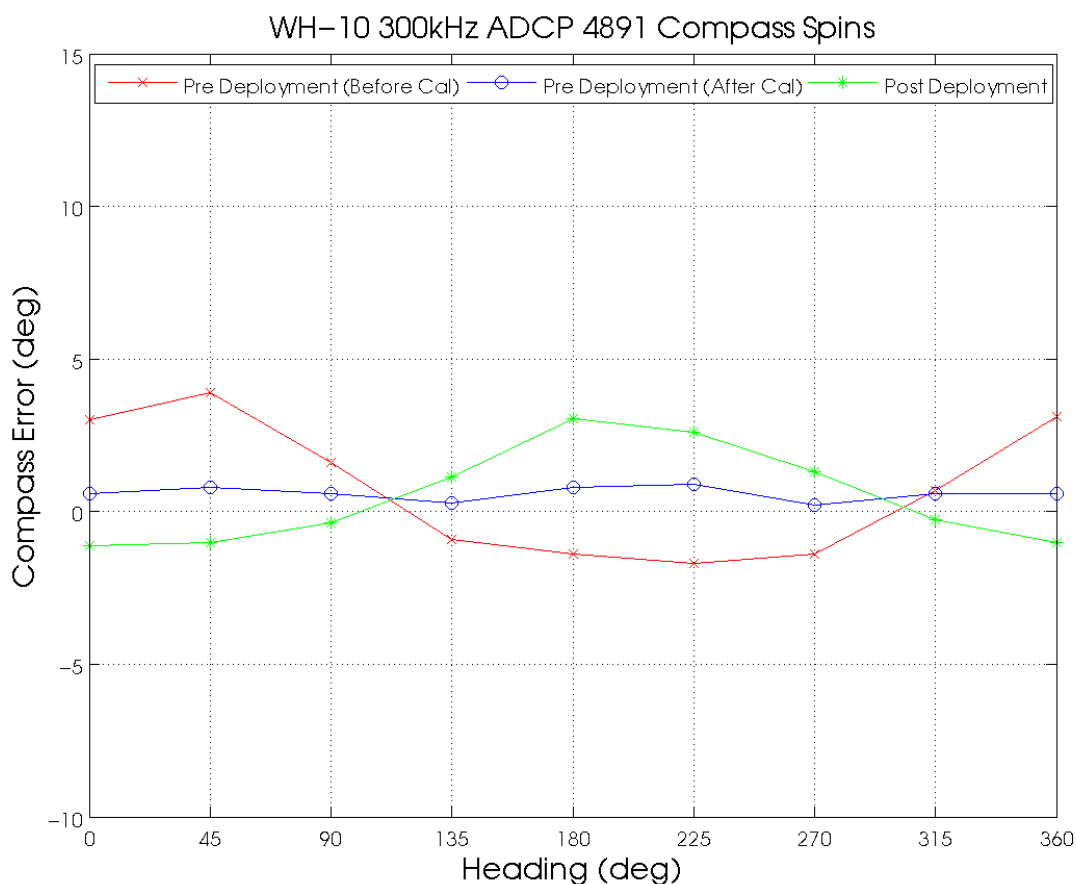


Figure 5-9. Results of the pre- (red, blue), and post-deployment (green) compass calibrations conducted on 30 May 2013 and 30 July 2014 respectively on 300 kHz ADCP SN 4891 at the University of Hawai'i at Manoa.

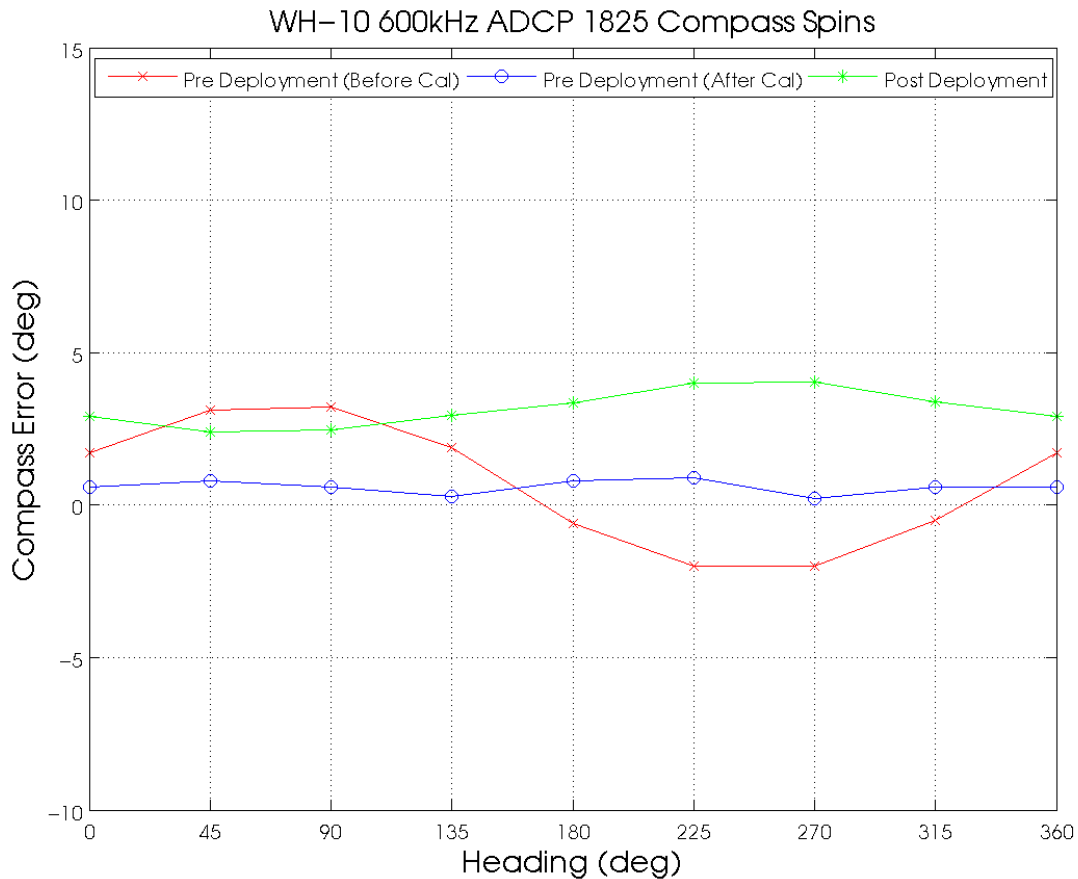


Figure 5-10. Results of the pre- (red, blue), and post-deployment (green) compass calibrations conducted on 30 May 2013 and 30 July 2014 respectively on 600 kHz ADCP SN 1825 at the University of Hawai'i at Manoa.

2. ADCP Configurations

Individual configurations for the two ADCP's on the WHOTS-10 mooring are detailed in Appendices 1 and 2. The salient differences for each of the ADCP's are summarized below.

300 kHz (125m)

The ADCP, set to a beam frequency of 300 kHz, was configured in a burst sampling mode consisting of 40 pings per ensemble in order to resolve low-frequency wave orbital motions. The interval between each ping was 4 seconds so the ensemble length was 160 seconds. The interval between ensembles was 10 minutes. Data were recorded in earth coordinates with a heading bias of 9.81° E used. This heading bias was corrected in post-deployment processing to a heading bias of 9.80° E. False targets, usually fish, were screened by setting the threshold maximum to 70 counts. Velocity data were rejected if the difference in echo intensity among the four beams exceeded this threshold.

600 kHz (47.5m)

The ADCP, set to a beam frequency of 600 kHz, was configured in a burst sampling mode consisting of 80 pings per ensemble. The interval between each ping was 2 seconds so the ensemble length was also 160 seconds. The interval between ensembles was 10 minutes. Data were recorded in earth coordinates with a heading bias of 9.81° E used. This heading bias was corrected in post-deployment processing to a heading bias of 9.80° E. The threshold maximum was also set to 70 counts. Velocity data were rejected if the difference in echo intensity among the four beams exceeded this threshold.

3. ADCP data processing procedures

Binary files output from the ADCP were read and converted to MATLAB™ binary files using scripts developed by Eric Firing's ADCP lab (<http://current.soest.hawaii.edu>). The beginning of the raw data files were truncated to a time after the mooring anchor was released in order to allow time for the anchor to reach the seabed and for the mooring motions that follow the impact of the anchor on the sea floor to dissipate. The pitch, roll, and ADCP temperature were examined in order to pick reasonable times that ensured good data quality but without unnecessarily discarding too much data (see Figure 5-11 and Figure 5-12). Truncation at the end of the data files were chosen to be the ensemble prior to the time that the acoustic release signal was sent to avoid contamination due to the ascent of the instrument. The times of the first ensemble from the raw data, deployment and recovery time, along with the times of the truncated records of both deployments are shown in Table 5-6.

Table 5-6. ADCP record times (UTC) during WHOTS-10 deployment.

	300 kHz	600 kHz
Raw file beginning and end times	06-Jul-2013 00:00 21-Jul-2014 18:51:33	06-Jul-2013 00:00 21-Jul-2014 20:06:45
Deployment and recovery times	10-Jul-2013 19:34 in water 11-Jul-2013 04:26 anchor over 20-Jul-2014 16:23 release triggered 21-Jul-2014 03:12 on deck	10-Jul-2013 19:22 in water in water 11-Jul-2013 04:26 anchor over 20-Jul-2014 16:23 release triggered 21-Jul-2014 03:22 on deck
Processed data beginning and end times	11-Jul-2013 00:30 20-Jul-2014 14:20	11-Jul-2013 00:30 20-Jul-2014 14:20

ADCP Clock Drift

Upon recovery, the ADCP clocks were compared with the ship's time server and the difference between the two was recorded. It was found that for 300 kHz (SN 4891) ADCP the clock on the instrument was fast by 8 minutes 27 seconds. The clock on the 600 kHz (SN 1825) was fast by 3 minutes and 15 seconds. Past deployments of the ADCP's suggest these differences aren't unusual. Since the drift represents just one ensemble out of a total of over 58,000, no corrections were made. However this drift may be significant if the data are used for time

dependent analysis such as tidal or spectrum analysis; a drift correction needs to be applied in those cases.

Heading Bias

As mentioned in the ADCP configuration section, the data were recorded in earth coordinates. A heading bias, the angle between magnetic north and true north, can be included in the setup to obtain output data in true earth coordinates. Magnetic variation was obtained from the National Geophysical Data Center ‘Geomag’ calculator. (<http://www.ngdc.noaa.gov/seg/geomag>). For a year long deployment a constant value is acceptable because the change in declination is small, approximately $-0.02^{\circ} \text{ year}^{-1}$ at the WHOTS location. A heading bias of 9.81° was entered in the setup of the WHOTS-10 ADCP’s, but was corrected to 9.80° during post-deployment processing.

Speed of sound

Due to the constant of proportionality between the Doppler shift and water speed, the speed of sound needs only be measured at the transducer head (Firing, 1991). The sound speed used by the ADCP is calculated using a constant value of salinity (35) and the temperature recorded by the transducer temperature sensor of the ADCP. Using CTD profiles close to the mooring during HOT cruises, HOT-254 to HOT-263, and from the WHOTS deployment/recovery cruises, the mean salinity at 125 dbar was 35.31 while the mean salinity at 47.5 dbar was 35.38. Mean ADCP temperature at 125 dbar was 21.48°C and 25.03°C at 47.5 dbar (Figure 5-13). The maximum associated mean sound velocity difference is less than 0.4 m s^{-1} which represents a change of less than 0.03%, so no correction was made.

WHOTS-10: 11-Jul-2013 to 20-July-2014: WH 300HKz ADCP
 Temperature : Raw Data

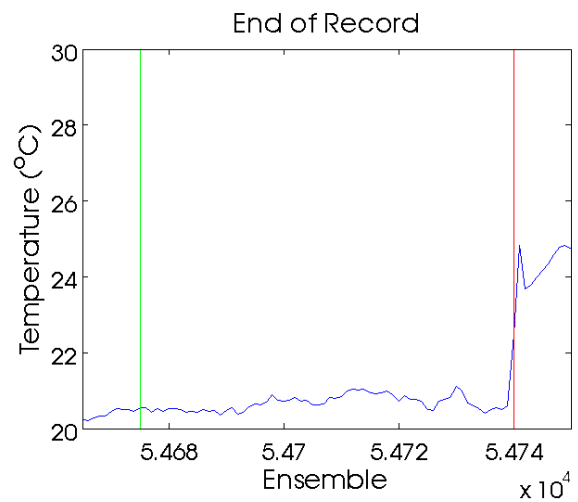
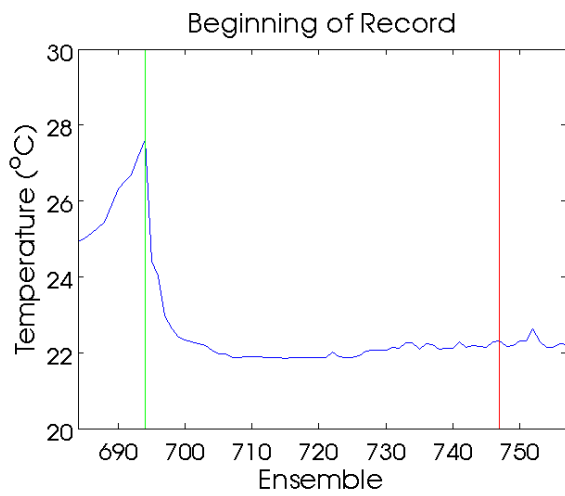
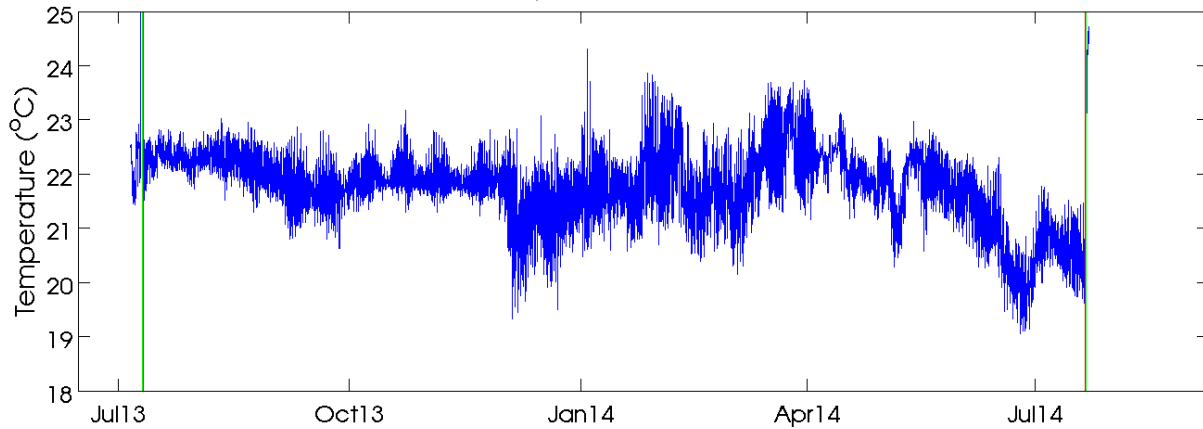


Figure 5-11. Temperature record from the 300 kHz ADCP during WHOTS-10 mooring (top panel). The bottom panel shows the beginning and end of the record with the green vertical line representing the in-water time during deployment and out-of-water time for recovery. The red line represents the anchor release and acoustic release trigger for deployment and recovery respectively.

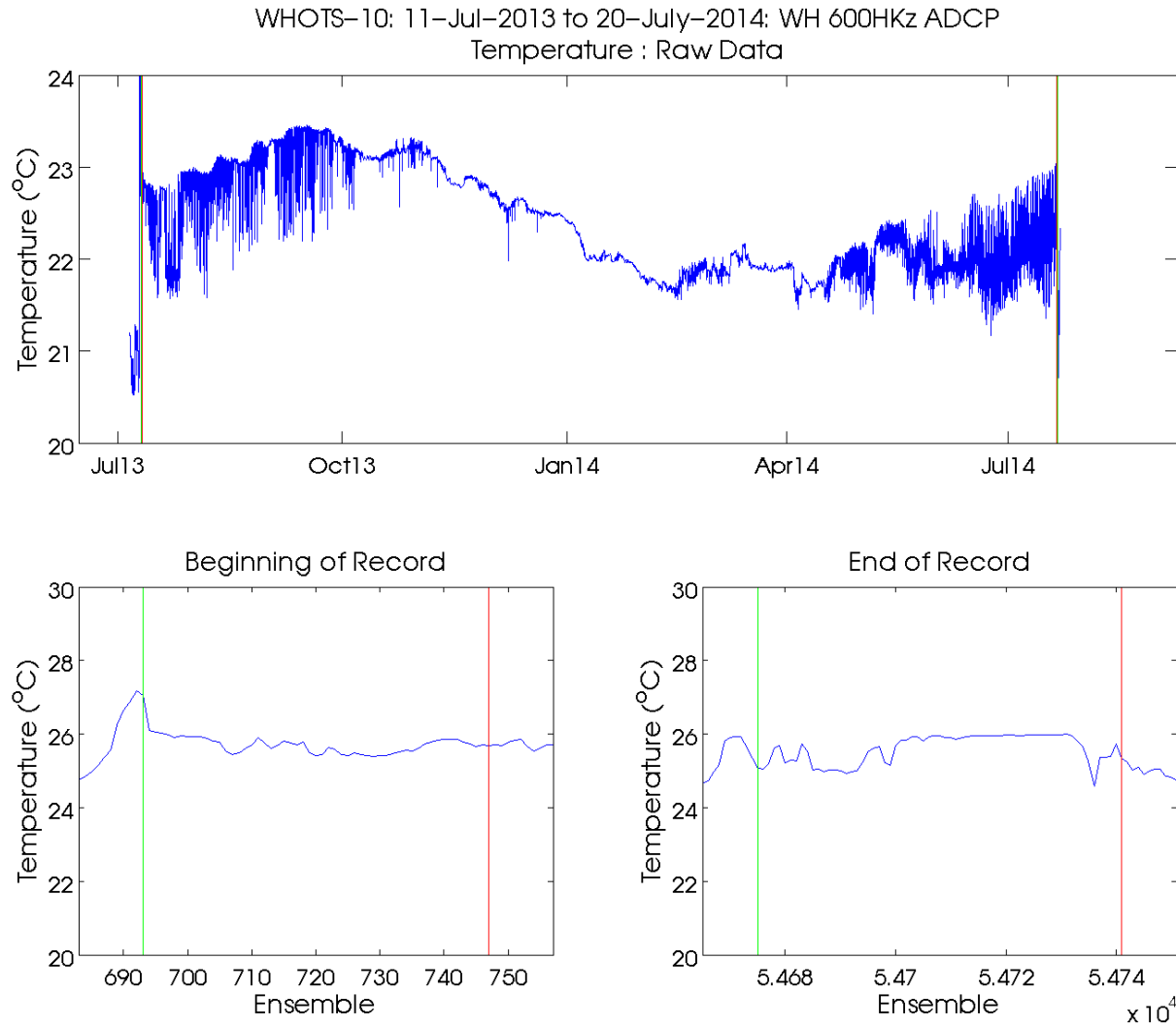


Figure 5-12. Same as Figure 5-26, but for the 600 kHz ADCP.

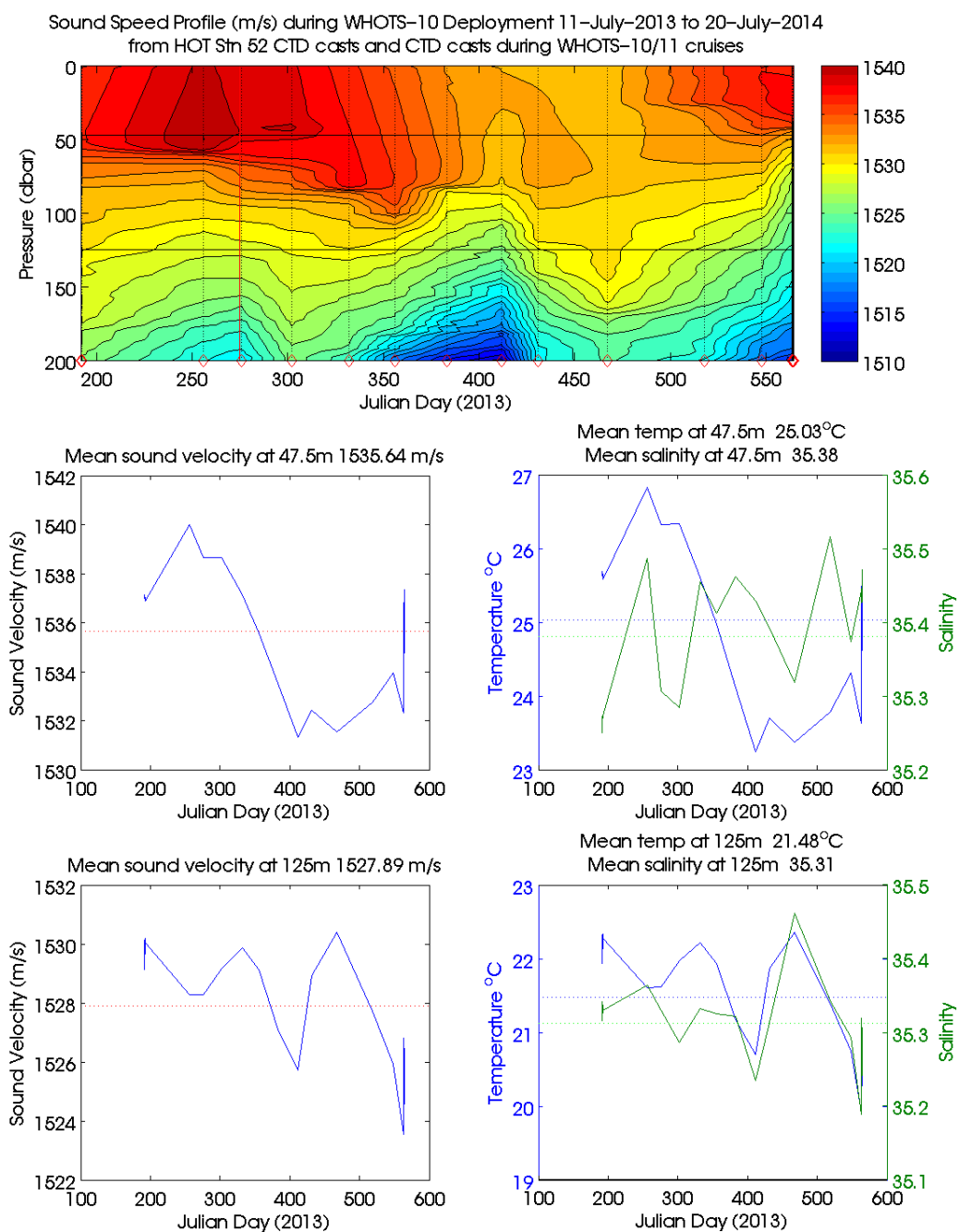


Figure 5-13. Sound speed profile (top panel) during the deployment of the WHOTS-10 mooring from 2 dbar CTD data taken during regular HOTS cruises and CTD profiles taken during the WHOTS-11 recovery/deployment cruise (individual casts marked with a red diamond). The bottom left panels show the sound velocity at the depth of the ADCP's (47.5 m and 125 m), with the mean sound velocity indicated with a red line. The lower right panels show the temperature and salinity at each ADCP depth for the time series with the mean temperatures indicated with blue lines and mean salinity indicated with green lines.

Quality Control

Quality control of the ADCP data involved the thorough examination of the velocity, instrument orientation and diagnostic fields to develop the basis of the QC flagging procedures. Details of the methods used can be found in the WHOTS Data Report 1 (Santiago-Mandujano et al., 2007). The following QC procedures were applied to the WHOTS-10 deployment ADCP data.

- 1) The first bin (closest to the transducer) is sometimes corrupted due to what is known as ringing. A period of time is needed for the sound energy produced during a transmit pulse at the transducer to dissipate before the ADCP is able to properly receive the returned echoes. The blanking interval is used to prevent useless data from being recorded. If it is too short, signal returns can be contaminated from the lingering noise from the transducer. The default value for the blanking interval, (expressed as a distance) of 1.76 m was used for the 300 kHz ADCP, whereas an interval of 0.88 m was used for the 600 kHz ADCP. Thus bin 1 was flagged and replaced with Not a Number (NaN) in the quality controlled dataset (Figure 5-14).

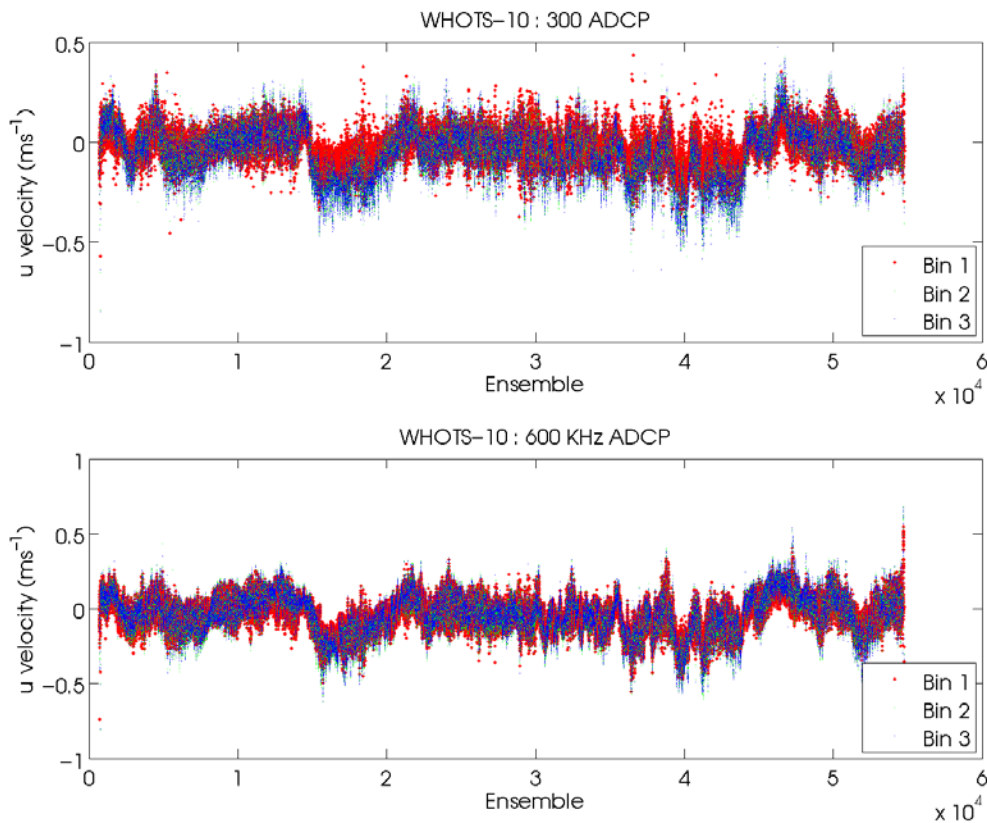


Figure 5-14. Eastward velocity component for the 300 kHz (top panel) and the 600 kHz (bottom panel) ADCPs showing the incoherence between depth 1 (red) and bins 2 (green) and 3 (blue).

- 2) For an upward-looking ADCP with a beam angle of 20° within range of the sea surface, the upper 6% of the depth range is contaminated with sidelobe interference (RDI, 1996). This is a result of stronger signal reflection from the sea surface (than from scatterers) overwhelming the sidelobe suppression of the transducer. Data are flagged using echo intensity (a measure of the strength of the return signal) from each beam to determine when the signal is contaminated with reflection from the sea surface. In practice, the majority of the data within the upper 4 bins ($\sim 14\%$ of the vertical range) were flagged. These upper 4 bins range from about 15 m up to the sea surface.
- 3) The use of four beams (along with instrument orientation) to resolve currents into their component earth-referenced velocities provides us with a second estimate of the vertical velocity. The scaled difference between these estimates is defined as the error velocity and it is useful for assessing data quality. Error velocities with an absolute magnitude greater than 0.15 m s^{-1} (a value comparable to the standard deviation of observed horizontal velocities) were flagged and removed.
- 4) An indication of data quality for each ensemble is given by the “percent good” data indicator which accompanies each individual beam for each individual bin. The use of the percent good indicator is determined by the coordinate transformation mode used during the data collection. With profiles transformed into earth coordinates (as in the case of the WHOTS-10 deployment) the percent good fields show the percentage of data that was made using 4 and 3 beam solutions in each depth cell within an ensemble, and the percentage that was rejected as a result of failing one of the criteria set during the instrument setup (see Appendix 1: WHOTS-10 300 kHz ADCP Configuration). Data were flagged when data in each depth cell within an ensemble made from 3 or 4 beam solutions was 20% or less.
- 5) Data were rejected using correlation magnitude, which is the pulse-to-pulse correlation (in ping returns) for each depth cell. If anyone beam had a correlation magnitude of 20 counts or less, that data point was flagged.
- 6) Histograms of raw vertical velocity data and partially cleaned data from the ADCP [see Figure 5-15 and the WHOTS Data Report 1 (Santiago-Mandujano et al., 2007)] showed vertical velocities larger than expected, some exceeding 1 m s^{-1} . Recall that the instruments’ burst sampling (4-second intervals for the 300 kHz and 2-second intervals for the 600 kHz, for 160 seconds every 10 minutes) was designed to minimize aliasing by occasional large ocean swell orbital motions (Section 3), and therefore are not the source of these large speeds in the data. These large vertical speeds are possibly fish swimming in the beams based on the histograms of the partially cleaned data; depth cells with an absolute value of vertical velocity greater than 0.3 m s^{-1} were flagged.

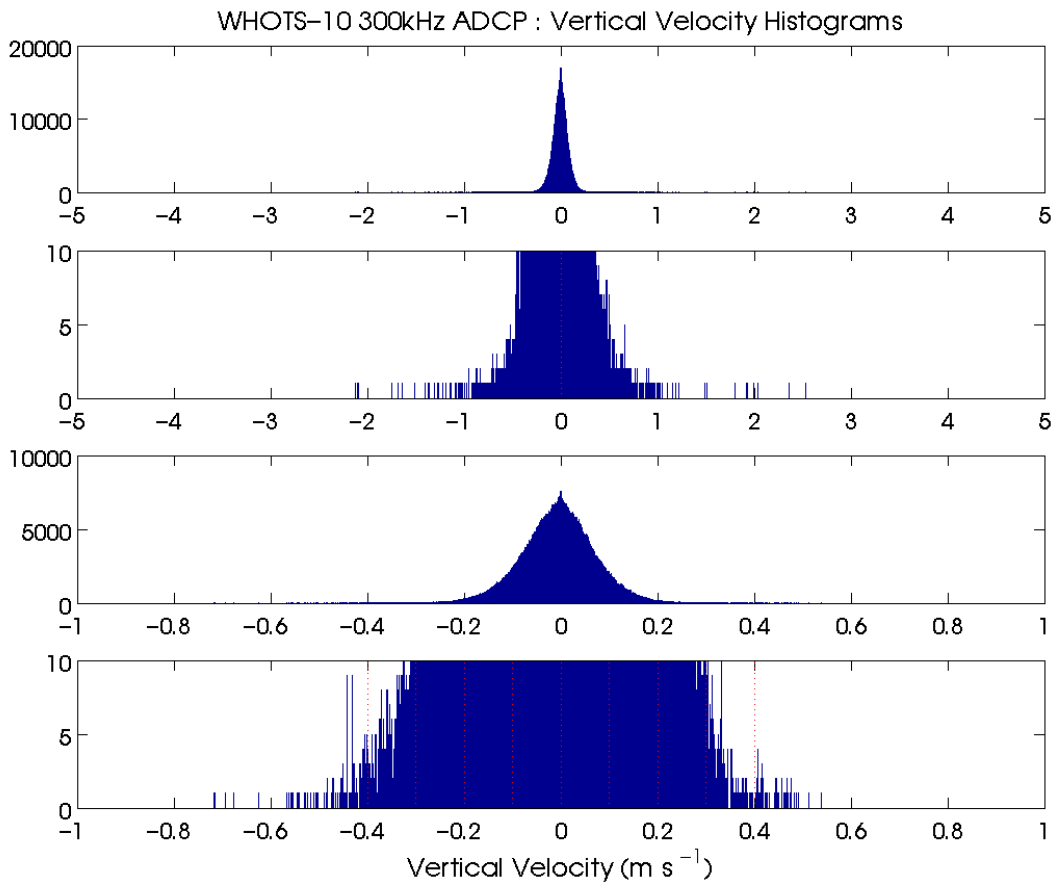


Figure 5-15. Histogram of vertical velocity of the 300 kHz ADCP for raw data (top panel) and enlarged for clarity (upper middle panel), and for partial quality controlled data (lower middle panel) and enlarged for clarity (bottom).

- 7) A quality control routine known as ‘edgers’ identifies outliers in surface bins using a five point median differencing method. The median velocity from surface bins was calculated for each ensemble, and then a five point running median of the surface bin median was calculated. This was then compared to individual velocity observations in the surface bins, and those differing by greater than 0.48 m/s were flagged.
- 8) A 5-pole low pass Butterworth filter with a cutoff frequency of 1/4 cycles/hour was used upon the length of the time-series to isolate low frequency flow for each bin independently. The low frequency flow is then subtracted giving a time series of high frequency velocity component fluctuations for each bin. Data points were considered outliers when their values exceeded four standard deviations from the mean (for each bin) and were removed.
- 9) A median residual filter used a 7-point (70 minute) median differencing method to define velocity fluctuations. A 7-point running median is calculated for each bin independently and the result is subtracted out giving time series of fluctuations relative

to the running median. Outliers greater than four standard deviations from the mean of the 7 points are flagged and removed for each bin.

- 10) Meticulous verification of all the quality control routines was performed through visual inspections of the quality controlled velocity data. Two methods were utilized; time-series of u and v components for multiple bins were evaluated as well as individual vertical profiles. The time-series methodology involved inspecting u and v components separately, five bins at a time, over 600 ensembles (100 hours). Any instance showing one bin behaving erratically from the other four bins was investigated further. If it seemed that there could be no reasonable rationale for the erratic points from the identified bin, the points were flagged [see Figure 5-16 and Figure 5-17 and the WHOTS Data Report 1 (Santiago-Mandujano et al., 2007)]. The intent of the vertical inspection of vertical profiles of the u and v components was to find entire profiles that were not aligned with neighboring profiles. Thirty u and v profiles were stacked at a time and were visually inspected for any anomalous data.

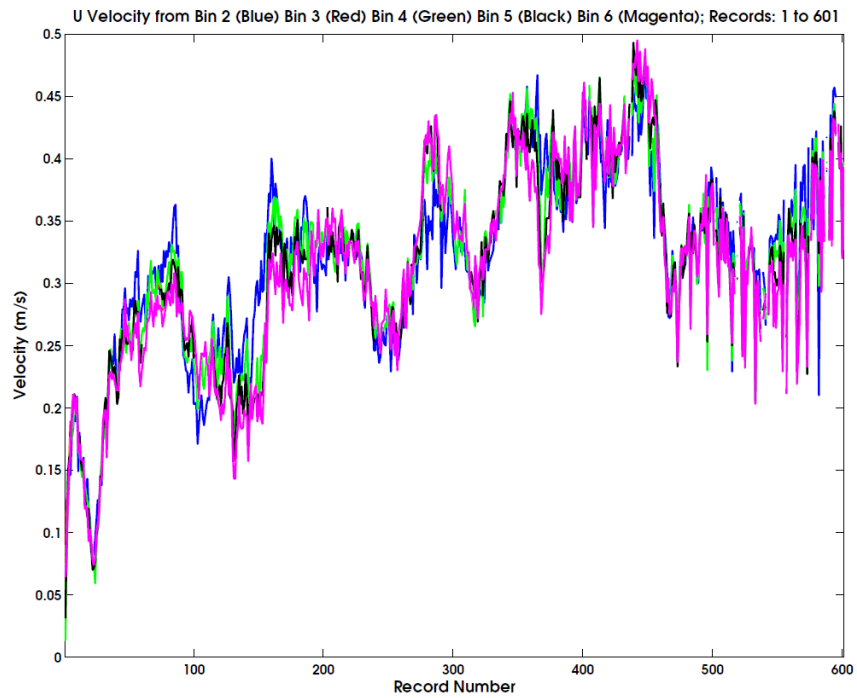


Figure 5-16. A sample of the horizontal inspection during WHOTS ADCP quality control

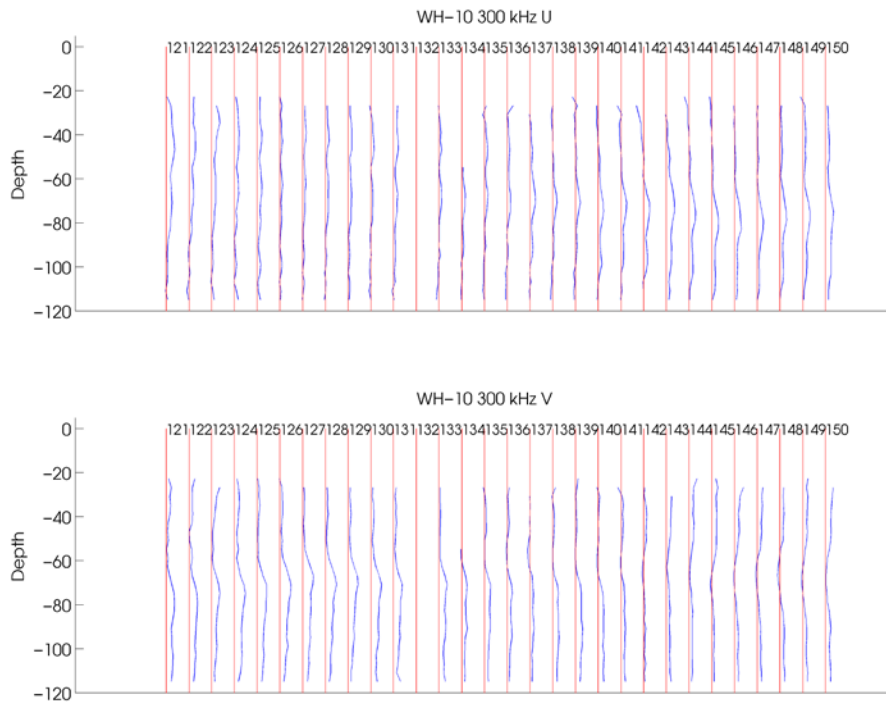


Figure 5-17. A sample of the profile consistency inspection from the WHOTS-10 ADCP quality control.

C. Vector Measuring Current Meter (VMCM)

Vector measuring current meters (VMCM) were deployed on the WHOTS-10 mooring at depths of 10 m and 30 m. VMCM data were processed by the WHOI/UOP group. A copy of the processing report is in Appendix 3 in Section 8.C. VMCM record times are shown in Table 5-7.

Table 5-7. Record times (UTC) for the VMCMs at 10 m and 30 m during the WHOTS-10 deployment

	WHOTS-10	
	VMCM016	VMCM019
Deployment and recovery times	10-Jul-2013 18:33 21-Jul-2014 05:12	10-Jul-2013 18:08 21-Jul-2014 05:24
Raw file beginning and end times	03-Jul-2013 18:53 24-Jul-2014 18:03	03-Jul-2013 18:55 24-Jul-2014 17:55

Daily (24 hour) moving averages of quality controlled 600 kHz ADCP data are compared to VMCM data interpolated to the ADCP ensemble times in the top panels of Figure 5-18 through Figure 5-21, and the difference is shown in the middle panels. The absolute value of the mean difference plus or minus one standard deviation is shown at the top of the middle panel. Velocities are not compared if greater than 80% of the ADCP data within a 24 hour average was flagged. The absolute value of mean differences for all deployments and both velocity components varied between 4 and 5 cm/s for most of the deployment, increasing to 10 cm/s at the end. The VMCM data does appear to degrade after May 2014. Propeller fouling may have dampened VMCM velocity magnitudes. Velocity differences between the 10m VMCM and the 600 kHz ADCP were smaller in comparison to the 30m VMCM.

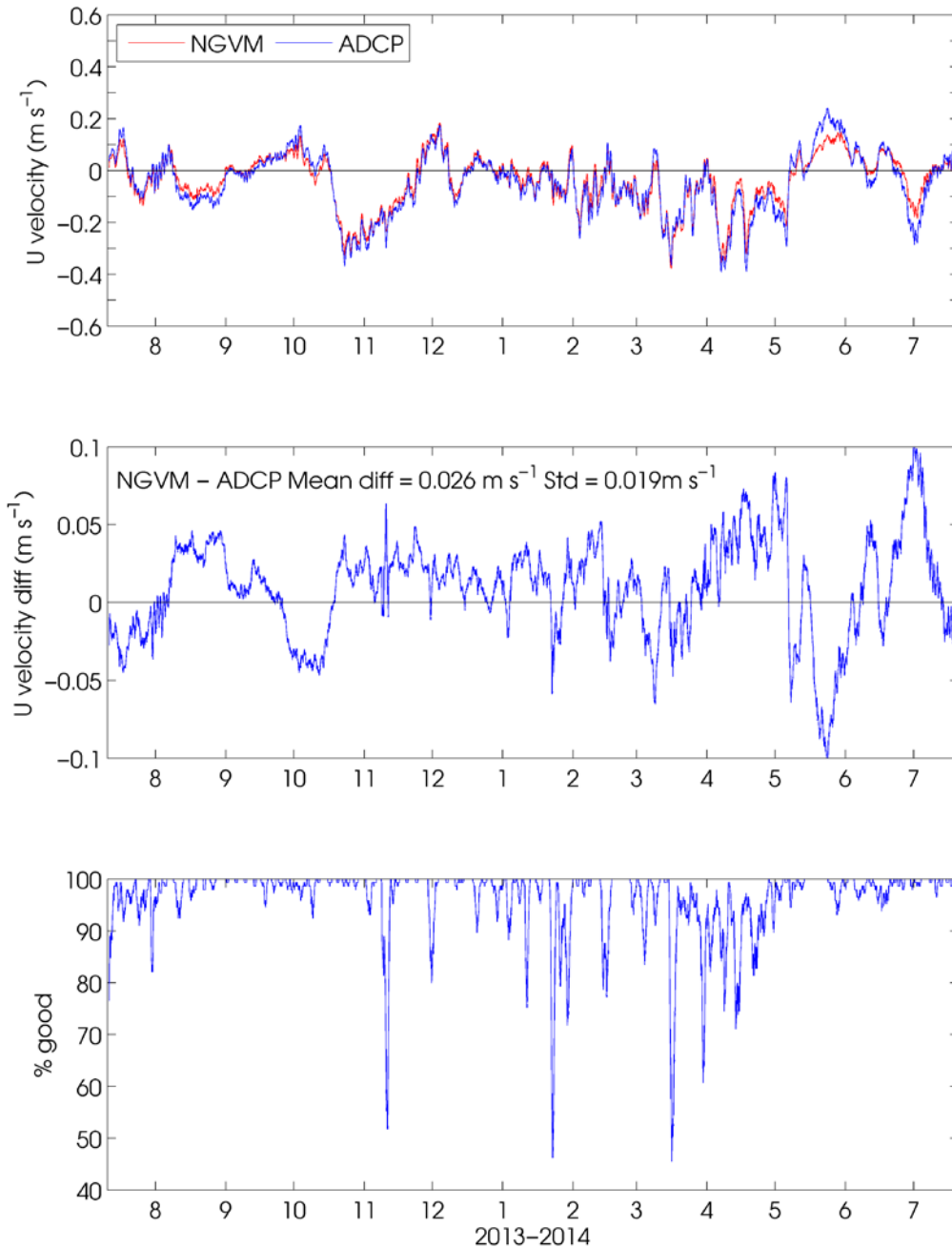


Figure 5-18. A comparison of 30 m VMCM and ADCP U velocity for WHOTS-10. The top panel shows 24 hour moving averages of VMCM zonal (U) velocity at 30 m depth (red) and ADCP U velocity from the nearest depth bin to 30 m (30.22 m). The middle panel shows the U velocity difference, and the bottom panel shows the percentage of ADCP data within the moving average not flagged by quality control methods. The dashed lines indicate a period of increased differences observed during spring months.

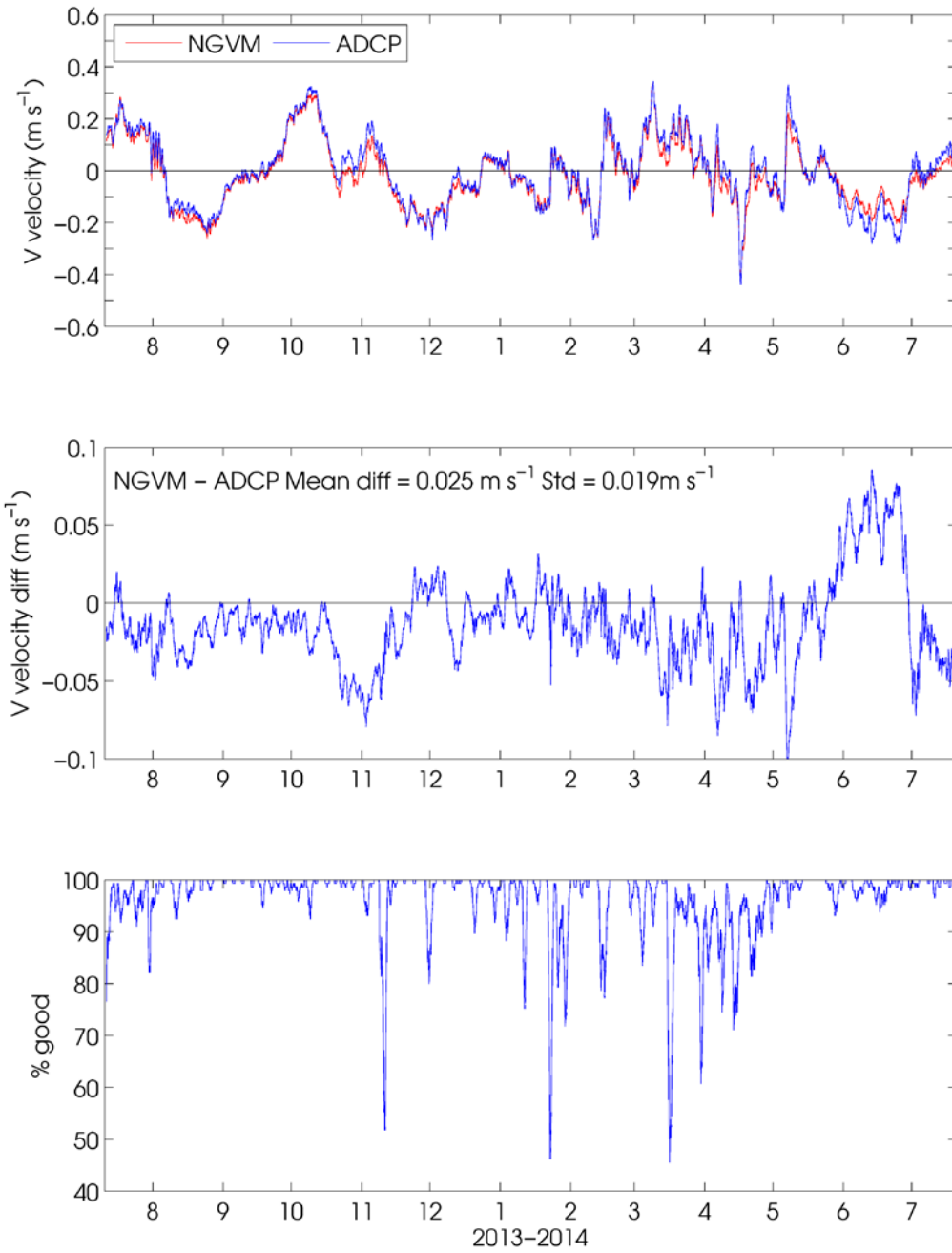


Figure 5-19. Same as in Figure 5-18 but for the meridional (V) velocity component.

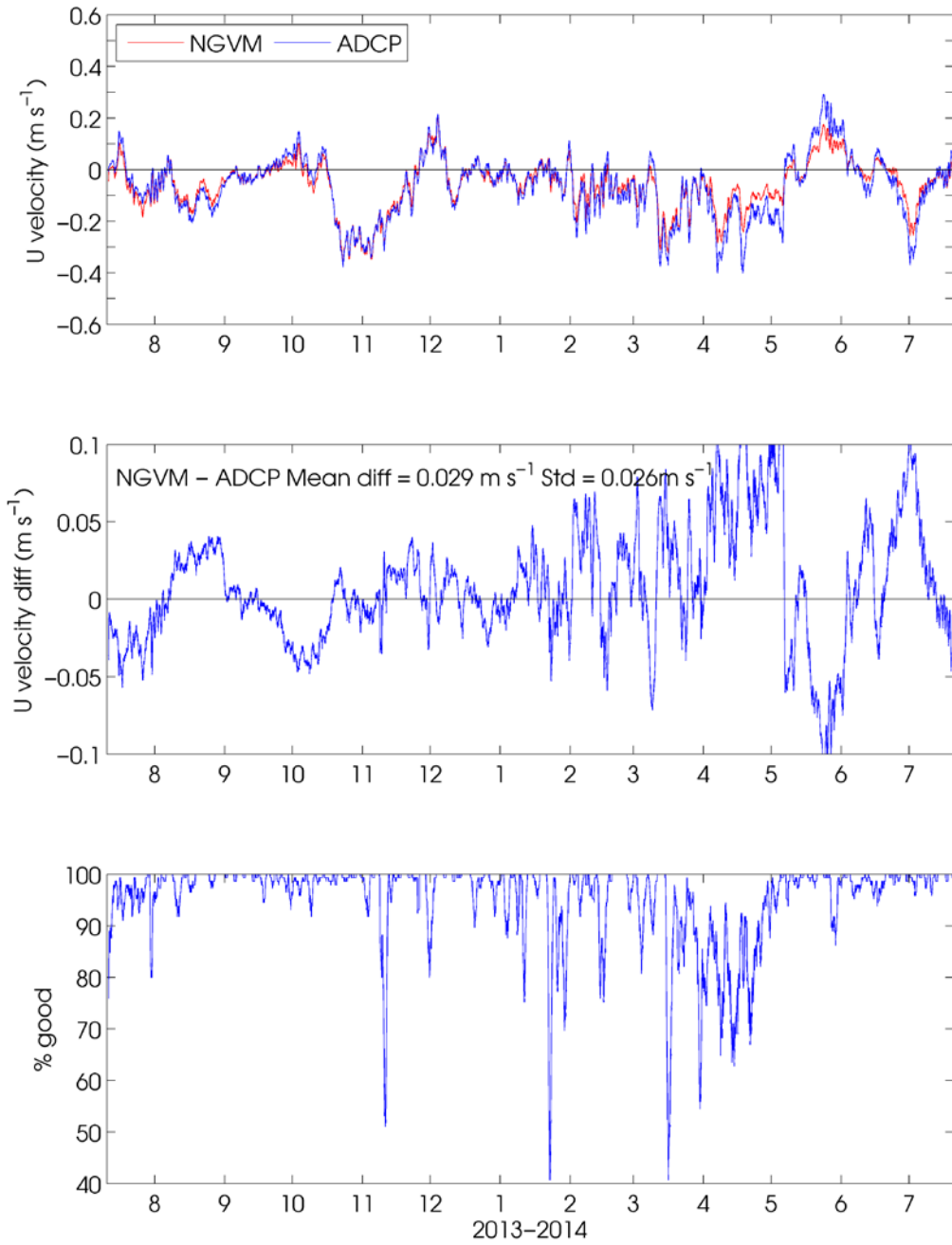


Figure 5-20. Same as in Figure 5-18 but for the 10 m VMCM.

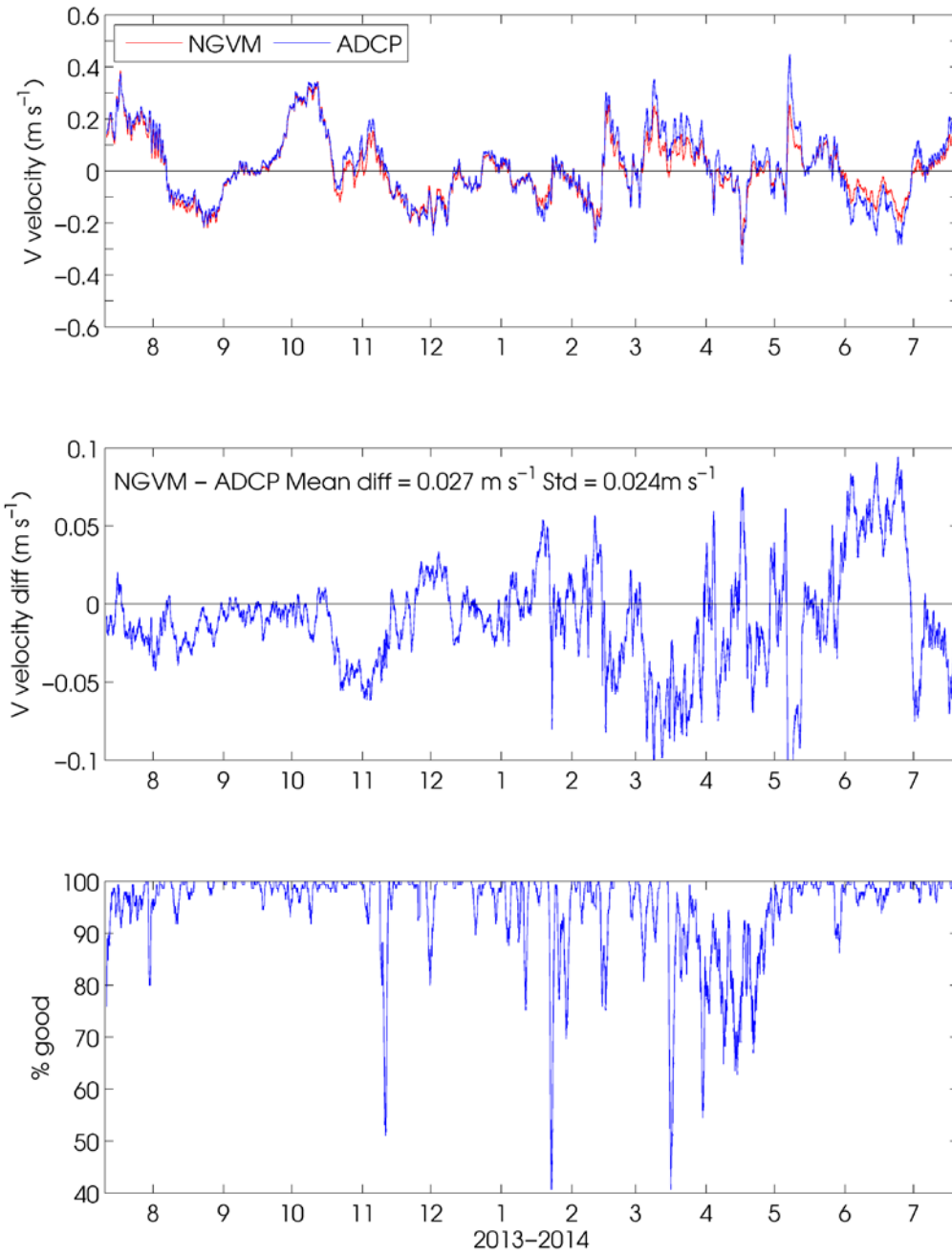


Figure 5-21. Same as in Figure 5-20 but for the V velocity component.

D. Global Positioning System Receiver and ARGOS Positions

A Xeos Global Positioning System receiver (SN 7580) and ARGOS beacon (SN 24576) were attached to the tower top of the buoy during the WHOTS-10 deployment. Data returns from the receivers were high.

Table 5-8. GPS and ARGOS record times (UTC) during WHOTS-10

WHOTS-10	Xeos GPS	ARGOS
Raw file beginning and end times	11-Jul-2013 06:11 22-Jul-2014 08:05	12-Jul-2013 06:04 20-Jul-2014 16:22

ARGOS positions were available during the WHOTS-10 deployment and they provided additional information on the buoy's motion. ARGOS data were recorded at 10 minutes intervals, although there are some small gaps at repeated times present in the records. Samples taken before mooring deployment were eliminated. Data were screened for points that were greater than 2.5 nautical miles from the surveyed anchor positions for each deployment which was considered to be the buoy watch circle radius. The velocity magnitude was calculated and positions that resulted in speeds greater than 1 m s^{-1} were removed. Data were interpolated onto a regular time grid in order to compute spectra.

For comparison, Figure 5-22 shows the ARGOS buoy's positions together with the GPS positions during the WHOTS-10 deployment. The standard deviation of the difference between these two records is about 380 m.

The ARGOS positions of the WHOTS-10 buoy for the duration of the deployment are in Figure 5-23 and shows the color-coded positions according to their data quality. The data quality is determined by its distance from the satellite track. Data of a better quality have a higher flag number: 3 is for a distance less than 150 m, 2 is for a distance between 150 and 350 m, and 1 is for a distance between 350 and 1000 m. For the duration of the deployment, the buoy had a mean position of about 3 km from the anchor, with a standard deviation of about 600 m.

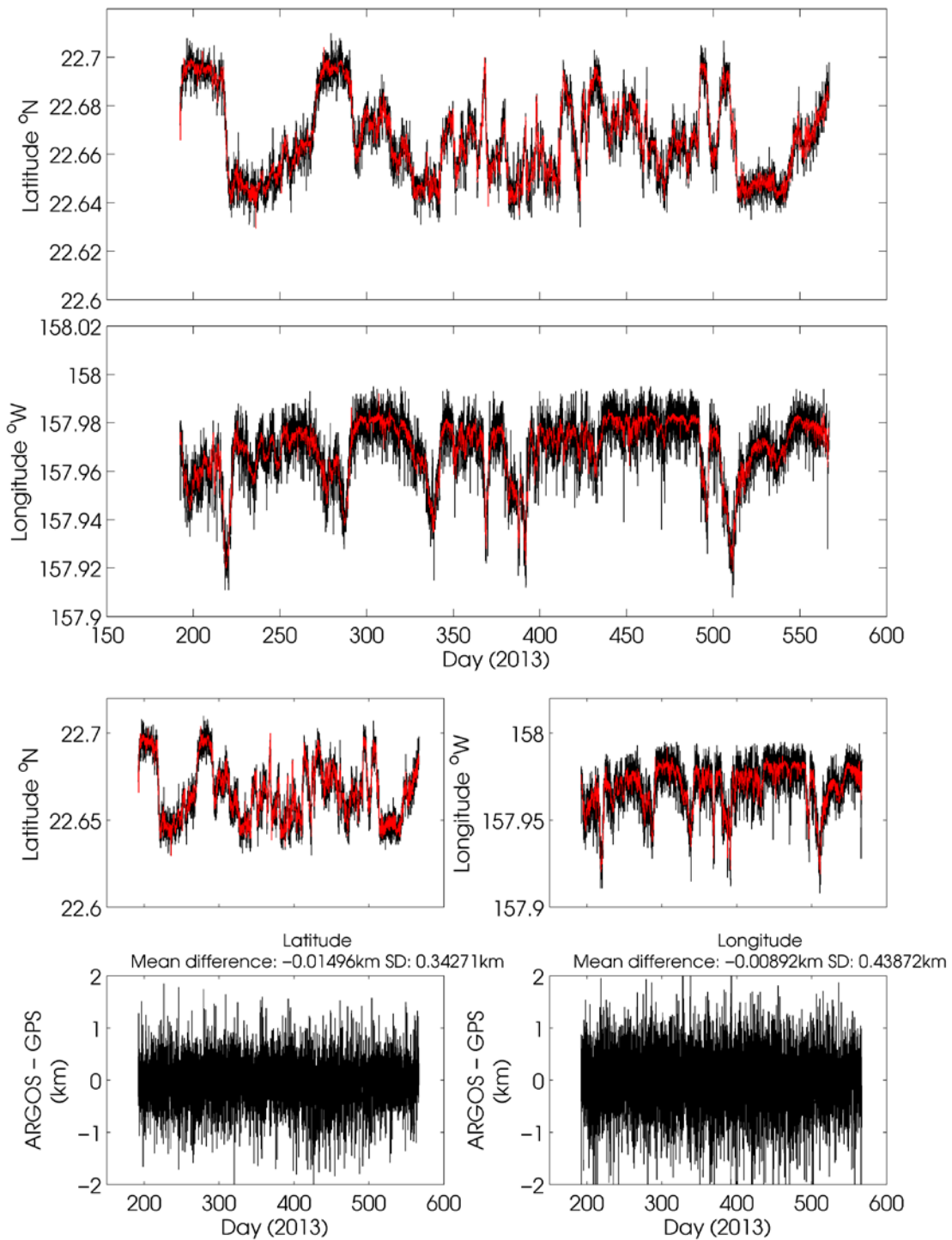


Figure 5-22. WHOTS-10 buoy position from ARGOS data (black line), and from GPS data (red line). The top and two middle panels show the latitude and longitude of the buoy. The bottom panel shows the difference between the GPS positions and the ARGOS positions interpolated to the GPS times.

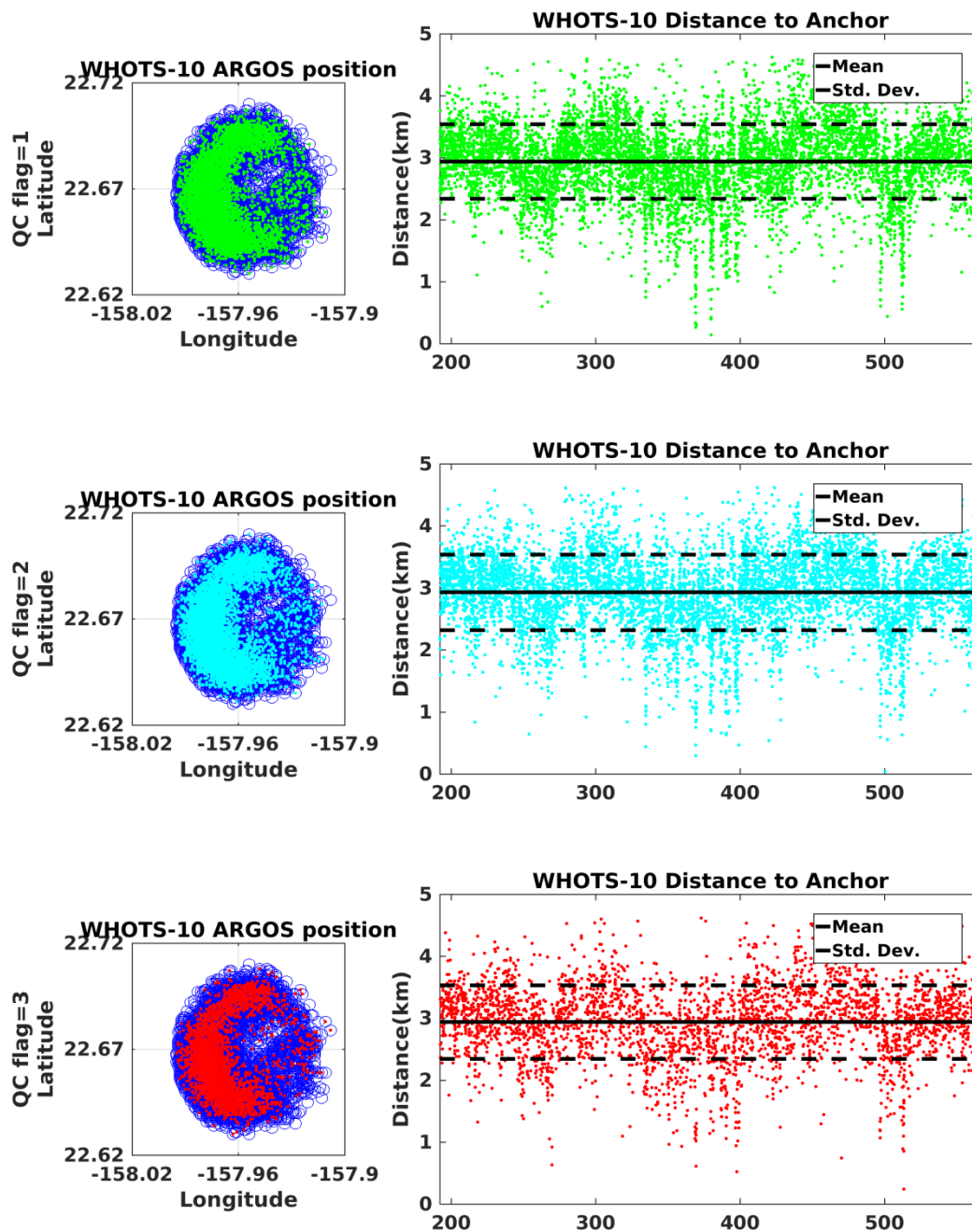


Figure 5-23. WHOTS-10 buoy ARGOS positions (circles, left panels), and distance from its anchor (dots, right panels). The data are colored according to their quality control flag, 1: green, 2: light blue, 3: red. The black circle in the center of the left side panels is the location of the mooring's anchor. The black line in the right panel plots is the mean distance between the buoy and its anchor, and the dashed line is the mean plus minus one standard deviation.

E. MAVS Acoustic Velocity Sensor

A Nobska MAVS acoustic velocity sensor (SN 10260) was deployed at 20 m on the WHOTS-10 mooring. Data return from the sensor was good until January 2014, when the velocity data show about a month of off-scale readings before returning to normal levels; data return ended in April 2014 (see Figure 5-24). Data from the 'A' and 'B' transducers lasted until recovery (transducer A wasn't working properly in January 2014), while transducers 'C' and 'D' failed in April (Figure 5-25). Data return issues have been observed in every deployment of the MAVS instrumentation on the WHOTS mooring. This failure has been evaluated by Nobska and it was determined that the bond between the piezoceramic transducer and the epoxy window delaminated, as electrically these transducers tested normal. This delaminated bond creates a thin air gap which separates the vibrating transducers from the water, attenuating the signal.

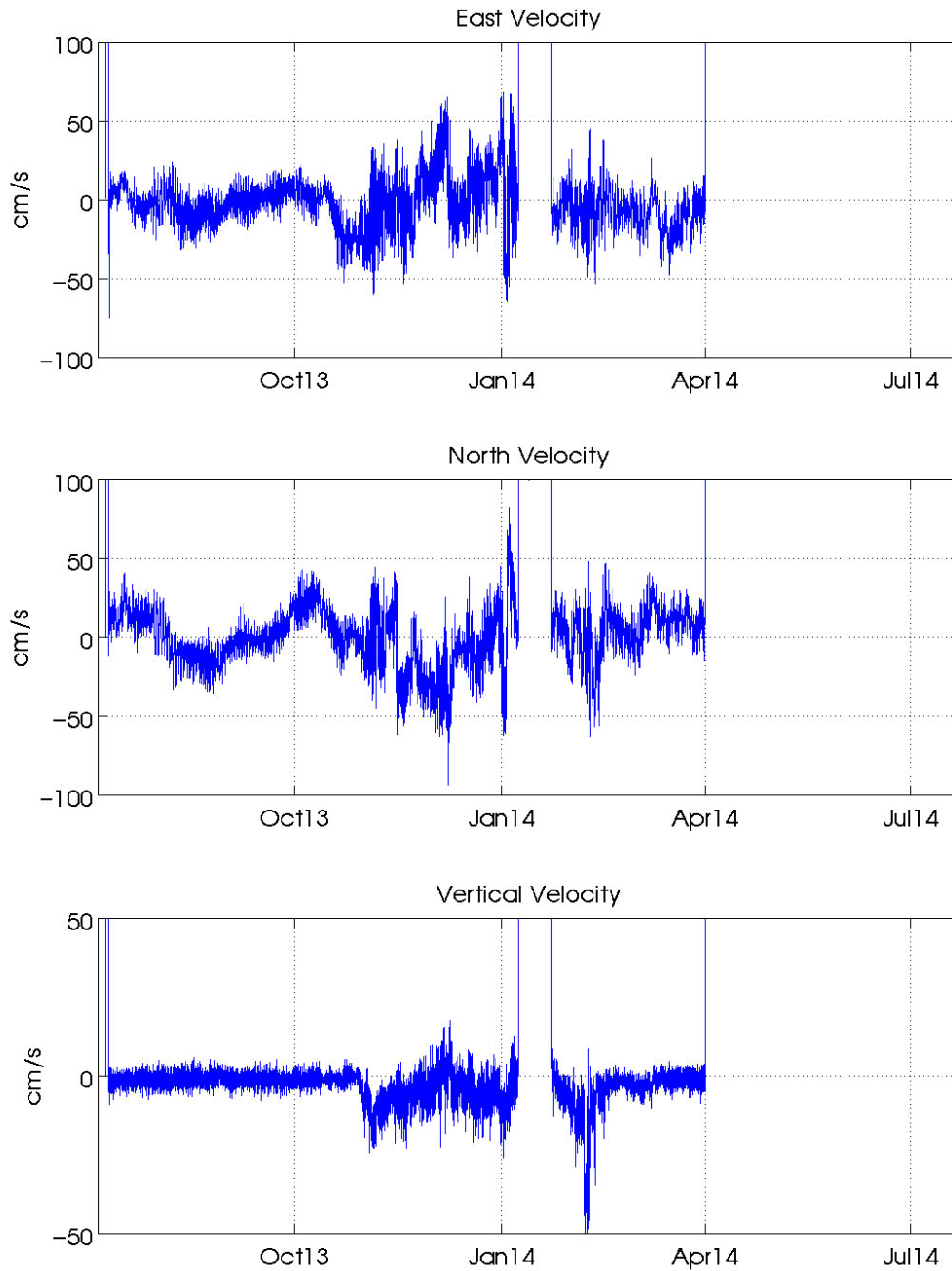


Figure 5-24. Eastward (upper panel), northward (middle panel), and upward velocity data (lower panel) as a function of time from the MAVS acoustic velocity sensor deployed at 20 m. Units are cm s^{-1}

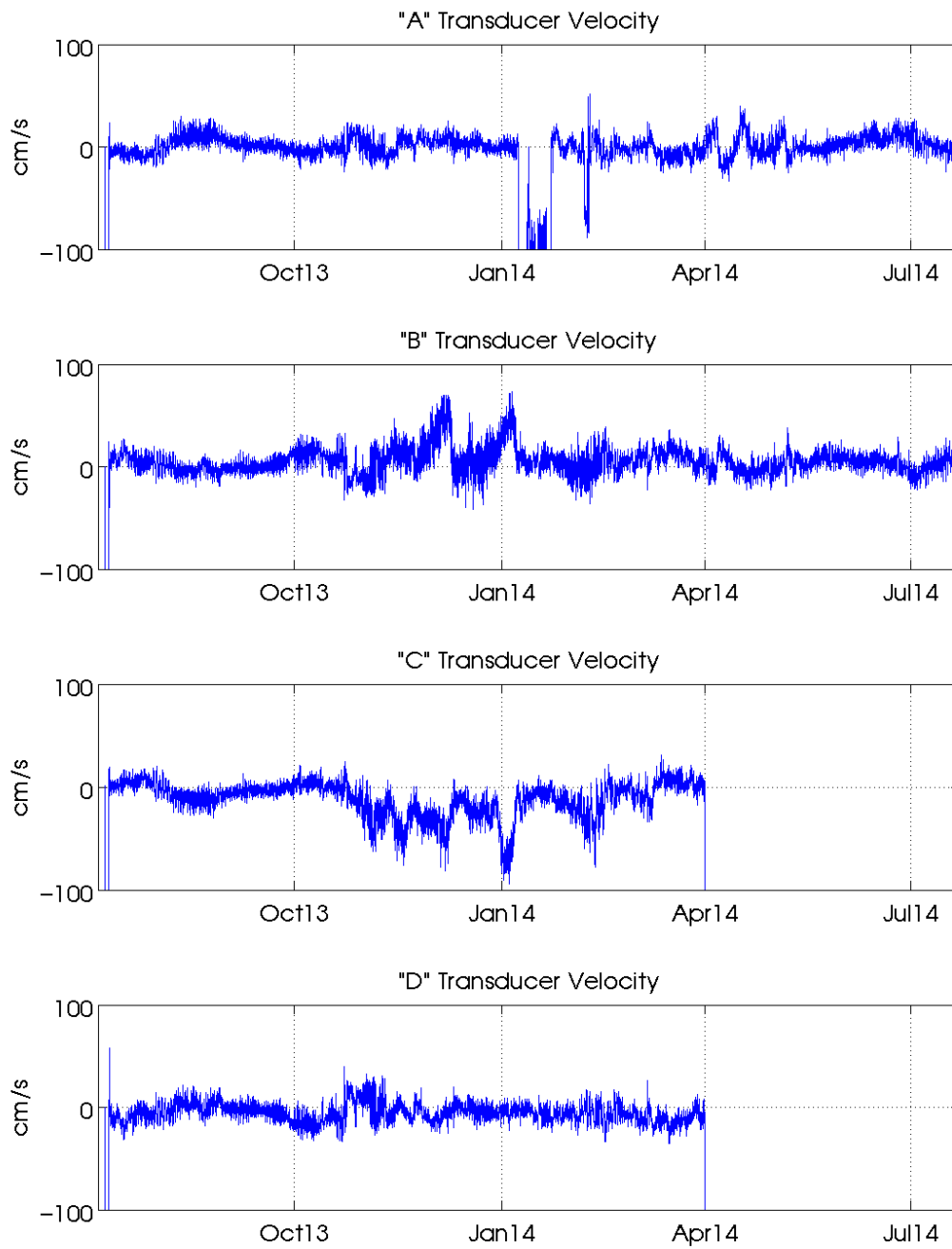


Figure 5-25. Time series of the raw acoustic velocity measured by each of the A, B, C and D transducers in $cm\ s^{-1}$ from the MAVS deployed at 20 m.

6. Results

During the WHOTS-10 cruise (WHOTS-10 mooring deployment), Station ALOHA was under the influence of the eastern North Pacific high pressure system. East-northeasterly trade winds were up to 25 kts on July 10, 2013, and slowed to 10-15 kts by July 14. A few intense squall lines with winds up to 25 kts and heavy rain passed through on July 14-15, causing an apparent drop in the sea surface salinity as indicated by the thermosalinograph record (Figure 6-12). Near-surface currents at Station ALOHA were strongly northward early on the cruise as shown by the shipboard ADCP data (Figure 6-24 and Figure 6-25), and turned NEward prior to recovery of the WHOTS-9 mooring, apparently associated with the spinup of a cyclonic eddy feature to the north of ALOHA that was interacting with an anticyclonic feature to the southeast. The developing eddy slowly moved towards the WSW as the anticyclone moved NNW. CTD casts conducted during the cruise (Figure 6-1 through Figure 6-5) showed a broad salinity maximum, with near-constant salinities between 50 and 200 dbar, and a small temperature gradient; conditions apparently associated with the anticyclonic eddy feature.

During the WHOTS-11 cruise (WHOTS-10 mooring recovery), Station ALOHA was under the influence of the eastern North Pacific high pressure system, and the associated east-northeasterly trade winds. Conditions were favorable for deployment of the WHOTS-11 mooring on 16 July, with 15-18 kt ENE winds. Weather conditions remained favorable during 17-19 July, with ENE wind speeds of 17 kts with occasional higher gusts. Tropical storm Wali started developing SE of Hilo, but weakened to below tropical storm status before reaching the islands. However Wali did cause overcast conditions and a few showers during the WHOTS-10 mooring recovery on 20 July causing an apparent drop in the sea surface salinity as indicated by the thermosalinograph record (Figure 6-14). Winds intensified to 20- 25 kts, with swells in the 8-10 ft range in the morning of the mooring recovery on 20 July, only to decrease to less than 10 kts soon after, and for the rest of the day. Winds were from the east in the 18-20 kt range on the morning of 22 July, but intensified to 25-40 kts with occasional higher gusts (up to 45 kts) for the rest of the day, causing the cancellation of additional CTD casts that were planned for that day. Near-surface currents were slightly westward during transit near Station ALOHA, turning NNEward at about 0.2 m/s during the WHOTS-11 mooring deployment, and fluctuating from NEward to NWward the rest of the cruise. There were no obvious cyclonic or anti-cyclonic eddies present, although a combination of internal semidiurnal and diurnal tides, along with near-inertial oscillations, were noticeable especially in vertical shear. CTD casts conducted near the moorings (Figure 6-6 through Figure 6-11), displayed a subsurface salinity maximum at 50 dbar.

The temperature MicroCAT records during the WHOTS-10 deployment (Figure 6-16 through Figure 6-19) show obvious seasonal variability in the upper 100 m, and a sudden drop during July 2013, between 35 and 65 m. The salinity records (Figure 6-20 through Figure 6-23) do not show an obvious seasonal cycle, but two instances of salinity decrease were recorded during October-November 2013 and April-May 2014 by the instruments located above 100 m.

Figure 6-28a and Figure 6-28b show contours of the WHOTS-10 MicroCAT data in context with data from the previous 9 deployments. The seasonal cycle is obvious in the temperature record, with record temperatures (higher than 26 °C) in the summer of 2004, and to a minor extent in the summer of 2005. Salinities in the subsurface salinity maximum were relatively low

during the first 6 years of the record, only to increase drastically after 2008, with some episodes of lower salinity in mid-2011, early 2012, April 2013 and April 2014. The salinity maximum extended to near the surface during some instances in early 2010, 2011, late 2012-early 2013, during February-March 2013, August-September 2013 and late 2013-early 2014. When plotted in σ_θ coordinates (Figure 6-28b), the salinity maximum seems to be centered roughly between 24 and 24.5 σ_θ .

Records from the WHOTS-10 SeaCATs (Figure 6-29) deployed near the bottom of the mooring (4728 m) detected temperature and salinity changes related to episodic ‘cold events’ apparently caused by bottom water moving between abyssal basins (Lukas et al., 2001). These events are being monitored by instruments at the ALOHA Cabled Observatory (ACO, Howe et al., 2011), a deep water observatory located at the bottom of Station ALOHA (about 6 nautical miles north from the WHOTS-10 anchor), since June 2011. Figure 6-29 shows temperature and salinity records from the WHOTS-10 SeaCATs superimposed on the ACO data. The SeaCAT data agreed with the temperature and salinity variability registered by ACO instruments during the WHOTS-10 period. Sudden drops in temperature of about 0.020 C occurred in September 2013 and January 2014, followed by a slow increase to “normal” temperatures lasting about 5 months. A sudden temperature drop followed by a fast recovery was also recorded on July 2014. These drops in temperature were accompanied by an increase in salinity.

Figure 6-33 through Figure 6-35 show time series of the zonal, meridional, and vertical currents recorded with the moored ADCPs during the WHOTS-10 deployment, and Figure 6-58 shows the currents at 10 and 30 m collected by the VMCMs. Figure 6-30 through Figure 6-32 show contours of the ADCP current components in context with data from the previous deployments. In spite of the gaps in the data, an obvious variability is seen in the zonal and meridional currents, apparently caused by passing eddies. On top of this variability there have been periods of intermittent positive or negative zonal currents, for instance during 2007-2008. The contours of vertical current component (Figure 6-32) show a transition in the magnitude of the contours near 47 m, indicating that the 300 kHz ADCP located at 126 m moves more vertically than the 600 kHz ADCP located at 47.5 m.

A comparison between the moored ADCP data and the shipboard ADCP data obtained during the WHOTS-10 cruise is shown in Figure 6-36 and Figure 6-37. Some of the differences seen especially in the zonal component may be due to the mooring motion, which was not removed from the data. A comparison between the WHOTS-11 ADCP mooring data and the shipboard ADCP data during the WHOTS-11 cruise (WHOTS-10 mooring recovery) is shown in Figures 6-38 and 6-39. Comparisons between the shipboard ADCP from HOT cruises and the mooring data are compiled in Table 6-1, and shown in Figure 6-40 through Figure 6-57. The mean difference between moored and shipboard ADCP ranged between -0.05 and 0.05 m/s, with greater variability in zonal than in meridional velocities.

The motion of the WHOTS-10 buoy was registered by the Xeos-GPS receiver, and its positions are plotted in Figure 6-59. The buoy was located west of the anchor for the majority of the deployment, except for short periods in July, October, December 2013, and January and May 2014, when it was east of it. Power spectrum of these data (Figure 6-60) shows extra energy at the inertial period (~31 hr). Combining the buoy motion with the tilt (a combination of pitch

and roll) from the ADCP data (Figure 6-61), showed that the tilt increased as the buoy distance from the anchor increased. This was expected since the inclination of the cable increases as the buoy moves away from the anchor.

A. CTD Profiling Data

Profiles of temperature, salinity and potential density (σ_θ) from the casts obtained during the WHOTS-10 deployment cruise near the moorings are presented in Figure 6-1 through Figure 6-5, together with the results of bottle determination of salinity. Figure 6-6 through Figure 6-11 correspond to the CTD profiles during the WHOTS-11 cruise.

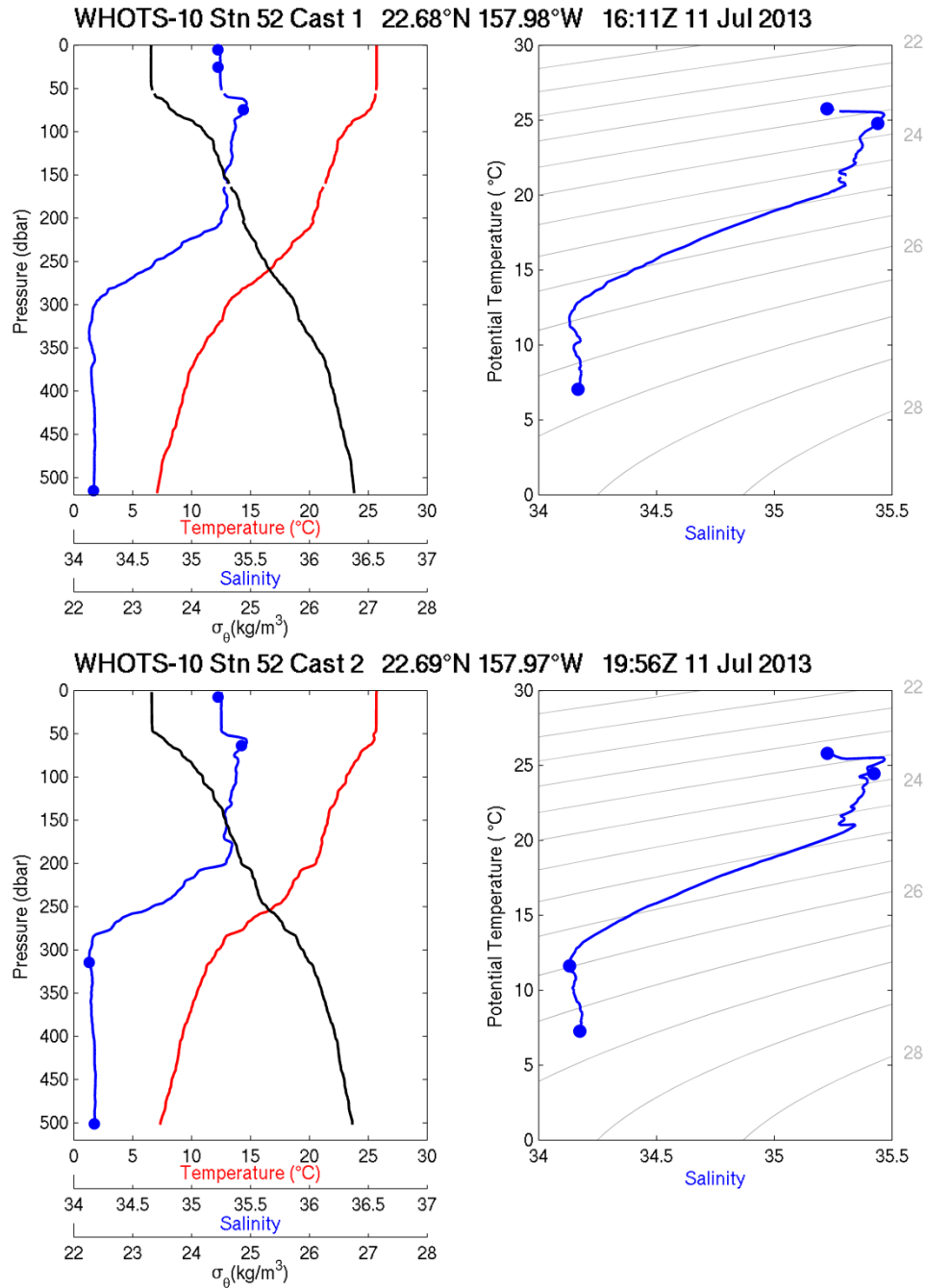


Figure 6-1. [Upper left panel] Profiles of CTD temperature, salinity, and potential density (σ_θ) as a function of pressure, including discrete bottle salinity samples (when available) for station 52 cast 1 during the WHOTS-10 cruise. [Upper right panel] Profiles of CTD salinity as a function of potential temperature, including discrete bottle salinity samples (when available) for station 52 cast 1 during the WHOTS-10 cruise. [Lower left panel] Same as in the upper left panel, but for station 52 cast 2. [Lower right panel] Same as in the upper right panel, but for station 52 cast 2.

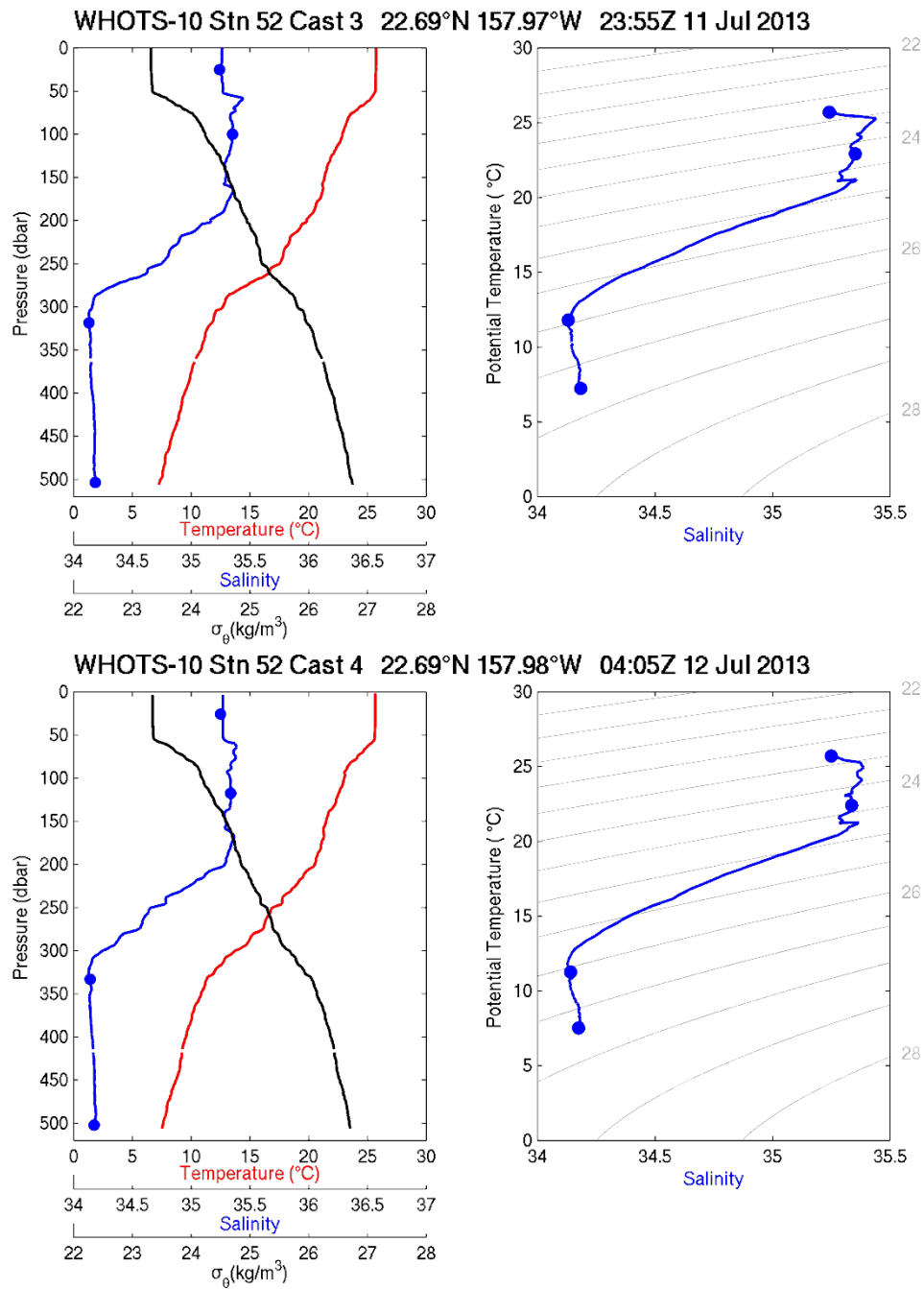


Figure 6-2. [Upper panels] Same as in Figure 6-1, but for station 52, cast 3. [Lower panels] Same as in Figure 6-1, but for station 52, cast 4.

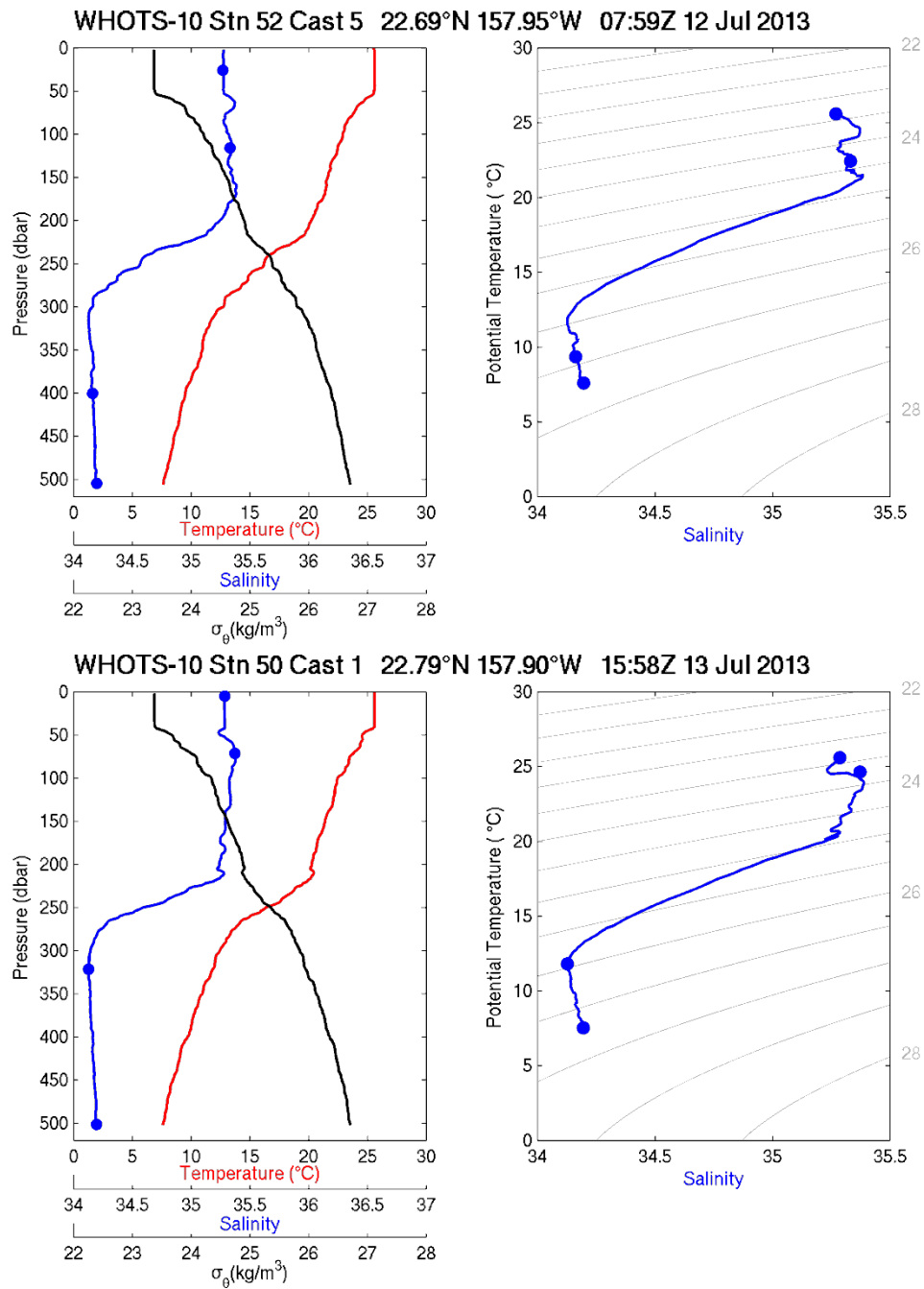


Figure 6-3. [Upper panels] Same as in Figure 6-1, but for station 52, cast 5. [Lower panels] Same as in Figure 6-1, but for station 50 cast 1.

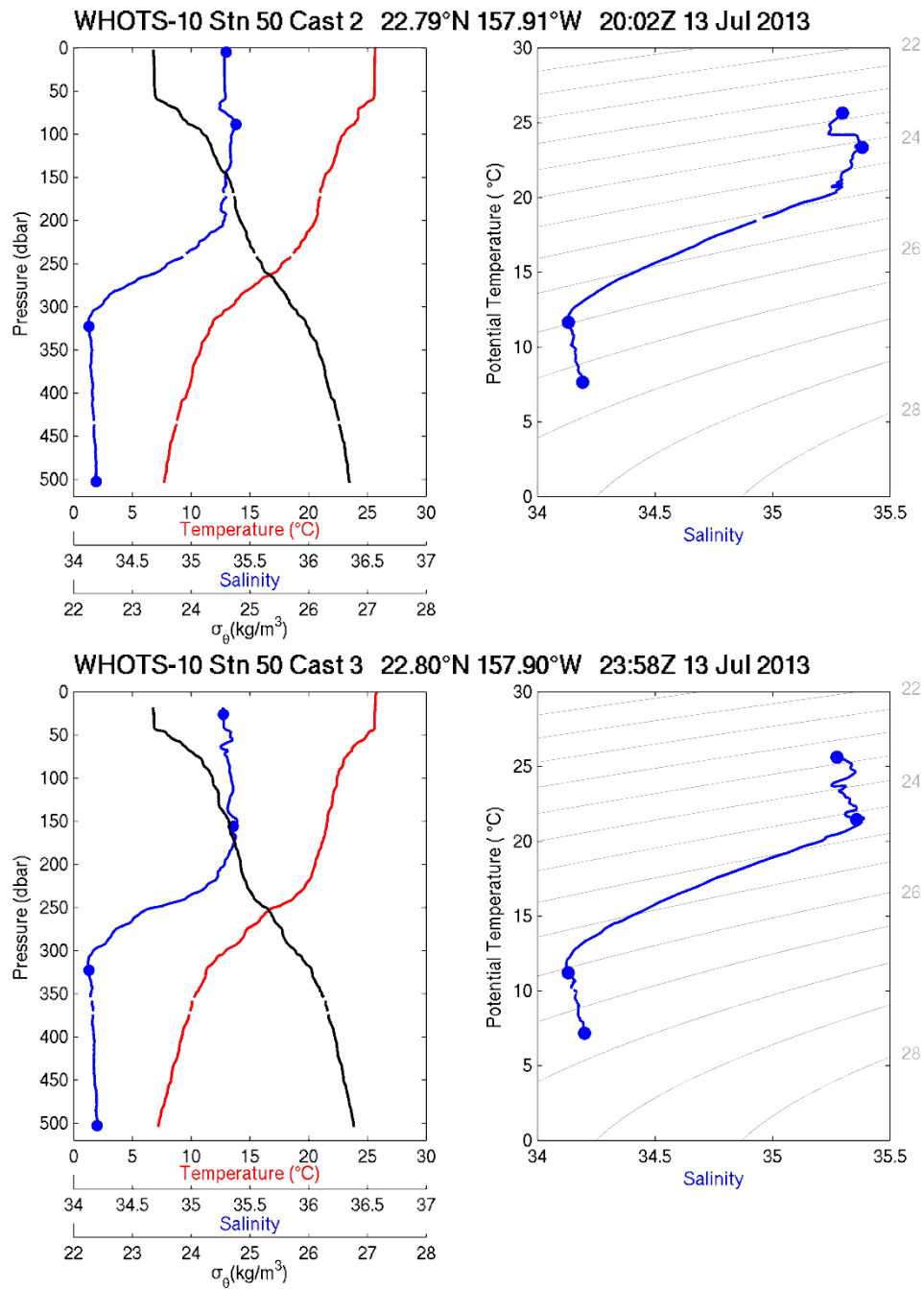


Figure 6-4. [Upper panels] Same as in Figure 6-1, but for station 50, cast 2. [Lower panels] Same as in Figure 6-1, but for station 50 cast 3.

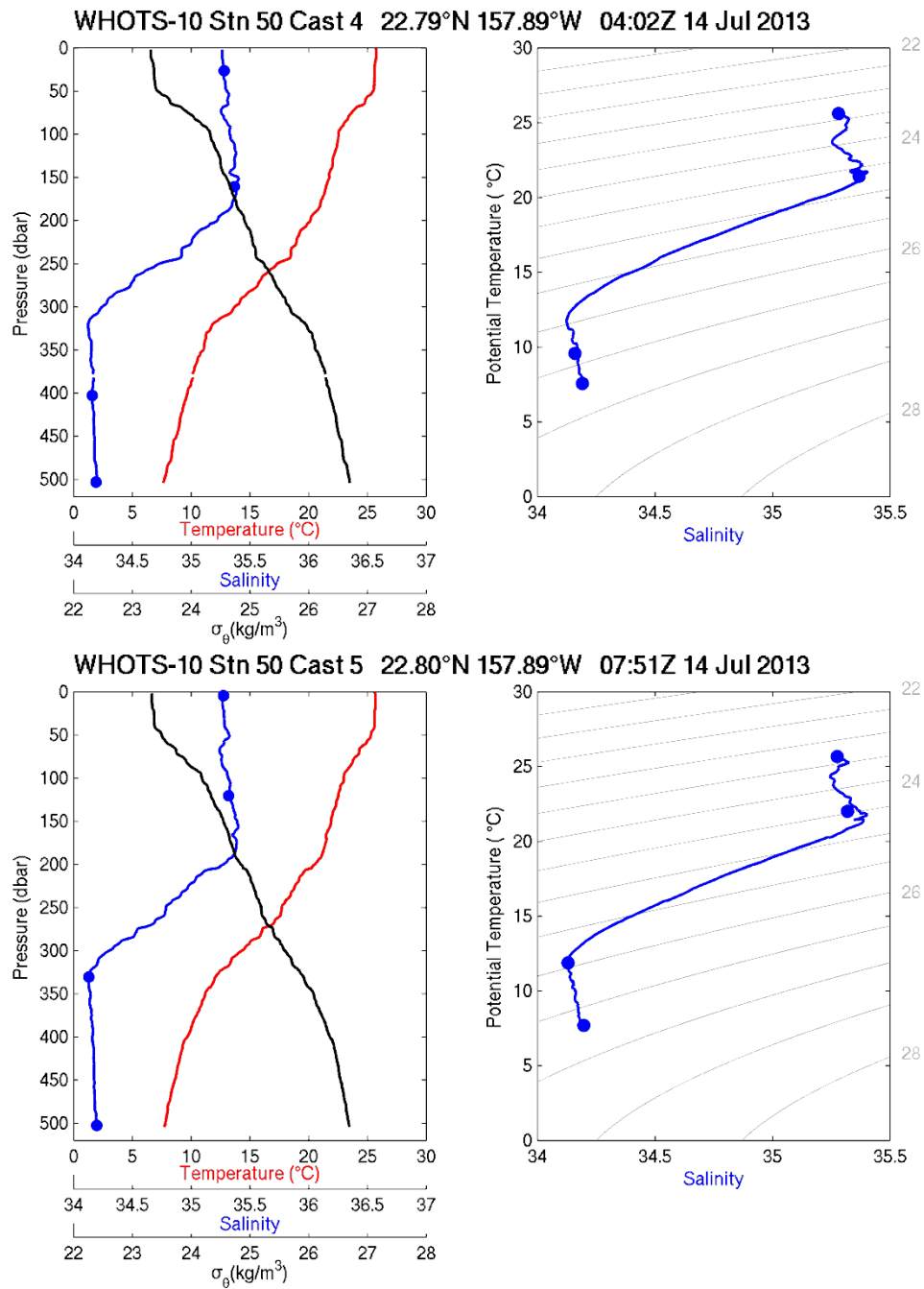


Figure 6-5. [Upper panels] Same as in Figure 6-1, but for station 50, cast 4. [Lower panels] Same as in Figure 6-1, but for station 50 cast 5.

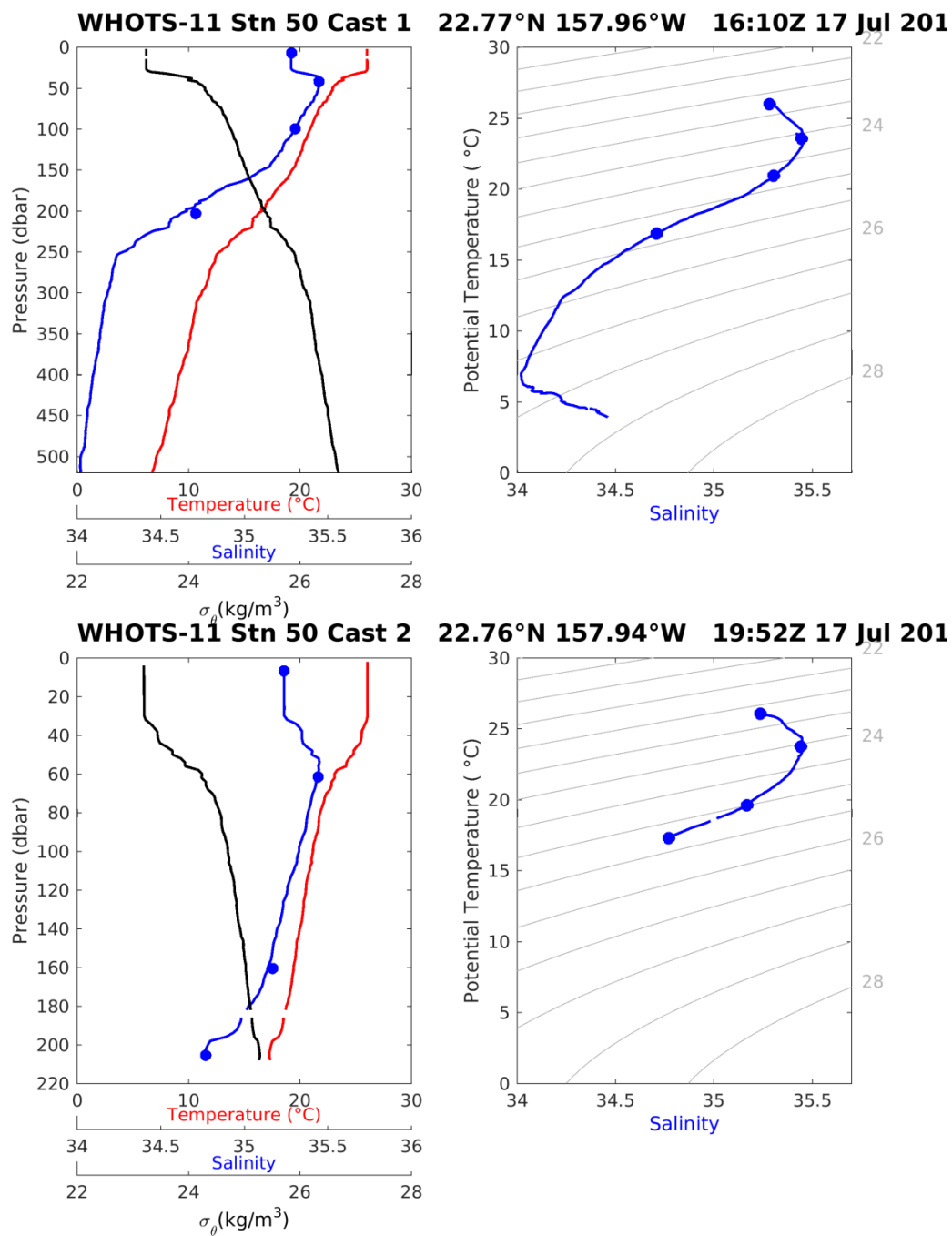


Figure 6-6. [Upper left panel] Profiles of CTD temperature, salinity, and potential density (σ_θ) as a function of pressure, including discrete bottle salinity samples (when available) for station 50 cast 1 during the WHOTS-11 cruise. [Upper right panel] Profiles of CTD salinity as a function of potential temperature, including discrete bottle salinity samples (when available) for station 50 cast 1 during the WHOTS-11 cruise. [Lower left panel] Same as in the upper left panel, but for station 50 cast 2. [Lower right panel] Same as in the upper right panel, but for station 50 cast 2.

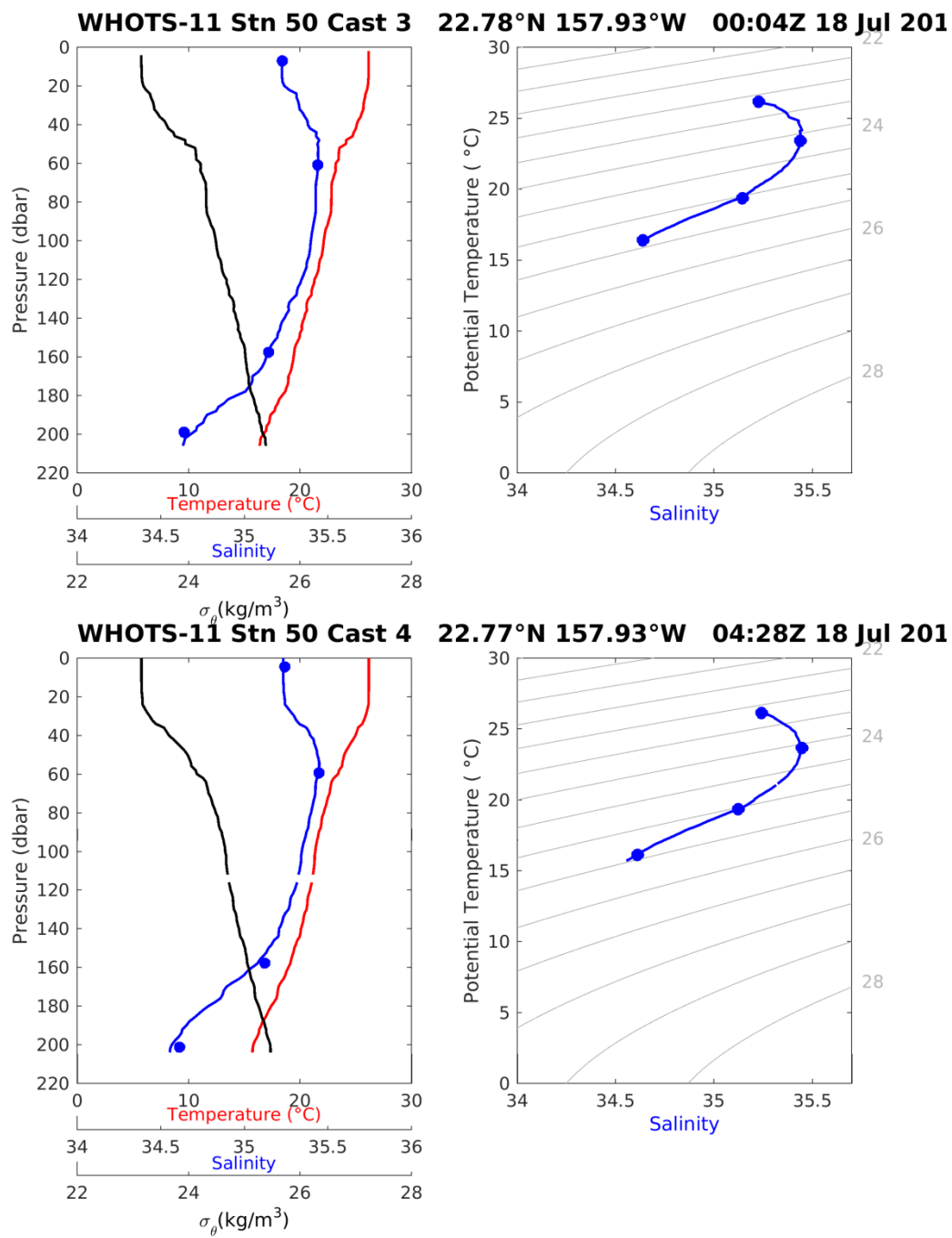


Figure 6-7. [Upper panels] Same as in Figure 6-6, but for station 50, cast 3. [Lower panels] Same as in Figure 6-6, but for station 50, cast 4.

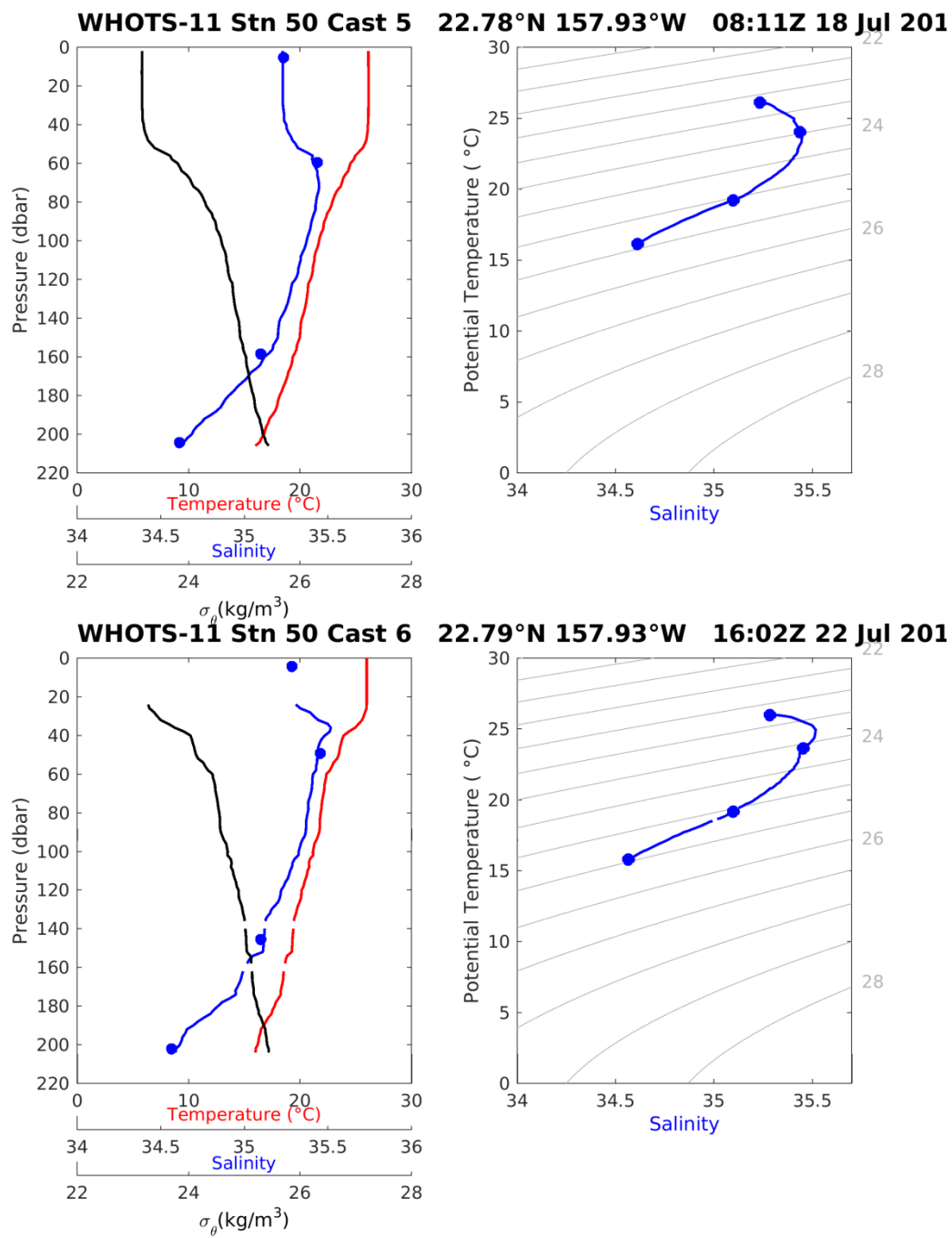


Figure 6-8. [Upper panels] Same as in Figure 6-6, but for station 50, cast 5. [Lower panels] Same as in Figure 6-6, but for station 50, cast 6.

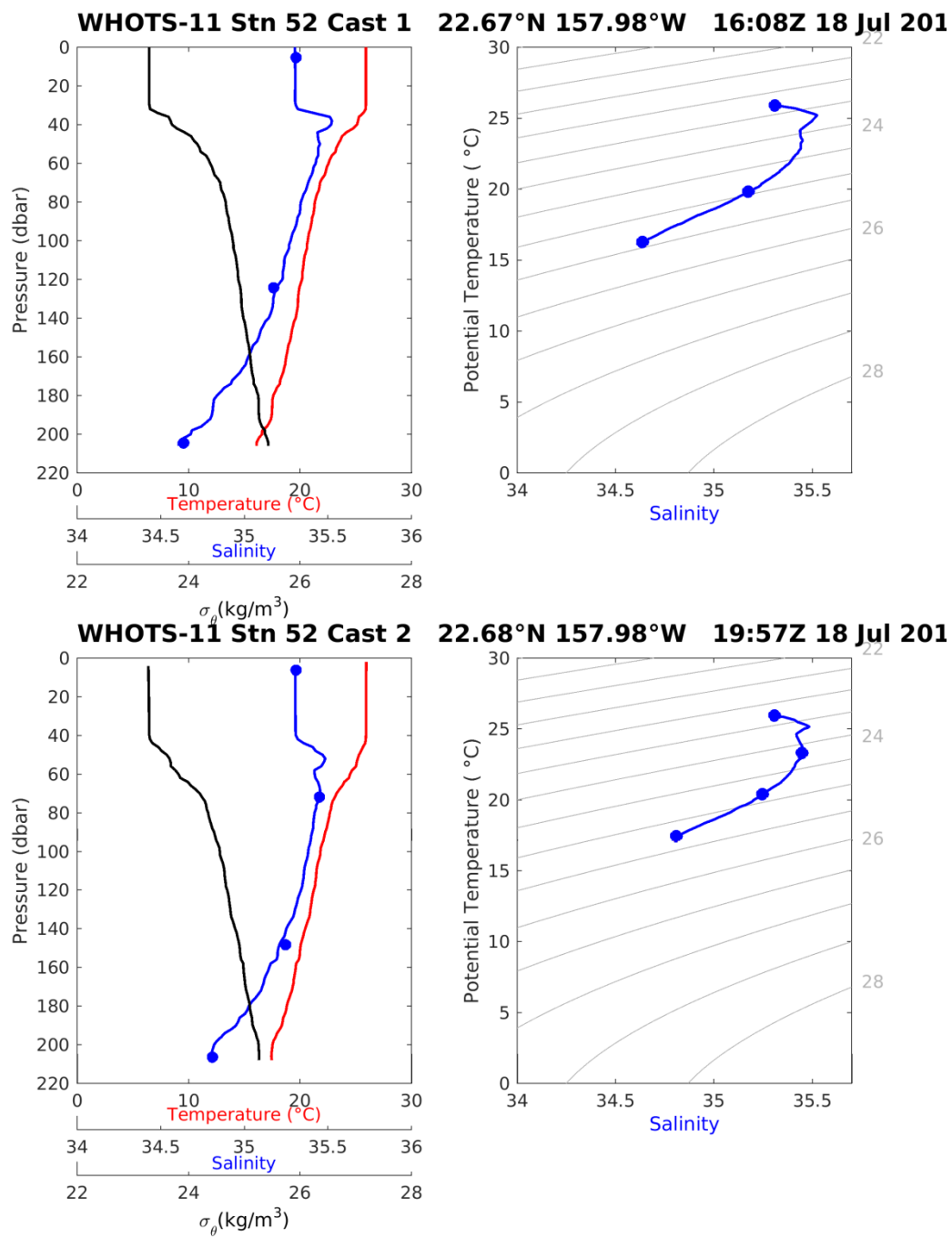


Figure 6-9. [Upper panels] Same as in Figure 6-6, but for station 52, cast 1. [Lower panels] Same as in Figure 6-6, but for station 52, cast 2.

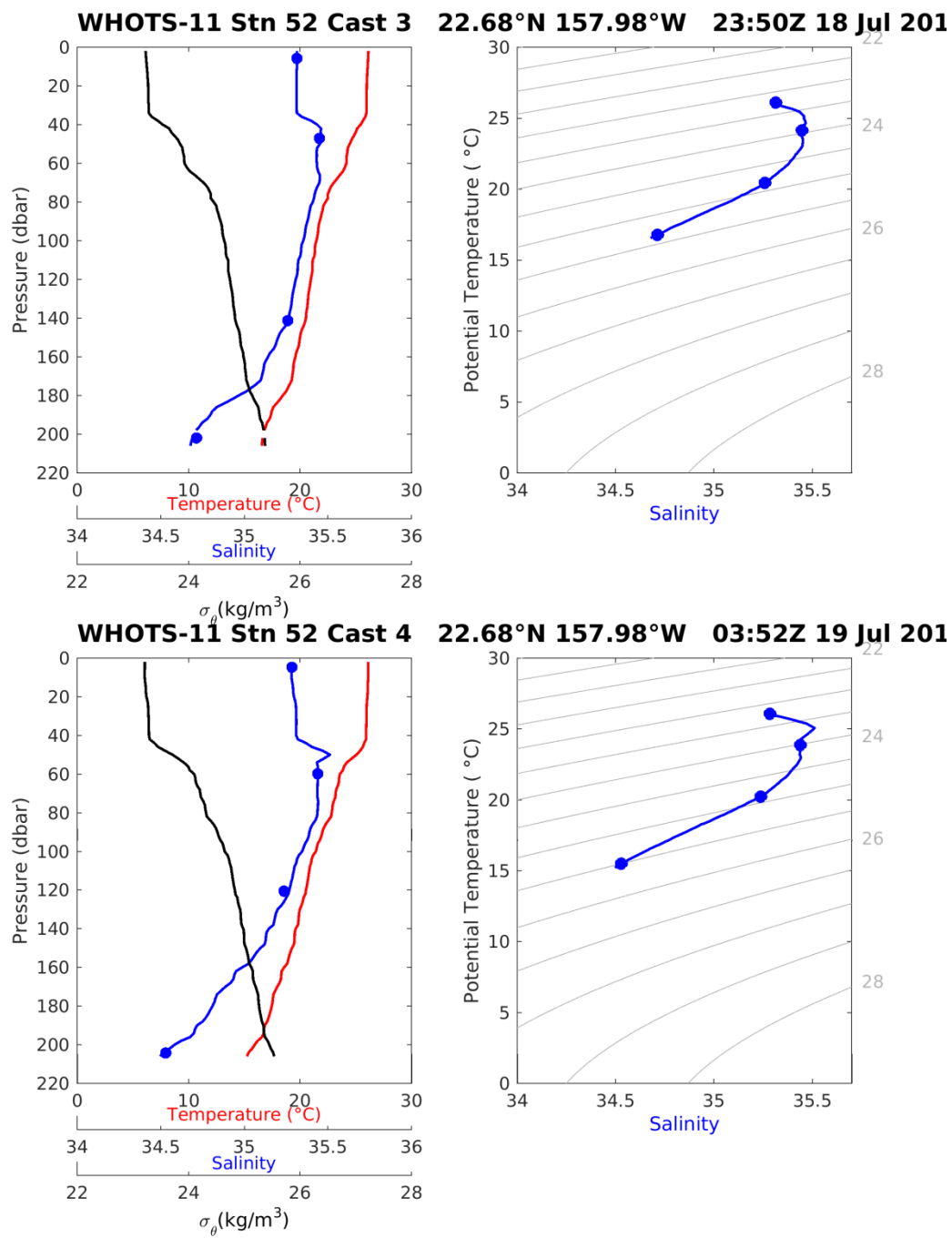


Figure 6-10. [Upper panels] Same as in Figure 6-6, but for station 52, cast 3. [Lower panels] Same as in Figure 6-6, but for station 52, cast 4.

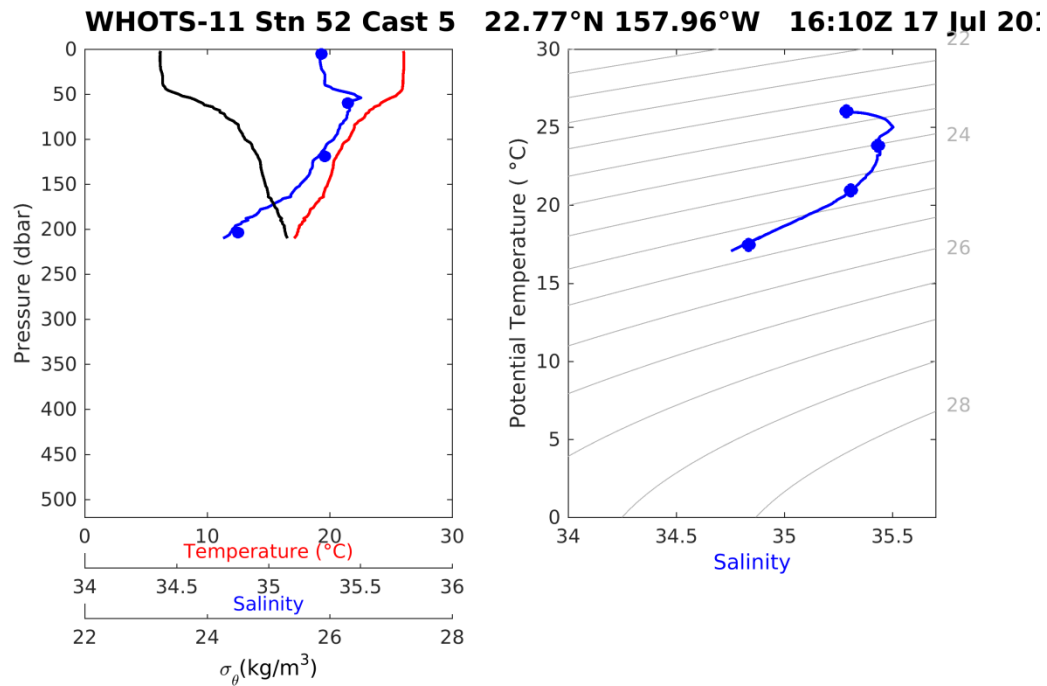


Figure 6-11. Same as in Figure 6-6, but for station 52, cast 5.

B. Thermosalinograph data

Underway measurements of near surface temperature and near surface salinity from thermosalinograph as well as navigation for the WHOTS-10 and WHOTS-11 cruises are presented in Figure 6-12 through Figure 6-15. Since external temperature data were not available in WHOTS-10, temperatures from the internal sensor are reported after correcting by an offset obtained by comparisons with the CTD cast data; however the internal sensor temperatures were affected by cooling and heating as the water traveled through the ship from the intake to the thermosalinograph (see Sect. 4.C.2), and therefore these data were flagged as uncalibrated. The external temperature sensor was installed prior to WHOTS-11 and functioned well throughout the cruise.

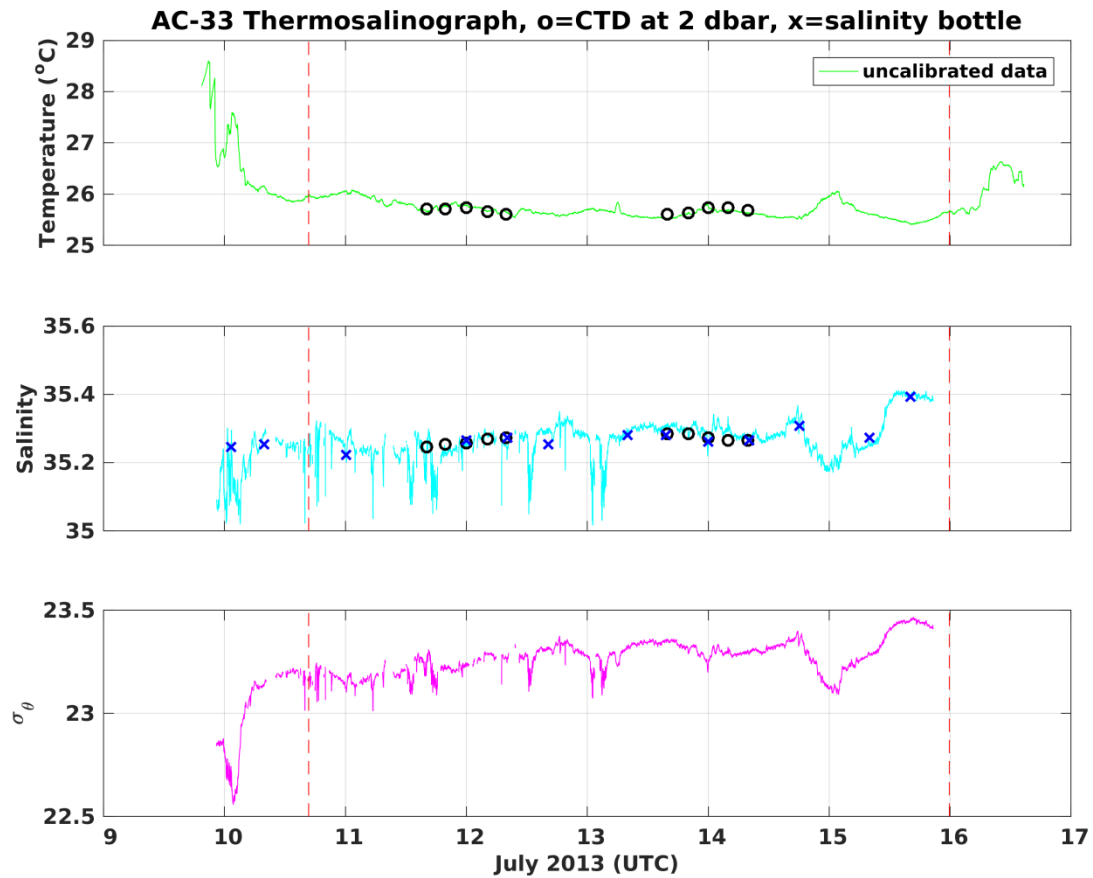


Figure 6-12. Final processed temperature (upper panel), salinity (middle panel) and potential density (σ_θ) (lower panel) data from the continuous underway system on board the RV Hi'ialakai during the WHOTS-10 cruise. Temperature and salinity taken from 6-dbar CTD data (circles) and salinity bottle sample data (crosses) are superimposed. The dashed vertical red line indicates the period of occupation of Station ALOHA and the WHOTS site.

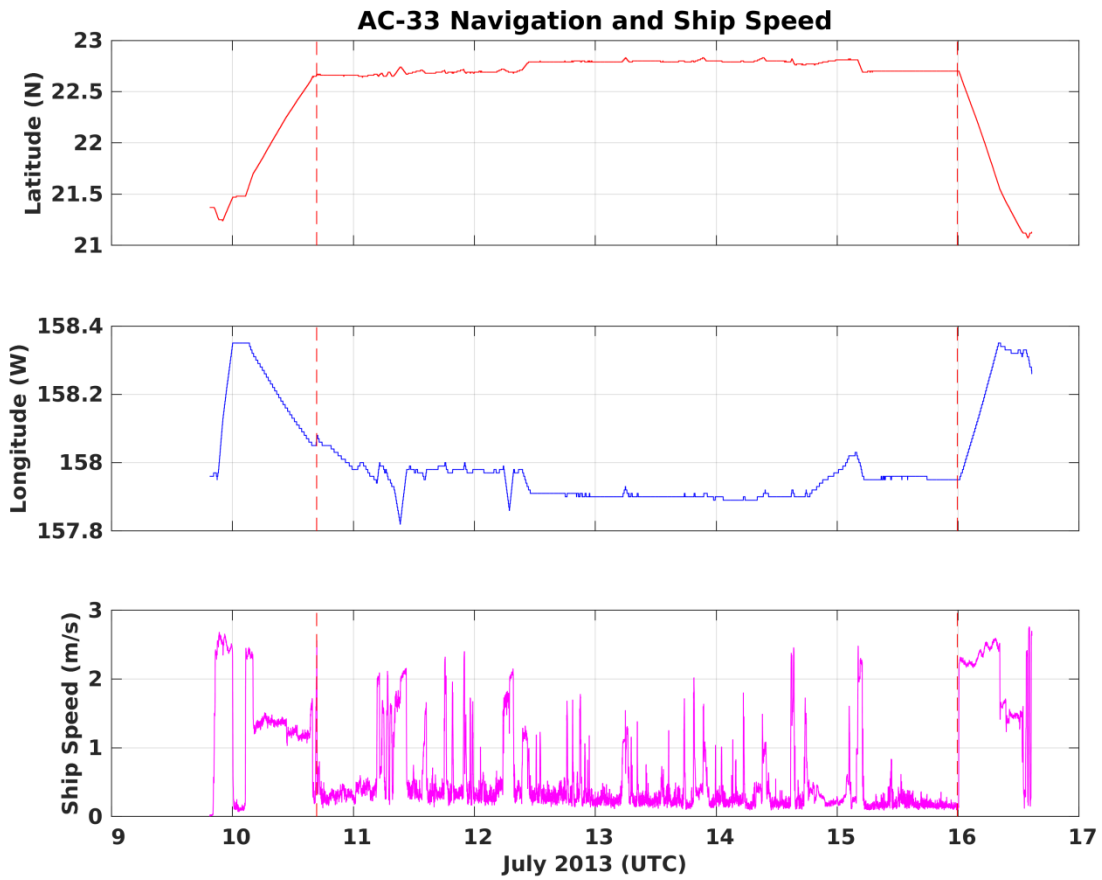


Figure 6-13. Timeseries of latitude (upper panel), longitude (middle panel), and ship's speed (lower panel) during the WHOTS-10 cruise.

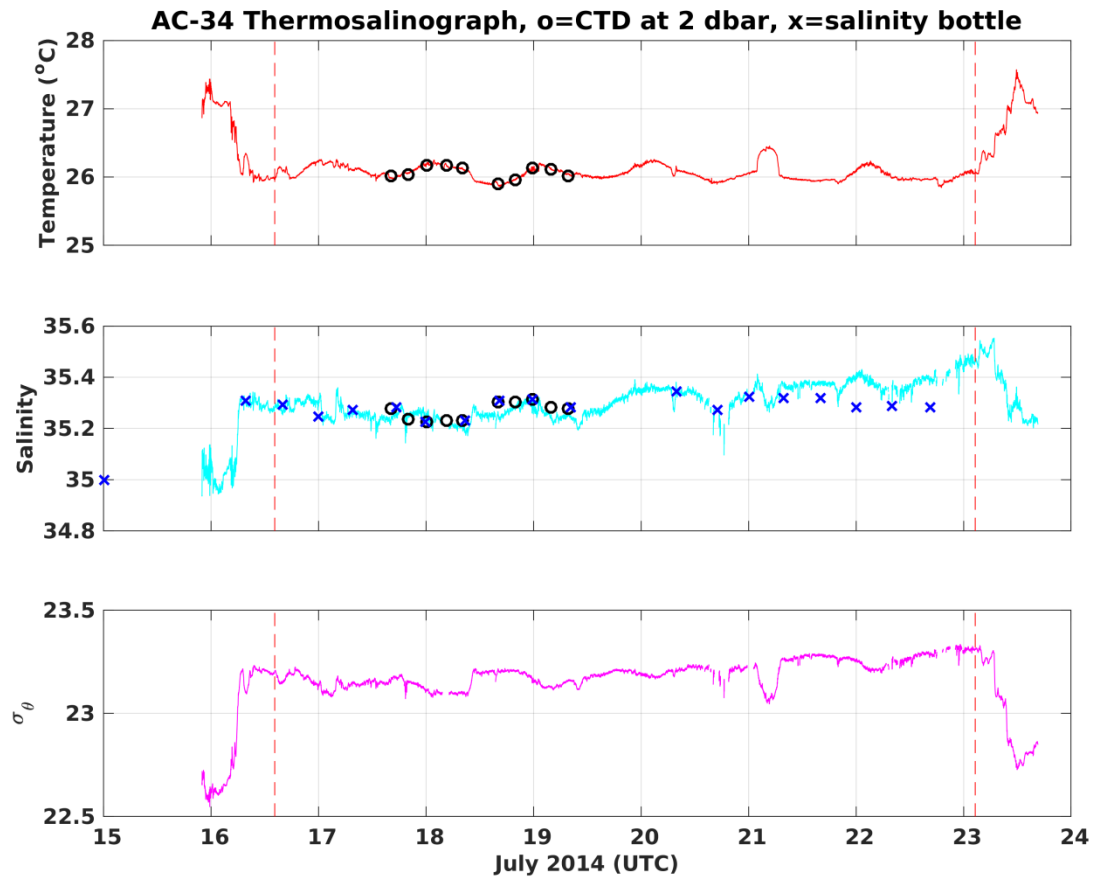


Figure 6-14. Final processed temperature (upper panel), salinity (middle panel) and potential density (σ_θ) (lower panel) data from the continuous underway system on board the RV Hi'ialakai during the WHOTS-11 cruise. Temperature and salinity taken from 6-dbar CTD data (circles) and salinity bottle sample data (crosses) are superimposed. The dashed vertical red line indicates the period of occupation of Station ALOHA and the WHOTS site.

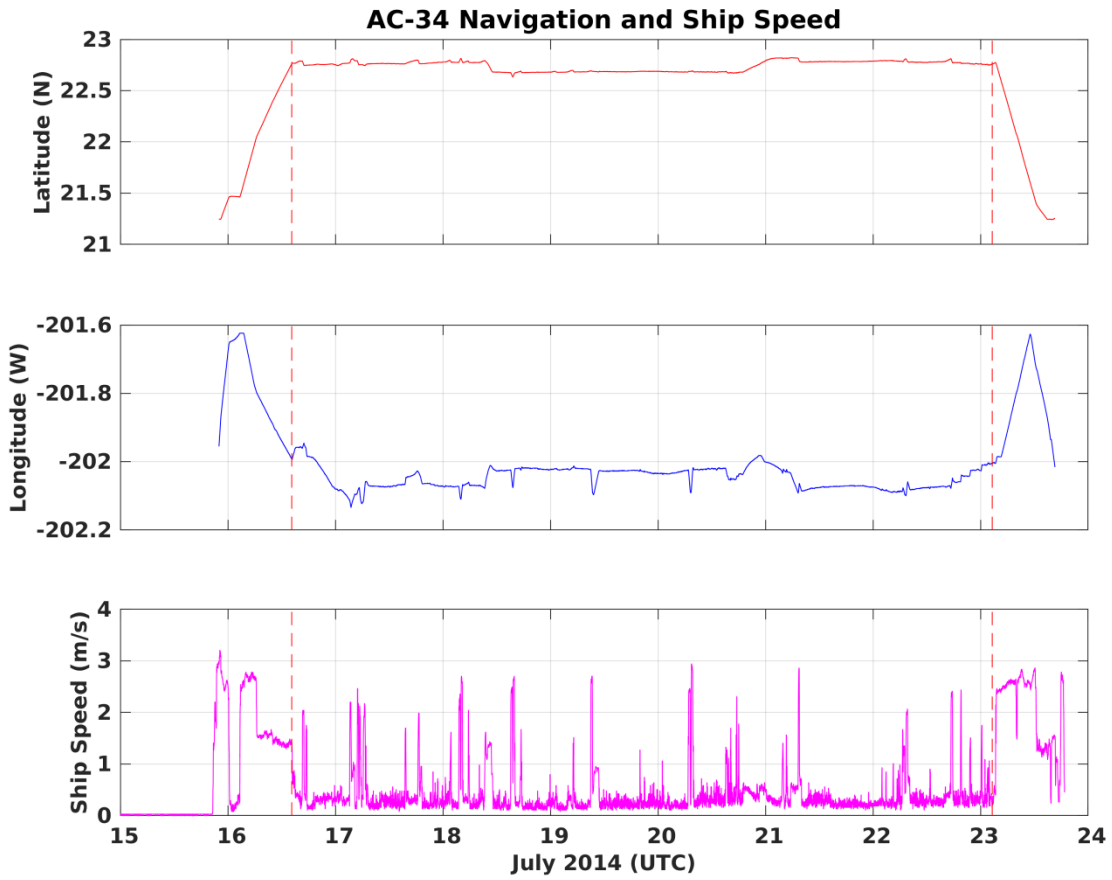


Figure 6-15. Timeseries of latitude (upper panel), longitude (middle panel), and ship's speed (lower panel) during the WHOTS-11 cruise.

C. MicroCAT/SeaCAT data

The temperature and salinity measured by MicroCATs during the mooring deployment are presented in Figure 6-16 to Figure 6-23 for each of the depths where the instruments were located. The potential density (σ_θ) is also plotted in Figure 6-24 to Figure 6-27.

Contoured plots of temperature and salinity as a function of depth are presented in Figure 6-28a; and contoured plots of potential density (σ_θ) as a function of depth, and of salinity as a function of σ_θ are in Figure 6-28b.

The potential temperature and salinity measured by the deep SeaCATs during the mooring deployment are shown in Figure 6-29. Also shown in the plot are the potential temperature and salinity data obtained with a MicroCAT (SBE-37) installed in the ALOHA Cabled Observatory, about 6 nautical miles north from the WHOTS-10 anchor, the instrument is located 2 m above the bottom.

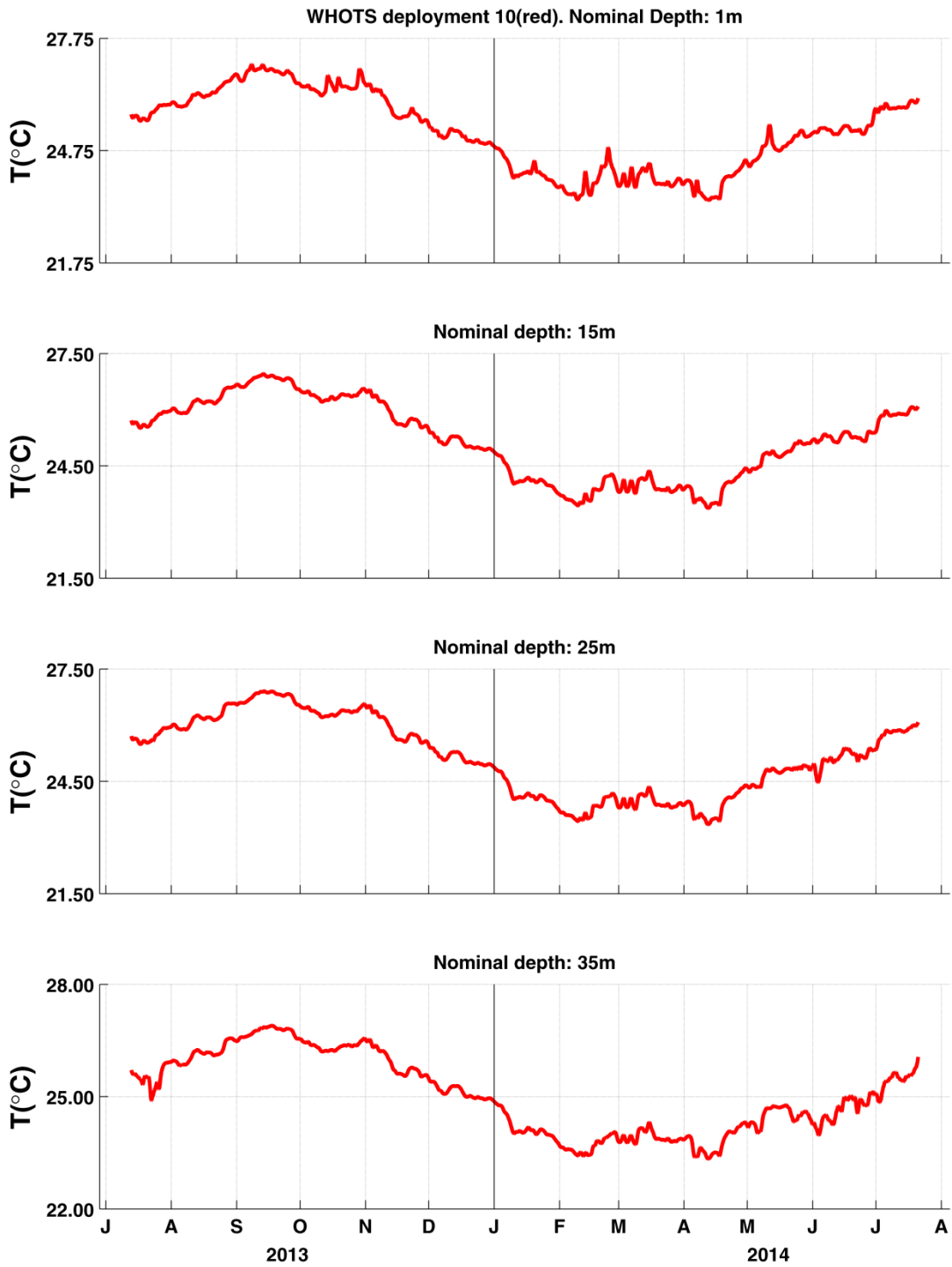


Figure 6-16. Temperatures from MicroCATs during WHOTS-10 deployment at 1, 15, 25, and 35 m.

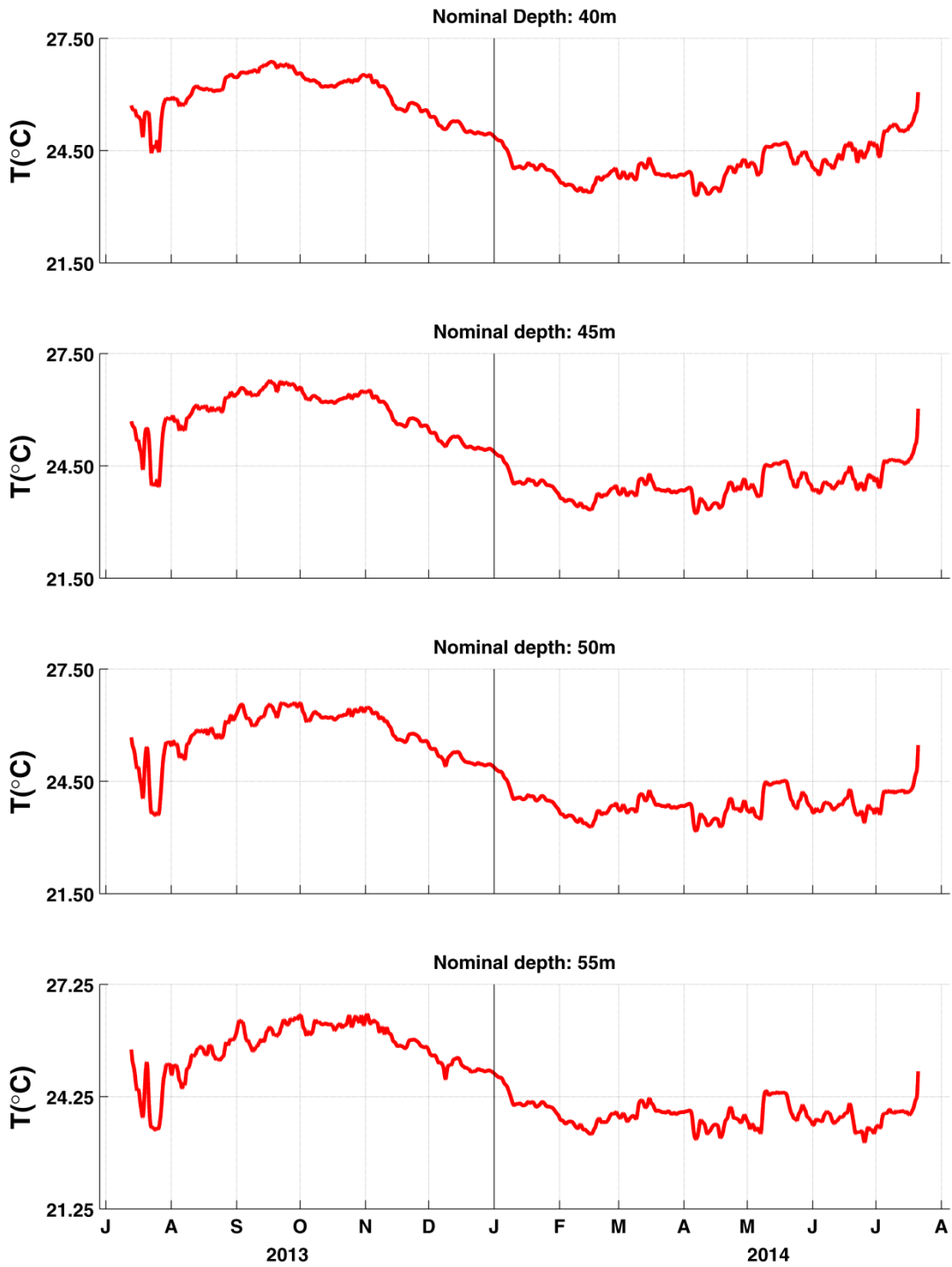


Figure 6-17. Same as in Figure 6-16, but at 40, 45, 50, and 55 m.

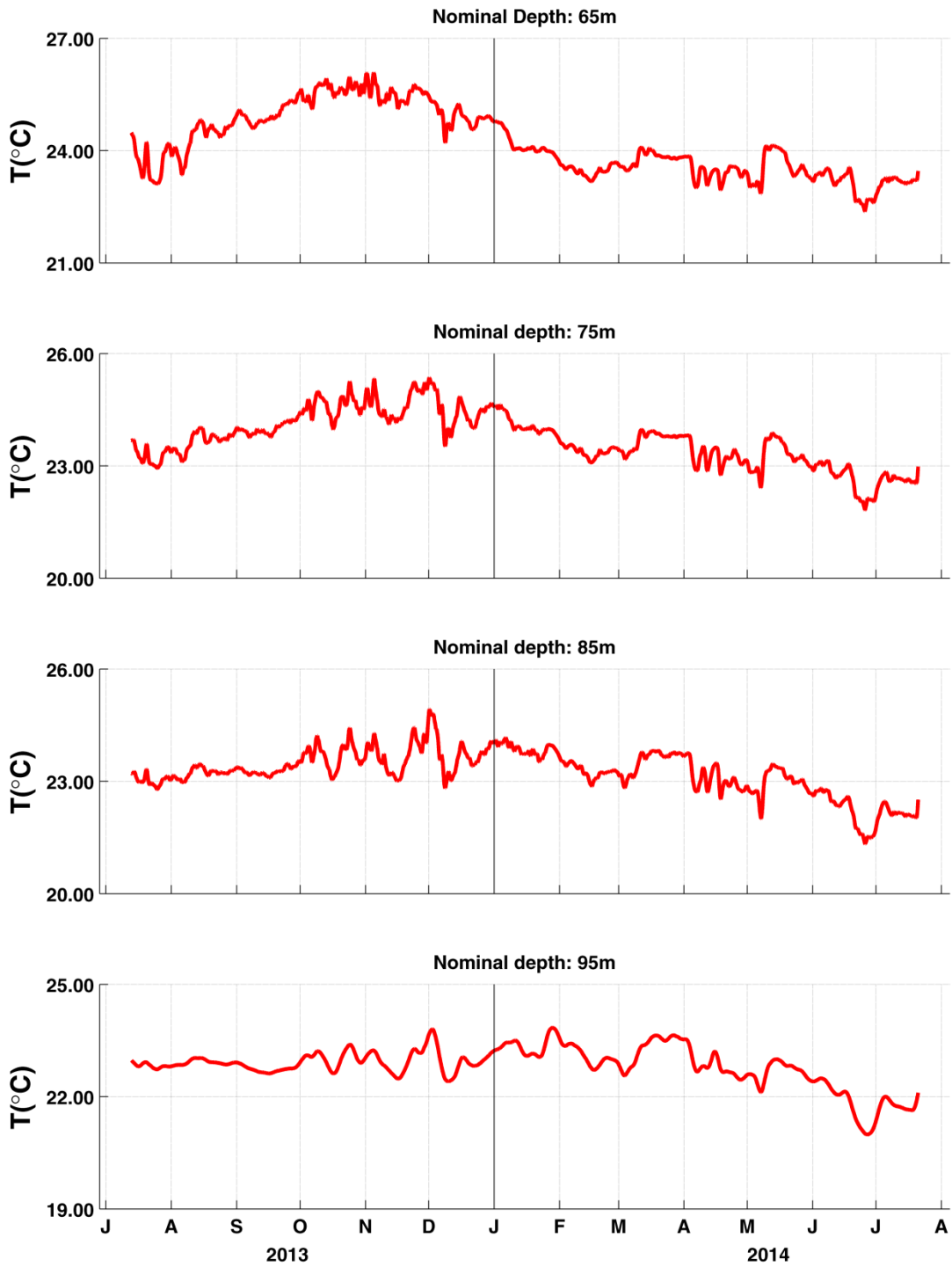


Figure 6-18. Same as in Figure 6-16, but at 65, 75, 85, and 95 m.

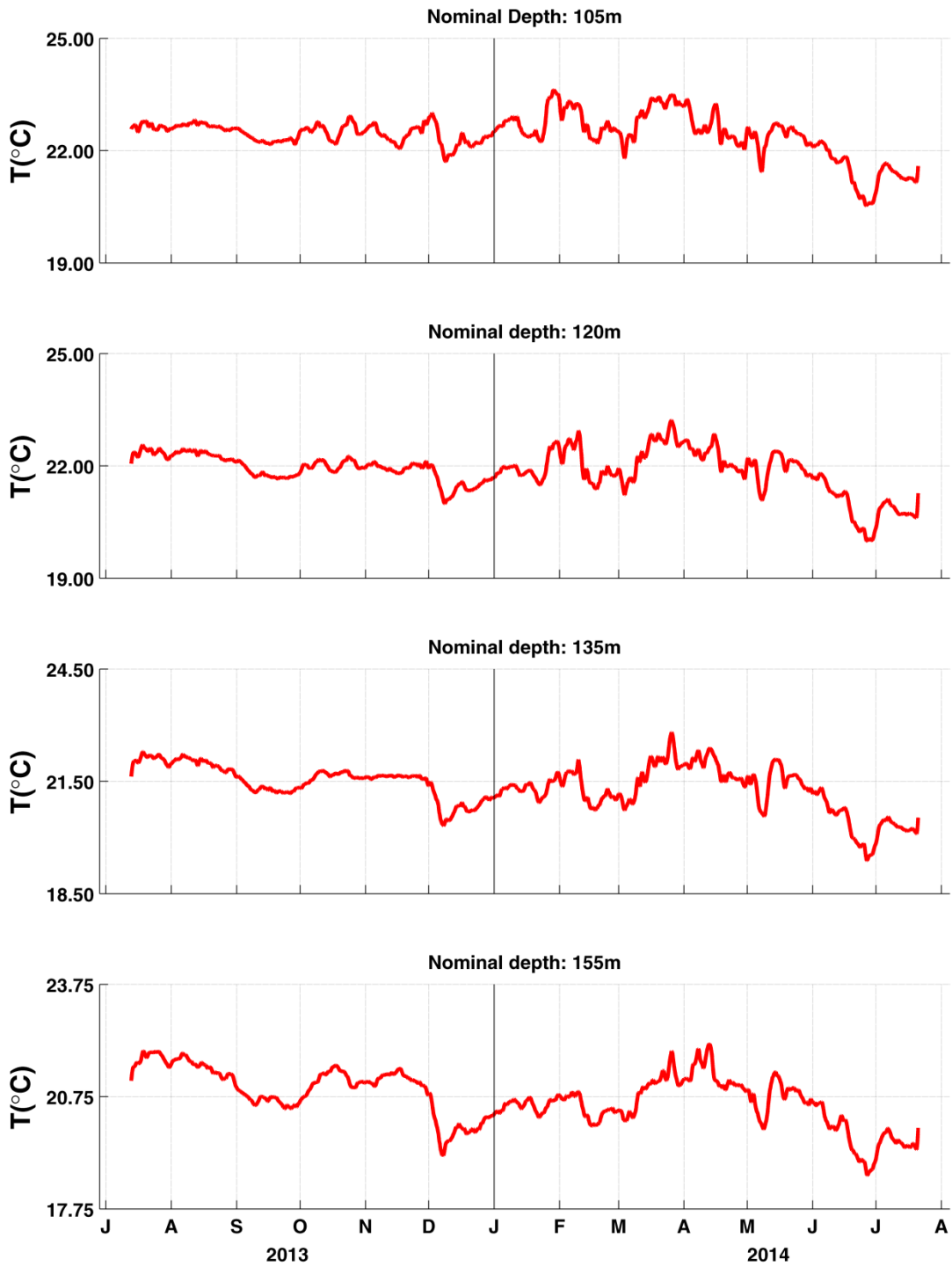


Figure 6-19. Same as in Figure 6-16, but at 105, 120, 135, and 155 m.

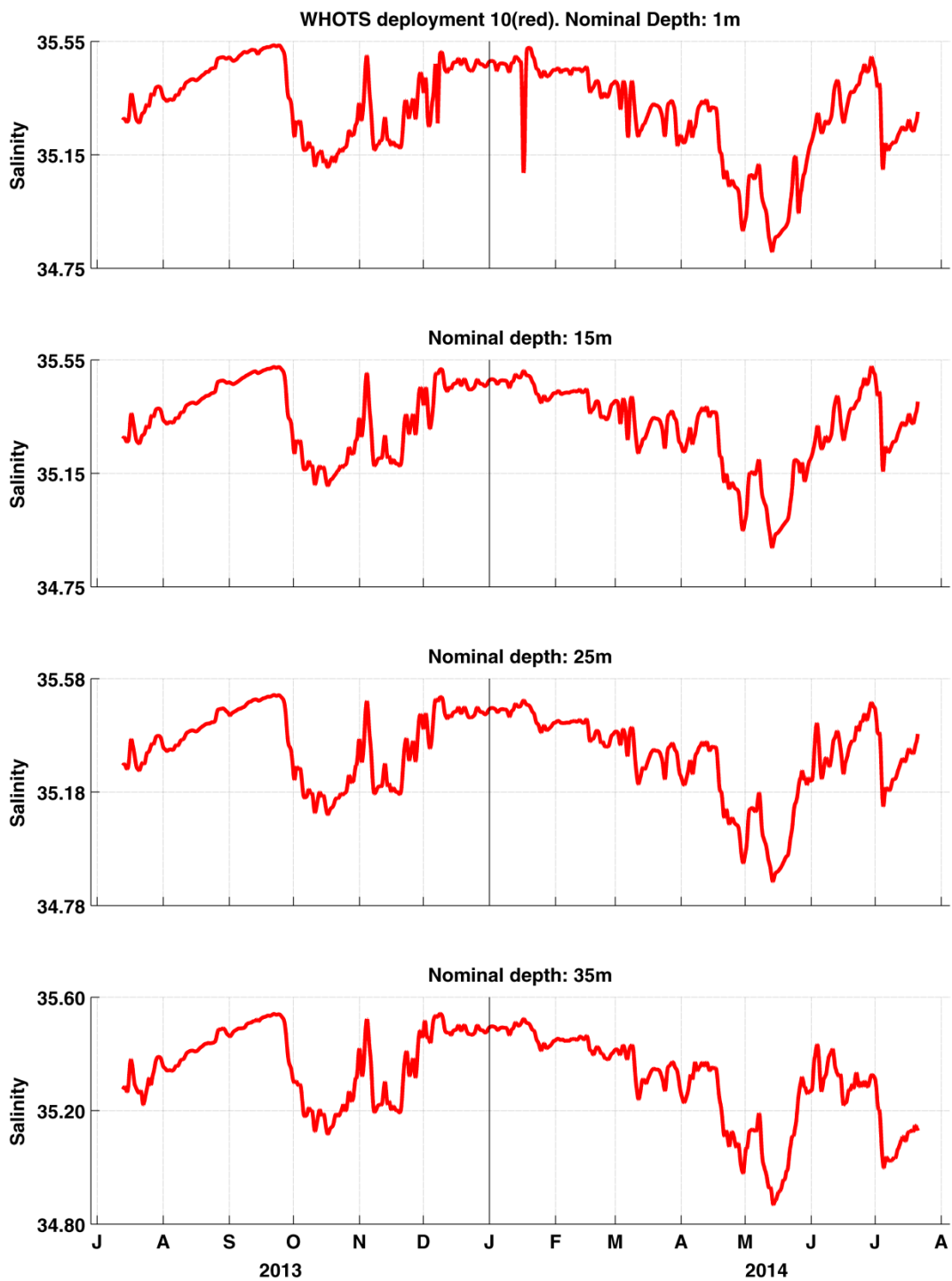


Figure 6-20. Salinities from MicroCATs during WHOTS-10 deployment at 1, 15, 25, and 35 m.

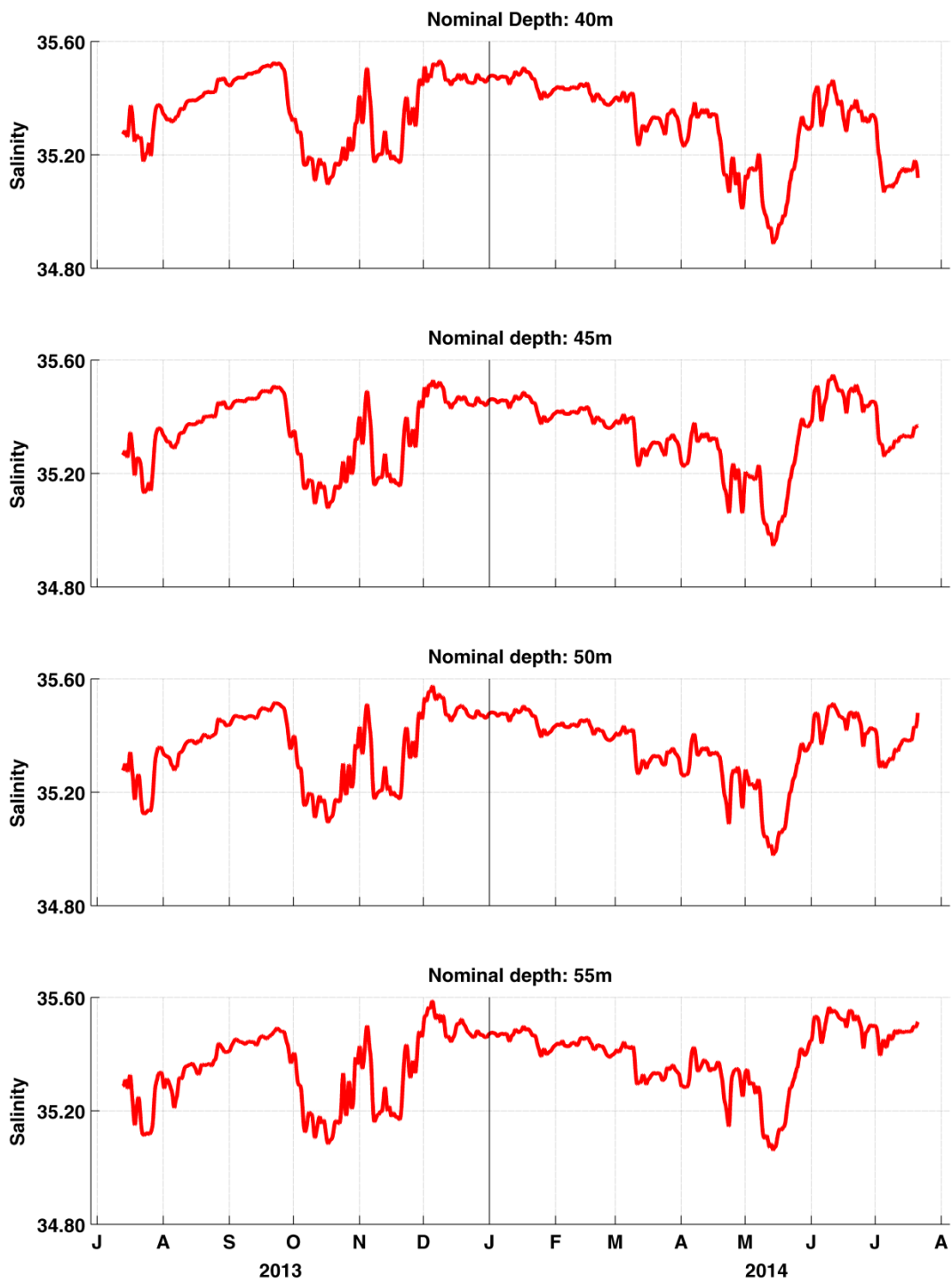


Figure 6-21. Same as in Figure 6-20, but at 40, 45, 50, and 55m.

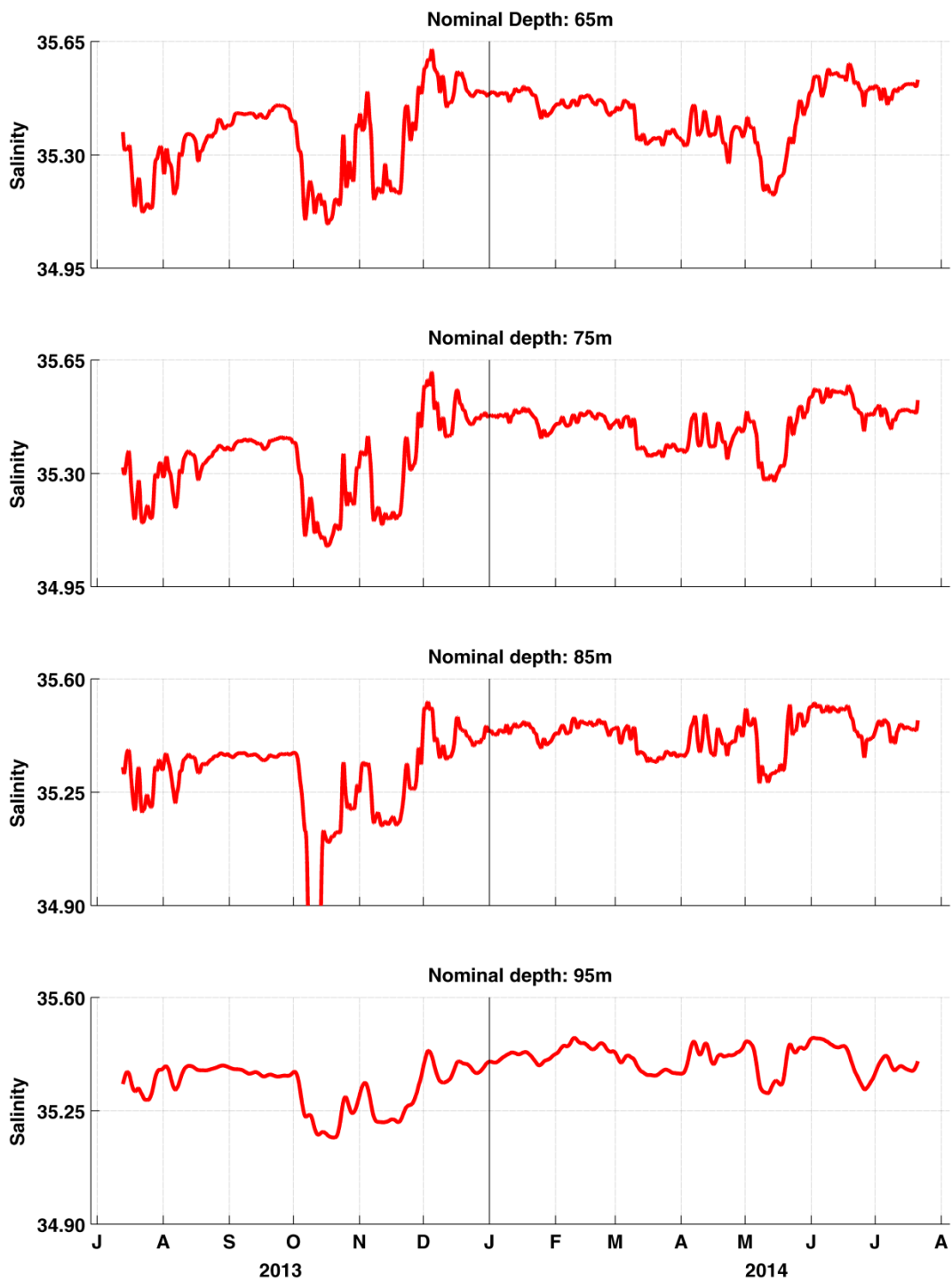


Figure 6-22. Same as in Figure 6-20, but at 65, 75, 85, and 95m.

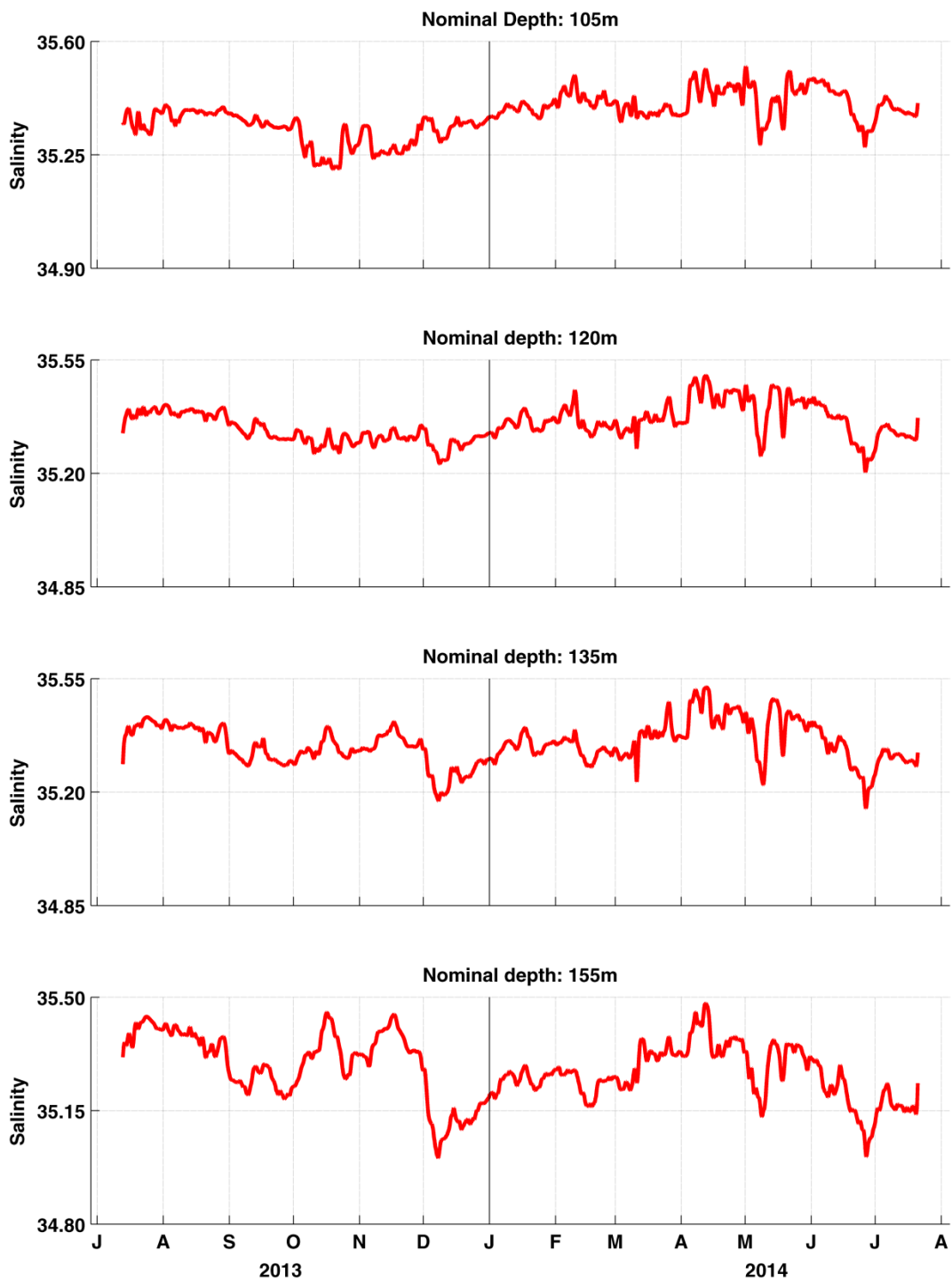


Figure 6-23. Same as in Figure 6-20, but at 105, 120, 135, and 155 m.

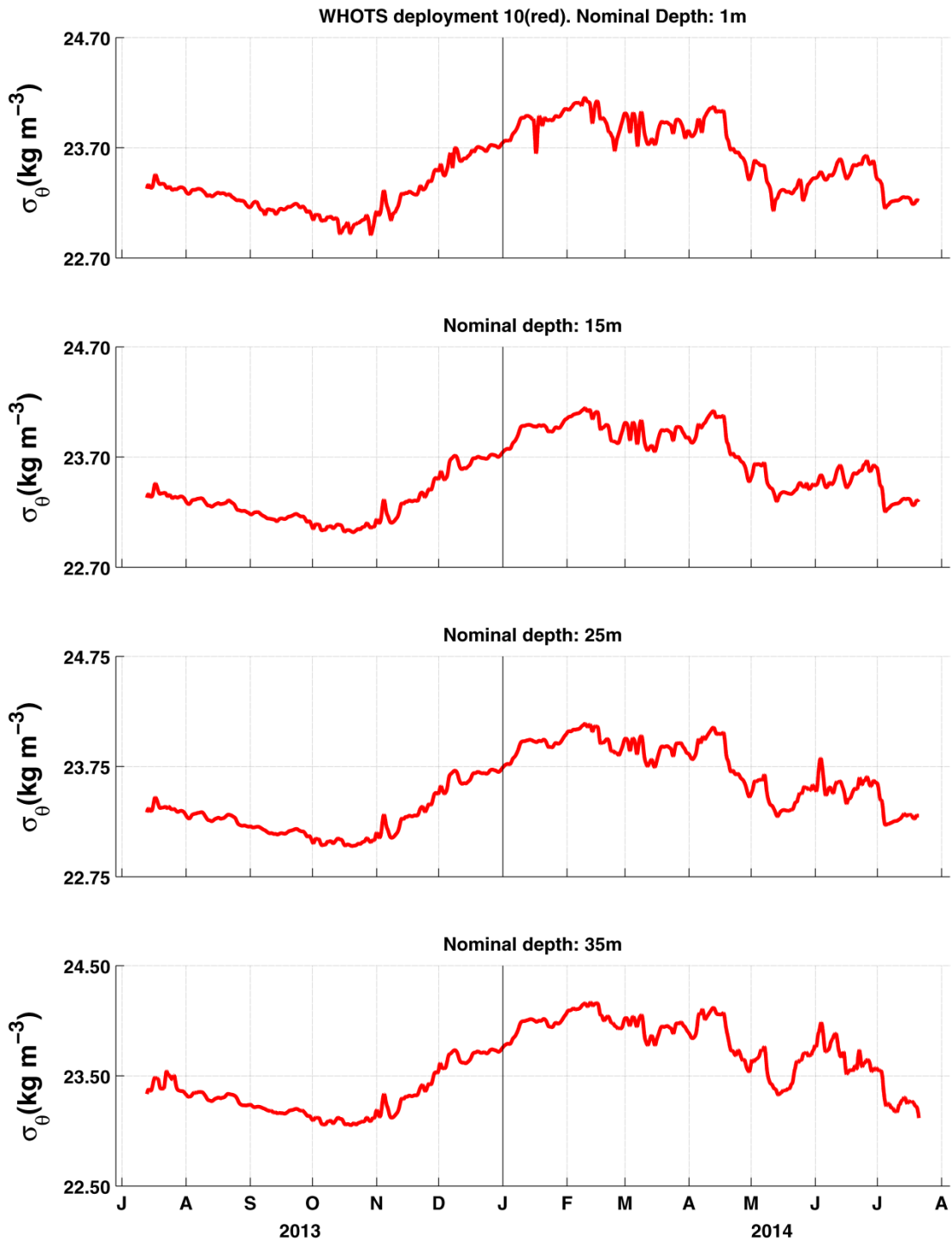


Figure 6-24. Potential density (σ_θ) from MicroCATs during WHOTS-10 deployment at 1, 15, 25, and 35 m.

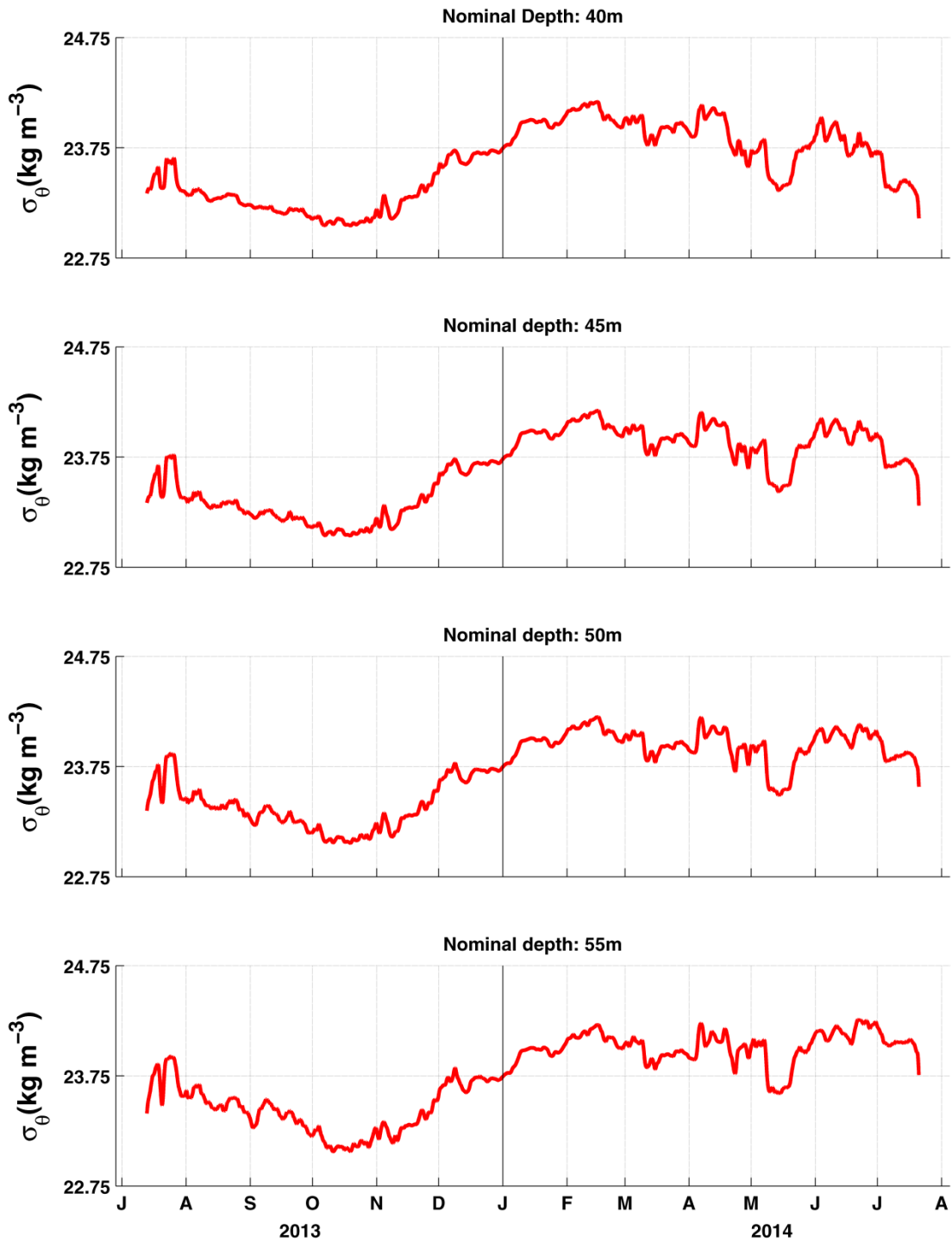


Figure 6-25. Same as in Figure 6-24, but at 40, 45, 50, and 55 m.

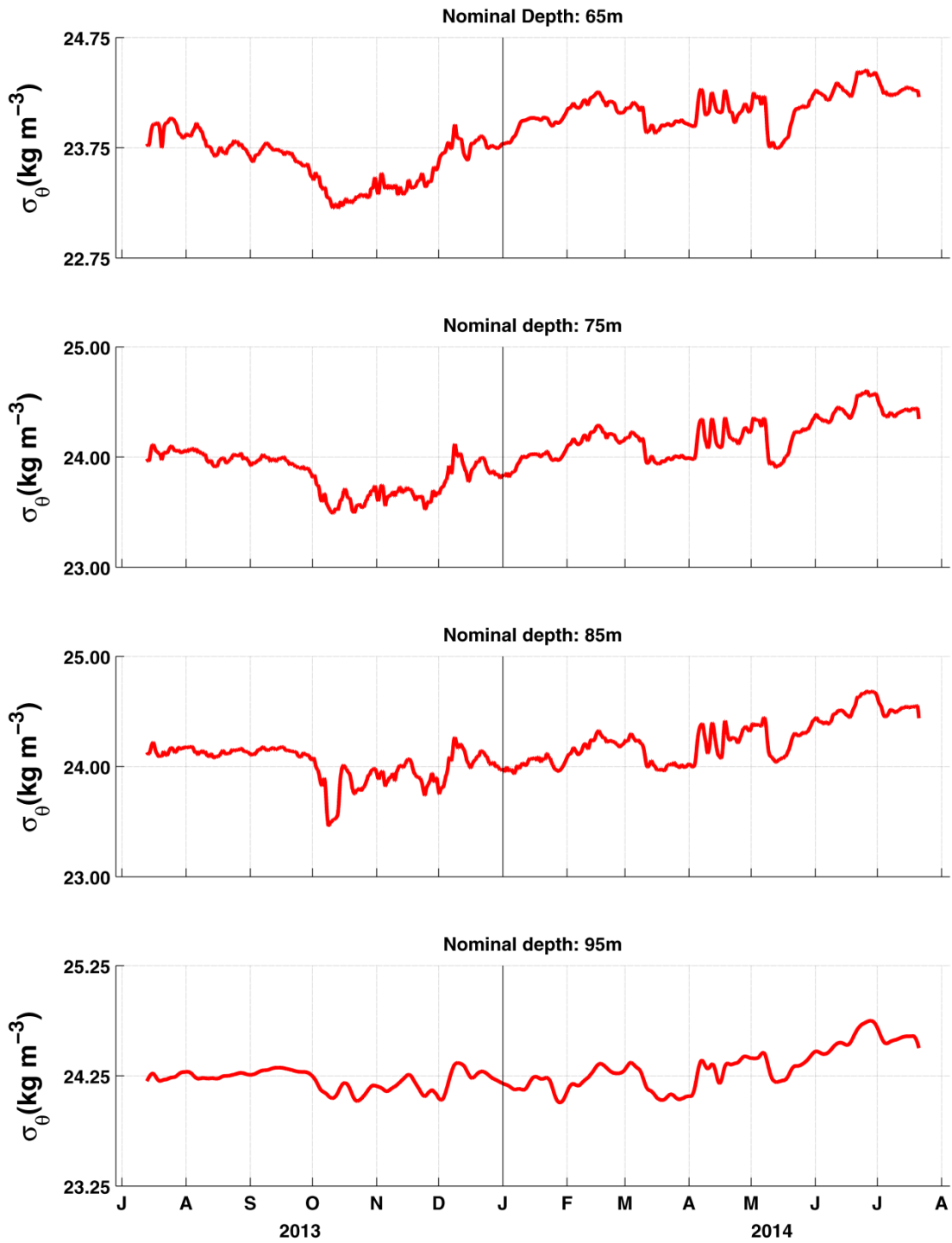


Figure 6-26. Same as in Figure 6-24, but at 65, 75, 85, and 95 m.

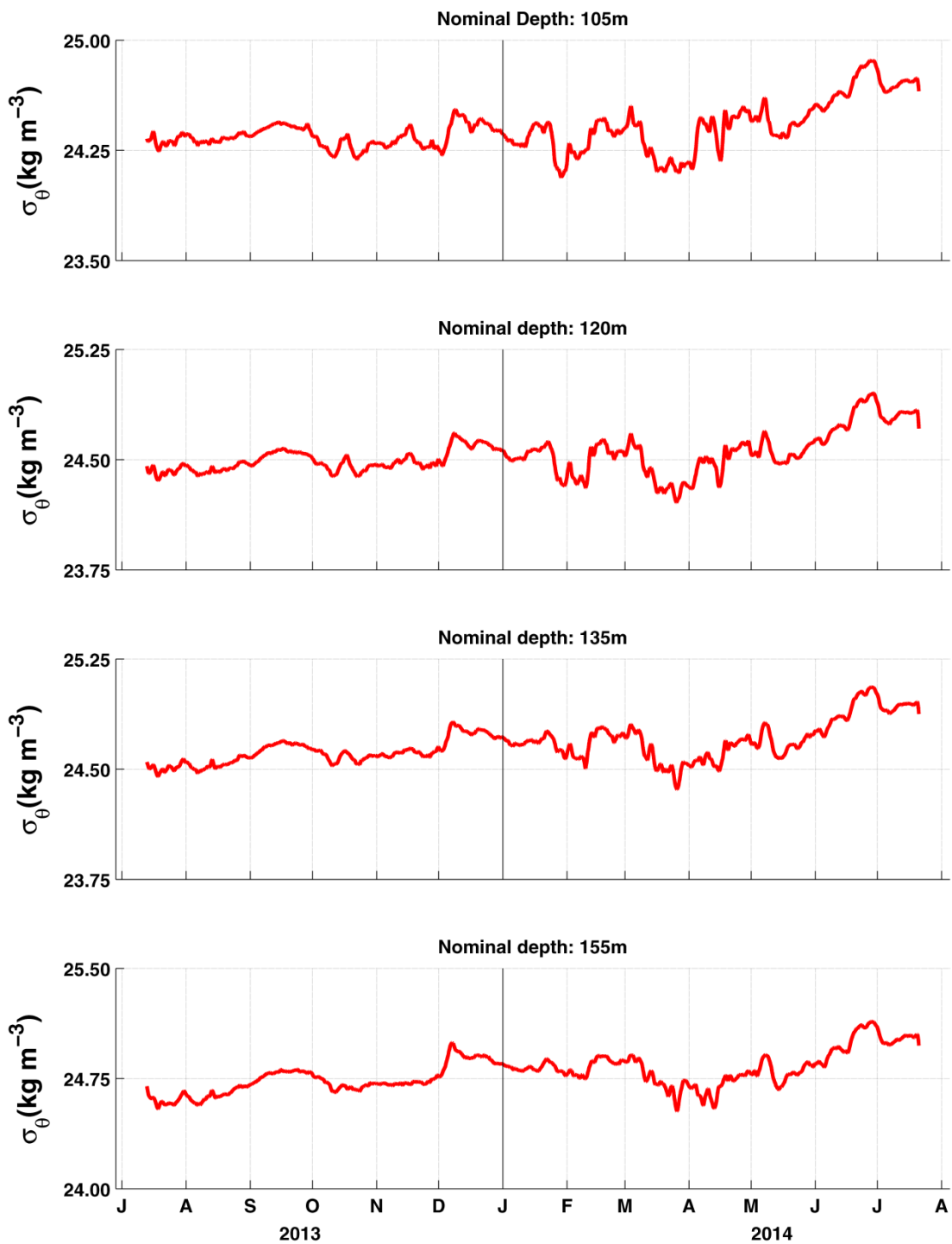


Figure 6-27. Same as in Figure 6-24, but at 105, 120, 135, and 155m.

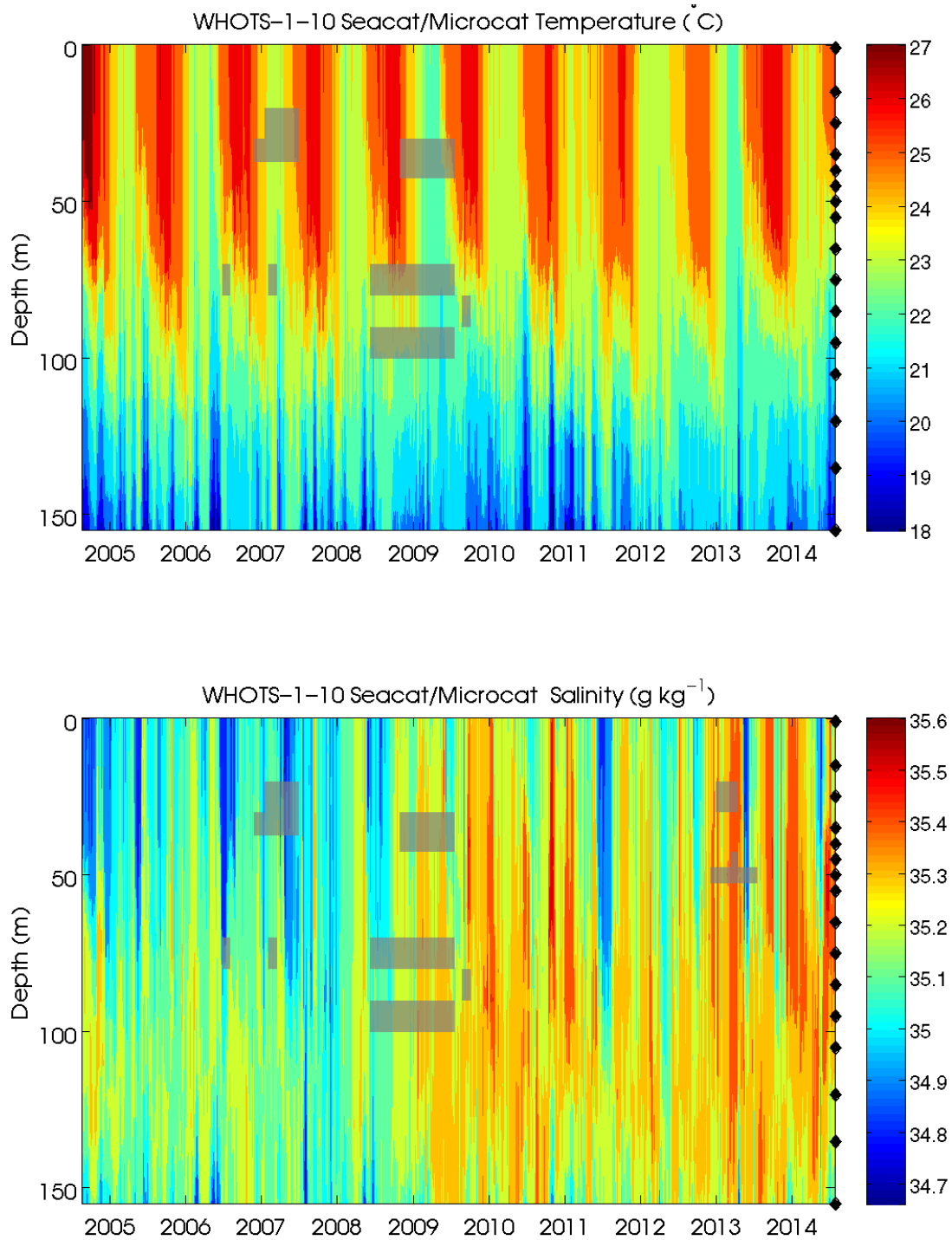


Figure 6-28 a. Contour plots of temperature (upper panel), and salinity (lower panel) versus depth from SeaCATs/ MicroCATs during WHOTS-1 through WHOTS-10 deployments. The shaded areas indicate missing data. The diamonds along the right axis indicate the instruments depths.

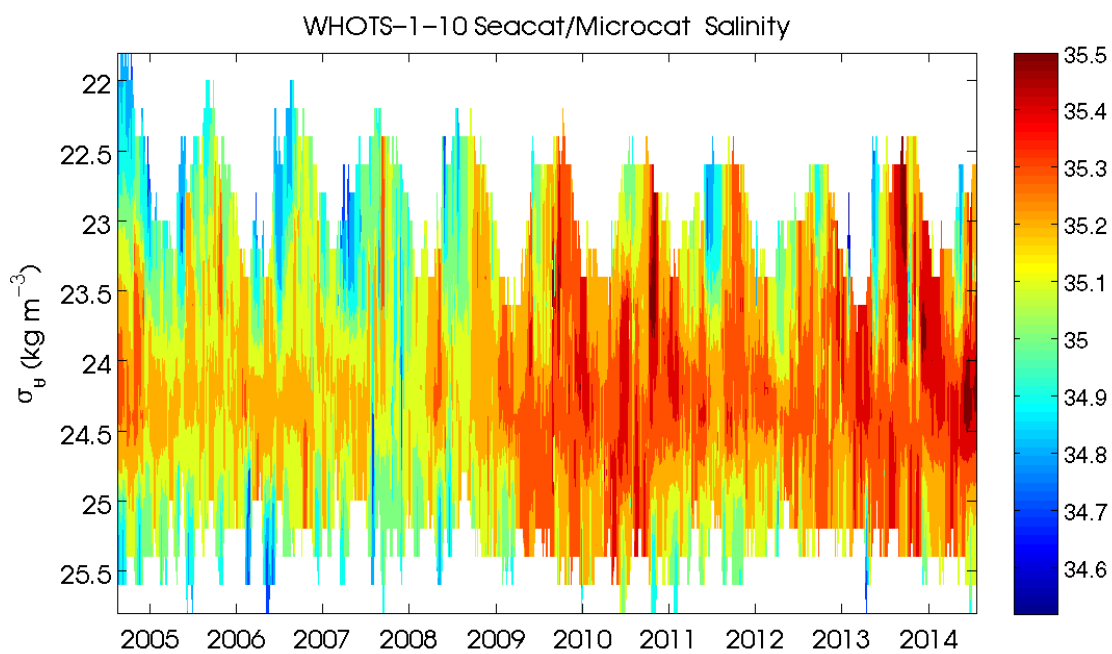
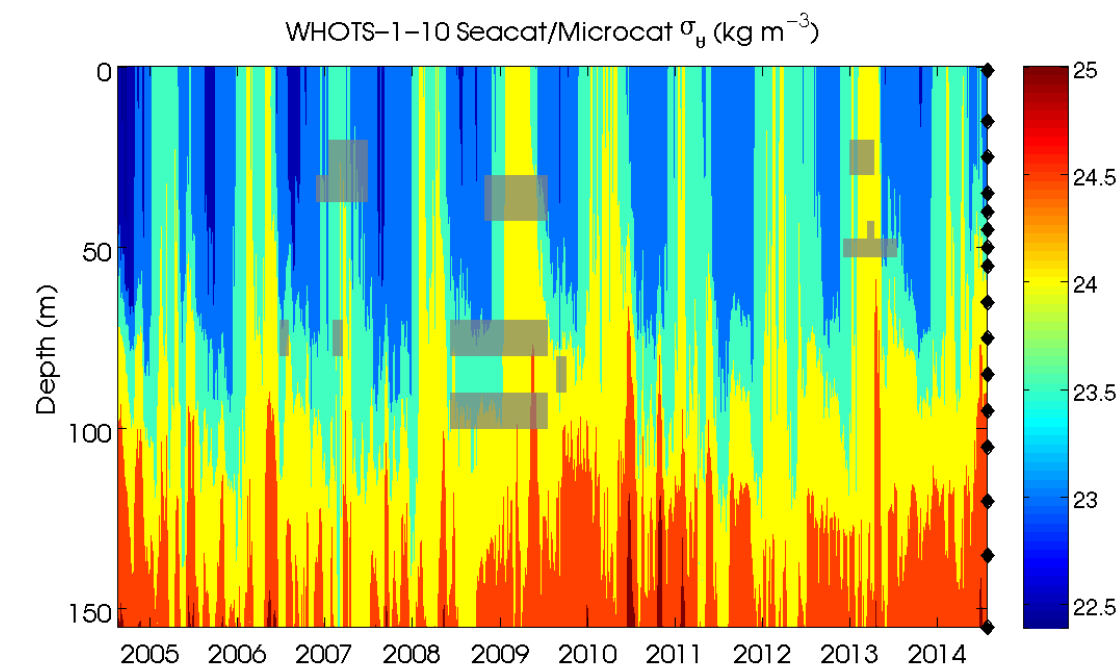


Figure 6-28b. Contour plots of potential density (σ_{θ} , upper panel), versus depth, and of salinity versus σ_{θ} (lower panel) from SeaCATs/MicroCATs during WHOTS-1 through WHOTS-10 deployments. The shaded areas indicate missing data. The diamonds along the right axis in the upper figure indicate the instruments depths.

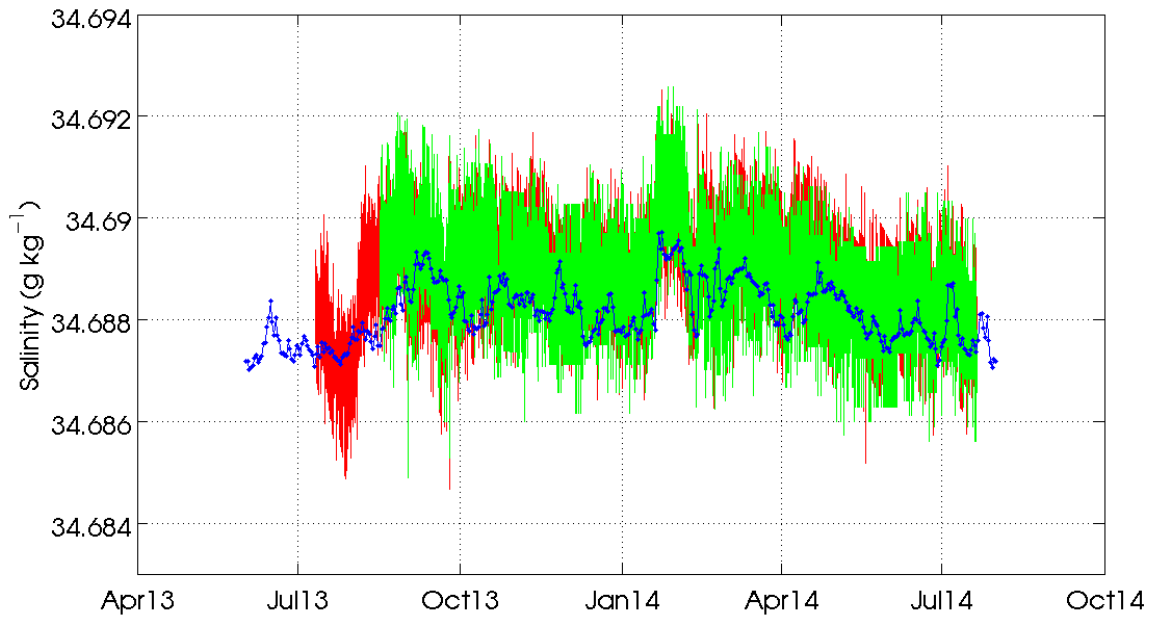
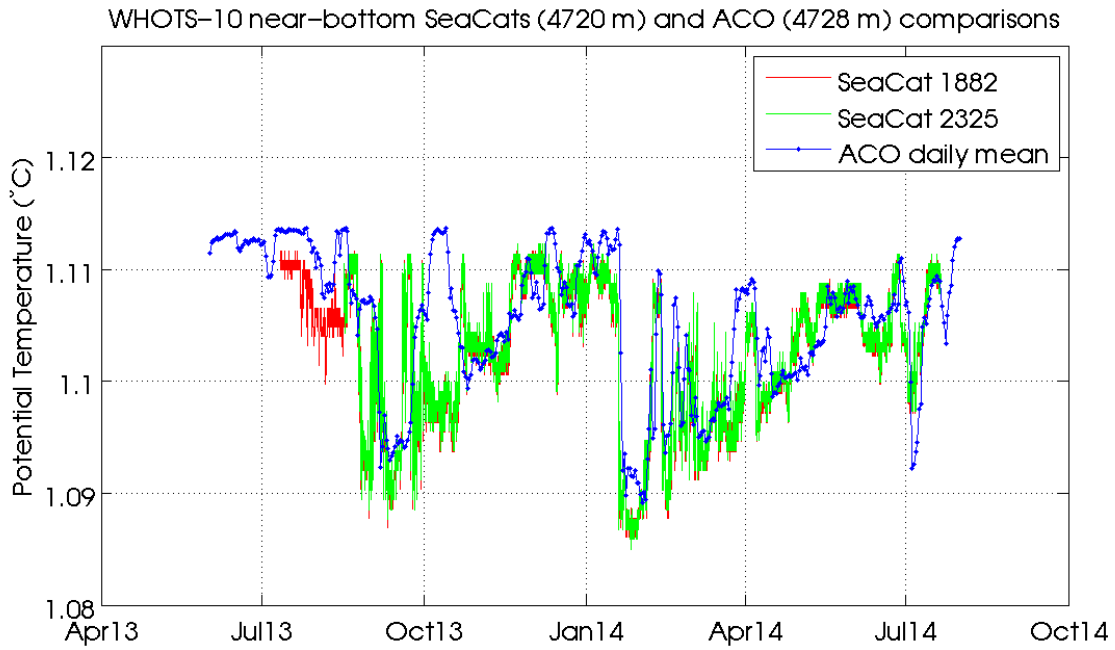


Figure 6-29. Potential temperature (upper panel) and salinity (lower panel) time-series from the ALOHA Cabled Observatory (ACO) sensors and from the WHOTS-10 SeaCATs 1882 and 2325.

D. Moored ADCP data

Contoured plots of smoothed horizontal and vertical velocity as a function of depth during the mooring deployments 1 through 10 are presented in Figure 6-30 to Figure 6-32. A staggered time-series of smoothed horizontal and vertical velocities are shown in Figure 6-33 to Figure 6-35. Smoothing was performed by applying a daily running mean to the data and then interpolating the data on to an hourly grid.

Contours of east and north velocity components from the Ship Hi'ialakai's Ocean Surveyor broadband 75 kHz shipboard ADCP, and the moored 300 kHz ADCP from the WHOTS-10 deployment as a function of time and depth, during the WHOTS-10 cruise are shown in Figure 6-36 and Figure 6-37. The corresponding plots during the WHOTS-11 cruise and WHOTS-11 deployment are shown in Figures 6-38 and Figure 6-39.

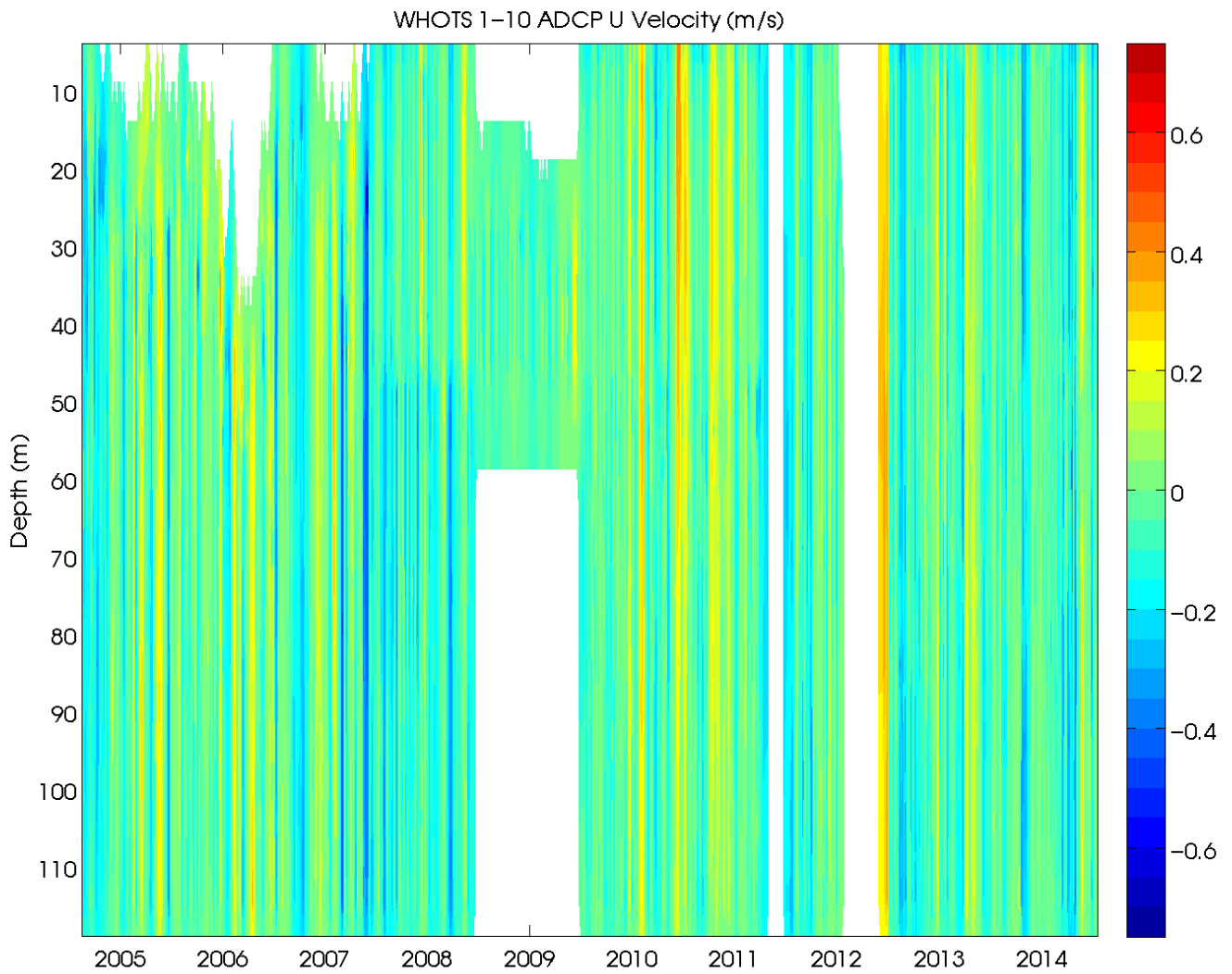


Figure 6-30. Contour plot of east velocity component ($m s^{-1}$) versus depth and time from the moored ADCPs from the WHOTS-1 through -10 deployments.



Figure 6-31. Contour plot of north velocity component ($m s^{-1}$) versus depth and time from the moored ADCPs from the WHOTS-1 through -10 deployments.

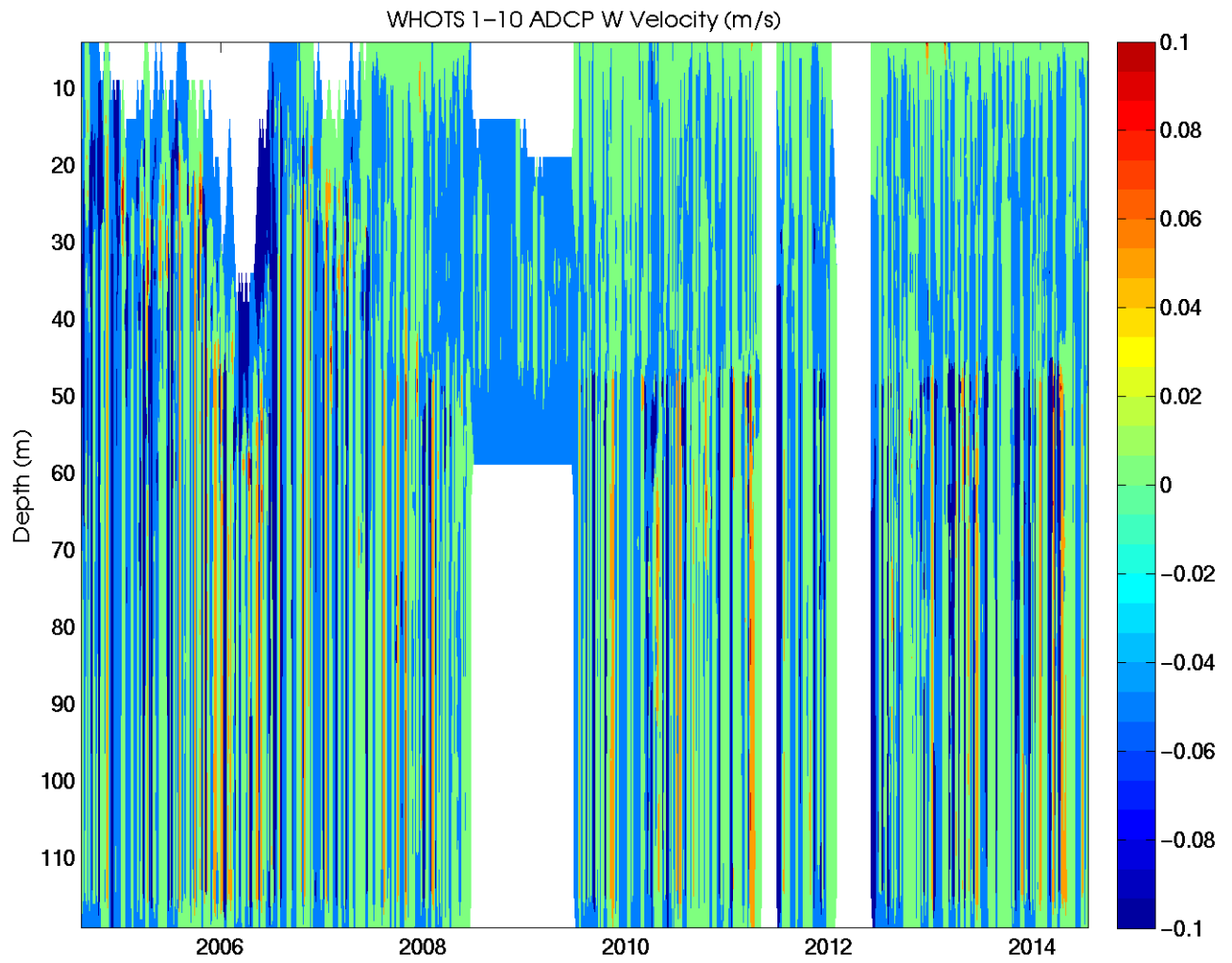


Figure 6-32. Contour plot of vertical velocity component ($m\ s^{-1}$) versus depth and time from the moored ADCPs from the WHOTS-1 through -10 deployments.

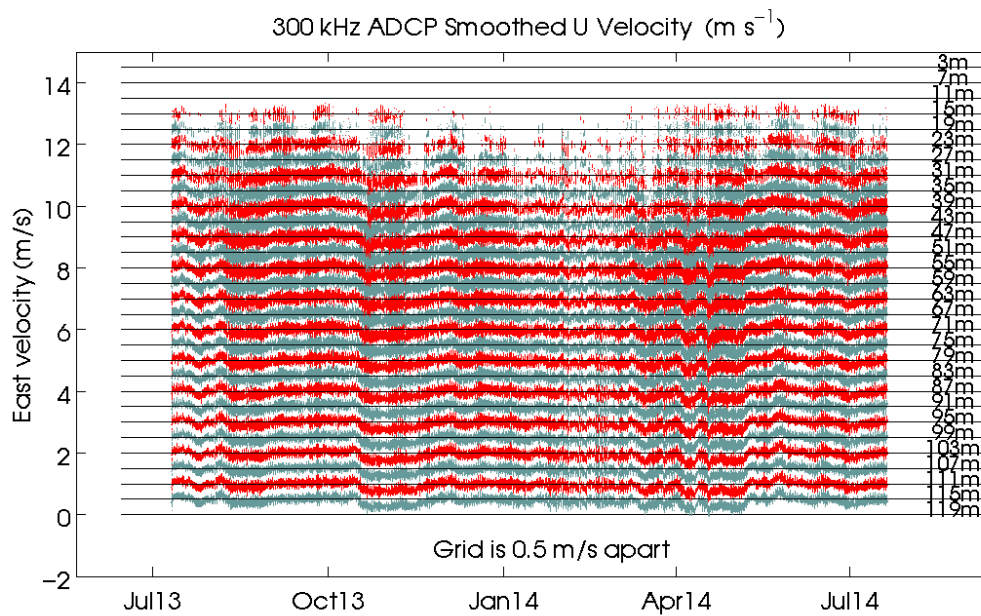
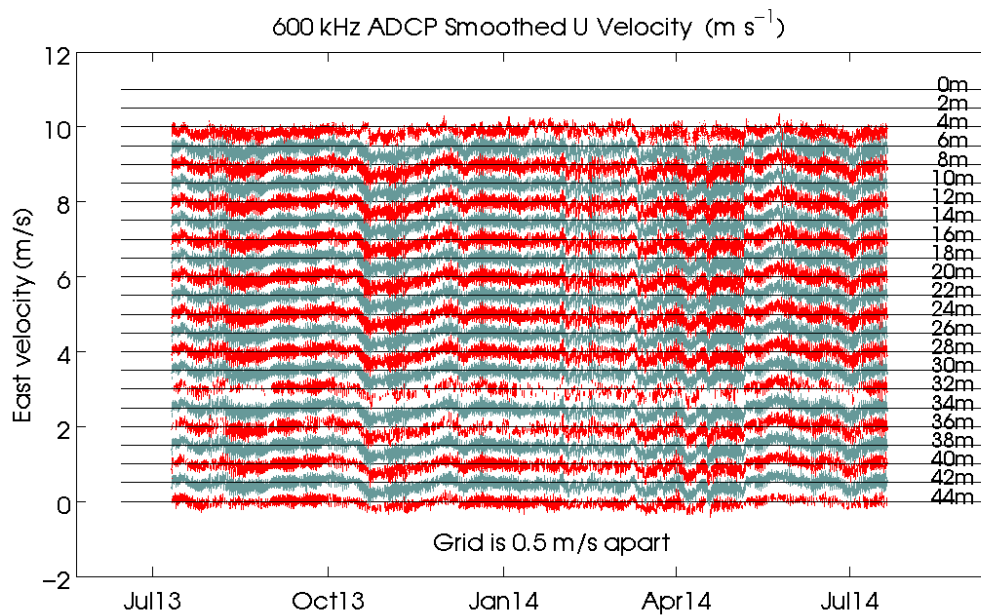


Figure 6-33. Staggered time-series of east velocity component (m s^{-1}) for each bin of the 600 kHz (upper panel), and 300 kHz (lower panel) moored ADCPs during WHOTS-10. The time-series are offset upwards by 0.5 m s^{-1} , the depth of each bin is on the right.

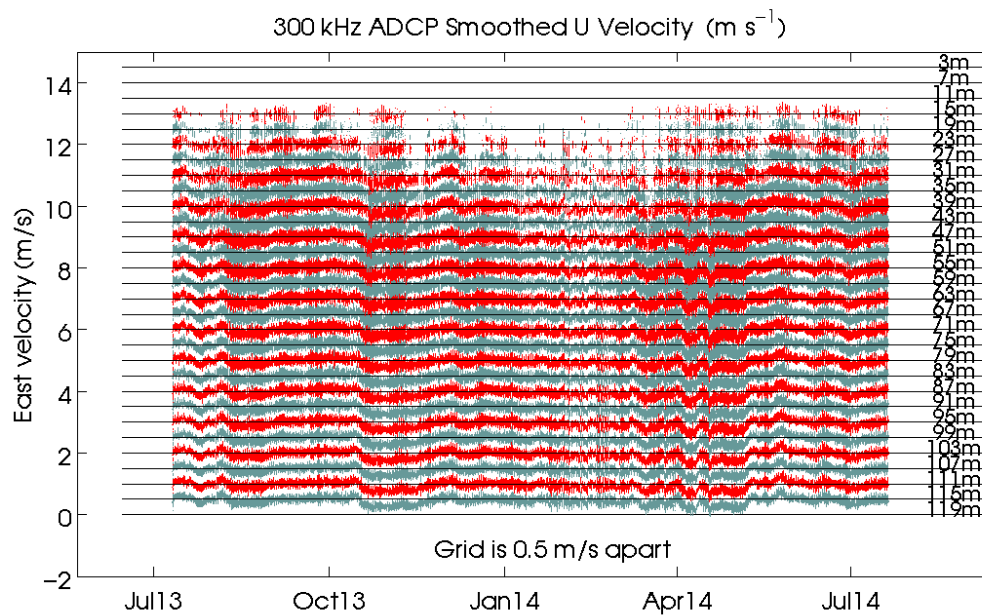
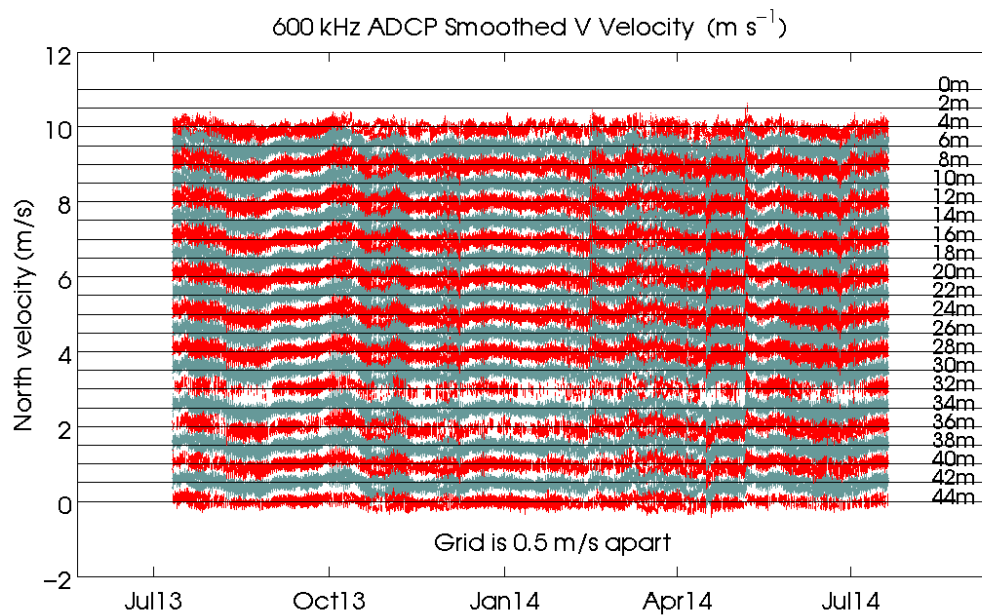


Figure 6-34. Staggered time-series of north velocity component (m s^{-1}) for each bin of the 600 kHz (upper panel), and 300 kHz (lower panel) moored ADCPs during WHOTS-10. The time-series are offset upwards by 0.5 m s^{-1} , the depth of each bin is on the right.

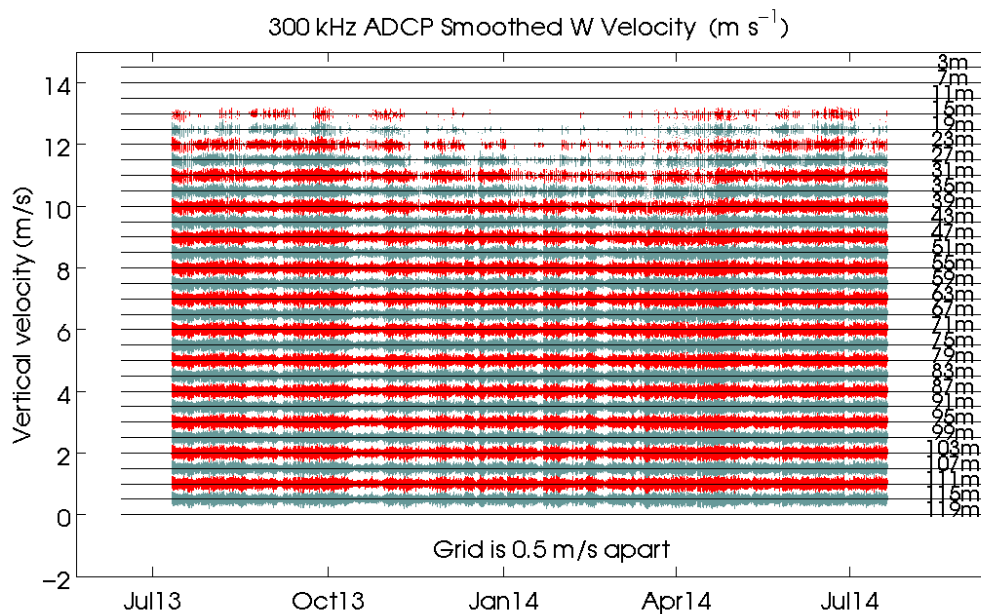
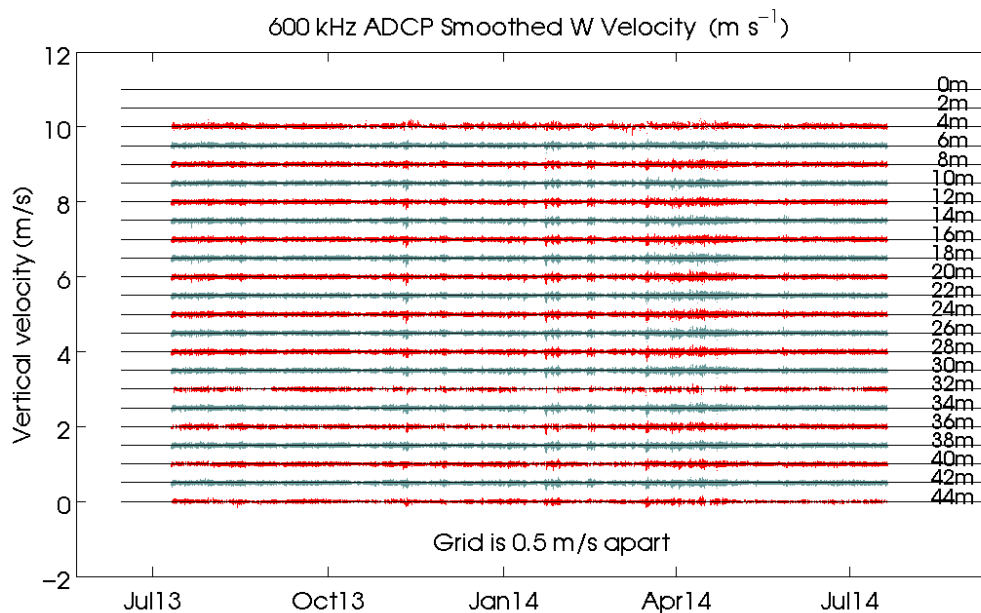


Figure 6-35. Staggered time-series of vertical velocity component (m s^{-1}) for each bin of the 600 kHz (upper panel), and 300 kHz (lower panel) moored ADCPs during WHOTS-10. The time-series are offset upwards by 0.5 m s^{-1} , the depth of each bin is on the right.

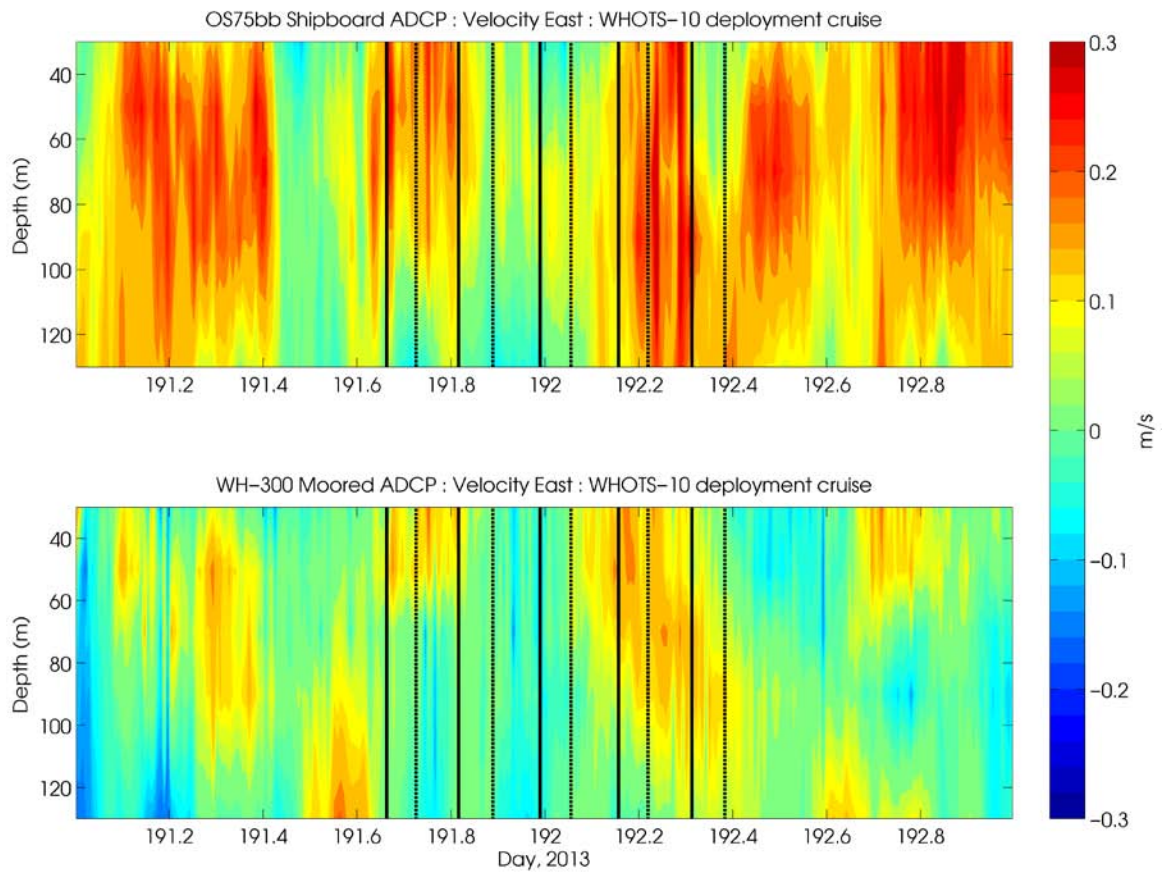


Figure 6-36. Contour of east velocity component ($m s^{-1}$) from the Ship *Hi'ialakai's* Ocean Surveyor broadband 75 kHz shipboard ADCP (upper panel), and the moored 300 kHz ADCP from the WHOTS-10 mooring as a function of time and depth, during the WHOTS-10 cruise (lower panel). Times when the CTD/rosette was in the water are identified between the two sets of black lines.

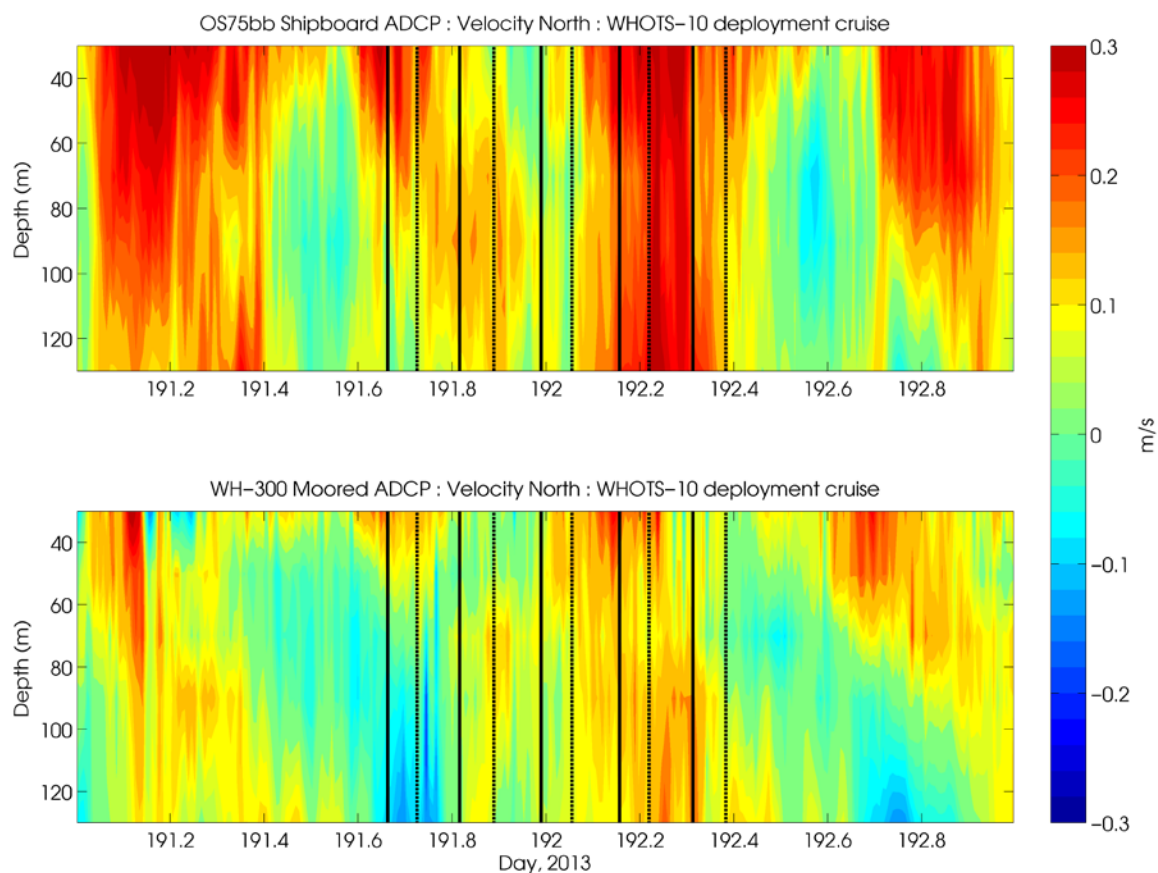


Figure 6-37. Contours of north velocity component ($m s^{-1}$) from the Ship *Hi'ialakai's* Ocean Surveyor broadband 75 kHz shipboard ADCP (upper panel), and the moored 300 kHz ADCP from the WHOTS-10 mooring as a function of time and depth, during the WHOTS-10 cruise (lower panel). Times when the CTD/rosette was in the water are identified between the two sets of black lines.

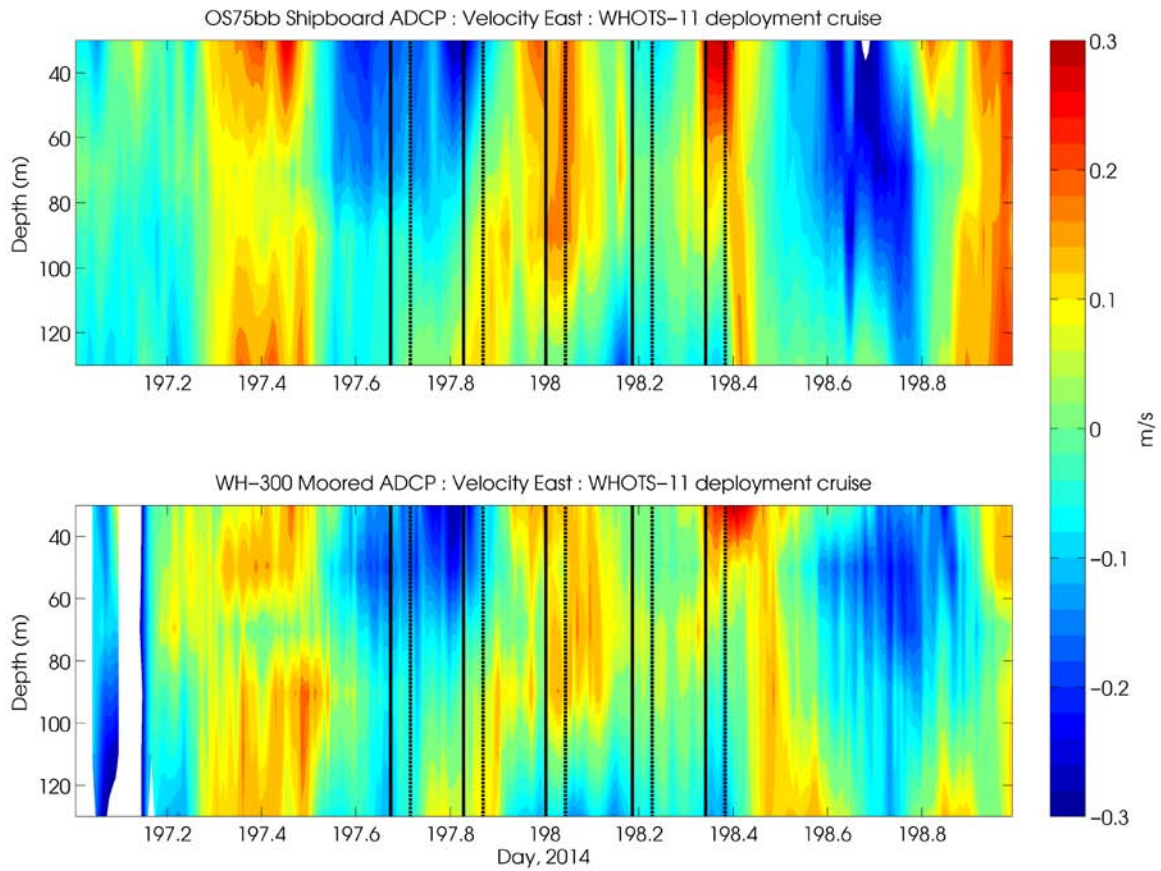


Figure 6-38. Contour of east velocity component ($m s^{-1}$) from the Ship *Hi'ialakai's* Ocean Surveyor broadband 75 kHz shipboard ADCP during the WHOTS-11 cruise (WHOTS-10 mooring recovery; upper panel), and the moored 300 kHz ADCP from the WHOTS-11 mooring as a function of time and depth during the WHOTS-11 cruise (lower panel). Times when the CTD/rosette was in the water are identified between the two sets of black lines.

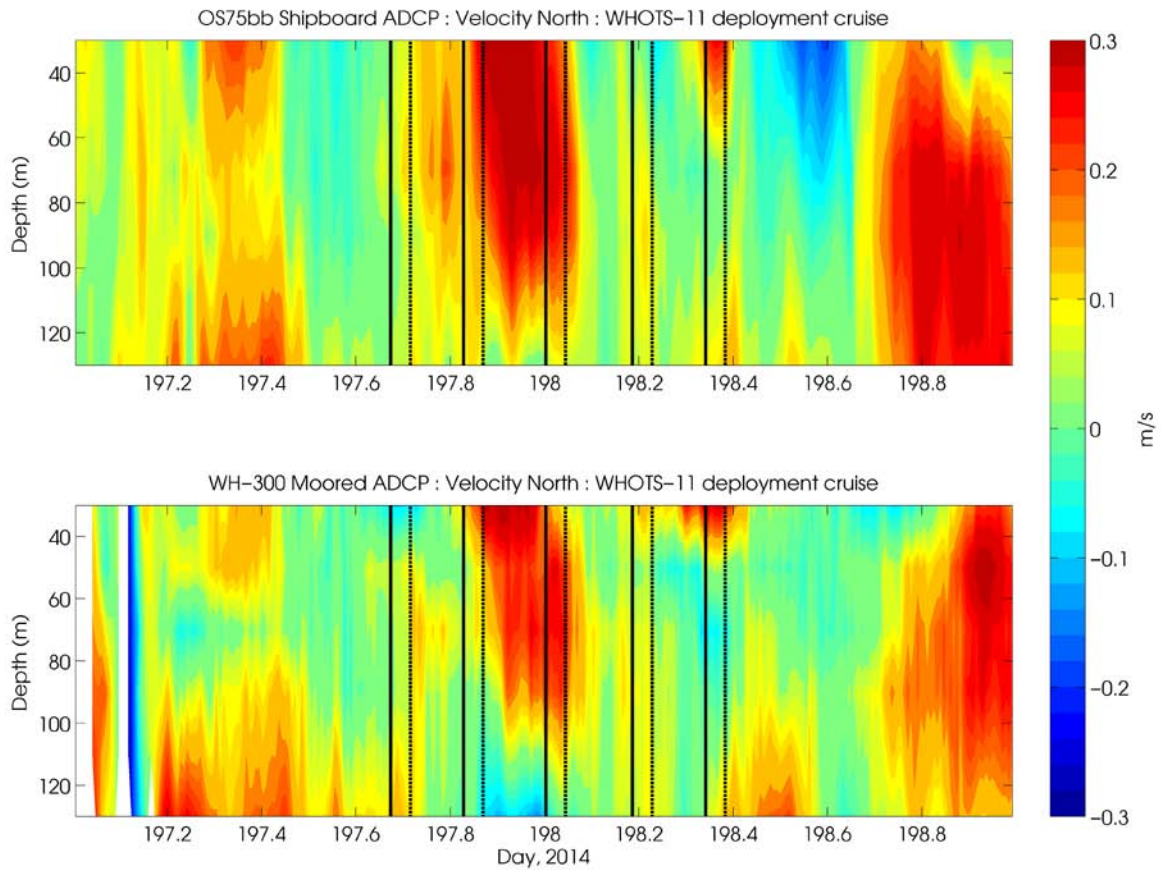


Figure 6-39. Contours of north velocity component ($m s^{-1}$) from the Ship Hi'ialakai's Ocean Surveyor broadband 75 kHz shipboard ADCP during the WHOTS-11 cruise (WHOTS-10 mooring recovery; upper panel), and the moored 300 kHz ADCP from the WHOTS-11 mooring as a function of time and depth, during the WHOTS-11 cruise (lower panel). Times when the CTD/rosette was in the water are identified between the two sets of black lines.

E. Moored and Shipboard ADCP comparisons

Comparisons between quality-controlled moored ADCPs during the WHOTS-10 deployment and available shipboard ADCP obtained during regular HOT cruises 254-260, 263, and 264 for the 300 kHz ADCP and cruises 254, 256-261, 263, and 264 for the 600 kHz ADCP are shown in Figure 6-40 to Figure 6-45 for the 300 kHz ADCP and Figure 6-49 through Figure 6-55 for the 600 kHz ADCP. HOT cruises with comparable ADCP data were conducted on the R/V *Kilo Moana* which featured a shipboard RD Instruments Workhorse 300 kHz ADCP (wh300) with 4 m bin size, reaching 100 m, and averaging ensembles every 2 minutes.

Current velocity profiles from each instrument were collected during the time when HOT CTD casts were being conducted near the WHOTS mooring specifically intended to calibrate moored instrumentation (see 5.A.4). In order to compare these HOT shipboard current profiles with moored ADCP data, each of the zonal (U) and meridional (V) current components from the moored vertical profiles were interpolated to the profile resolution of the shipboard ADCP. Data from depth bins were rejected if more than 30% of the available data during the cruise comparison period from either source were flagged as bad. The comparison period during each cruise was typically an hour and a half to two hours long. Mean difference and RMS difference values were then calculated for each bin. The vertical average of mean and RMS differences (moored – shipboard) for each of the U and V components are shown in Table 6-1.

Mean U and mean V differences for the 300 kHz and 600 kHz comparisons were between -0.05 and 0.05m/s, with generally larger differences in V than in U. RMS difference for both ADCP comparisons exhibited similar characteristics in U and V, ranging between 0.02 and 0.10 m/s, but with larger differences in V. There was significant variability with depth for both the mean and RMS difference profiles for the majority of cruises.

Table 6-1. Vertical average of mean and RMS differences between shipboard (300 kHz) and moored (300 kHz[top] and 600 kHz[bottom]) ADCP profiles taken during HOT CTD casts next to the mooring.

HOT Shipboard ADCP vs WHOTS Moored 300 kHz ADCP					
Cruise	Ship ADCP Type	Vertical average of mean U differences (m/s)	Vertical average of RMS U differences (m/s)	Vertical average of mean V differences (m/s)	Vertical average of RMS V differences (m/s)
HOT – 254	wh300	0.0547	0.0670	0.0159	0.0431
HOT – 255	wh300	-0.0063	0.0260	-0.0449	0.0708
HOT – 256	wh300	-0.0064	0.0302	-0.0202	0.0471
HOT – 257	wh300	-0.0105	0.0289	0.0418	0.0629
HOT – 258	wh300	-0.0584	0.0658	-0.0280	0.0378
HOT – 259	wh300	0.0040	0.0136	-0.0282	0.0331
HOT – 260	wh300	0.0009	0.0375	-0.0352	0.0438
HOT – 263	wh300	-0.0263	0.0527	0.0294	0.0551
HOT – 264	wh300	-0.0196	0.0474	-0.0255	0.0431

HOT Shipboard ADCP vs WHOTS Moored 600 kHz ADCP					
Cruise	Ship ADCP Type	Vertical average of mean U differences (m/s)	Vertical average of RMS U differences (m/s)	Vertical average of mean V differences (m/s)	Vertical average of RMS V differences (m/s)
HOT – 254	wh300	0.0379	0.0421	0.0142	0.0187
HOT – 256	wh300	-0.0045	0.0188	-0.0155	0.0196
HOT – 257	wh300	-0.0289	0.0434	0.0203	0.0244
HOT – 258	wh300	-0.0145	0.0213	0.0026	0.0079
HOT – 259	wh300	0.0377	0.0457	-0.0253	0.0368
HOT – 260	wh300	0.0056	0.0431	-0.0239	0.0346
HOT – 261	wh300	-0.0101	0.0146	0.0282	0.0403
HOT – 263	wh300	-0.0112	0.0355	0.0461	0.0554
HOT – 264	wh300	-0.0080	0.0295	-0.0128	0.0308

HOT-254 Shipboard vs WHOTS-10 Moored ADCP Comparisons

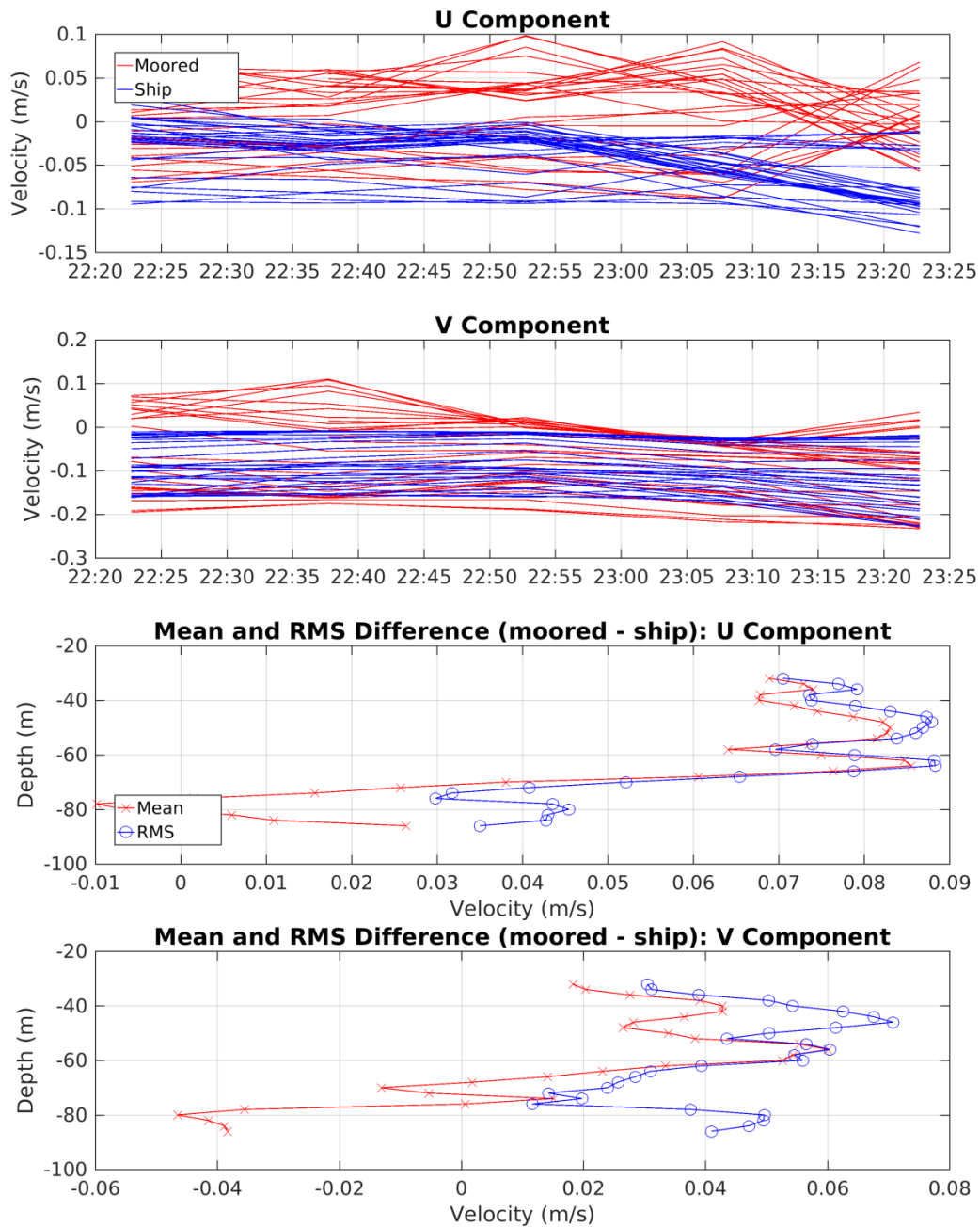


Figure 6-40. Shipboard ADCP (blue) versus moored 300 kHz ADCP (red) intercomparisons from HOT-254. Top panels show east and north velocity components (respectively) from every bin over the length of the CTD cast next to the mooring during the cruise, bottom panels show east and north (respectively) average mean difference and average RMS difference vertical profiles.

HOT-255 Shipboard vs WHOTS-10 Moored ADCP Comparisons

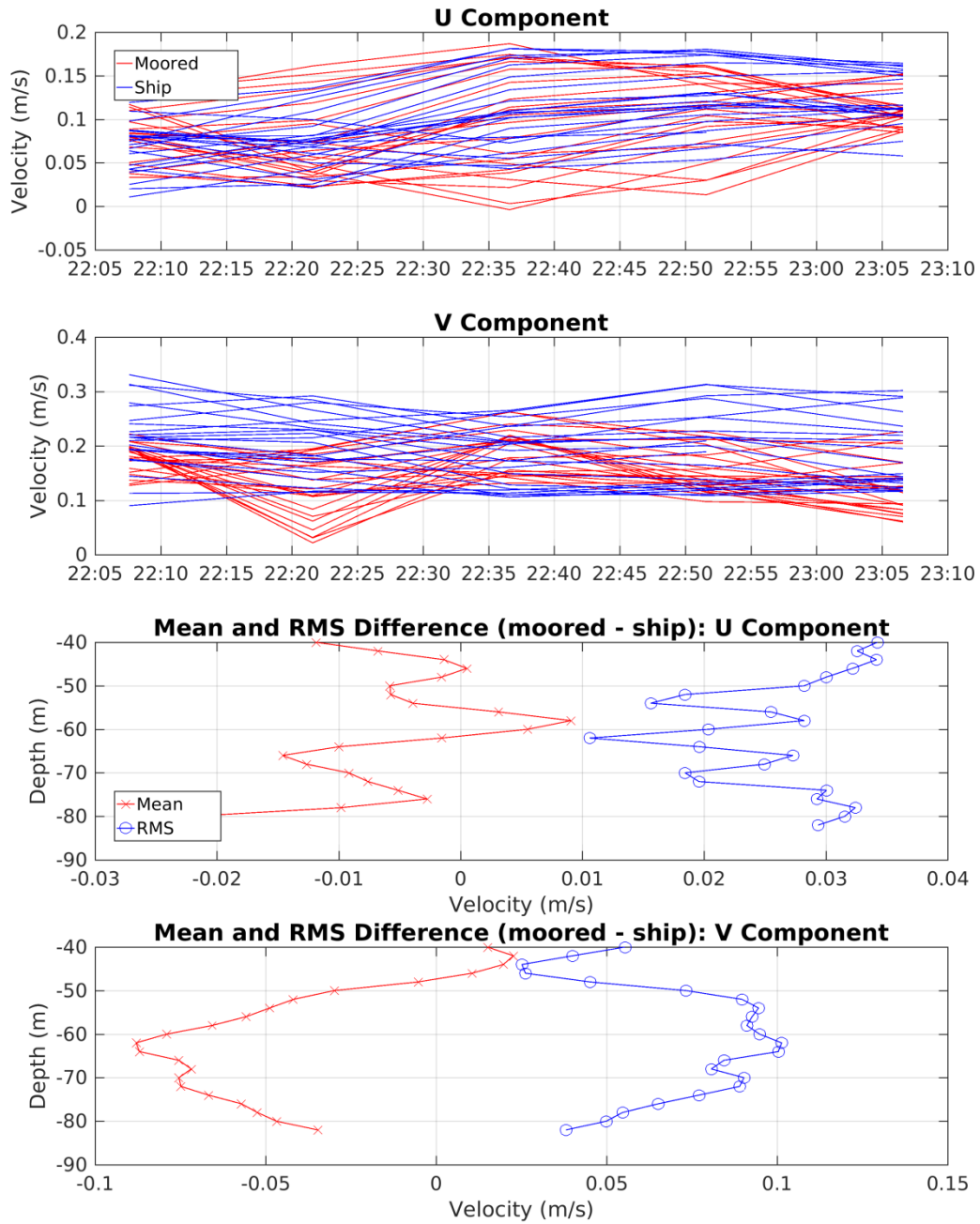


Figure 6-41. Same as in Figure 6-40, but for HOT-255.

HOT-256 Shipboard vs WHOTS-10 Moored ADCP Comparisons

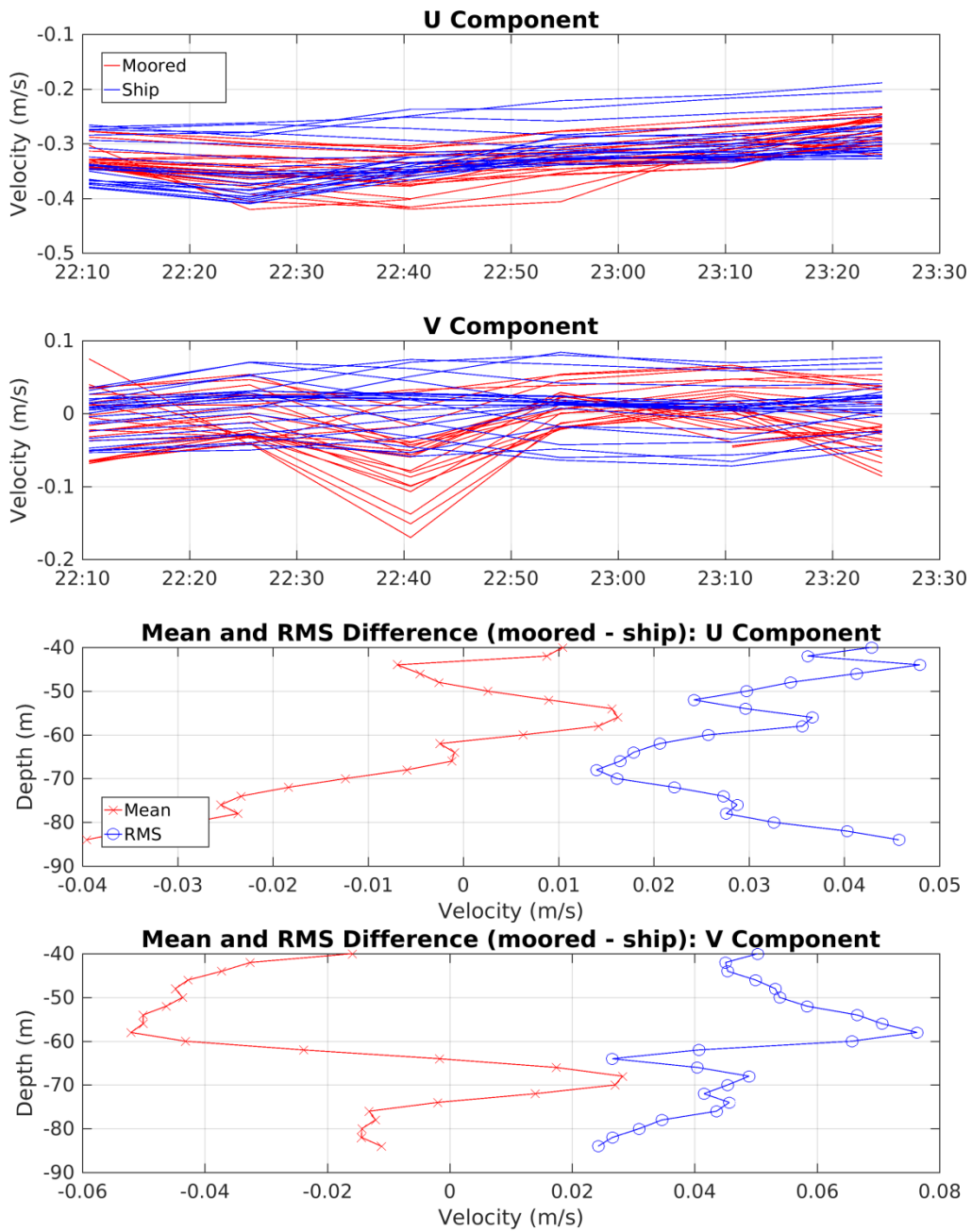


Figure 6-42. Same as in Figure 6-40, but for HOT-256.

HOT-257 Shipboard vs WHOTS-10 Moored ADCP Comparisons

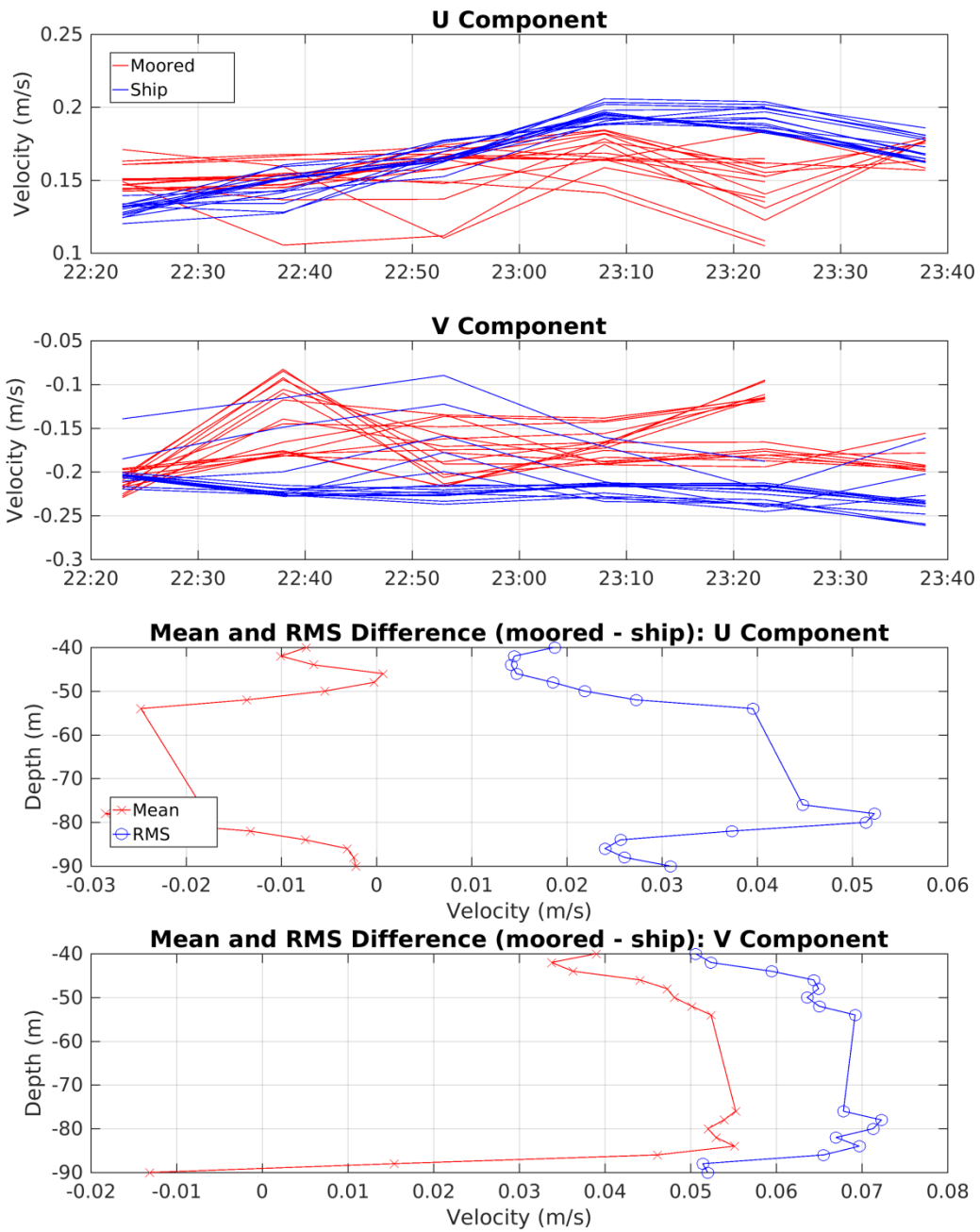


Figure 6-43. Same as in Figure 6-40, but for HOT-257.

HOT-258 Shipboard vs WHOTS-10 Moored ADCP Comparisons

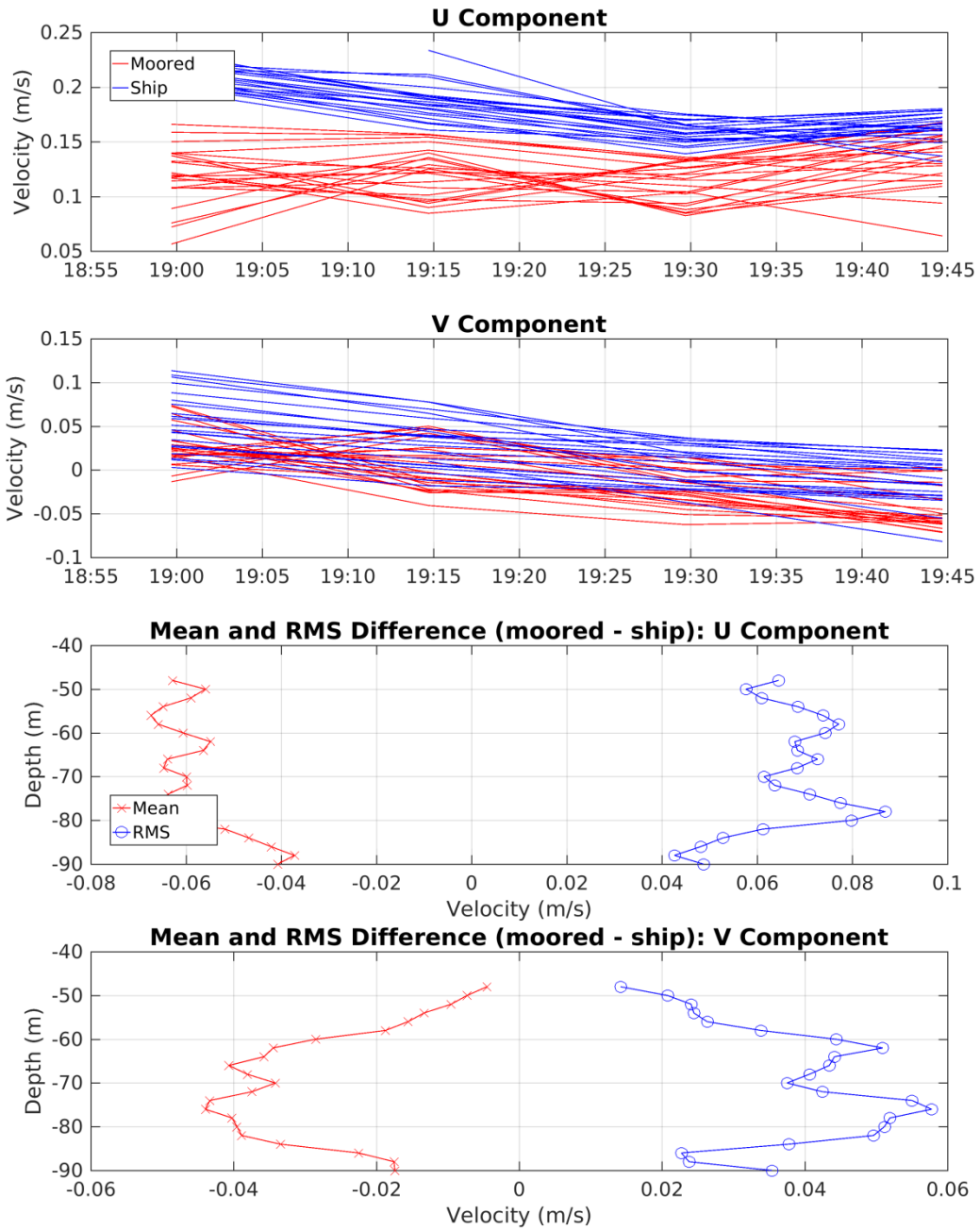


Figure 6-44. Same as in Figure 6-40, but for HOT-258.

HOT-259 Shipboard vs WHOTS-10 Moored ADCP Comparisons

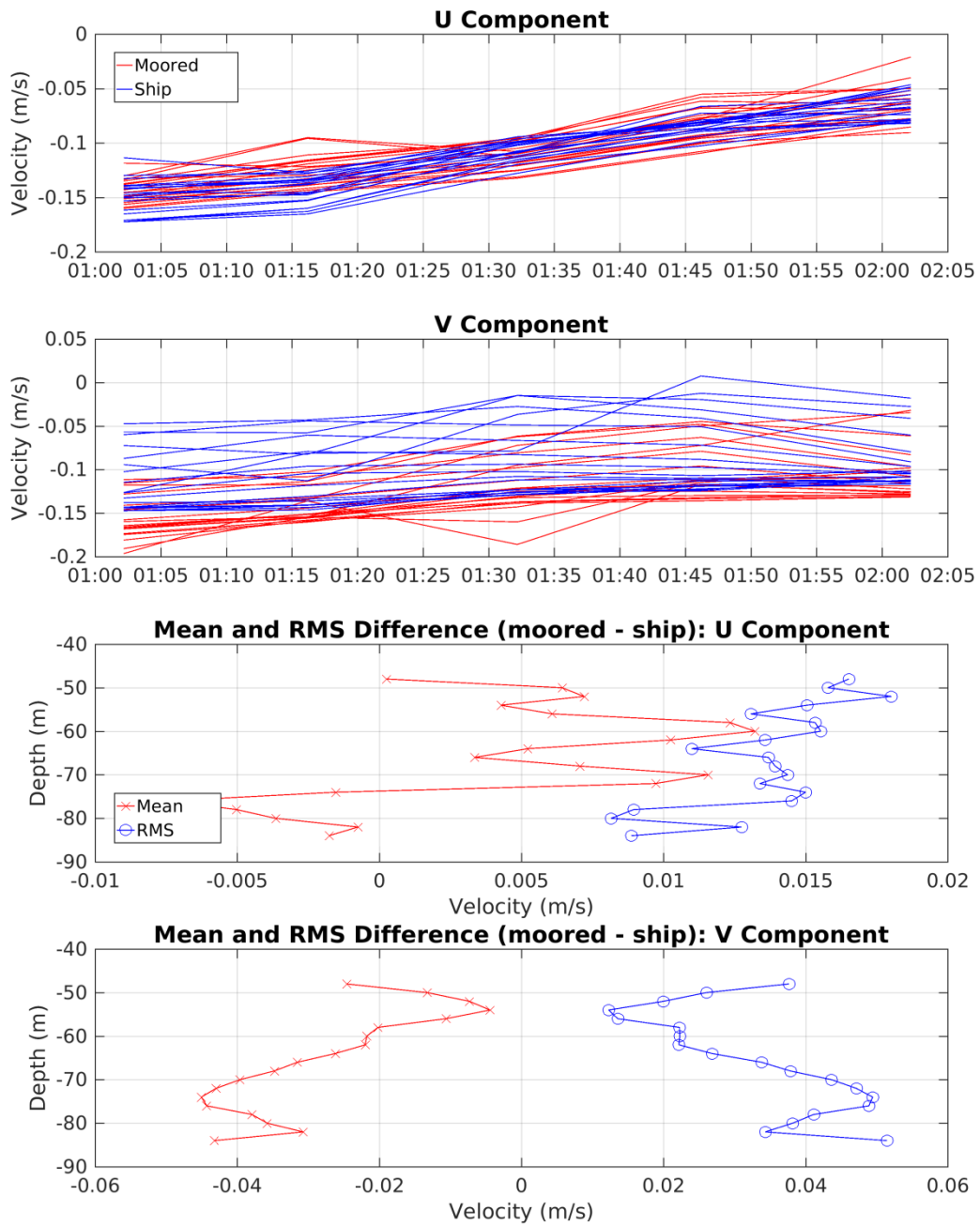


Figure 6-45. Same as in Figure 6-40, but for HOT-259.

HOT-260 Shipboard vs WHOTS-10 Moored ADCP Comparisons

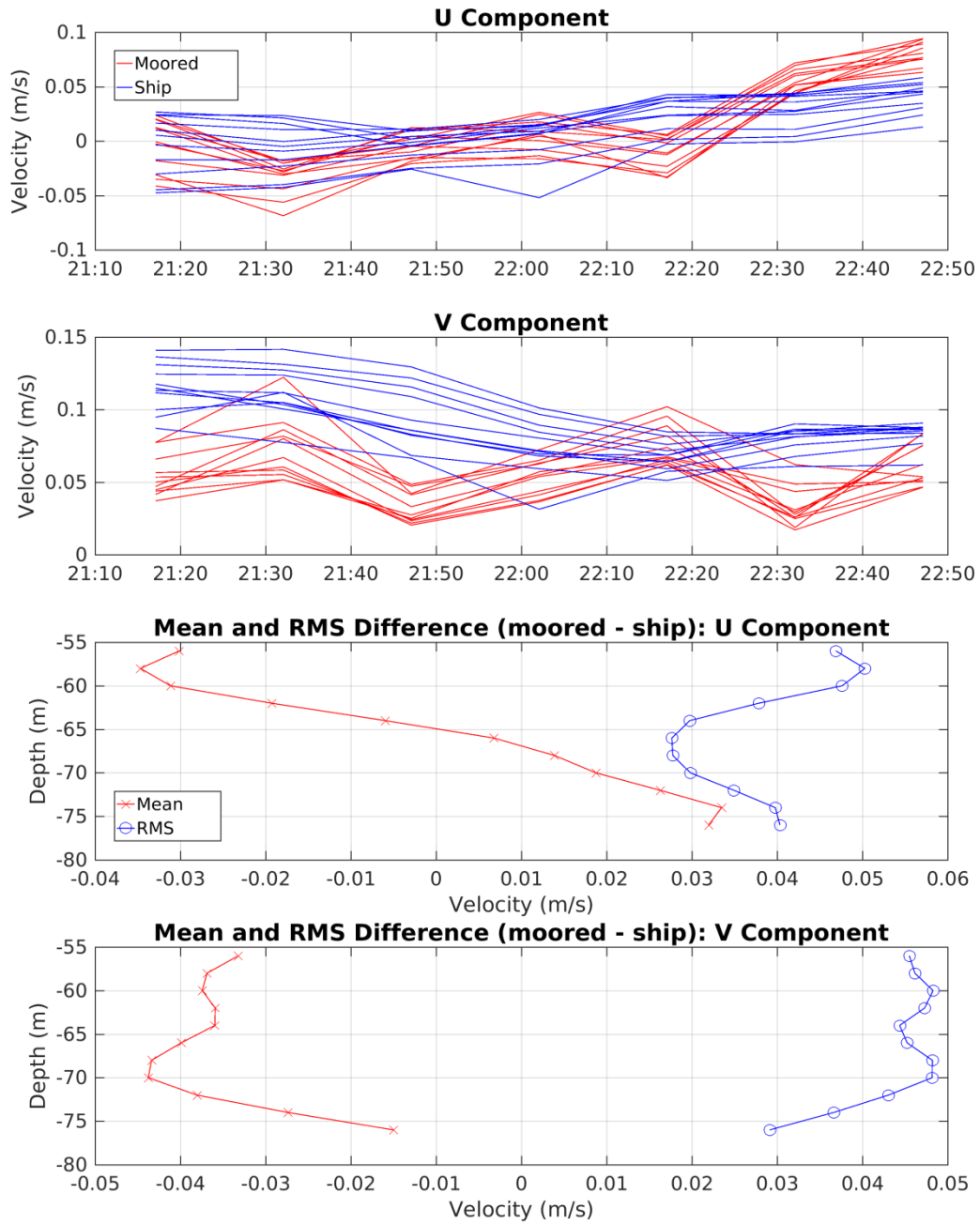


Figure 6-46. Same as in Figure 6-40, but for HOT-260.

HOT-263 Shipboard vs WHOTS-10 Moored ADCP Comparisons

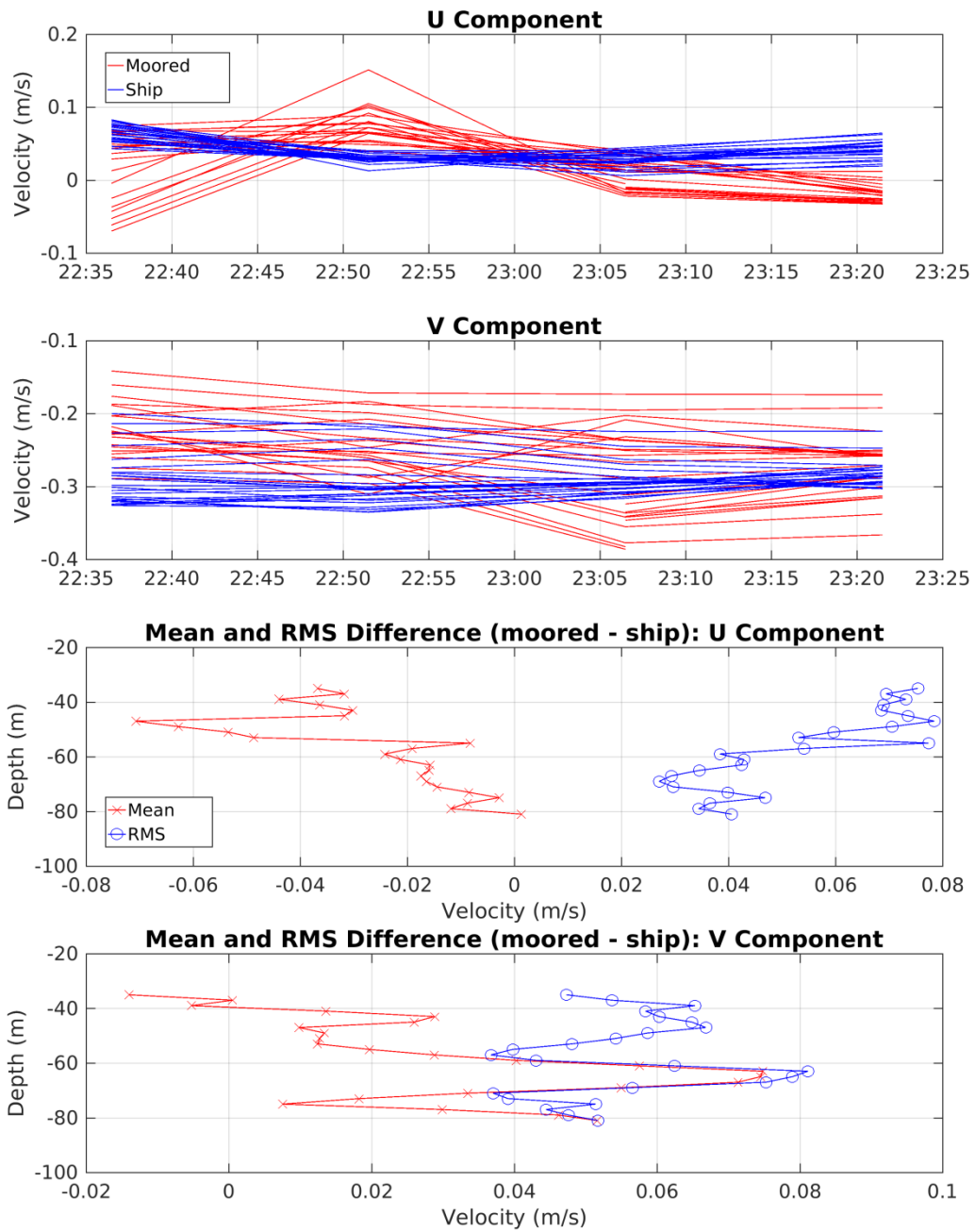


Figure 6-47. Same as in Figure 6-40, but for HOT-263.

HOT-264 Shipboard vs WHOTS-10 Moored ADCP Comparisons

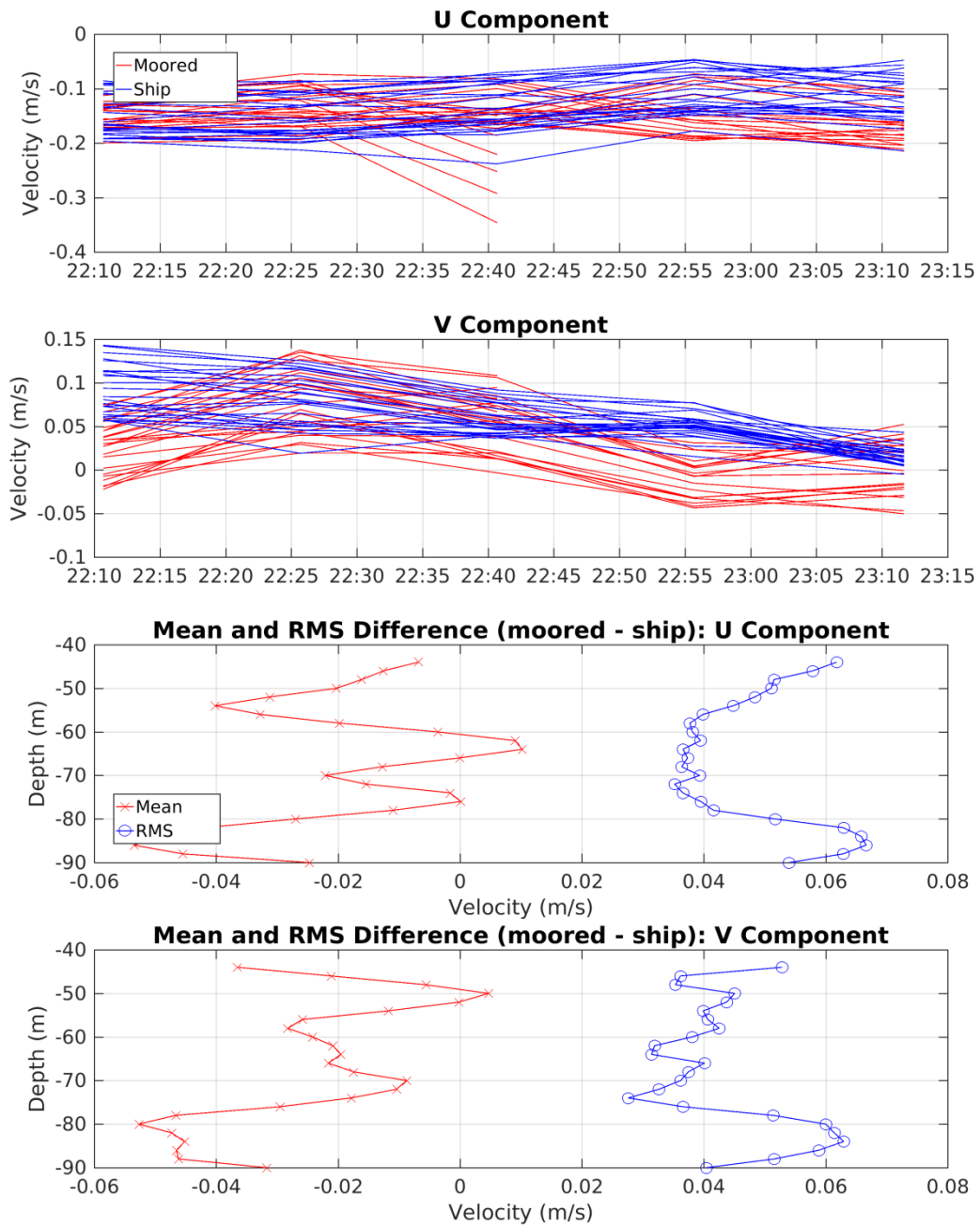


Figure 6-48. Same as in Figure 6-40, but for HOT-264.

HOT-254 Shipboard vs WHOTS-10 Moored ADCP Comparisons

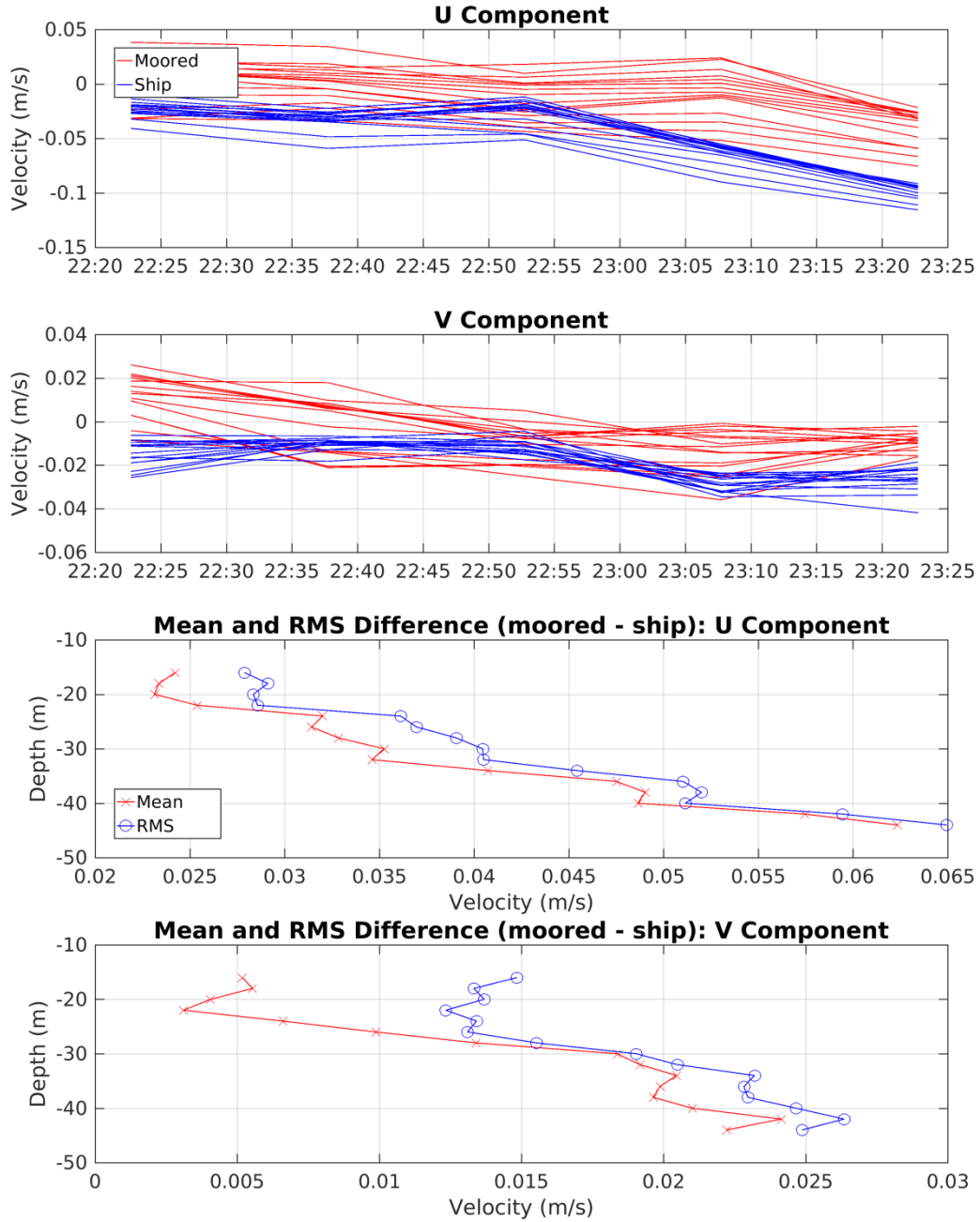


Figure 6-49. Shipboard ADCP (blue) versus moored 600 kHz ADCP (red) intercomparisons from HOT-254. Top panels show east and north velocity components (respectively) from every bin over the length of the CTD cast next to the mooring during the cruise, bottom panels show east and north (respectively) average mean difference and average RMS difference vertical profiles.

HOT-256 Shipboard vs WHOTS-10 Moored ADCP Comparisons

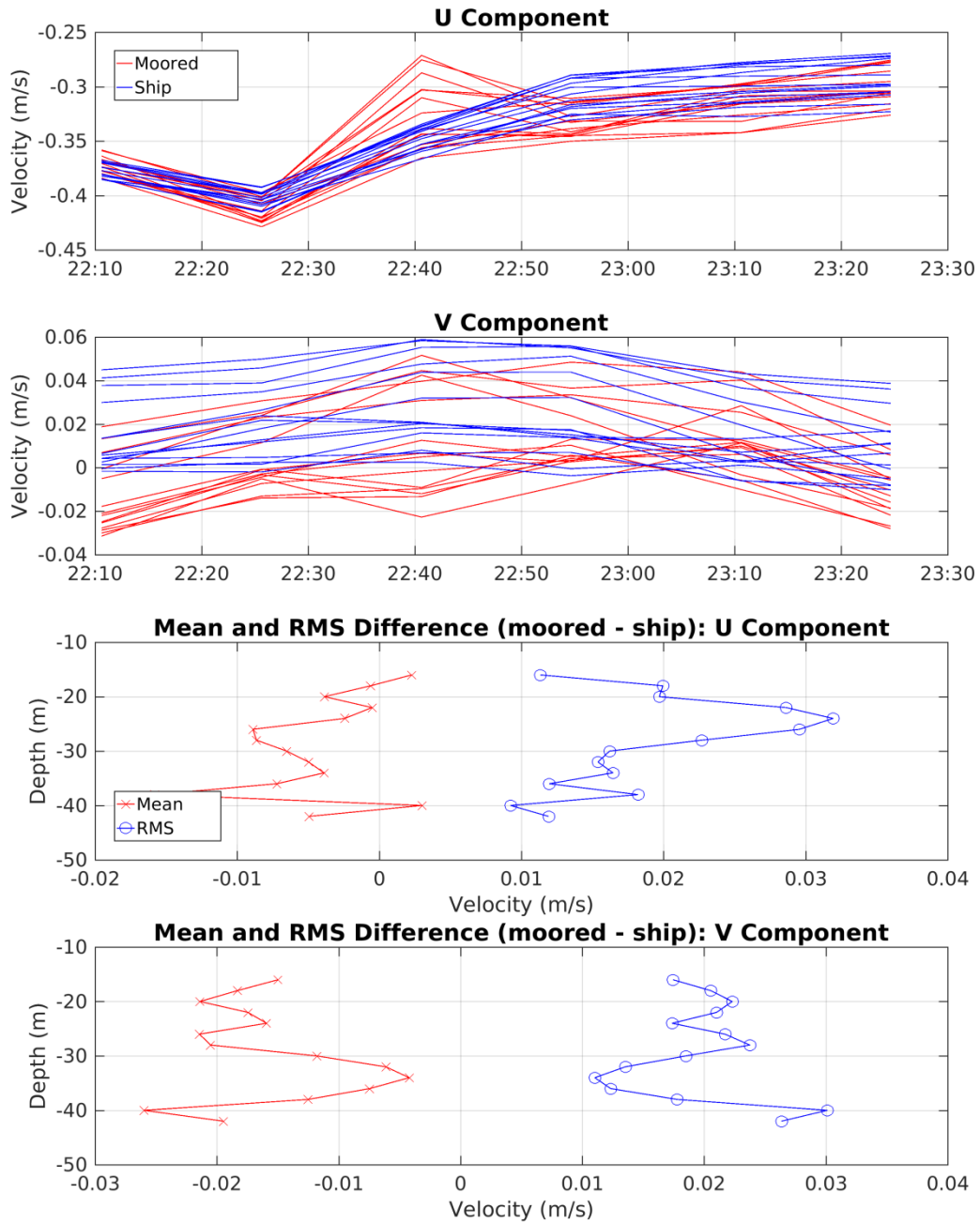


Figure 6-50. Same as in Figure 6-49, but for HOT-256.

HOT-257 Shipboard vs WHOTS-10 Moored ADCP Comparisons

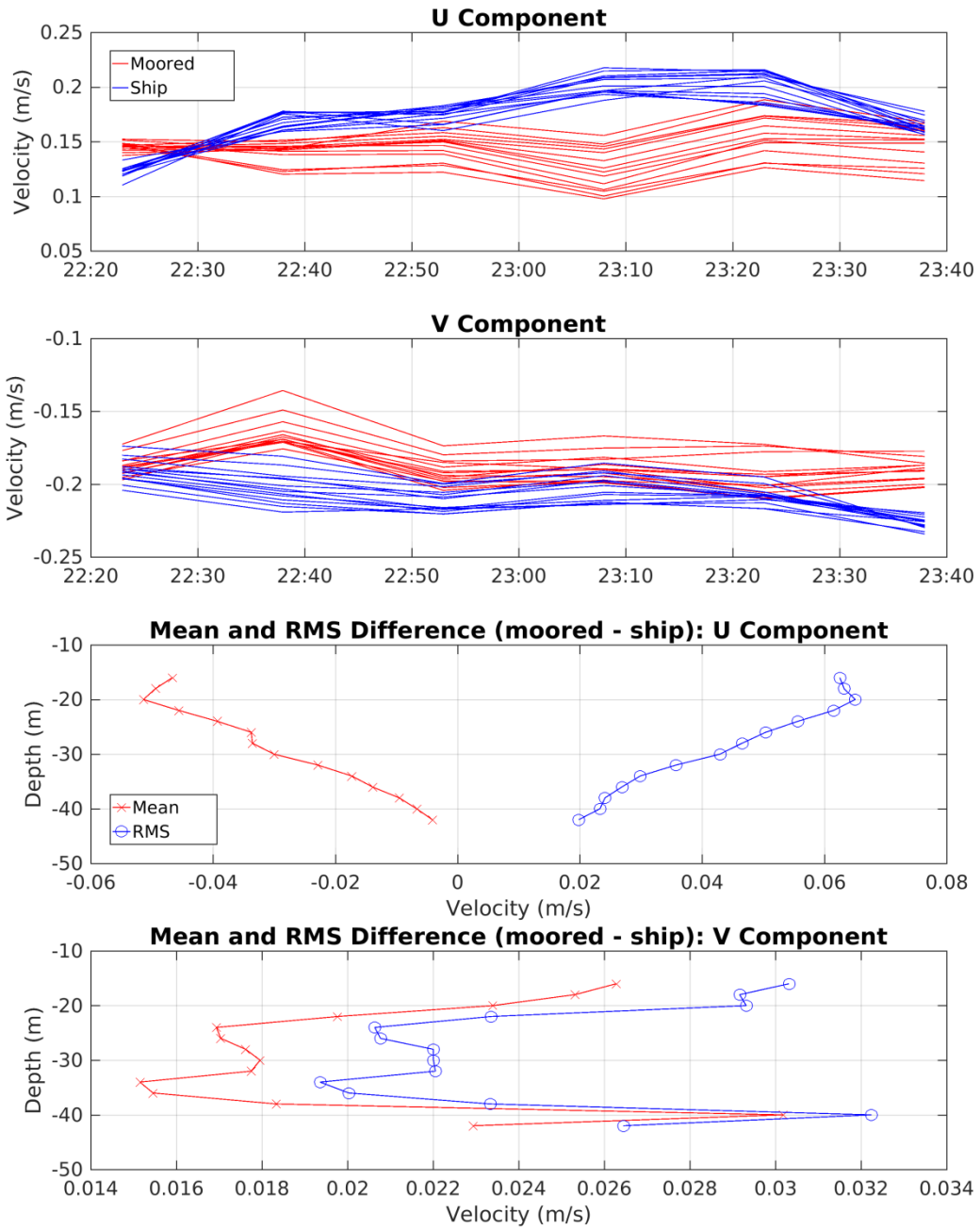


Figure 6-51. Same as in Figure 6-49, but for HOT-257.

HOT-258 Shipboard vs WHOTS-10 Moored ADCP Comparisons

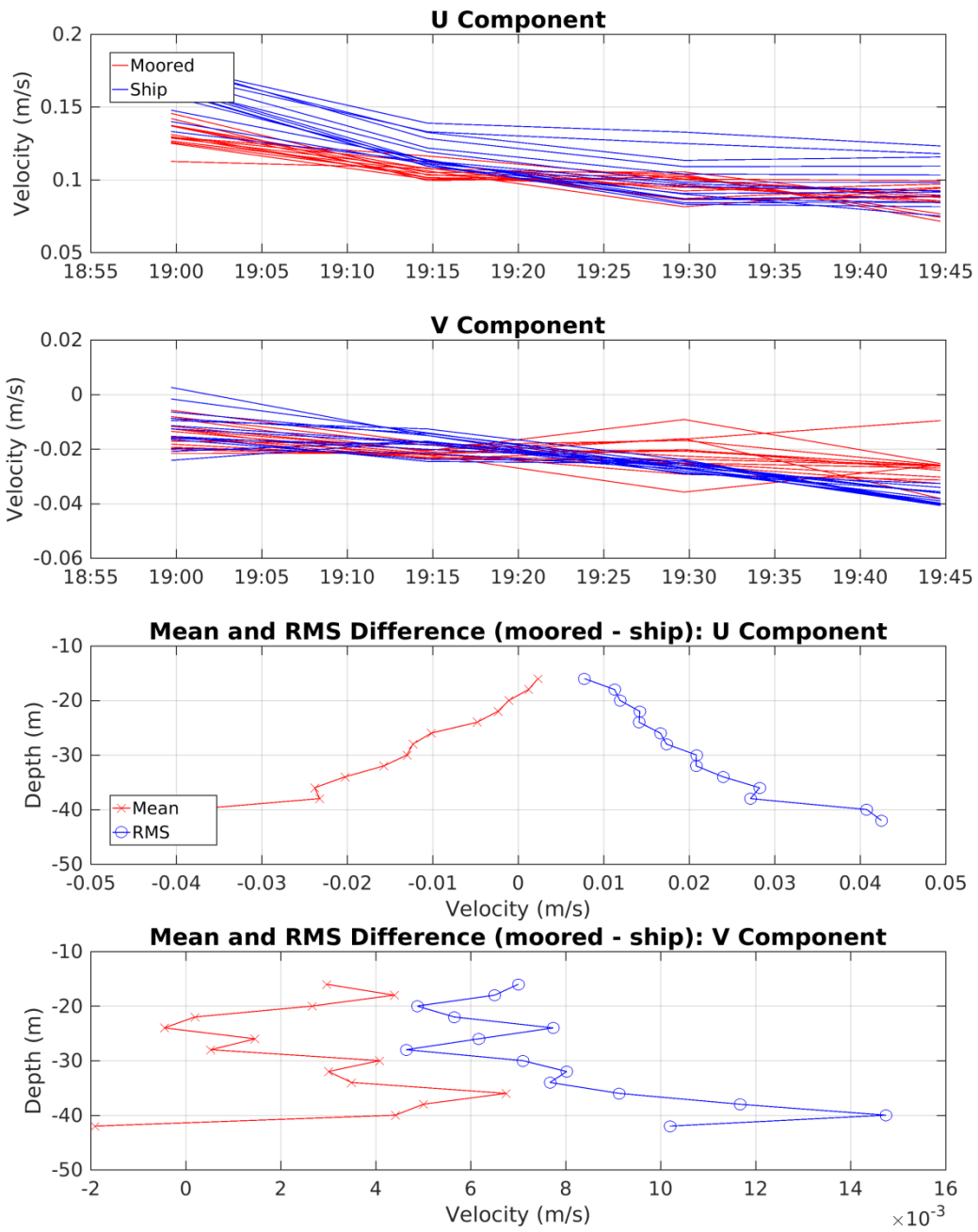


Figure 6-52. Same as in Figure 6-49, but for HOT-258.

HOT-259 Shipboard vs WHOTS-10 Moored ADCP Comparisons

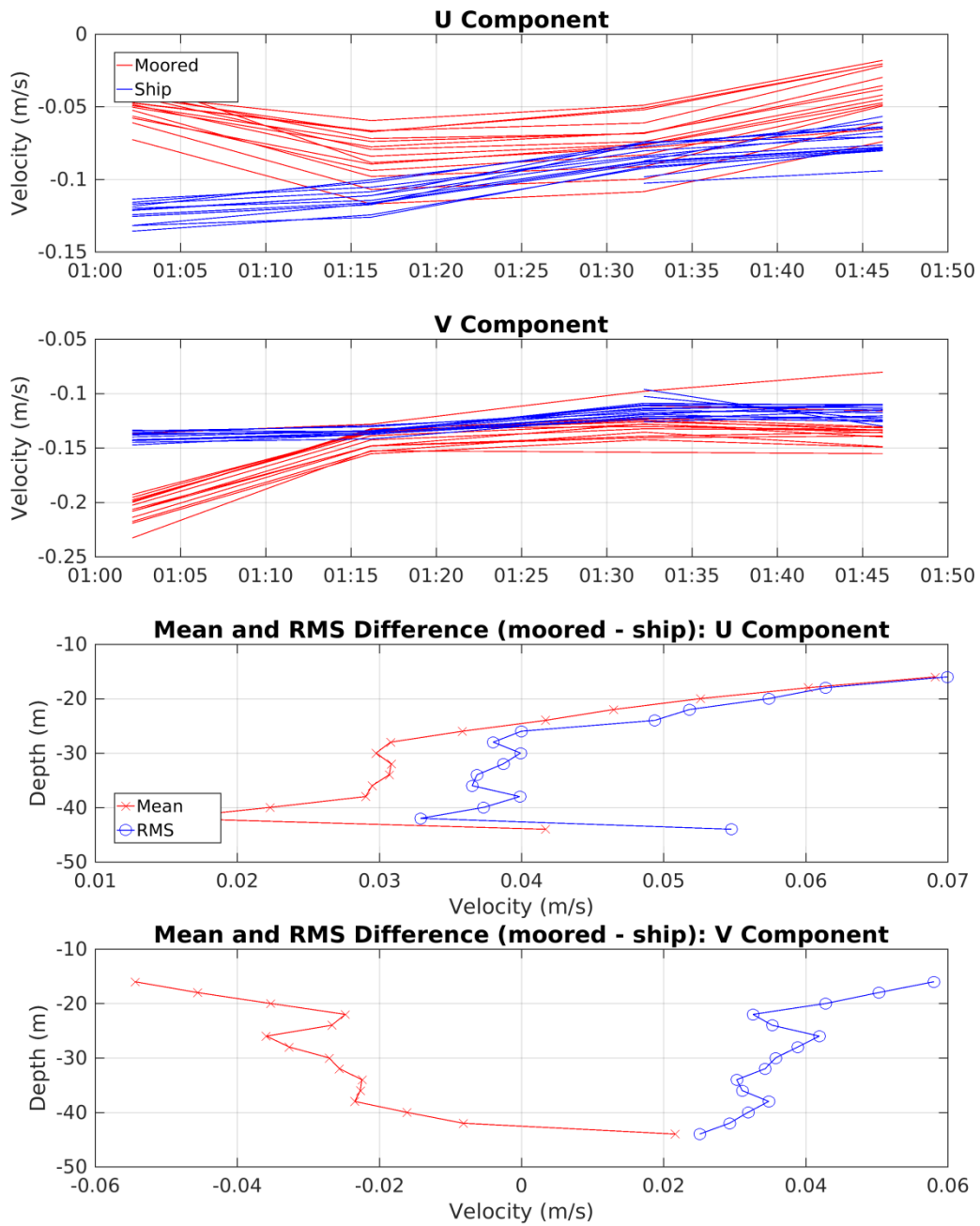


Figure 6-53. Same as in Figure 6-49, but for HOT-259.

HOT-260 Shipboard vs WHOTS-10 Moored ADCP Comparisons

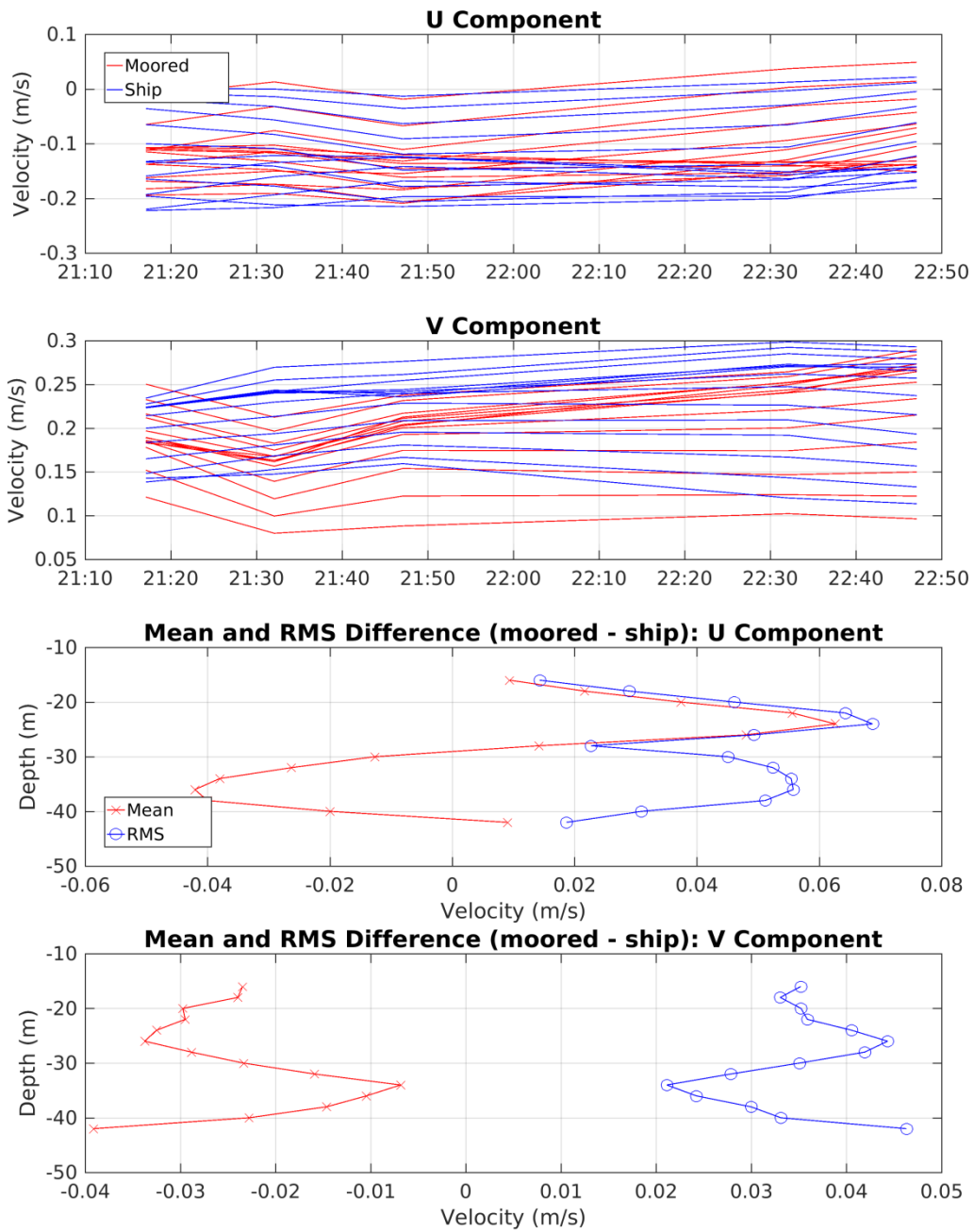


Figure 6-54. Same as in Figure 6-49, but for HOT-260.

HOT-261 Shipboard vs WHOTS-10 Moored ADCP Comparisons

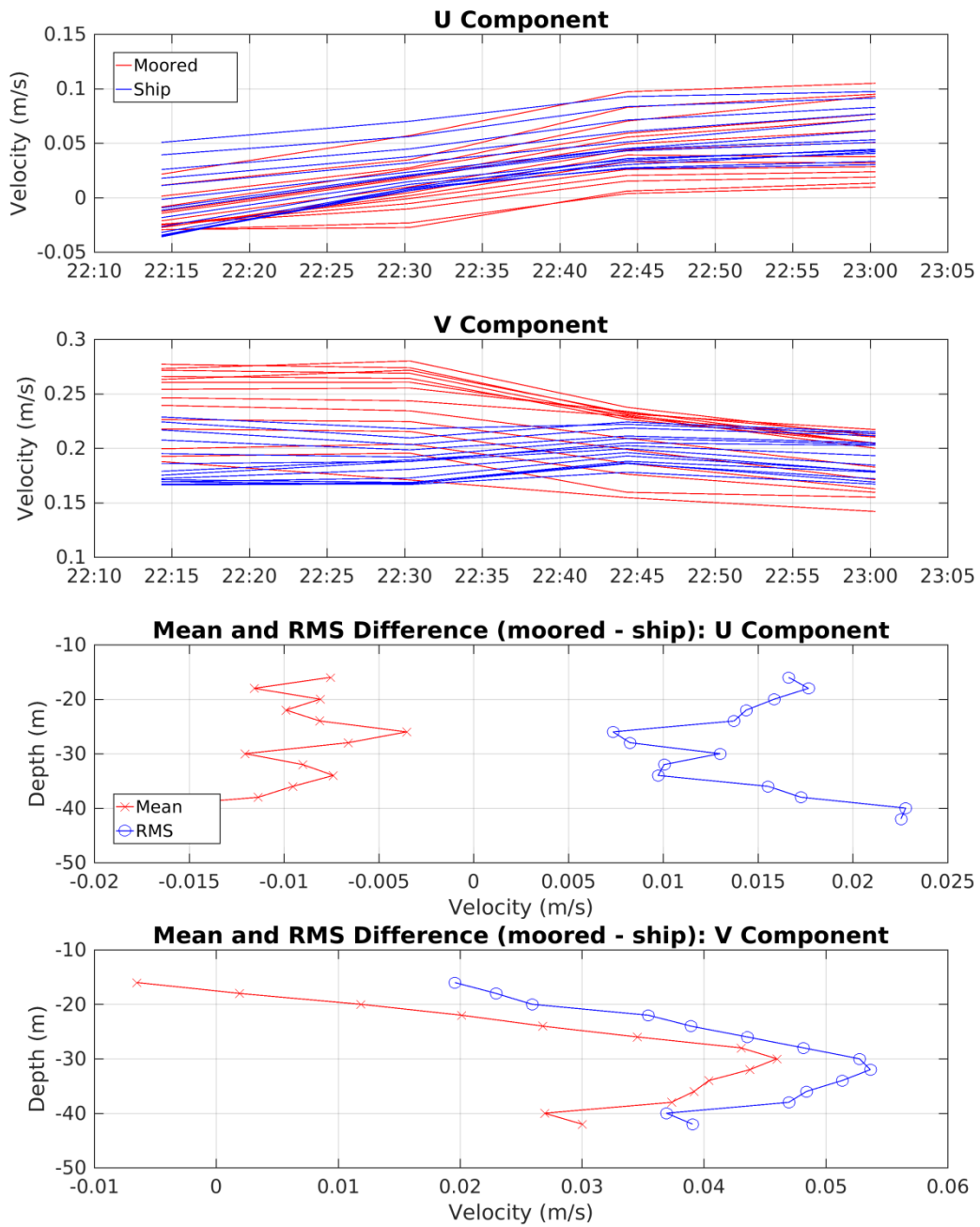


Figure 6-55. Same as in Figure 6-49, but for HOT-261.

HOT-263 Shipboard vs WHOTS-10 Moored ADCP Comparisons

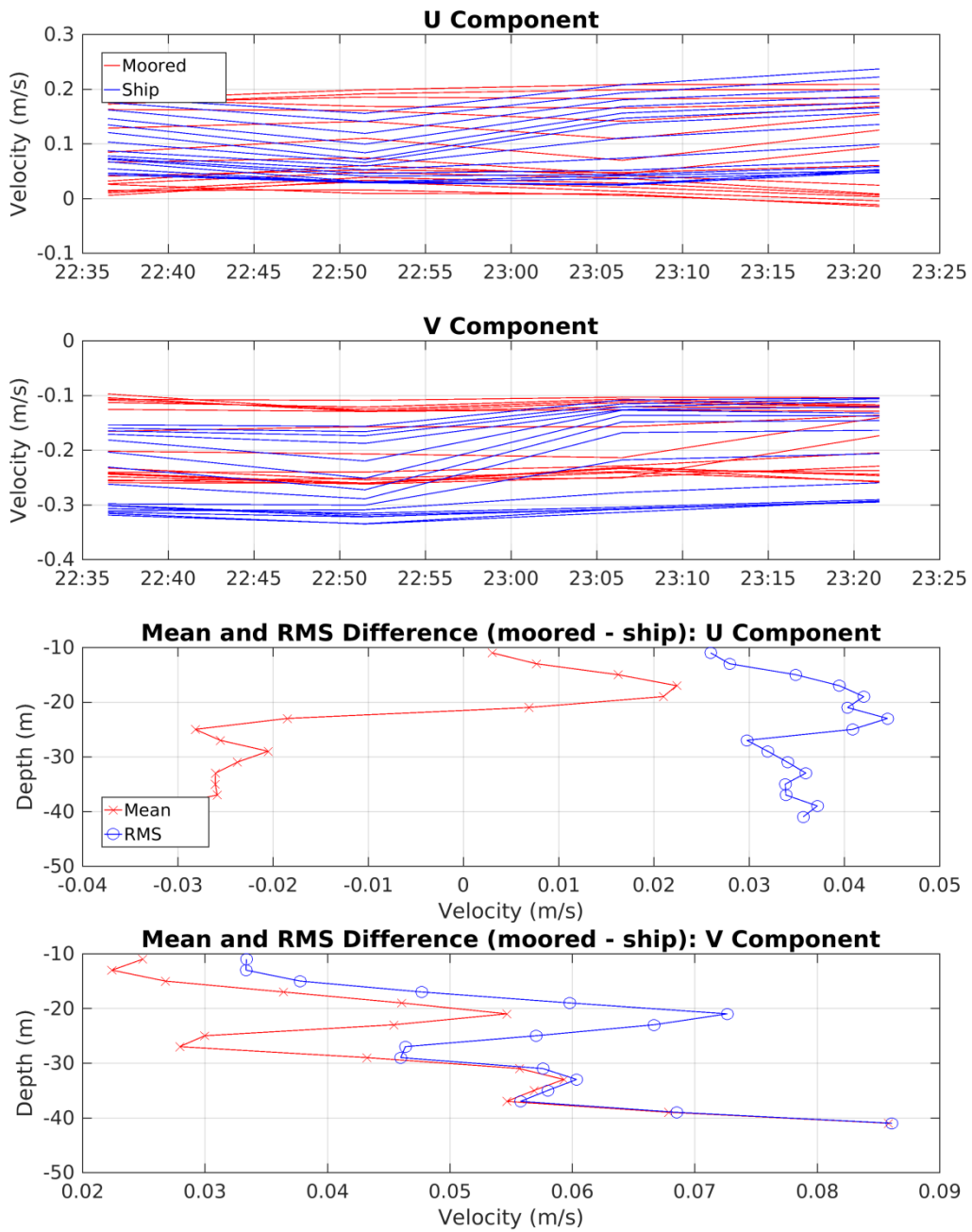


Figure 6-56. Same as in Figure 6-49, but for HOT-263.

HOT-264 Shipboard vs WHOTS-10 Moored ADCP Comparisons

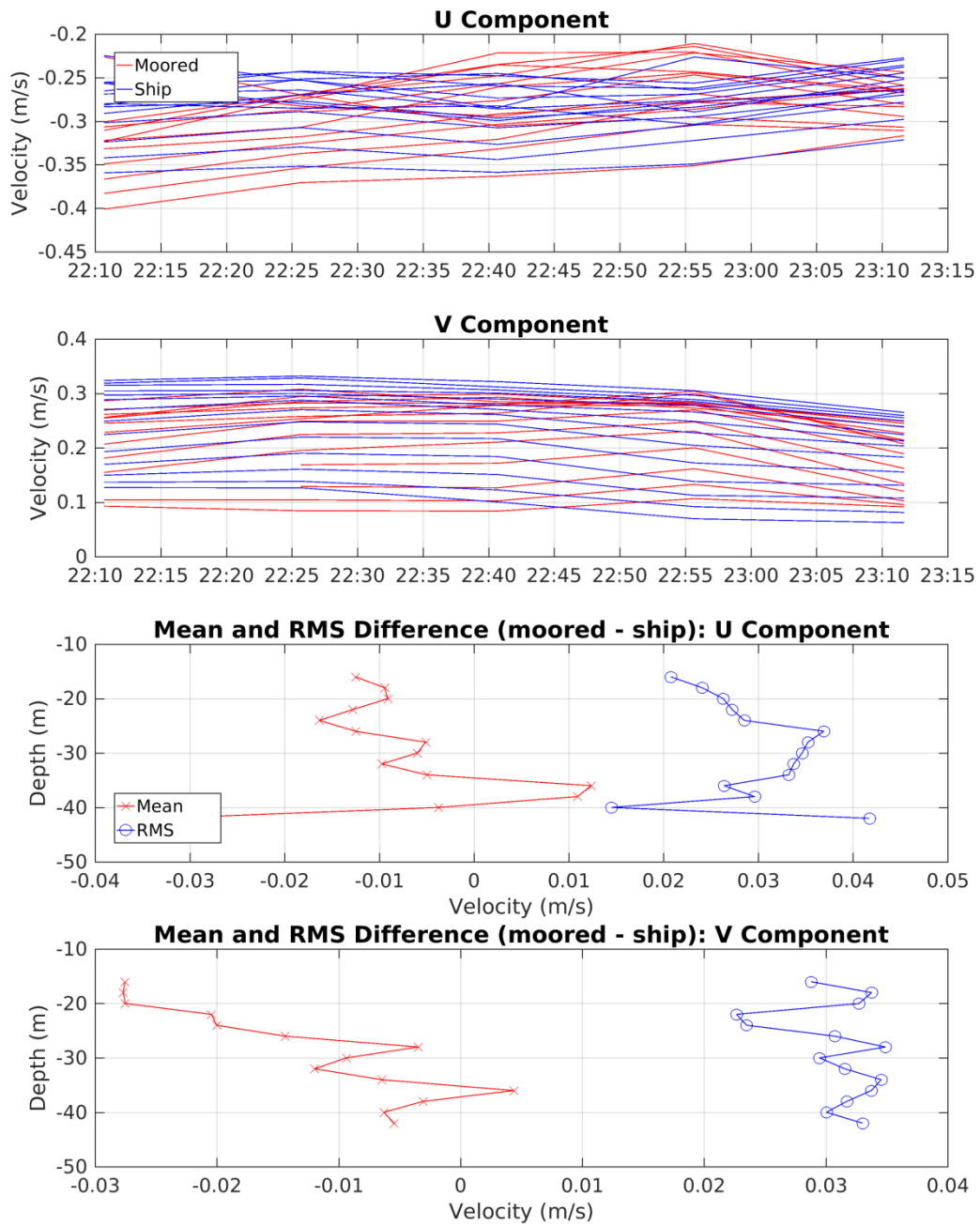


Figure 6-57. Same as in Figure 6-49, but for HOT-264.

F. Next Generation Vector Measuring Current Meter data (VMCM)

Time-series of daily mean horizontal velocity components for the VMCM current meters deployed during WHOTS-10 at 10 m and 30 m are presented in Figure 6-58.

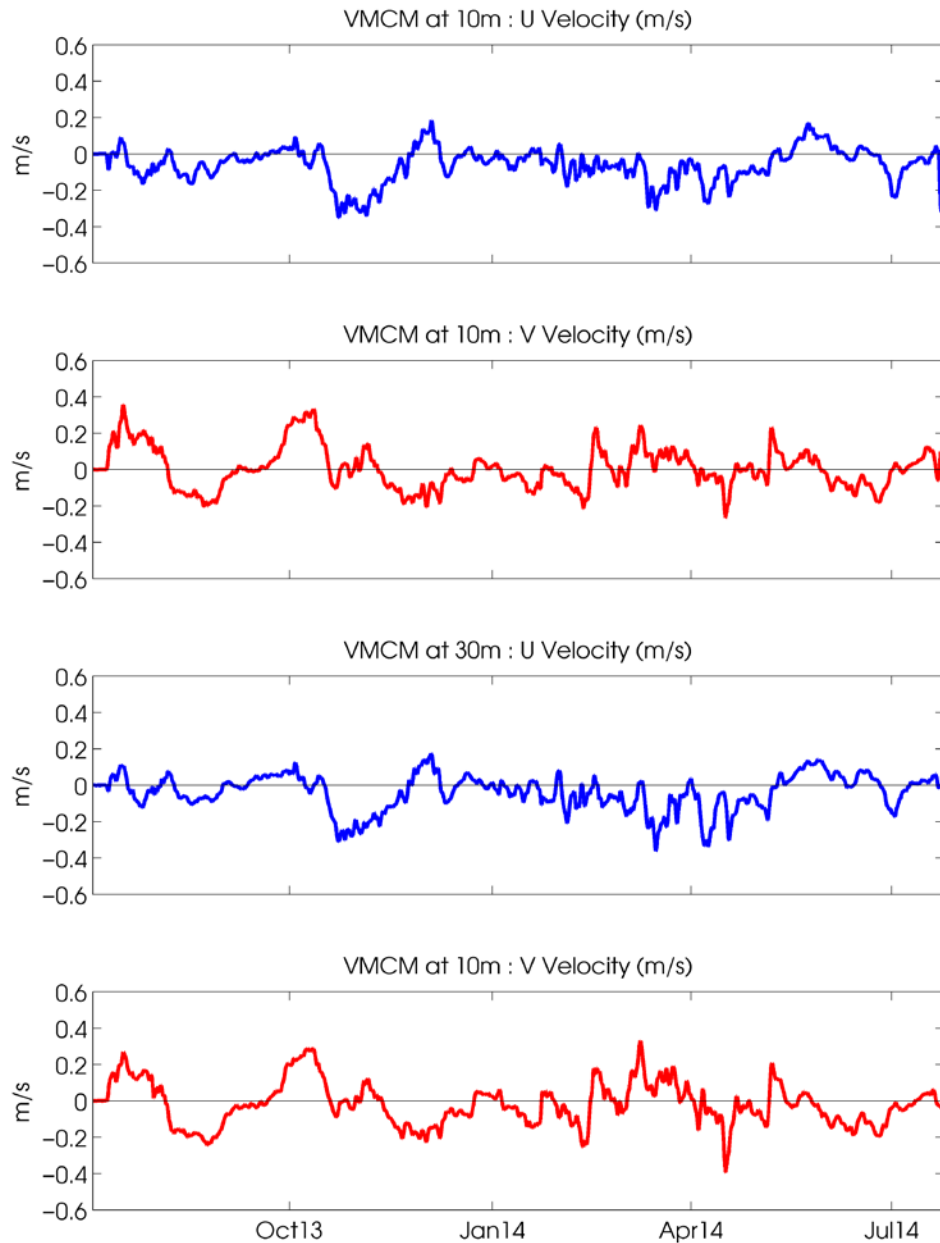


Figure 6-58. Horizontal velocity data (m/s) during WHOTS-10 from the VMCMs at 10 m depth (first and second panel) and at 30 m depth (third and fourth panel).

G. GPS data

Time-series of latitude and longitude of the WHOTS-10 buoy from GPS data are presented in Figure 6-59 and spectra of the time-series is shown in Figure 6-60.

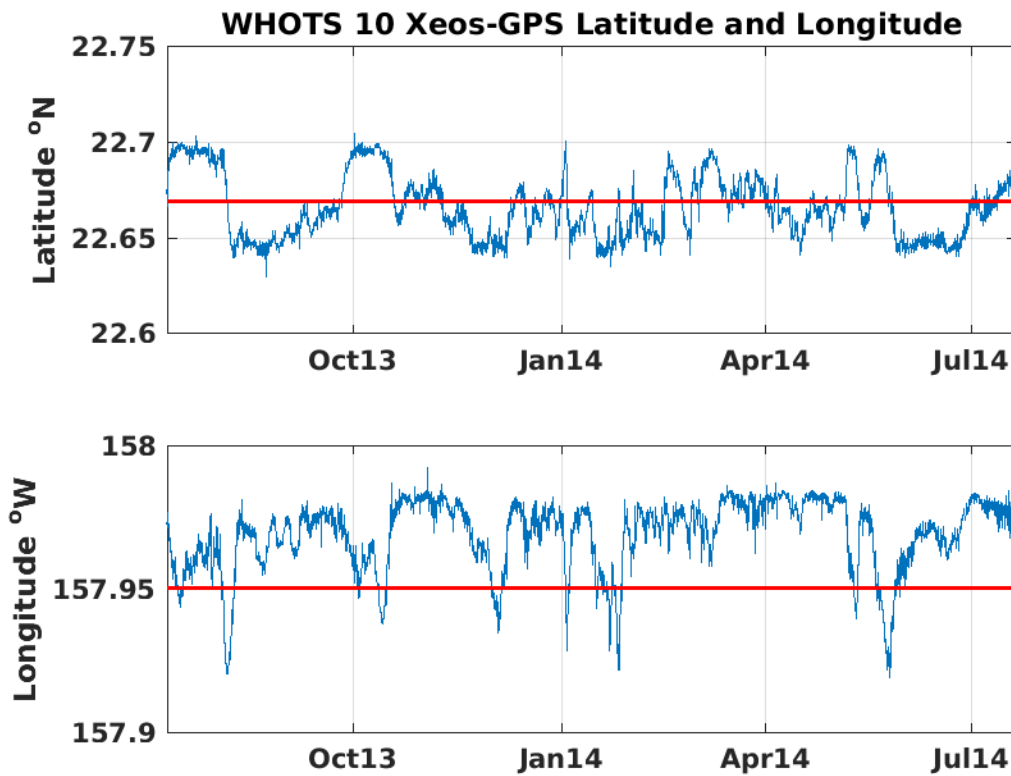


Figure 6-59. GPS Latitude (upper panel) and longitude (lower panel) time series from the WHOTS-10 deployment. The position of the anchor is shown in red.

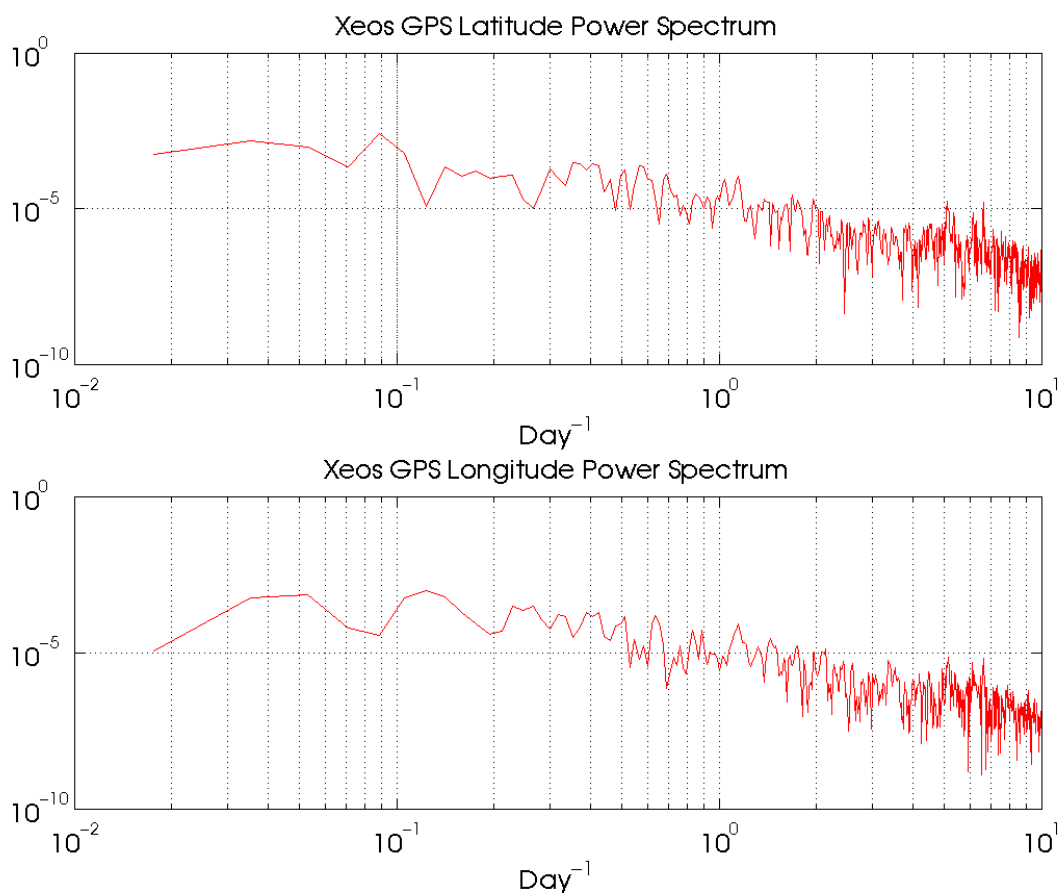


Figure 6-60. Power spectrum of latitude (upper panel) and longitude (lower panel) for the WHOTS-10 deployment.

H. Mooring Motion

The position of the mooring with respect to its anchor was determined from the ARGOS positions as shown in Section 5.D. Additional information of the mooring motion was provided by the ADCP data of pitch, roll and heading, shown in this section.

Figure 6-61 shows the ADCP data of the instrument's tilt (a combination of the pitch and roll), plotted against the buoy's distance from its anchor (derived from ARGOS positions), for both WHOTS ADCP's. The red line in the plot is a quadratic fit to the median tilt calculated every 0.2 km distance bins. The figure shows that during both deployments, the ADCP tilt increased as the distance from the anchor increased. This tilting was caused by the deviation of the mooring line from its vertical position as it was pulled by the anchor. The tilting of the line also caused the rising of the instruments attached to the line.

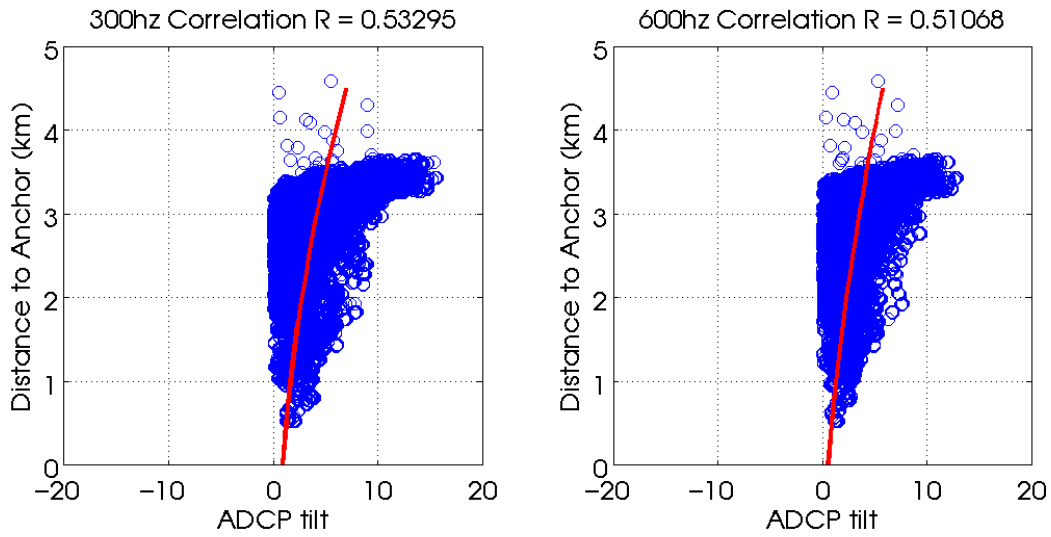


Figure 6-61. Scatter plots of ADCP tilt and distance of the buoy to its anchor for the 300 kHz (left panel), and the 600 kHz ADCP deployments (right panel, blue circles). The red line is a quadratic fit to the median tilt calculated every 0.2 km distance bins.

7. References

- Colbo, K., R. Weller, 2009. Accuracy of the IMET Sensor Package in the Subtropics. *J. Atmos. Oceanic Technol.*, 26, 1867-1890.
- Firing, E., 1991. Acoustic Doppler Current Profiling measurements and navigation. In *WOCE Hydrographic Operations and Methods*. WOCE Operations Manual, WHP Office Report WHPO 91-1, WOCE Report No. 68/91, 144pp.
- Freitag, H. P., M. E. McCarty, C. Nosse, R. Lukas, M. J. McPhaden, and M. F. Cronin, 1999. COARE Seacat data: Calibrations and quality control procedures. NOAA Technical Memorandum, ERL PMEL-115. 93 pp.
- Fujieki, L.A., F. Santiago-Mandujano, R.W. Deppe, D. McCoy, R. Lukas, and M. Church, 2016a. Hawaii Ocean Time-series Data Report 25:2013. School of Ocean and Earth Sciences and Technology (SOEST) Report, 434 pp. (www.soest.hawaii.edu/HOT_WOCE/data.report.html).
- Fujieki, L.A., F. Santiago-Mandujano, R.W. Deppe, D. McCoy, R. Lukas, and M. Church, 2016b. Hawaii Ocean Time-series Data Report 26:2014. School of Ocean and Earth Sciences and Technology (SOEST) Report, 435 pp. (www.soest.hawaii.edu/HOT_WOCE/data.report.html).
- Hosom, D. R. Weller, R. Payne, and K. Prada, 1995. The IMET (Improved Meteorology) Ship and Buoy Systems. *J. Atmos. Oceanic Technol.*, 12, 527-540.
- Howe, B. M., R. Lukas, F. Duennebieer, and D. Karl, ALOHA cabled observatory installation, *OCEANS 2011*, 19-22 Sept. 2011.
- Kara, A. B., P. A. Rochford, and H. E. Hulbert, 2000. Mixed layer depth variability and barrier layer formation over the North Pacific Ocean, *J. Geophys. Res.*, 105, 16,803–16,821.
- Lukas, R., F. Santiago-Mandujano, F. Bingham and A. Mantyla, 2001. Cold bottom water events observed in the Hawaii Ocean time-series: Implications for vertical mixing. *Deep-Sea Res. I*, 48 (4), 995-1021
- Owens, W. B. and R. C. Millard, 1985. A new algorithm for CTD oxygen calibration. *Journal of Physical Oceanography*, 15, 621-631.
- Plueddemann, A.J., R.A. Weller, R. Lukas, J. Lord, P.R. Bouchard, and M.A. Walsh, 2006, WHOI Hawaii Ocean Timeseries Station (WHOTS): WHOTS-2 Mooring Turnaround Cruise Report, Woods Hole Oceanographic Institution, Technical Report WHOI-2006-08, 68 pp.
- Plueddemann, A.J., B. Pietro, S. Whelan, R. Lukas, J. Snyder, C. Fumar, E. Roth, B. Nakahara, D. McCoy, J. George, and D. Wolfe, 2014, WHOI Hawaii Ocean Timeseries Station (WHOTS): WHOTS-10 Mooring Turnaround Cruise Report, Woods Hole Oceanographic Institution, Technical Report WHOI-2014-02, 114 pp.

Plueddemann, A. J., B. Pietro, S.P. Whelan, R. Lukas, J. Snyder, F. Santiago-Mandujano, B. Nakahara, D. McCoy, R. Tabata, T. Tran, K. Lance and B. Blomquist. 2015. WHOI Hawaii Ocean Timeseries Station (WHOTS): WHOTS-11 2014 Mooring Turnaround Cruise Report, Woods Hole Oceanographic Institution, Technical Report WHOI-2015-041, 105 pp.

Santiago-Mandujano, F., P. Lethaby, R. Lukas, J. Snyder, Weller, A. Plueddeman, J. Lord, S. Whelan, P. Bouchard, and N. Galbraith, 2007. Hydrographic Observations at the Woods Hole Oceanographic Institution (WHOI) Hawaii Ocean Timeseries (HOT) Site (WHOTS): 2004-2006. School of Ocean and Earth Science and Technology, University of Hawaii. (http://www.soest.hawaii.edu/whots/data_report1.html)

Tupas, L., F. Santiago-Mandujano, D. Hebel, R. Lukas, D. Karl, and E. Firing 1993. Hawaii Ocean Time-series Data Report 4, 1992, School of Ocean and Earth Science and Technology, University of Hawaii, 93-14, 248 pp.

Tupas, L., F. Santiago-Mandujano, D. Hebel, C. Nosse, L. Fujieki, E. Firing, R. Lukas, D. Karl, 1997. Hawaii Ocean Time-series Data Report 8, 1996, School of Ocean and Earth Science and Technology, University of Hawaii, 97-7, 296 pp.

UNESCO. 1981. Tenth Report of the Joint Panel on Oceanographic Tables and Standards. UNESCO Technical Papers in Marine Science, No. 36, UNESCO, Paris.

Whelan S., R. Weller, R. Lukas, F. Bradley, J. Lord, J. Smith, F. Bahr, P. Lethaby, J. Snyder, 2007. WHOI Hawaii Ocean Timeseries Station (WHOTS): WHOTS-3 Mooring Turnaround Cruise Report. Technical Report. Woods Hole Oceanographic Institution, WHOI-2007-03, 103 pp.

8. Appendices

A. Appendix 1: WHOTS-10 300 kHz ADCP Configuration

File Size 41,388,568 bytes

Data Structure BB/WH/OS
Ensemble Length 752 bytes

Program Version 50.4

System Frequency 300 kHz
Convex
Sensor Configuration #1
Transducer Head Attached TRUE
Orientation UP
Beam Angle 20 Degrees
Transducer 4 Beam Janus

Real Data

CPU Serial Number: 71288

False Target(WA) 70 counts
Band Width (WB) 0
Cor. Thres. (WC) 64 counts
Err Thres. (WE) 2000 mm/s
Blank (WF) 1.76 m
Min PGood (WG) 0
Ref Layer (WL) 1, 5 first bin, last bin
Mode (WM) 1
Bins (WN) 30
Pings/Ens (WP) 40
Bin Size (WS) 4.00 m

Head Align (EA) 0.00 degrees
Head Bias (EB) 9.81 degrees
Coord Xform (EX) 00011111 Earth Coordinates Using Tilts, 3 Beam Solutions, and Bin Mapping
Sens Source (EZ) 01111101 cdhprst
Sens Avail 00011101 cdhprst

Time/Ping (TP) 00:04.00

Hardware 4 Beams
Code Reprs. 9
Lag Length 0.49 m
Xmt Length 4.42 m
1st Bin 6.22 m

BT Pings/Ens (BP) 0
BT Ens Delay (BD) 0
BT Cor.Thres. (BC) 0 counts
BT Eval. Thres. (BA) 0 counts

BT PG Thres. (BG) 0
BT Mode (BM) 0
BT Err Thres. (BE) 0 mm/s
BT Max Range (BX) 0 dm

First Ensemble 00000001 06-Jul-2013 00:00:00
Last Ensemble 00054891 22-Jul-2014 04:19:59

B. Appendix 2: WHOTS-10 600 kHz ADCP Configuration

File Size 35,900,022 bytes

Data Structure BB/WH/OS
Ensemble Length 652 bytes

Program Version 50.4

System Frequency 600 kHz
Convex
Sensor Configuration #1
Transducer Head Attached TRUE
Orientation UP
Beam Angle 20 Degrees
Transducer 4 Beam Janus

Real Data

CPU Serial Number: 70122

False Target(WA) 70 counts
Band Width (WB) 0
Cor. Thres. (WC) 64 counts
Err Thres. (WE) 2000 mm/s
Blank (WF) 0.88 m
Min PGood (WG) 0
Ref Layer (WL) 1, 5 first bin, last bin
Mode (WM) 1
Bins (WN) 25
Pings/Ens (WP) 80
Bin Size (WS) 2.00 m

Head Align (EA) 0.00 degrees
Head Bias (EB) 9.81 degrees
Coord Xform (EX) 00011111 Earth Coordinates Using Tilts, 3 Beam Solutions, and Bin Mapping
Sens Source (EZ) 01111101 cdhprst
Sens Avail 00011101 cdhprst

Time/Ping (TP) 00:2.00

Hardware 4 Beams
Code Reps. 9
Lag Length 0.25 m
Xmt Length 2.21 m

1st Bin 3.11 m

BT Pings/Ens (BP) 0
BT Ens Delay (BD) 0
BT Cor.Thres. (BC) 0 counts
BT Eval. Thres. (BA) 0 counts
BT PG Thres. (BG) 0
BT Mode (BM) 0
BT Err Thres. (BE) 0 mm/s
BT Max Range (BX) 0 dm

First Ensemble 00000001 06-Jul-2013 00:00:00
Last Ensemble 00054892 22-Jul-2014 04:30:00

C. Appendix 3: WHOTS-10 VMCM report

WHOTS 10 Preliminary Processing
VMCMs
2014/08/12 Nan Galbraith

Deployment info

Anchor over: 2013/07/11 04:26:53 UTC
Anchor release 2014/07/20 16:23:00 UTC
Deployment Cruise HA-13-03
Recovery Cruise HA-14-03
Water depth 4756 m
Deck height 65 cm
Watch circle 4.4nm

VMCMs deployed

SN	Depth	Start Date	Start Time
16	10	3-Jul-2013	18:52:30
19	30	3-Jul-2013	18:54:30

VMCMs sampled at 1 minute; compasses were configured for 2 seconds on, 13 seconds off.

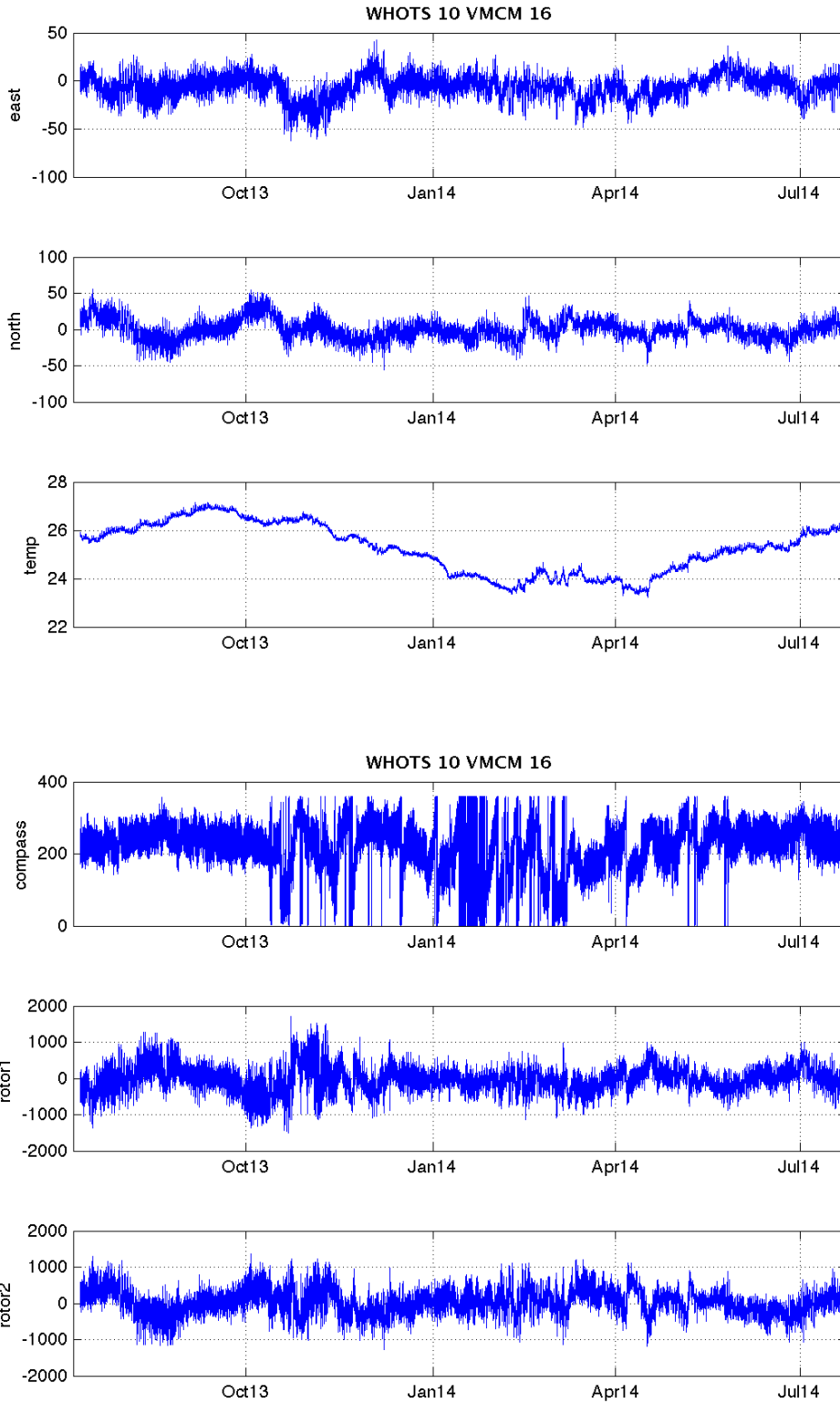
Data return

Inventory

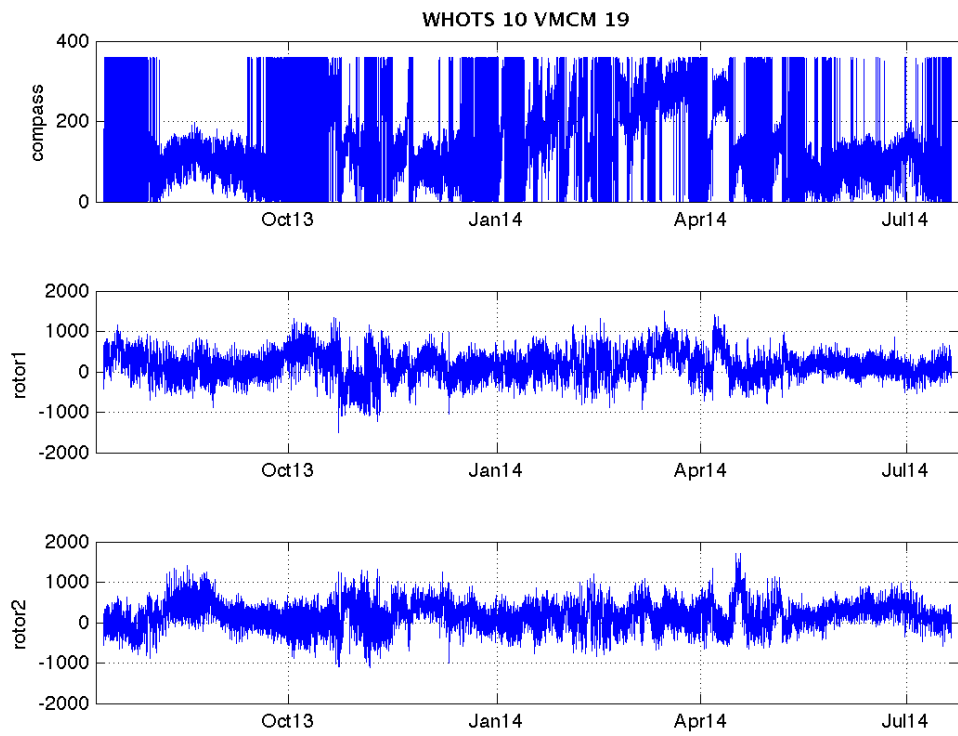
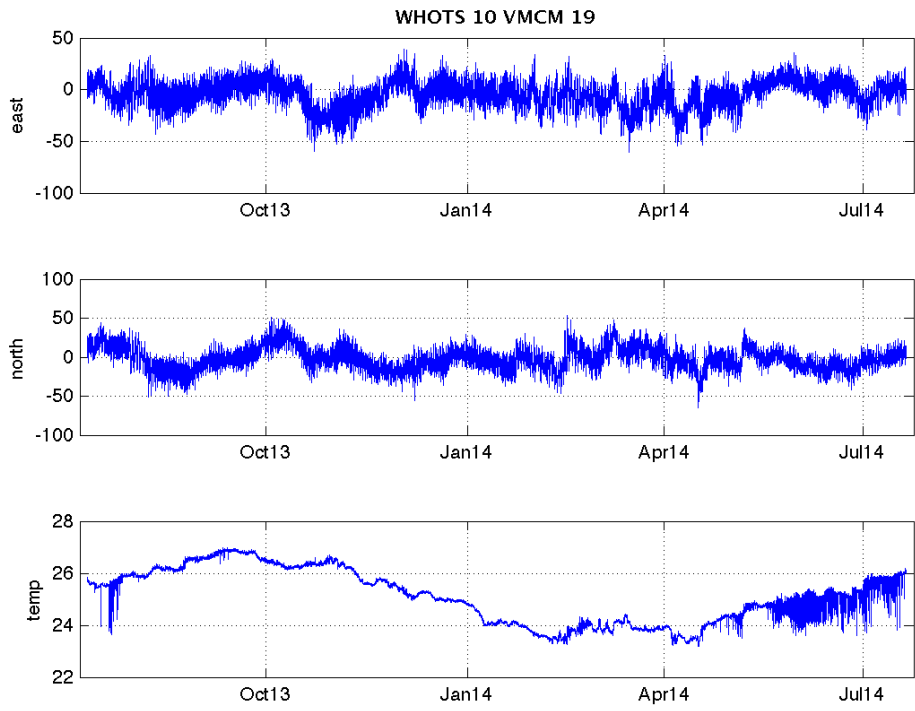
SN	first	last	#points	#expt	%Ret
16	11-Jul-2013 04:27:30	20-Jul-2014 16:22:30	539276	539276	100
19	11-Jul-2013 04:27:45	20-Jul-2014 16:22:45	539276	539276	100

Plots

VMCM 16



VMCM 19



Timing marks

Pre-deployment

SN	Depth	Start Date	Start Time	Spike Start	Spike Stop
16	10	3-Jul-2013	18:52:30	7/3/13 20:26	7/3/13 20:28
19	30	3-Jul-2013	18:54:30	7/3/13 20:22	7/3/13 20:24

Post-recovery

SN	Clock check	Time	Internal Date	Internal Time	Stop Samp	Records
16	24-Jul-2014	18:01:00	24-Jul-2014	18:03:23	18:02:00	555791
19	24-Jul-2014	17:54:00	24-Jul-2014	17:54:19	17:54:30	555780